Thèse présentée pour obtenir le grade de

Docteur de l'Université Louis Pasteur

Strasbourg I

Discipline : Géographie

par **Annett Wania**

# Urban vegetation – detection and function evaluation for air quality assessment

Soutenue publiquement le 12 Novembre 2007

**Membres du jury**

| | |
|---|---|
| Directeur de Thèse : | **Mme Christiane WEBER, Directeur de Recherche CNRS** *Université Louis Pasteur I* |
| Rapporteur Interne : | **M Dominique SCHWARTZ**, **Professeur** *Université Louis Pasteur I* |
| Rapporteur Externe : | **Mme Laurence HUBERT-MOY**, **Professeur** *Université de Rennes II* |
| Rapporteur Externe : | **M Jürgen BREUSTE**, **Professeur** *Universität Salzburg, Autriche* |
| Examinateur : | **M Michael BRUSE**, **Professeur** *Universität Mainz, Allemagne* |

***It is particularly ironic that the battle to save the world's remaining healthy ecosystems will be won or lost not in tropical forests or coral reefs that are threatened but on the streets of the most unnatural landscapes on the planet.***

(Worldwatch Institute 2007)

## Acknowledgments

This thesis was developed and authored at the ‘Laboratoire Image et Ville’, Department of Geography and Planning at the Louis Pasteur University in Strasbourg, France.

First of all thank you Christiane Weber, head of the ‘Laboratoire Image et Ville’, for guiding me through this thesis and sharing your insights and views on the French urban ecology. I am deeply grateful for the opportunity you gave me to live and work in France.

Thank you Prof. Laurence Hubert-Moy, Prof. Jürgen Breuste, Prof. Dominique Schwartz and Prof. Michael Bruse for investing your time and effort in the evaluation of this thesis.

Many thanks to you, Michael Bruse, for your patient help and discussions concerning the ENVI-met model and for your insights on atmospheric modelling.

Thank you Nadège Blond for your discussions and critical comments on the air quality simulations.

Thanks, Alexandre Blansché, for processing my data using MACLAW and the opportunity you gave me to view the process of image analysis through the eyes of a programmer. In this context thanks also to Pierre Gançarski for his insights.

For your input on remote sensing, thank you Jacky Hirsch, Aziz Serradj, Dong Binh Tran, Stéphane Lhomme, and Marc Lennon.

Furthermore, I thank ‘l’Association pour la Surveillance et l’Etude de la Pollution Atmosphérique en Alsace’ (ASPA) for providing me the STREET database and meteorological data as well as the ‘Service des Espaces Verts, des Jardins Familiaux et des Forêts’ of the municipality of Strasbourg for providing me data from the tree database.

This thesis would not have been the same without my companions from room 417: Thank you all for sharing your time, tea, and biscuits with me. Merci beaucoup au LIV!

For your support in verbalizing this thesis in proper English, I thank you Amy and Patrick.

I am particularly thankful to Florian for sharing with me the beauties of life…and the end of this thesis. Thanks to my family for supporting me in my projects even from far away.

And finally, thank you FIP!

# TABLE OF CONTENT

# LIST OF FIGURES

# LIST OF TABLES

# INTRODUCTION

Cities experience continuous population growth and at the same time they concentrate most of the Earth's environmental problems. Although they draw together many of the Earth's major environmental problems, cities paradoxically hold the best chance for building a sustainable future (UNFPA 2007). Today, the concept of sustainable development is a guiding political concept and most municipalities have put quality of life on their political agendas. Discussions on sustainable urban development require consideration of the urban form and the elements in urban systems. The present work contributes to this discussion by particularly focussing on urban vegetation as an important element of the urban ecosystem. Vegetation is associated to the quality of life and considered as a key element for sustainable urban development. Vegetation might help compensate for the effects of urbanisation. Research has proven the psychological, social, economic and ecological benefits of urban vegetation. Nevertheless, planning uses vegetation still primarily as an element of urban design and its ecosystem services are not fully realised. The study addresses the role of vegetation for air quality in urban areas and more precisely, the influence of vegetation on air pollution.

Air pollution affects health and life quality especially in urban areas. It is estimated that more than one billion people are exposed to outdoor air pollution annually (UNEP 2007). Urban air pollution is linked to up to one million premature deaths and one million pre-natal deaths each year. Even if emission levels could be reduced in terms of fuel quality and emission reduction technologies, they won't fall under certain limits and will continue deteriorating the air we breathe. The development of technical solutions to reduce emission levels is one solution to improve urban air quality. The second solution is to develop adapted planning strategies in order to reduce human exposure to air pollution in the urban fabric. The present work focuses on the second solution and investigates the influence of vegetation on air pollution in built environments. In general, three effects of vegetation on air pollution can be distinguished. First, by emitting substances (e.g. hydrocarbons) vegetation adds pollutants to unnatural emissions. Second, vegetation can help to reduce pollutants by absorption into the plant's tissue or by removal on the plant's leaves or other surfaces. Third, by its physical presence plants modify the air flow and consequently the dispersion of pollutants. In the frame of this study we were focussing on the second and third effect, the removal and influence on the dispersion of pollutants. The removal of pollutants by plants was addressed in many studies leading to the conclusion that vegetation can help in reducing pollutants. As a consequence of this evidence, planning strategies generally favour increasing vegetation cover. The influence of vegetation cover on the air flow in general was extensively described in rural and above all forest areas where the slow down effect on wind speed was shown. However, this influence was few analysed in built environments.

The considered effects can be studied either by measurements or by modelling. In the present work, it is evaluated using computational modelling. Models are an abstraction of reality and help understanding complex processes such as atmospheric processes in the heterogeneous built pattern of urban areas. Furthermore, models provide the possibility to compare scenarios such as different vegetation configurations in the same built environment. Air quality models operate on different scales and the choice of a model implies the definition of an appropriate scale. In general, air quality models operate either on macro- or microscale. Macroscale models consider the whole of regional objects –a city for example. In contrast, microscale models simulate processes at the scale of single objects like buildings, streets, trees, etc. The latter was chosen for the present study as we were mainly interested in the processes happening at the interface plant-atmosphere in built environments. Aiming to find planning solutions to reduce human exposure, the focus is on the influence of vegetation on pollution concentration levels in the immediate surrounding of vegetation objects. The analysis is performed using the three-dimensional microclimate model ENVI-met (Bruse and Fleer 1998, Bruse 1999) that combines the simulation of plant induced processes with the microscale atmospheric processes in built environments.

Air pollution models need two kinds of input data: first, data on the objects present in the area and second, emission data and meteorological data to set up the frame of atmospheric processes. Microscale models, like the model used in this study, need precise object information, i.e. the object’s shape, height, location and material. Such information can be obtained from different sources. In urban areas official databases might provide enough information on the built environment. However, the possibility to obtain information on vegetation from these sources is rather limited. First, they comprise almost always only vegetation in public places. Second, they were built for a certain objective and may not provide the required detail of information, and third, the access to these databases is often restrained. In this context the present work aims to evaluate the possibility to obtain precise information on the whole urban vegetation cover from remotely sensed images. Besides the differentiation between herbaceous areas and trees/shrubs the objective was to extract tree species. We examine the potential to use hyperspectral image data. More precisely, we analyse a high spatial and spectral resolution image acquired with the Compact Airborne Spectrographic Imager (CASI) in September 2005 over the city of Strasbourg (France). Acquired in a high number of continuous and narrow spectral bands, hyperspectral images offer precise spectral object information. They are therefore especially interesting for applications on highly heterogeneous areas like cities. Till today, they have been little used for the analysis of urban vegetation cover. The advantageous high information content results in increased complexity of the data and restrains the application of methods developed for multispectral image data. Furthermore, the high number of spectral bands leads to increased spectral redundancy. Consequently, for the analysis of these data adapted methods are needed and in the present work methods for dimensionality reduction and consequent supervised classification are used. Besides different algorithms for feature extraction, we evaluate the potential to use the unsupervised classification algorithm developed by Blansché *et al.* (2006) for band selection in hyperspectral images.

The objective of this thesis was thus twofold. One objective was to evaluate the potential to extract plant species from remotely sensed hyperspectral images. The second objective was to evaluate the influence of vegetation on pollution concentrations in the built environment.

The work is divided into three parts. Part I deals with the theoretical framework of the present work. In the first chapter, the concept of sustainable development is quickly presented, focussing on the discussions about the sustainability of urban areas and political actions to improve the urban environment. In the second chapter, the ecosystem approach is adopted to present cities as urban ecosystems and argue the various functions of vegetation in the urban ecosystem. Part II of the work deals with the detection of urban vegetation using hyperspectral images. The analysis is performed on image extracts mainly covering the densely built city centre of Strasbourg. Part III focuses on the evaluation of the influence of vegetation on air quality. We focus on the effect of street trees on the removal and dispersion of pollution particles and their consequent concentrations at the height of the human respiratory tract. The simulations are performed for street canyons with different height-to-width ratios, varying inflow conditions and different vegetation configurations. At the example of a planning project recently realised in the city of Strasbourg we show the interest to use the applied model to evaluate the changes of air quality induced by modified vegetation cover.

As a major outcome of this study we encourage to improve actual planning practice in order to optimise the functions of urban vegetation and underline that plantings should not be based solely on aesthetic and design aspects. We underline that smaller vegetation objects such as street trees need more attention as their ecological function is not well considered by planning.

# PART I: THEORETICAL FRAMEWORK

# 1 SUSTAINABLE DEVELOPMENT AND URBAN AREAS

The concept of sustainable development is shortly presented in the following in order to build a general basis for the discussion performed in this work. Not all aspects stressed by the concept are presented and we mainly concentrate on the notion of the provision of a healthy and sustainable living environment with basic services for all that refers to the quality of life. At the end of this chapter, the link between the concept of sustainable development and urban vegetation is established by means of the concept of indicators.

## 1.1 Sustainable development

In 2005, the world population reached 6.5 billion people and the UN estimates an increase to nine billion people for 2050 (UN 2006). This population is in face of a deteriorating environmental situation mainly induced by human activities (MA 2005). In general, there is a widespread agreement on the contribution of human activities to environmental degradation and the continual release of varying assessment reports, international conventions, and agreements shows the importance of the subject (recently e.g. the publication of the Millennium Assessment Report in 2005, the new ratification of the Kyoto Protocol in 2006). Very recently, the release of the fourth assessment report of the Intergovernmental Panel on Climate Change (IPCC[1]) has given new drive to the discussion about the role of humans in climate change.

Humans started serious reflections on the future of life on earth and existential problems of the human being in the second half of the last century. One of the first studies about the situation and future scenarios was "The Limits of the Growth" of the Club of Rome published in the seventies (Meadows *et al.* 1972). In the late eighties the publication of the report of the United Nations World Commission on Environment and Development (WCED) "Our Common Future", also called Brundtland[2] report, introduced the concept of '*sustainable development*' in the discussions (WCED 1987). Approaching the environmental and development problems worldwide, the report emerged a new broad political vision that should become a leading concept for future development (Barth and Lang 2003). The following definition of sustainable development is the most cited:

***„Sustainable development is the development that meets the needs of the present without compromising the ability of future generations to meet their own needs." (WCED 1987, page 43).***

A number of definitions were set up since the adoption of the concept (Keiner 2005). Common to all definitions are three dimensions or pillars: economic, social development and environmental protection. The dimensions are interdependent and mutually reinforcing (DSD

---

[1] The IPCC was established by the World Meteorological Organization (WMO) and the United Nations Environment Programme (UNEP) recognizing the problem of potential global climate change. Former reports were published in 1990, 1995 and 2001.

[2] The Norwegian Gro Harlem Brundtland was the Chair of the World Commission on Environment and Development (WCED) convened by the UN in 1983.

2007). Figure 1.1 shows the three dimensions and their key elements. Accordingly, sustainable development means to continue economic growth to satisfy the needs of the worlds population, reduce the worldwide social and health disparities, while avoiding environmental degradation and provide a liveable environment to future generations (WCED 1987). In this context, we want to underline the formulated need for provision of a healthy and sustainable living environment with basic services for all.

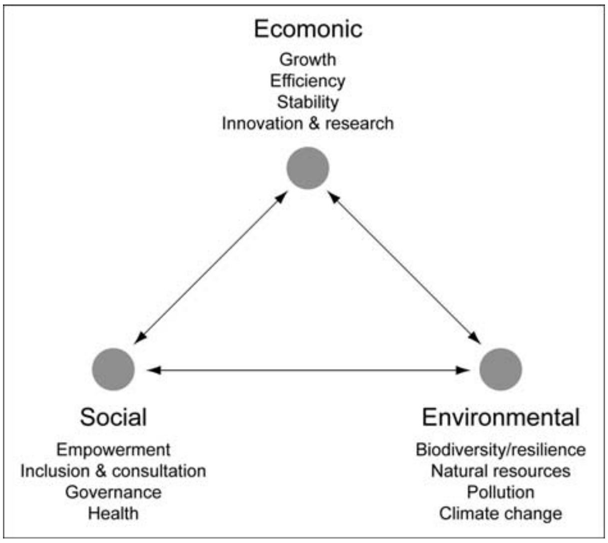


*Figure 1.1: The three key dimensions of sustainable development and the main subjects to be addressed in each dimension (Allemand 2006, IPCC 2007).*

The basic frame for the worldwide actions concerning sustainable development is set by the United Nations document Agenda 21 that was developed during the Earth Summit of the United Nations in Rio de Janeiro in 1992. By signing the document the nations commit to define actions at all levels of governance, from the national to the local level (Local Agenda 21) (UN 1992).

***Sustainable development to assure the quality of life?***

In the definition of the concept it is referred to the need of humans to meet their own needs. These needs concern above all a livable environment but comprise the well being of humans as well. The discussion on sustainable development implies the notion of the quality of life. In this sense, the aim of sustainable development is to provide a certain quality of life for every human being. The quality of life can be defined as the degree of goodness of the conditions of life and of the life of a person (Clark 1985, Glatzer and Zapf 1984). It may be interpreted as people's subjective feeling of satisfaction with their living conditions and life-style (Clark 1985). Nevertheless, the evaluation of the factors influencing the quality of life is subjective and may vary from one individual to another, from one society to another.

Consequently, the quality of life comprises also the quality of the natural and built environment that is particularly addressed in this study and we will come back later to these aspects.

***Measuring sustainable development***

Chapter 40 of the Agenda 21 asks to provide information about sustainable development through indicators. At the national and international level (governmental and non-governmental organizations) indicators should be set up and used to monitor the development (UN 1992). Indicators are means to measure the process of sustainable development comprising social, economic, and environmental (or ecological) aspects (OFD 2002).

Since then, a large number of indicators and indicator systems have been developed. With the platform Earthwatch[3] the United Nations provide an overview of indicators developed at international level. An Austrian platform[4] gives an overview of European indicators. Furthermore, the European Commission developed ten indicators for urban sustainable development. The International Council for Local Environmental Initiatives ICLEI developed the ecoBUDGET to help local governments or councils to manage and measure sustainability (ICLEI 2006). Actually, a plethora of indicators exist and research on the development of indicators is still ongoing.

## 1.2 Urban areas –a chance for sustainability?

### 1.2.1 Urbanisation and city growth

Special attention is paid to urban areas in the discussion on sustainable development. They concentrate not only half of the Earth's population, but also embody the environmental damage. In 2008, more than half of the worlds population, 3.3 billion people, will live in urban areas (UNFPA 2007). By 2030, this is expected to increase to almost 5 billion, meaning an increase of 11 % between 2005 and 2030 (see Figure 1.2).

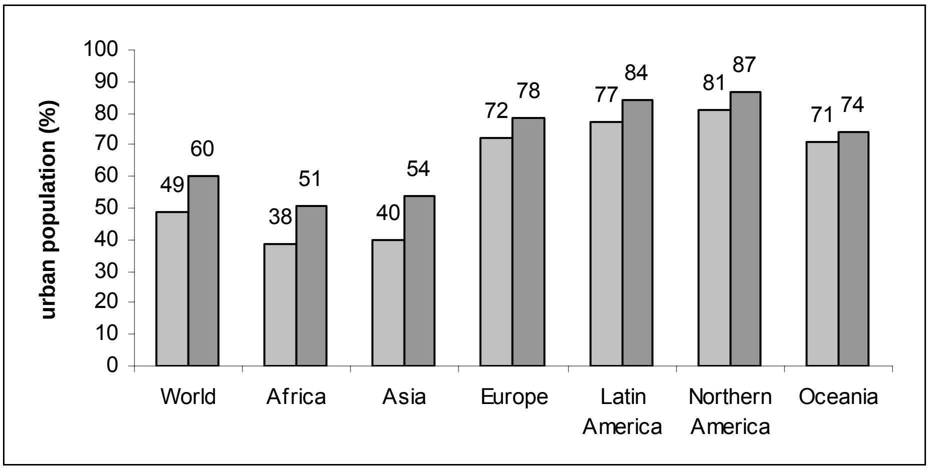


*Figure 1.2: Urban population as percentage of total population for 2005 (left column) and predicted for 2030 (right column) (medium variant) (UN 2006).*

[3] http: //earthwatch.unep.ch/indicators

[4] http://www.nachhaltigkeit.at

Urbanisation is not an industrialised-world phenomenon and regional rates of urbanisation widely vary (Figure 1.2). In high-income countries typically 70-80 % of the population is urban. Some developing country regions, such as parts of Asia, are still largely rural, while Latin America, by 2005 at 77 % urban, is distinguishable from high-income countries in this regard (MA 2005). According to the report of the UNFPA, the next few decades will see an unprecedented scale of urban growth in the developing world that will be particularly notable in Africa and Asia (see Figure 1.2) (UNFPA 2007). On both continents, the urban population will double between 2000 and 2030. Recent UN estimations prospected that towns and cities in the developing world made up 72 % of the world's urban population in 2005 and will swell to 85 % in 2030 (UN 2006). This ongoing trend shows that more and more people choose to live in cities, especially in the developing world, where the influx of rural populations into urban areas will continue. Cities are the heart of economic growth attracting people especially in developing countries (UNFPA 2007). Although they concentrate poverty they also represent the best hope of escaping it. The differences between the developing and developed world are not considered any further.

Besides this population concentration, cities concentrate also most of the environmental problems such as poor air quality, noise, water pollution, green house gas emission, great volumes of waste, etc. (Douglas 2002). Referring back to the concept of sustainable development, providing a healthy and sustainable living environment is both especially necessary and difficult.

### 1.2.2 A chance for sustainability?

Experts and policymakers increasingly recognise the potential of cities to long-term sustainability. Although they draw together many of the Earth's major environmental problems they paradoxically hold the best chance for sustainable future (UNFPA 2007). Cities embody the environmental damage, creating environmental problems but also containing the solutions. They concentrate half of the Earth's population on less than 3 % of its land area (UNFPA 2007). With the prospected population growth, demographic concentration gives sustainability better chances. The dispersion of population and economic activities would make problems worse rather than better. Environmental problems are not necessarily aggravated by urban concentration but rather by unsustainable patterns of production and consumption and to inadequate urban management. Urbanisation based on ecologically, economically and socially sound principles may be a solution. From a demographic point of view, dense settlements have greater capacity than rural areas to 'sustainably' absorb large populations. From the standpoint of biodiversity conservation and ecosystem management, maximally concentrating human activities may be a solution rather than a barrier to achieving sustainability.

Consequently, managing urban growth has become one of the most important challenges of the 21st century. Solving the problems of the city would make a major contribution to solving the most pressing global environmental problems (CEC 1996). Accordingly, approaches for the anticipation of urban growth, the managing, and catering for urban populations are needed.

### 1.2.3 Political action for a sustainable urban environment

Since the World Summit in Rio de Janeiro in 1992, many programmes, encouraging and promoting sustainable city development, were developed. The United Nations Agenda 21 that identifies local activities as being the root of most of the problems and also solutions is basic to many of them (UN 1992). Accordingly, local authorities are the level of governance closest to the people playing an important role for the promotion of sustainable development. They are invited to adopt a Local Agenda 21 in order to initiate special projects.

There exist a number of national and international programmes. The United Nations Human Settlements Programme UN-HABITAT, for example, was launched with the mission to promote socially and environmentally sustainable human settlements development with the goal of providing adequate shelter for all (UN 2007a). The URBAN Community Initiatives are an equivalent on the European level (URBAN I and URBAN II, see Table 1.1). The initiatives provide funding for neighbourhoods in extreme deprivation. Problems of isolation, poverty and exclusion are addressed through interventions that improve the ensemble of the physical and social environment (UN 2007b).

At European level, the need to intensify political action concerning the urban environment was already expressed at the end of the 1980 (see Table 1.1). This was even before the concept of sustainable development was adopted in the Treaty on European Union agreed at Maastricht in 1992. Consequently, the urban environment was first advocated in the Fourth Environment Action Programme EAP (1987-1992) (CEC 1990). The publication of the Green Paper on the Urban Environment and the constitution of the Expert Group on the Urban Environment followed. In the frame of the European Sustainable Cities Project, sustainable development of urban areas was first addressed. An important milestone of the European urban sustainable development process is the commitment of local authorities to establish Local Agenda 21 actions by signing the Aalborg Charter (1994). The number of signing local authorities increased. Today, more than 2000 local and regional authorities from 34 European countries have signed up the charter. Urban issues are still addressed in the last EAP running until 2012, and among the seven Thematic Strategies the sixth EAP seeks to develop one addresses especially urban issues (Table 1.1). The Strategy on the Urban Environment, adopted in January 2006, sets out measures to support and facilitate the adoption of integrated approaches to the management of the urban environment at all authority levels (CEC 2006). The aim is to support the process by facilitating the exchange of experiences, providing platforms, guidance, training, etc.

Table 1.1 is not exhaustive but the overview gives an impression how increasing awareness on the importance of urban environmental quality influenced political action in Europe. The cited programmes and actions induce initiatives on the national, regional and local level. To make a list of all of these actions would be a challenging task. The European framework programmes are not mentioned in this figure but one has to be mentioned in this context: the fifth Framework Programme (1998-2002). With this programme and especially within the fourth Key Action ‘City of Tomorrow and Cultural Heritage’[5] research on strategies for urban environmental quality was promoted. A number of research projects on urban sustainability were performed. Some are shortly presented in the following.

[5] Key Action within the thematic programme ‘Energy, Environment and Sustainable Development’.

*Table 1.1: Important programmes and documents reflecting the increasing relevance of urban environmental issues in the European Union (former European Community) actions (CEC 1990, 1991, 1996, 2001).*

| | |
|---|---|
| 1987-1992 | ***Fourth Environment Action Programme***<br>First expression of the need to intensify political action concerning the urban environment. |
| 1990 | ***Green Paper on the Urban Environment***<br>One of the major conclusions: The improvement of the urban environment contributes both to the quality of life and to the develoment of the urban economy. |
| 1991 | ***Expert Group on the Urban Environment***<br>Composed of national representatives and indepent experts. Should take forward the core ideas of the Green Paper. Constitues the first pillar of the European Sustainable Cities Project. |
| 1993 | ***European Sustainable Cities Project***<br>Was launched to promote urban sustainability across Europe. Aims to encourage the exchange of experience and dissemination of good local practice and seeks to influence policy at all levels.<br>Two pillars: 1) Expert Group on the Urban Environment<br>2) Sustainable Cities and Towns Campaign |
| 1994 | First ***Congress on Sustainable Cities and Towns*** in Aalborg (Denmark)<br>Marks the beginning of the ***Sustainable Cities and Towns Campaign***.<br>80 European local authorities signed the ***Aalborg Charter***. With signing the Charter they commited themselves to establish Local Agenda 21 processes and long-term local environmental action plans. A series of conferences followed (Lisbon, Por. 1996; Hannover, Ger. 2000; Aaalborg, Dan. 2004; Seville, Esp. 2007). |
| 1994-1999 | ***URBAN I Community Initiative of the European Commission***<br>Funding for urban districts in extreme deprivation to improve the physical and social environment. |
| 2000-2006 | ***URBAN II Community Initiative of the European Regional Development Fund***<br>(follow-up of URBAN I) |
| 2002-2012 | ***Sixth Environment Action Programme***<br>Requires the preparation of Thematic Strategies on seven different areas among them the ***Thematic Strategy on the Urban Environment.*** |
| 2006 | ***Thematic Strategy on the Urban Environment***<br>Adoption by the European Commission and setting out of cooperation measures and guidelines aimed at the Member States and the local authorities. It is a process parallel to the local Aalborg Commitments that are considered as a complement to the Strategy. |

## 1.3 Urban green and urban sustainability

Urban green is part of the urban environment and generally associated to the quality of life (Van Herzele and Wiedemann 2003, Bonaiuto *et al.* 2006a, CEC 2007). It is identified as a key for making cities more worth living. The role of urban green in the discussion on sustainable development is based on the approved ecological, economic, social and psychological benefits of vegetation in general. Most of them are considered in the next chapter.

The value of urban green for urban sustainable development is among others reflected in the indicators set up to evaluate the sustainable performance of a city. Commonly indicators of urban sustainable development comprise a measure for the provision and accessibility of green areas (OFD 2002, CEC 2007). The indicators of the Urban Audit of the European Commission for example include a criteria of green space accessibility and the walking distance to the next green urban area (CEC 2007). The portal 'Sustainable Urban Development Laboratory' (SUD-LAB) provides a tool to obtain a ranking of cities based on criteria such as the percentage of green area and the percentage of population with 15 min walk to a green space. However, indicators related to green spaces are only one or two out of a number of indicators.

The special interest in the role of urban green for sustainable development can be furthermore observed at the example of political actions that aim to encourage the valuing of urban green for city development in general. In this context a number of research projects on urban green were realised within the fifth European Framework Programme (1998-2002). They were all addressing the role of urban green for the quality of life namely 'Benefits of Urban Green Spaces' (BUGS), 'Greenspace', 'Rediscovering the urban realm and open spaces' (RUROS), 'Communicating Urban Growth and Green' (GREENSCOM) and 'Development of Urban Green Spaces to Improve the Quality of Life in Cities and Urban Regions' (URGE). They were brought together later in the so-called 'Greencluster'. BUGS, RUROS and Greenspace were mainly addressing ecological functions of urban green such as air quality, noise, biodiversity. 'Greenspace' combined aesthetical aspects with ecological functions. The URGE project elaborated an interdisciplinary catalogue of methods and measures to evaluate ecological, social, economical, and planning issues of urban green spaces. GREENSCOM focused on instruments and tools for planning practice and management of urban growth and green issues.

Furthermore, a number of COST Actions (European Cooperation in the Field of Scientific and Technical Research) addressed urban green. Examples are the COST Action C11 on 'Greenstructures and Urban Planning' created to exchange knowledge and experiences with urban development and green structures. The COST Action E12 'Urban Forests and Trees' gathered researchers on the whole of urban trees. Recently, the EC Community Initiative 'GreenKeys' was launched (Interreg III B CADSES). The list of research project is quite long and urban green and sustainable development is still a running subject that is addressed in numerous international and national projects and with this study we want to contribute to the discussion focussing on the functions of urban vegetation.

# 2 URBAN VEGETATION – AN ELEMENT OF THE URBAN ECOSYSTEM

This chapter discusses the role of vegetation[6] in the urban ecosystem. To analyse the different functions of urban vegetation, the ecosystem approach was adopted to consider cities as ecosystems. As we will show in the next paragraphs, considering (eco)systems in environmental sciences helps to understand nature[7]. Since many centuries humans try to describe complex natural processes and phenomena. At the beginning it was mainly driven by curiosity. Since the second half of the last century one main motivation originates from environmental problems. The human being is one of various organisms living worldwide. Organisms depend on each other as they depend on their non-living environment, the notion of ecosystems. Even if advances in technology help people to manipulate and to copy natural processes to build their own 'improved' world, we still depend on nature and especially intact nature (Douglas 2002). Men strongly modified nature, consequently real untouched nature only exists in some places in the world (mostly extremes of nature e.g. rainforest in some places, polar zone, deserts). Cities express to what extend nature can be modified: impervious surfaces, building structures, aligned and concreted watercourses, reduced vegetation cover. Like other organisms humans settle and build their own home. But humans went further on developing a world dominated by technical advances, facilitating life.

With this chapter we want to build a frame for the understanding and analysis of urban vegetation. First, we therefore adopt the ecosystem approach to argue secondly urban areas, their characteristics and functioning. Third, vegetation is argued as an element within this ecosystem exerting various functions induced by its interactions with the ecosystem elements.

## 2.1 The System and Ecosystem Approach

Since humans noticed the detrimental environmental situation, they try to understand the ecosystem functioning often motivated by the possibility to intervene and change situations in the positive sense. A system or more precisely an ecosystem view provides a valuable concept to enable us to better understand urban settlements. In the following paragraphs a short overview of the system approach is given. In the following, the application of systems for the description of ecological systems – ecosystems – is described to finally lead over to the urban ecosystem.

### 2.1.1 The system approach

In the 1940's the biologist Ludwig von Bertalanffy's introduced the system theory in his textbook entitled 'General System Theory'. He proposed to use the term 'system' describing those principles which are generally common to systems. Systems theory was furthered by William Ross Ashby in his textbook 'Introduction to cybernetics' in 1956. Cybernetics and systems theory are closely related and many concepts used by system scientists come from cybernetics. Cybernetics were first introduced by the mathematician Norbert Wiener and his

---

[6] The term 'vegetation' is used in the following to simplify but will be defined later.

[7] The word 'nature' is derived from the latin word 'nasci' that means to be born, emerge from itself without foreign action. Accordingly, as nature we consider all phenomena and processes emerging without the influence of humans.

book 'Cybernetics, or Control and Communication in the Animal and Machine' (1948). The word derives from the Greek word *kybernetes* and means steersman, governor, pilot, or rudder. Accordingly, cybernetics studies the control mechanisms in a system. It is the study of feedback and derived concepts such as communication and control in living organisms, machines and organisations (=system) through regulatory feedback.

System theory is applied in nearly all disciplines to 1) conceive, develop, create complex technical systems and 2) to study and explain natural systems in order to interact in different disciplines (e.g. agriculture, medicine, economy, politics) and to know the basic principles of (human) life (Le Gallou and Bouchon-Meunier 1992).

Central part of systems theory and cybernetics is the system that is defined as a collection of components that work together to perform a function (Le Gallou and Bouchon-Meunier 1992). The most simplified model of a system is presented in Figure 2.1. It shows a system with different elements linked by interactions as well as system inputs and outputs.

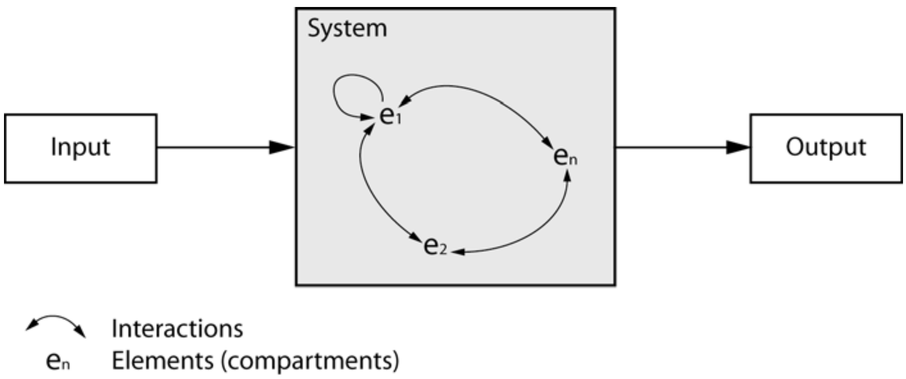


*Figure 2.1: Simplified system model (Le Gallou and Bouchon-Meunier 1992, Park 2001).*

A system is defined as a number of *elements* (or compartments, components) and the relationships between the elements. In natural science these elements are active because each element is influenced by elements of the same or another system resulting in a dynamic system. The coupling of active or functional elements results in relationships or *interactions* such as flows of energy, materials or information (Figure 2.1). While the sense of energy and material flows is determined (unique), information transfer between two elements happens either in only one or two directions (reciprocal). An element might also act on itself in the sense of auto-control (see Figure 2.1, element $e_1$). System relationships or flows characterise a system and its ability to adapt or adjust and the way how it interacts with other systems. System elements can be regulators as well as processes.

Systems can be defined at different scales what mainly depends on the purpose of a study (the observer) (Le Gallou and Bouchon-Meunier 1992).

The elements of a system might be considered as systems too, and each system itself might be a sub-system of a larger system and each has its own properties (Figure 2.2). A system element thus refers to a portion of the (larger) system and can be considered as sub-system that has its own specific properties. The structure of these coupled systems or system elements can be represented in a scheme depicting *organisation hierarchy* (Figure 2.2). The notion of hierarchy in system analysis is important. Hierarchy exists if at least two systems exist while one is imposed to another. At each hierarchical level a system might be linked to other systems of the same level (Figure 2.2). But hierarchy exists even between system elements constituting compartments that make a subsystem and finally several subsystems form a system (nesting hierarchy, Figure 2.2). It is a hierarchy where each level enriches that below it and cannot be reduced to it. Furthermore, the properties of a system cannot be explained on the basis of the individual parts alone (notion of *emergent properties*).

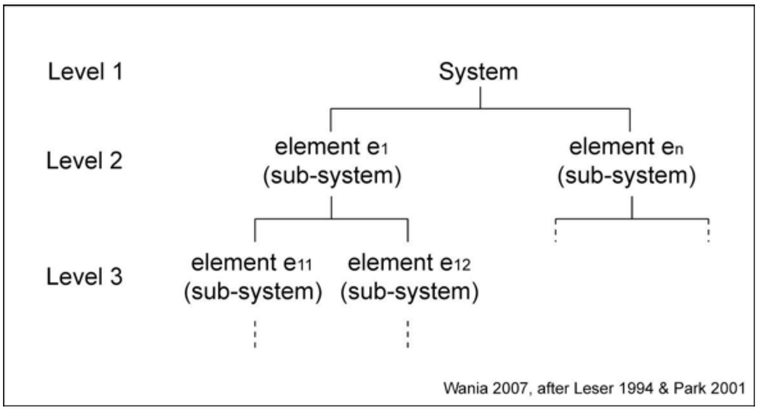


*Figure 2.2: Organisation hierarchy in systems. Each element in a system has specific properties and is a sub-division of the whole system (sub-system). A sub-system is composed of elements too that might each constitute another system again (nesting hierarchy).*

The *boundaries* of a system are defined such that they include all interacting system elements. The definition of boundaries depends on the aim of this study. Boundaries define the scale of systems and refer to the system type according to systems *inputs and outputs* (see Figure 2.3). There are three types: isolated, open and closed systems. *Isolated systems* have no exchange of energy and material across the boundaries and are quite rare in the natural world (only under controlled conditions). *Closed systems* that can exchange energy but not materials across the boundaries (e.g. the global water cycle) are more common in the environment. Finally, most environmental systems are *open systems* that exchange energy and materials across the system boundaries (e.g. drainage basin). Outputs from one open system can become inputs to another. The distinction between open and closed systems is sometimes a matter of scale (e.g. water cycle and an individual drainage basin).

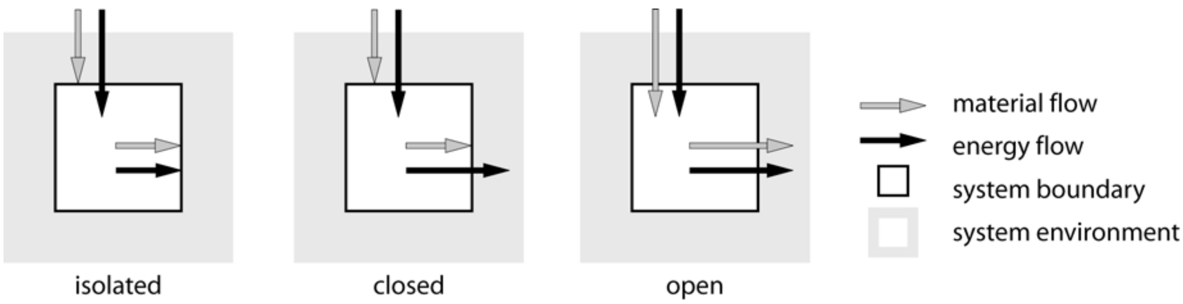


*Figure 2.3: The three system types (Park 2001).*

Ultimate goal of system analysis is to understand system behaviour and in our special context understand the behaviour of environmental systems. System analysis facilitates the study, description, interpretation and modelling of the environment where *processes* are of particular interest. Such processes might be purposive (i.e. to reach the system's goal) or processes tending to stabilise or destabilise the system. The way how a system reacts on disturbances characterises its *stability*. Complex systems show higher stability than simple systems. Due to the higher number of elements and accordingly higher number of interactions they can better adapt to changing conditions.

The definition of a system depends strongly on the type of system dealing with. Which system type is analysed is determined by the minimum entity of interest and strongly depends on the observer originating from different disciplines. Nowadays system theory is applied in nearly all scientific domains as for example in physiology, economy, sociology, physics and chemistry. Some examples for systems are computer systems, social systems, political systems or road systems. Systems can be defined at a variety of scales and even may overlap. The planet Earth for example is an integrated system with four main environmental systems namely the lithosphere, atmosphere, hydrosphere and biosphere (Odum 1959). Organisms or plants itself are systems and each consist in sub-systems.

Finally, systems can be modelled and simulated and depending on the aim of the study static or dynamic models can be applied (Le Gallou and Bouchon-Meunier 1992). Static models are used to learn about the behaviour of a system at rest (e.g. statistic models used to calculate the forces needed to keep an object at rest). Dynamic models are used to study the dynamics of a system, how their interactions of system elements change over time. Growth, decay, and oscillations are the fundamental patterns of dynamic systems. They are modelled by means of *system dynamics*. The field of system dynamics originates in the 1960s with the work of Jay Forrester who applied concepts from feedback control theory to the study of industrial systems (Forrester 1961).

As will be shown later system language is used to describe ecosystems mainly to quantify flows, in- and outputs but also to show the relationship between the system elements.

### 2.1.2 The ecosystem approach

Ecosystems are central to the hierarchy of ecological abstractions and are the fundamental block sof the biosphere (Hinckley 1976, Park 2001). They are the most important to understand the relations between plants and animals. The term introduced by A.G. Tensley in 1935, is the term used for systems in ecology. It is a contraction of the words *ecological* and *system*. Ecology is the English translation of *Ökologie* a term coined by the German biologist Ernst Haeckel at the end of the 19th century. Derived from the greek words *oikos* (household) and *logos* (study) ecology is the study of the household and especially the household of nature. To understand the 'nature's household' it is necessary to know the relationships and interdependencies between organisms and between organisms and their non-living, abiotic environment.

Tensley used the term ecosystem to define a unit that covers all living organisms of a given area (biocoenosis), the relations between them as well as to their inorganic environment (biotope). The organisms within an ecosystem form a biocoenosis; their inanimate environment is called a biotope. Thus, ecosystems consist in *biotic and abiotic elements* and the *relationships and interactions* between them. The most important abiotic elements are weather, climate, energy flows, the lithosphere and the water cycle. Ecosystems have no size definition, nevertheless elements and interactions exist in some defined area (Hinckley 1976). The definition strongly depends on the observed elements and interactions.

The main distinction within the *biotic elements* is between animals and plants and a hierarchical structure of organisms is based on the distinction between producers and consumers revealing one kind of the various relationships. If an organism is considered as producer or consumer depends strongly on feeding habits. The food chain differentiates between different hierarchical levels that designate where organisms get their energy. Energy is produced by food. Accordingly the following trophic levels are: producers (plants) => primary consumers (herbivores) => secondary consumers (carnivores) => tertiary consumers (scavengers, e.g. humans) (see Figure 2.4). Decomposers like bacteria, fungi and other micro-organisms link the biotic world to the abiotic world on the other side of the food chain by breaking down dead tissue from producers and consumers into its constituent elements that are important for the development of soils, an abiotic ecosystem element.

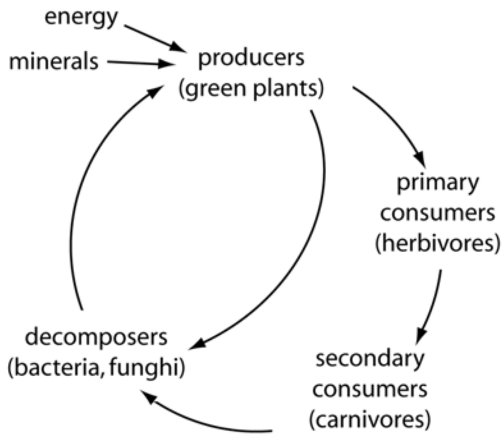


*Figure 2.4: Simplified model of material and energy flows in an ecosystem (after Odum 1959).*

*Flows* of *energy* stand behind this hierarchy of biotic elements. Energy plays a key role in all ecosystems because all phenomena are accompanied by energy transformations and many forms of energy are involved in different processes. Examples are the energy in photons of sunlight, in water waves, in magnetic fields, in chemicals and in water of rivers. Figure 2.4 shows the simplified energy flows between biotic elements in an ecosystem. Thermodynamic open systems are influenced by the flows in and out of the systems. According to the energy conservation law (first law of thermodynamics) the change in the internal energy of an open system is equal to the amount of energy added to the system by materials flowing in and by heating, minus the amount lost by material flowing out and in the form of work done by the system. The flows of energy and material cause that open systems might adopt a steady state far away from the thermodynamic equilibrium in contrast to closed systems, which quest towards the thermodynamic equilibrium (Sitte *et al.* 2002).

Further, *material* flows are another kind of flow existing in ecosystems (Odum 1959). Flows are generated by the active elements (see Figure 2.4) working together and making ecosystems *dynamic systems*. Accordingly flows of energy and material represent most of the relationships between elements. Main movements through ecosystems are energy flows and nutrients cycle, energy derived ultimately from solar radiation and nutrients from rock weathering, soil formation and biological decay. Energy consumption in ecosystems is inefficient with decreasing energy loss at higher trophic levels (Odum 1959). Energy can be used but not reused in contrast to material that can be recycled. The reuse of material is necessary as material supply is finite (e.g. water, carbon) and especially necessary for materials having few inflows. In contrast, the loss of energy is somehow compensated by the infinite energy supply (solar energy). Nutrients for example are used by the organisms, first taken up by plants they pass the trophic levels, are recycled by decomposers and finally released back to the cycle. Generally, these flows inside the ecosystem are strongly influenced by factors outside (e.g. rain drives a river ecosystem). Energy and material can be stored for various times before being released back into flows (e.g. water stored in vegetation).

The drive for ecosystem dynamic is assured by continuous throughput of energy and materials from outside the ecosystem *boundaries*. In turn energy and materials are output either back to the environment or to adjacent ecosystems. Due to this exchange of material and energy with the ecosystem environment, ecosystems are *open systems*. Both, inputs and outputs drive the system.

These cycles and flows can be interrupted leading to ecosystem imbalance. But each ecosystem has the tendency to maintain or return to its *equilibrium* by action and counteraction (*feedbacks*). Ecosystems are self-regulating interacting systems characterised by a steady-state equilibrium. It is an dynamic equilibrium defined by the persistence of short term variations around an unchanging average state. More precisely, equilibrium is given when the number of individuals (due to equal mortality and birth rates), ecological niches (constant environmental conditions), and the number of species (due to constant individual number and niches) remain more or less constant. Impacts from disturbances from the environment can be stabilised by ecosystem constraints and by the process of self-adjustment (homeostasis). The ability to recover depends strongly on the functioning of the biotic and abiotic factors and systems *resilience*. For each ecosystem there is a critical level of disturbance beyond which natural recovery is very difficult. Critical thresholds are rarely known as they become often apparent only when they have been reached or exceeded or irreparable damages and changes happened. In general, natural ecosystems have greater resilience than anthropogenic systems (agricultural ecosystem). Park (2001) distinguishes between three types of pressure: gradual changes (e.g. climate, sea level), disturbances (e.g. hurricanes, introduction of new elements) and natural periodicities (e.g. cycles of dry and wet seasons). While relationships between elements exist, changes on one element trigger changes to another (at least one). In general, changes in ecosystems are generally nonlinear, which produces considerable complexity in dynamics and potential for unpredictable change.

The presence of biotic elements in an ecosystem is closely related to its ability to survive. If changes affect the environment in such a manner, that the maximum and minimum limits of the optimal range of species abundance are exceeded, the species will die (see Figure 2.5). This *tolerance range* considers above all abiotic elements, for some species the presence of other species might be a determining factor too. *Limiting factors* in the abiotic environment are solar radiation, nutrient supply, water and temperature. If one of these elements is in short supply, species abundance is endangered (e.g. absence of vegetation in deserts due to missing water supply). The productivity of an ecosystem strongly depends on the availability of these factors.

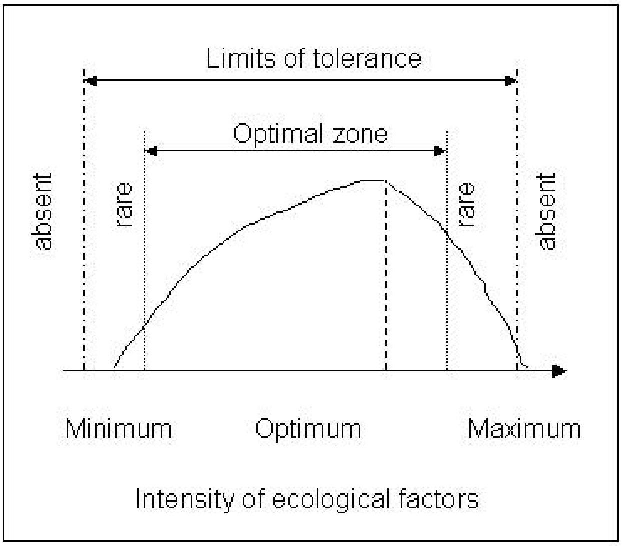


*Figure 2.5: Generalised scheme of species tolerance depending on the intensity of the ecological factor (Odum 1959).*

Systems are integrated functional units that can not be dissected. If so, they function improperly. Ecosystems or environmental systems of the earth are all interrelated and any action on one element (or ecosystem) might ultimately influence any other system in one way or another. Such a chain of reactions is the origin of most environmental problems that are rarely positive from the ecological point of view.

According to Tansley (1935) ecosystems can be of any size, as long as the concern is with the interaction of the organisms and their environment in a specified area. Further, boundaries are drawn to answer a particular question. Thus, the choice of scale and boundary defining any ecosystem depends upon the question asked and is the choice of the investigator. Typical examples for ecosystems are forest, lake, river and grassland ecosystems (Odum 1959). Another possibility is to refer to the degree of human influence on ecosystems and consequently differentiate between natural and anthropogenic ecosystems (Leser 1994). The examples cited above are accordingly natural ecosystems but a nearly untouched rain forest is much more natural than a forest in central Europe where forestry optimises wood production, introducing foreign, better resisting tree species. Another more extreme example are agricultural ecosystems with anthropogenic nutrient and water supply and selective species promotion and removal. But certainly one of the most extreme examples for anthropogenic ecosystems is the urban ecosystem. After the description of ecosystems in general, in the following the urban ecosystem will be described.

## 2.2 The urban ecosystem

The ecosystem approach was adopted by different disciplines in order to study cities or urban areas. Despite the same approach, each discipline has another interpretation and focuses on other system aspects. Urban ecology is a general term used to summarise research about cities based on the ecosystem approach. The science in the different disciplines has different origins and is used differently in Europe and America, or France and Germany for example. The different points of view of urban ecology are described in the following and one will be adopted to describe subsequently more specifically the urban ecosystem.

### 2.2.1 Approaches to urban ecology

In general, cities are the subject of research in many disciplines. Among them two claim an urban ecological approach. A first one is the approach applied in natural sciences, the second one the approach of the social sciences. Finally, another approach is shortly presented whose aim is the description of the urban system as a whole by means of system languages. It is another view on urban ecosystems increasingly considered in urban ecological studies that tries to quantify the throughputs of the system.

#### 2.2.1.1 Urban ecology in the natural sciences

Traditionally, urban ecology in natural sciences is based on the ecology established by Haeckel in the 19$^{th}$ century that is directed towards flora and fauna. Botanists were the first addressing attention to the ecology of cities and towns and consequently introduced urban ecology in Europe (Sukopp 1990). For a long time it was thought that urban areas are not worth studying with regard to ecology. Early investigations discovered that even on man-made sites, characteristic combinations of organisms could be found under similar conditions, and not just as coincidental co-habitats. In the 60s and 70s of the last century, a number of floristic studies have shown the considerable variety of sites, organisms and communities in European cities (Duvigneaud 1980, Sukopp 1998). Besides the purely botanical description first ecological considerations were made on the urban metabolism, i.e. the exchange and transformation of energy and matter (Wolman 1965, Duvigneaud 1980). Early investigations on urban vegetation and the environment were also performed in North-American cities (Kieran 1959).

With increasing awareness about the inadequate adaptation of human societies to their surroundings natural scientists from other disciplines were addressing themselves to cities. Pioneer work was about the urban climate established by Kratzer (Kratzer 1956), Landsberg (Landsberg 1970), and Oke (Oke 1980). Later on it was started to investigate soils (Blume 1998).

The ecology of the natural sciences is the basis for environmental discussion. The need of ecological evaluation of the relationship between human society and its environment, based on the evaluation of the living conditions, increased in the last decades. This is especially true for urban ecology as important relationships between Man and environment are pronounced in cities, and more and more people live in urban areas. Although the origins of urban ecology in natural sciences lie in biology, today, almost all natural sciences consider the urban environment.

#### 2.2.1.2 Urban ecology in the social sciences

Another approach of urban ecology was developed in the social sciences and mainly emerged from the work of the Chicago School founded by R. Park in the early 20$^{th}$ (Burgess 1925). The American scientists R. Park, E.W. Burgess, H. Hoyt, R.D. McKenzie, and others focused on the spatial organisation and the reasons of intra-urban differentiation of a city (Grafmeyer and Joseph 1979). Referring to the models in animal and plant ecology, this approach considers cities as a ‘super-organism’.

Theory of urban ecology in the social sciences is founded on three steps (Timms 1971, Lichtenberger 1998):

1) The setting up of spatial models by the Chicago School in the early 20th century. The work of the Chicago School issued in the setting up of different city models expressing the spatial organisation of the urban society. The three basic models are the model of zonal model of Burgess (1925), the sector model of Hoyt (1939), multiple nuclei model of Harris & Ullmann (1945). The models are based on information such as dominance of residences or working areas, type of working places (industry or business) and the dominant social class.

2) The development of the theory of social space (social area analysis) mainly introduced by Shevky & Bell in the 50s. The theory is based the concept of homogeneous units composing a city that are defined by specific economic, social, and cultural characteristics.

3) Factorial ecology mainly set up by Berry in the 60s in Chicago. It comprises the application of factor analysis to data describing the residential differentiation of the population (demographic, socio-economic, housing data). The differentiation of a city is consequently based on statistical units, i.e. *a priori* there exists no link with the physical structure of the city (Goheen 1970).

In the centre of interest of this urban ecology is the relationship between the society and the city. In contrast to the urban ecology of the natural sciences, social urban ecology as defined by Park and Burgess focuses on one sector that is sociology.

Finally, it has to be mentioned that out of the classical social ecology approach other lines of research emerged that include political, economic, and anthropological aspects (Hannerz 1983, Pickett *et al.* 2001).

#### 2.2.1.3 System analysis

A third approach to urban ecology should be mentioned here as it is an approach that considers the system as a whole. Although it is not considered as urban ecology as such, it was used to prospect the urban system by means of models. The idea of system analysis is to build models to describe and understand the urban system or ecosystem. In this context, only two examples will be mentioned but they are the most cited and to our opinion each of it concerns one out of the two traditional approaches to urban ecology.

The work of Odum H.T. in the 1970s is especially known for ecological models. Ecological models are often designed to improve our general understanding or to guide research efforts (Odum 1983). The radiation ecologist Howard T. Odum developed a general systems language known as Energy Systems Language based on the circuit language of electronics. In such budgetary approaches to urban ecosystem research the metabolism of an urban area is described to reveal dependencies and to quantify inputs and outputs. Ecological models mainly help understanding the interactions between the urban development and environmental change (Pickett *et al.* 2001). However, ecological models do not claim to make precise predictions as basic inputs in ecosystems are random and cannot be measured or quantified. An example for such a model of the urban system will be given later.

In the social sciences urban systems were first considered in the context of system theory. In his textbook ‘Urban Dynamics’ Forrester explained rapid urban population growth and subsequent decline that has been observed in North-American cities (Forrester 1969). He constructed a model to portray a city as a system of interacting industries, housing, and people. The approach of Forrester was finally used in the Limits of Growth (Meadows *et al.* 1972), a study on global prospects of growth in human population and industrial production that is known to be one of the milestones in the debate about future development of the human society. Others prospected the urban system as the whole of four sub-systems: systems of population, production (economic), housing, decisional system (politics), and a constructed biophysical system (Weber 1997).

#### 2.2.1.4 Conclusions and adoption of one approach

From the comparison of the described approaches we conclude that all have in common the systems approach. One might even say that the ecosystem approach is underlying but the approach in the social sciences is limited to humans and their interactions with the environment. In most cases other living organisms or the natural environment are not considered. The same, the natural sciences approach does not include social components in its ecosystem concept, although adapting the ecosystem concept to urban systems requires normally inclusion of human and social components. Main differences lie also in the definition of (eco)system. Figure 2.6 shows a comparison between the definition of a forest ecosystem as defined in natural sciences to that of a city as defined in the social sciences. Accordingly, besides the physical limit, social sciences define also time as a limit (Figure 2.6). The elements defined in the city ecosystem are above all the urban inhabitant. In the approach of Forrester (1969) housing and industry are further elements. Natural sciences consider more varying biotic and abiotic elements and especially the abiotic environmental elements the system is built on. The main difference here is that natural sciences describe the whole space, i.e. the surrounding air, underlying soil, etc. are considered as part of the ecosystem. Interactions happen between abiotic and biotic elements while in the city ecosystem interactions are generated finally only by the actions of humans.

| | Forest ecosystem | Urban system |
|---|---|---|
| **Boundaries** | physical limit | physical limit, time (24 hours) |
| **Elements** | animals, plants, soil, atmosphere, water | people, housing, industry |
| **Flows** | water, nutrients, heat, organic material, etc. | transport, information, goods, money, services, etc. |
| **Stocks** | soil, water bodies, wood, etc. | city area |

Wania 2007, after Odum (1959), Forrester (1969), Vicari (1981)

*Figure 2.6: Differences in the understanding of ecosystems in the natural and social sciences explained at the example of boundaries, elements, flows, and stocks. Comparison of the definition of a forest (eco)system (Odum 1959) with the urban system as viewed by the social sciences (Forrester 1969, Vicari 1981).*

There is increasing awareness that urban ecology needs both the ecology of the social and natural sciences (Pickett *et al.* 2001, Alberti and Marzluff 2004). All the more sustainable development asks simultaneously for ecological, social and economic sound development. Discussions on the quality of life touch both disciplines and environmental problems are no more only a task of natural sciences. Urban ecology in the sense of the natural sciences copes with the consequences of human activities that affect the environment. The tasks are to describe the effects, to look for solutions for problems or, and this is probably the most important task to prevent (further) damage. But ecological problems are also a social task as they touch the way of life of urban citizens. Finally, humans are the main drivers of urban ecological processes (social and environmental) as they influence themselves the ecosystem. Some conceptual models combine ecological and social processes to analyse the dynamic of the ecosystem as a whole (Pickett *et al.* 2001, Alberti and Marzluff 2004). To a certain degree the approach in system analysis integrates all elements and understands the ecosystem as a whole. However, the links between the biotic and abiotic elements are described and analysed by the natural and social sciences.

While at the time of their introduction the urban ecology of the natural and social sciences were two disciplines performed on two different continents (the first in Europe, the second in North-America), both are nowadays performed everywhere in the world (Wittig and Sukopp 1998). Nevertheless, in some countries like France urban ecology is still associated with the social sciences and urban ecological research in the sense of natural sciences is performed separately in each discipline and not labelled as such. In contrast, in Germany the pioneer botanical approach still dominates over the urban ecology of the other environmental sciences.

In the present work, the approach of urban ecology in natural sciences is generally adopted to characterise the habit of urban ecosystems. The urban ecosystem is understood as the unit that covers all living organisms of a given area, the relationships between them and their inorganic environment. This description aims to lead over to the ecosystem element vegetation and its interactions with the environment and other living organisms. However, for the understanding of the system as a whole it is important to include the human being. He is the main driving force of the system and shapes it more than just the physical environment.

## 2.2.2 Characteristics of urban ecosystems

### 2.2.2.1 Structure and metabolism

#### *2.2.2.1.1 Boundaries*

Urban ecosystems are those in which people live at high densities, or where the built areas cover a large proportion of the land surface (Pickett *et al.* 2001). For an ecological understanding of urban ecosystems it is impossible to give one definition based on precise density and population numbers as settled areas strongly vary in size, form and density. Not only the urban core area but also less densely built areas must be included because of reciprocal flows and influences between densely and sparsely settled areas. However, boundaries of urban ecosystems are set in the same way as boundaries of any other ecosystem. In the broadest sense urban ecosystems comprise the urban core as well as suburban areas and sparsely settled villages connected by commuting corridors or by utilities but also the hinterlands directly managed or affected by the energy and material from the core and suburbs. The term ‘hinterland’ is used here to refer to areas that are functionally connected to the city although they cannot be precisely defined in space.

#### *2.2.2.1.2 Elements*

Urban ecosystems are very complex with a structure similar to that of natural ecosystems but due to human activities it is not possible to describe it the same way as natural ecosystems. Main characteristic is that these ecosystems are based on initially natural ecosystems that were strongly modified to meet the requirements of the urban metabolism (Douglas 2002).

Figure 2.7 shows a simplified model of the urban ecosystem with three groups of main elements. Additionally to the nature borne biotic and abiotic elements, man made or technical elements are present in the ecosystem (Tomášek 1979, Leser 1994). Human beings are among the biotic elements and their activities induce many interactions that do not occur in other ecosystems. They create the technical elements like roads, buildings, and all types of infrastructure (Figure 2.7). As in natural ecosystems, the abiotic elements soil, atmosphere, water, and bedrock build the basis of the ecosystem.

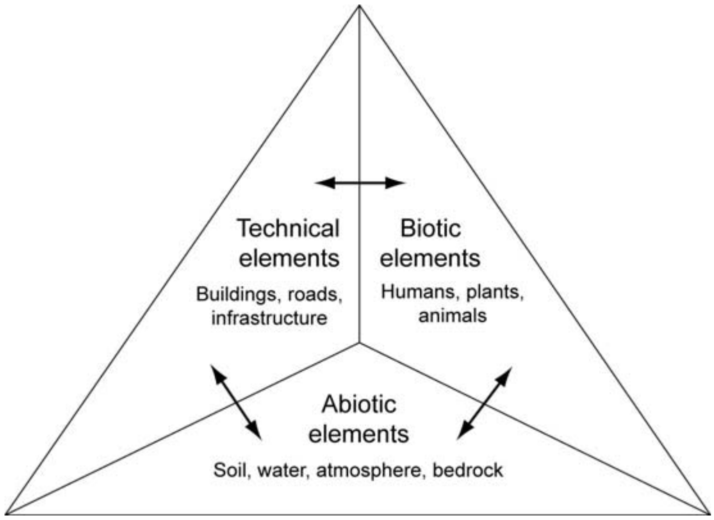


*Figure 2.7: Urban ecosystem model after Tomášek (1979). Like natural ecosystems urban ecosystems consist of biotic and abiotic elements but additionally technical or Man made elements are present. All elements are linked by interactions (arrows).*

Most of the ecosystem elements constitute a system on its own. Humans, plants, the soil, water bodies, the atmosphere constitute systems on their own. But also technical elements such as buildings and the road network might be considered as systems. Like any system the urban ecosystem consists in various sub-systems that each consist of sub-systems too. A single urban area itself is part of a larger system. Regarding economic or political action, a city can be part of a city system on a regional or even global scale. If an area is limited based on a watershed, a city constitutes an element inside this system.

#### *2.2.2.1.3 Metabolism*

Like organisms and other ecosystems the urban ecosystem consumes substances and energy (Odum 1983). Like other consumers, they have pulses, long periods, and major controlling actions, and their basis in the feedback loops to and from their support region. The exchange processes may be called the urban metabolism. The urban metabolism is presented in the following paragraphs focussing on the features induced by human activities. Explication of flows between other biotic elements and the abiotic elements are not detailed in the frame of this study.

***Flows***

Nowadays, the urban ecosystems as a whole is considered as an open system characterised by inflow and outflow of substances, energy and information between the system and its environment, causing key elements within the system to change continuously in response to these flows (feedback). Energy, natural resources, transportation, information and waste can be regarded as flows (CEC 1996). Additionally, flows exist between the biotic, abiotic as well as technical elements (e.g. buildings, infrastructure) and can be induced by the human being or based on natural processes.

As in the traditional ecosystem concept, flows are shaped by three main categories of ‘actors’: producers, consumers and regenerators. Producers create the substance and energy including outputs from farming forestry, animal husbandry and fishing in the hinterlands, mineral resources, solar and geothermal energy but also human knowledge and craftsmanship (Zhang *et al.* 2006a). Consumers are humans and enterprises but also plants and animals. However, there is a preponderance of the consumer, man, as well as little primary production and weak presence of decomposers (Sukopp and Werner 1983). Regenerators are mainly enterprises involved in waste recovery, disposal and utilisation. Further, the natural environment serves as a vital role in metabolic processes of the urban ecosystem (Zhang et al. 2006a) providing functions such as the modulation of the climate, the purification of the atmosphere or the prevention of soil erosion. Additionally, economic, political, and social conditions are system regulators maintaining the system functioning. Each of these regulators might constitute itself an independent subsystem.

***In- and Outputs***

Energy, water, food and other materials, which support human activity, are system inputs imported from outside the urban area (see Figure 2.8) (Park 2001). Further system inputs are people coming from outside into the considered city. The inputs are necessarily manufactured and used resulting among others in production of goods and different materials (food, chemical substances, material for technical installations, construction material, etc.) that either remain in the system or are exported back out to the hinterland. At the same, wastes, heat, sewage and air pollutants are 'produced' with some of them remaining in the system but most of them are considered as main system outputs (see Figure 2.8). The increased system inputs induce of course increased outputs and waste management is one of the main problems in urban ecosystems. Biological degradation in urban ecosystems is very low compared to the amount of waste produced and some substances must be artificially disposed and decomposed (Zhang *et al.* 2006a).

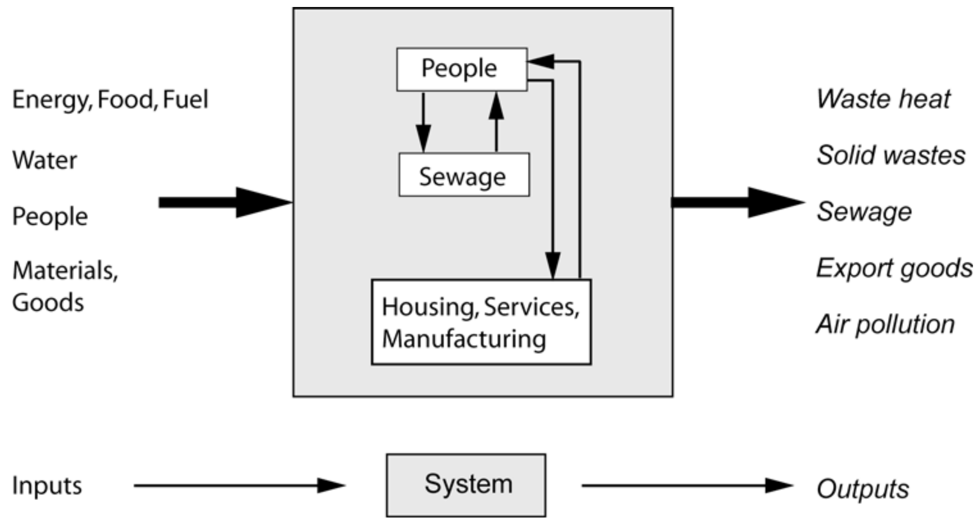


*Figure 2.8: The urban system and its main inputs and outputs (modified after Park 2001). Flows are not specified, they consist in energy, natural resources, transportation, information and waste.*

***Equilibrium***

The urban ecosystem is a self regulating system, exclusively driven by the human being. In contrast to natural ecosystems (e.g. forests, lakes), the steady state of the urban ecosystem is only maintained by permanent and high energy supply (Leser 1994, Douglas 2002). In traditional ecological terms the urban ecosystem is more unbalanced than other ecosystems

(Collins *et al.* 2000). While natural ecosystems mainly depend on solar radiation, urban ecosystems are an energy-intensive ecosystem and depend on supplementary energy sources such as wood, coal, gas and oil.

### *Footprint*

Intensity of human influence is linked with the ecosystem need of energy for self regulation (Leser 1994, Schulte 1995). Consequently, larger cities need more supply from the surrounding rural areas. The urban footprint is used to describe the perimeter of urban consumption (Hinckley 1976). The ecological footprint concept is based on the idea that for every item of material or energy consumption, a certain amount of land in one ore more ecosystem categories is required to provide the consumption-related resource flows and waste sinks (Rees 1997). Urban footprints spread beyond the immediate vicinity of cities and especially in urban ecosystems boundaries do not contain all the influences that are important for the ecosystem (Pickett *et al.* 1997). Rising incomes and consumption in urban areas lead to increasing pressure on natural resources, triggering land-use and land-cover changes in their zones of influence, sometimes over vast areas. This causes greater losses of habitat and ecosystem services than urban expansion itself (UNFPA 2007).

Cities depend on their hinterland (Hinckley 1976, Odum 1983). As a consequence, probability of damaging the surrounding environment increases with the city size and human influence intensity. Nevertheless, the couplings depend not only on natural factors like mass air exchange, groundwater flow and species migration but imply social as well as economic conditions (Adam 1985). Evidently, urban areas in developing countries do not have the same footprint as those in developed countries.

### *Modeling the urban metabolism*

Research is performed to quantify the urban metabolism in order to asses the consequential environmental effects of urbanization. Based on models the complexity of cities is related to ecological principles and energy flows. Producers, consumers, sources and sinks, driving functions, energy circuits and money flows are described employing techniques of energetic analysis (Odum 1983, Huang and Chen 2005, Zhang *et al.* 2006a, Huang *et al.* 2007).

Figure 2.9 shows such a quantification of the metabolism. It shows the components of a city and its main driving energy circuits (arrows). Among the different elements it shows the dependence of the city on a supporting region. The main consumers are people and the government. Natural ecosystems and agriculture provide main inputs like resources and food (producers). Industry is based on (re)sources (energy, material, water) and agriculture produces nutrition for humans but also material for industry. This kind of metabolism model helps to estimate the ecological footprint of urban ecosystems. Such a general model of a city is considered as a budgetary approach to ecosystems because it is used to quantify in- and outputs to a city region (Pickett *et al.* 2001).

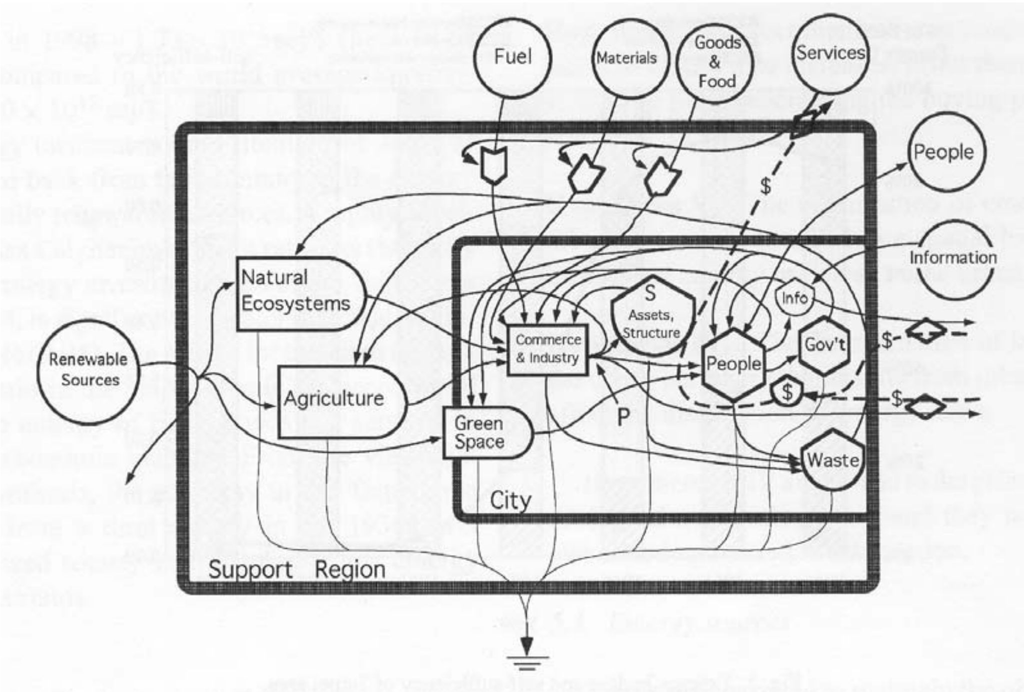


*Figure 2.9: Energy system diagram of a city and its support region (Huang and Chen 2005). For the language see Figure AC2-1 (Annex). Producers are the natural ecosystem, agriculture and green space. Fuel, materials, goods and food, services, people, information and renewable resources are considered as sources. People and the government (Gov't) are consumers. As energy tanks are considered waste, assets, and information. The arrows indicate the energy circuits between the elements.*

Such models combine ecological, social, and economic aspects. They are potentially useful to evaluate the sustainability of the urban system. However, the economic aspect dominates because all flows of in- and outputs are expressed to financial numbers. The cost of environmental damage is not explicitly considered.

***Concluding remarks***

The ecosystem concept emphasizes the city as a complex system characterized by continuous processes of change and development (Hinckley 1976, CEC 1996). It was shown that cities can be described as a complex, physical ecosystem in a similar way to wetlands or forests. Like organisms and other ecosystems the urban ecosystem consumes substances and energy and emits substances. Cities can be modelled in terms of flows of energy, nutrients, abiotic materials and the effects can be analysed on other physical ecosystems (such as the surrounding countryside). All interactions are greatly influenced by the structures humans have built and the energy they import but also their cultures, behaviours, social organisation and economy (Douglas 2002).

It is obvious that urban ecosystems are not yet well developed systems based on features such as their rapid growth, inefficient use of resources, very high energy supply and waste production (Zhang *et al.* 2006b). Understanding the city as an ecosystem and building system models helps understanding the functioning of urban ecosystems. Urban areas are a key element in global environmental change and nowadays, to consider cities as ecosystems is one of the running themes through literature on urban sustainability (Newman 1999). The urban metabolism leads to profound changes in natural processes and affects biotic ecosystem elements such as soil, water, plants, animals and the atmosphere (Rees 1997). After having focussed on the metabolism of the urban ecosystem and ecosystem features such as flows, equilibrium and in- and outputs, the features of the physical environment or the abiotic ecosystem elements are addressed in the following paragraph. Special focus is on the atmosphere.

#### 2.2.2.2 Physical environment

The urban ecosystem differs in many ways from non-urban ones. Urban ecosystems are some of the most profoundly altered ecosystems on the planet. Within their boundaries are found some of the most diverse ecological conditions. The modifications of the physical environment are profound and affect all abiotic elements. The human influence increases from the urban fringe to the centre (Sukopp 1990). Figure 2.10 shows an idealised cross-section of a large city and the main modifications of the elements atmosphere (referred to climate), soil, water, relief, as well as the two biotic elements plants (flora) and animals (fauna). In the following paragraph the modifications of the atmosphere, soil and water are described. In the frame of this study, we focus mainly on atmospheric phenomena and especially air pollution that are considered in Part III. A short paragraph considers the resources soil and water.

Main characteristics of the atmosphere over densely built urban area are air pollution, generally warmer air and reduced humidity (Figure 2.10). The urban roughness leads to air circulation reduction, as we will show later. Furthermore, surface sealing that increases surface water runoff, and the channelling of water courses lead to reduced ground water levels. Atmosphere, soils, and water bodies show generally higher pollution levels. Building activities modify the relief leading in general to a lowering of the original Earth surface. The original flora and fauna is changed or destroyed.

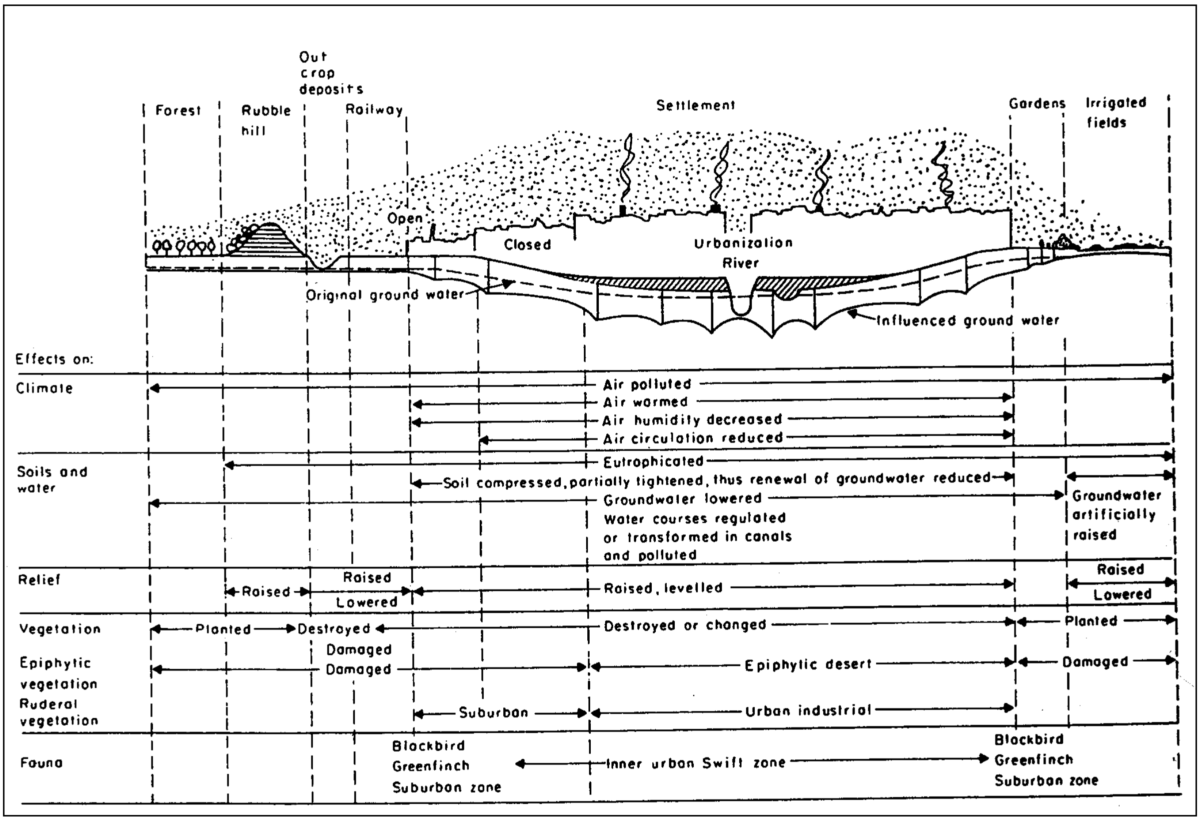


*Figure 2.10: Idealized cross-section of a large city with varying physical environment features (Sukopp 1990). Human influence is lower at the urban fringe than in the centre. The figure depicts some main characteristics of climate, soils and water, relief, vegetation, and fauna.*

#### *2.2.2.2.1 Soils and water*

Soils in urban areas are strongly modified by the human activity. They are sealed in and built over to a large extent (Blume 1998). In large German cities for example, more than half of the surfaces are sealed (Sukopp 2004). Soils in urban areas are restricted in their environmental functions[8] and urbanisation leads to soil degradation and the complete loss of soil function (Baize and Rossignol 1995, Blume 1998). They may vary from naturally developed soils with intact functions, disturbed and altered soils, that might have lost their environmental key role and totally artificial, mixed, technological prepared substrates. Often they are made of rubble or very sandy infertile soils dominate (Sukopp and Werner 1983). Large quantities of unnatural rubbish or anthropogenic admixtures often form a thick layer that can rise to as much as several meters thick increasing the distance to the ground water level. According to the characteristics of the upper soil layer Baize and Rossignol (1995) differentiate between transformed, artificial, and reconstituted soils ('anthroposol').

A major feature of urban soils is compaction, occuring due to pedestrians, riding, biking, vehicle traffic, parking, construction activities, wrong soil preparation techniques and maintenance (Sieghardt *et al.* 2005). Further, natural aggregation and structural formation is reduced due to lower frequency of wet-dry or freeze-thaw cycles, a consequence of the urban climate. Consequently, root systems in compacted soils are shallow and sparsely branched

---

[8] Soil are basis for the growth of organisms (root medium, supply of air, water, nutrients), play a major role in the hydrologic system and filter, buffer and eliminate pollutants that might affect organisms or contaminate ground water (Blume 1998).

and circulation of water and nutrients is changed with slower movement rates. Bad drainage negatively influences soil aeration.

The chemical composition is altered in urban soils (Blume 1998). In contrast to natural forest soils, urban soils tend to higher pH-values due to alkaline dust and waste, and organic fertilizers. In alkaline substrates, the plant availability of micronutrients is reduced because they remain insoluble (e.g. B, Zn, Fe, Mn, Cu) (Sieghardt *et al.* 2005). Urban soils lack organic matter mainly because nutrient containing-litter is generally removed during maintenance. The less natural the urban site the more it is characterised by nutrient deficiency and imbalances in the chemical composition occur (N, P, K, Mg are frequently lacking elements). Furthermore, urban soils are affected by atmospheric pollutants, or animal husbandry and agricultural production (herbicides, fertiliser), or even due to de-icers in winter. Additionally, leaking tubes and industrial sites increase concentration of pollutants such as heavy metals. Generally, the high pollutant load negatively affects the plants metabolism.

The hydrological features of urban soils are altered by soil compaction, increased surface sealing, higher amounts of coarse material, addition of technogene substrates. Consequences are reduced water infiltration rates, increased surface runoff and reduced evapotranspiration. On one hand, reduced groundwater formation leads to drought problems for plants. On the other hand, the increased storm water runoff leads to fluctuations of ground water level and consequently aeration problems. Water shortage in soils is also induced by the modified temperature balance and evapotranspiration due to building density.

#### *2.2.2.2.2 Atmosphere*

Urban areas are known to induce modifications of the climate compared to the non-built surrounding landscape. The urban geometry (size, shape, orientation of buildings and streets), the nature of urban surfaces (albedo, heat capacity, thermal conductivity, wetness) and the large inputs of materials and energy and the resulting solid, liquid, gaseous wastes lead to a specific urban climate differing from the original local conditions (Oke 1987, Kuttler 1998). Differences concern the urban atmosphere, the energy and radiation budgets, and air convection. Main responsible factors are (Kuttler 1998):

1) transformation of natural surfaces into areas mostly sealed by artificial material,

2) modifications of the biosphere mainly induced by reduction of vegetated areas, and

3) influences of technical installations such as thermal and hygienic modifications due to traffic, industry and trade as well as domestic fuel.

To understand the influence of an urban area on the atmosphere, we consider in the following first, the urban heat island and second, the urban boundary layer.

***Urban heat island***

Cities are usually warmer than surrounding rural areas as a consequence of the modification of energy and radiation fluxes and especially the increased sensible[9] heat flux (Oke 1987) (Figure 2.11). The climatic phenomenon induced by urban areas is known as the ‘urban heat island’. The cross-section of a typical urban heat island in Figure 2.11 shows a steep temperature gradient at the rural-urban boundary (Cliff) followed by a weaker but steady horizontal gradient of increasing temperature towards the city centre (Peak). The continuous temperature increase is interrupted by distinct ‘cooler’ land uses such as parks, lakes and open areas and ‘warmer’ land uses like industrial, commercial sites. The difference between the temperature in urban areas and the surrounding rural area might reach up to 4°C km $^{-1}$ (Oke 1987).

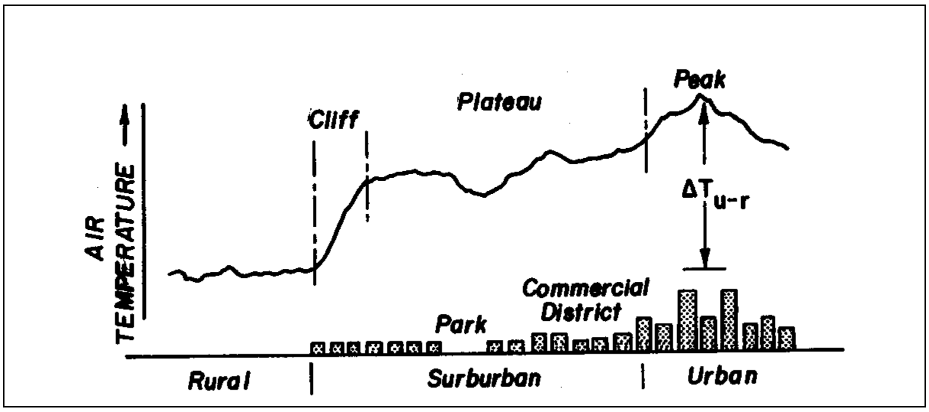


*Figure 2.11: The urban heat island: generalised cross-section from a rural to an urban area and related temperature difference ($\Delta T_{u-r}$ = difference between urban and rural temperature) (Oke 1987).*

The temperature differences between rural and urban areas are induced by modifications of the energy balance and several underlying features are distinguished (Table 2.1) (Oke 1987). The atmospheric exchange near the surface is first affected by the increased surface roughness induced by building structures. Increased surface area and reflection increase the absorption of short-wave radiation that modifies the initial radiation budget[10] (Table 2.1 A). It also leads to general wind speed reduction and consequently reduced heat transport (Table 2.1 G). Construction materials used in urban areas to built houses and streets modify the physical surface characteristics by influencing the reflection and absorption potential and heat capacity (increased thermal admittance, Table 2.1 E). On the one hand, the dense pattern of squares, buildings and streets increases the total area available for radiation and energy conversion (Table 2.1 C, E). On the other hand, surface sealing and compaction leads to reduced evapotranspiration and water retention (Table 2.1 F). The latter effect is even complemented by the heavily reduced vegetated areas that are the origin of cold, humid, fresh air (see below vegetation functions). The impact of technical installations is mainly due to combustion

[9] Sensible heat flux (direct) arises as a result of the difference in the temperatures of the surface and the air above (Arya 2001). The latent heat flux (indirect) is a result of evaporation, evapotranspiration, or condensation at the surface. In this case, heat is stored as water vapour, thus not sensible as heat.

[10] The net radiative flux is one out of four types of heat energy fluxes at the surface. During daytime it is dominated by solar radiation directed towards the surface, during night the flux is directed away from the surface. Solar radiation is confined to short wavelengths, terrestrial to long wavelengths.

processes and consequently heat production and pollutants emission. Main pollution sources are traffic, combustion and industry. Air pollution influences radiation by absorption and re-emission. Incoming solar radiation is reduced by gases and aerosols but at the same these air pollutants increase downward longwave radiation (Table 2.1 B). Anthropogenic heat released by motor vehicles, power plants, industrial processes and heating increases the radiative heating in urban areas (Table 2.1 D).

*Table 2.1: Hypothesised causes of the urban heat island (Oke 1987). Main factors are the geometric characteristics of the building constructions (canyon geometry), construction materials, and air pollution.*

| | **Altered energy balance terms leading to positive thermal anomaly** | **Features of urbanisation underlying energy balance changes** |
|---|---|---|
| A | Increased absorption of shortwave radiation | Canyon geometry – increased surface area and multiple reflection |
| B | Increased longwave radiation from the sky | Air pollution – greater absorption and re-emission |
| C | Decreased longwave radiation loss | Canyon geometry – reduction of sky view factor |
| D | Anthropogenic heat source | Building and traffic heat losses |
| E | Increased sensible heat storage | Construction materials – increased thermal admittance |
| F | Decreased evapotranspiration | Construction materials – increased ‘water-proofing’ |
| G | Decreased total turbulent heat transport | Canyon geometry – reduction of wind speed |

Even if the causes of urban heat island listed in Table 2.1 are hypothesised, they show the main modifications of the urban climate and their responsible factors. Their relative role is not yet certain and their importance changes over the day and with the seasons (Oke 1987).

Form and size of the urban heat island vary in time and space as a result of meteorological conditions, the location and urban characteristics. Heat island intensity varies through the day. The urban area warms up slower after sunrise and cools slower down after sunset (Oke 1987). The maximum intensity for a given city occurs in clear and calm conditions, a few hours after sunset (3 to 5 hours later). The intensity usually slightly declines through the night and is rapidly eroded after sunrise. Weather conditions induce modifications in this general profile.

The heat island intensity is also related to city size and population number. Oke (1987) related population number to the urban-rural temperature difference and stated that European large cities with 100.000 to 1.000.000 inhabitants the difference can reach up to 8°C. A much stronger correlation and apparently unique relationship is obtained between the maximum heat island intensity and the geometry of the street canyons in the city centre, as characterised by the average height-to-width ratio (H/W) (Oke 1987). Based on data from different North American, Australian, and European cities Oke (1987) defined a regression relationship that indicates that urban geometry exerts a fundamental control on the urban heat island.

Other features of the urban climate are generally reduced humidity, extreme winds with higher wind speeds (e.g. jet streams induced by deflection on buildings and inside street canyons), less snow (converted to rain), and cloud formation in the lee of a city (Oke 1987).

***Urban boundary layer***

The described phenomena modify the climatic characteristics of the Urban Boundary Layer (UBL). As UBL the portion of the Planetary Boundary Layer (PBL) above the urban canopy is considered. The urban heat island described above extents through the whole depth of the UBL but its intensity is maximum at the surface. Besides the urban heat island, the increased roughness that is induced mainly by the buildings modifies the UBL. The increased drag and turbulence results in a deeper zone of frictional influence within which wind speeds are reduced in comparison with those at the same height on a rural site (Oke 1987). The local slowing of the air flow causes it to pile-up over the city (i.e. it converges), and this is relieved by uplift. This induced vertical motion adds to that brought by the heat island effect.

Remember, that the maximum intensity occurs in clear and calm conditions and in this case the heat island induced thermal modifications of the boundary layer dominates over the roughness effects (Arya 2001). The thermally induced circulation leads to the formation of a 'dome' over the city like shown schematically in Figure 2.12. The circulation inside the dome is radially inward toward the city centre at lower levels and outward from the city centre at upper levels with a rising motion over the centre and subsidence over the surrounding areas. During the day this dome might reach the base of the lowest inversion. As the mixing of air is restricted to the layer below the inversion, smoke, dust, and haze from urban emissions accumulate during stagnant conditions (i.e. in case of temperature inversion). This is the reason why this phenomena is also termed 'dust dome'.

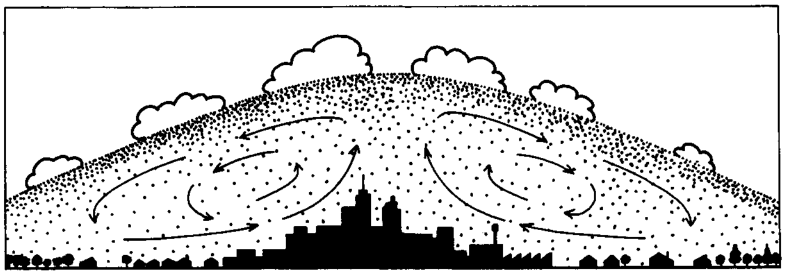

*Figure 2.12: Scheme of the dust dome and thermally induced circulations over a large city under calm wind conditions (Arya 2001). The circulation inside the dome is radially inward toward the city centre at lower levels and outward from the city centre at upper levels with a rising motion over the centre and subsidence over the surrounding areas.*

***Influence of the urban canopy on the flow near the surface***

The urban roughness leads to specific features of air flow near the surface. Buildings are the main objects in urban areas disturbing the approaching flow. Deflection occurs at building walls leading to wind speed reduction, deflection and formation of recirculation regions (Oke 1988). The flow field around a single building is characterised by three zones of disturbance (Figure 2.13): first, a small downward flow at the upwind ground-level corner of the building. Second, a lee or cavity eddy behind the building that is drawn into the low pressure zone due to the sharp edges of the building top and sides, and third, a building wake further downstream characterised by increased turbulence and lower horizontal wind speed.

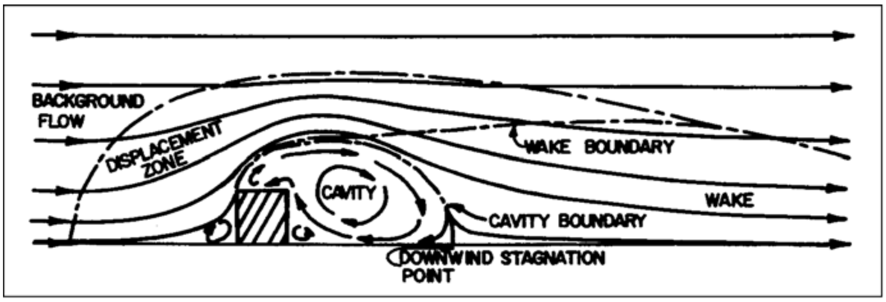


*Figure 2.13: Scheme of the main displacement, cavity, and wake flow zones around a two-dimensional building (Arya 2001).*

The complexity of the flow around buildings from a three-dimensional point of view is again more complex. Major features are schematically presented in Figure 2.14 and the description of all phenomena would go beyond the frame of this work. Nevertheless, some are considered in the frame of the air quality simulations in Part III. The scheme should simply give an idea of the complex flow patterns induced by buildings. We want to refer especially to the increased turbulence and formation of intermittent vortices occurring at the corners of buildings and the horseshoe vortex wrapping around any isolated building (Oke 1988, Ahmad *et al.* 2005). They are important features that influence the ventilation at this height. The wind profile on the left of Figure 2.14 shows how the wind is affected when the flow meets a building.

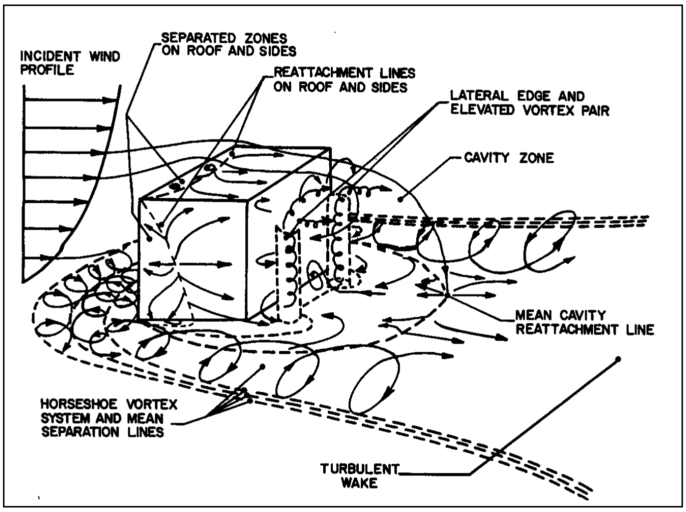


*Figure 2.14: Schematic representation of the complex of flows and vortex systems around a three-dimensional building (Arya 2001).*

In urban areas, buildings are placed in clusters of individual houses, high rise or flat buildings what makes the flow pattern more complex. When the spacing between two adjacent buildings is less than 10 to 20 building heights, which is generally the case in urban areas, the wakes and cavities described above interact (Arya 2001). All flow patterns strongly depend on building aspect ratios and the relative spacing between them, and they become more complex when buildings differ considerably in their heights and aspect ratios. The result is a variety of complicated and often discomforting flows.

However, the flows occurring at buildings and in streets are related to the flow characteristics in the boundary layer. More information on flow regimes near the surface in built environments can be found among others in Oke (1988) and Ahmad *et al.* (2005).

### *Air pollution*

Most of the mentioned atmospheric conditions and phenomena are relevant features for the higher air pollution levels, generally observed in urban areas. Higher air pollution is a result of both higher emissions and reduced capacity for atmospheric dispersal due to reduced wind speed and ventilation (Oke 1987).

After release, the dispersion of pollutants is controlled by atmospheric motion (wind and turbulence) on many scales. Near the surface, dispersion is affected by the complex flow patterns created by building structures. Narrow streets flanked by high rise buildings generally promote high pollution concentrations especially in the leeward canyon side (Figure 2.15). The vertical movement of air pollutants in the whole of the UBL is controlled by the prevailing stability conditions, and therefore the air stratification. Dispersion of pollution is suppressed in case of stable UBL and temperature inversion. The height of the PBL is generally referred to as the mixing height or depth, since it represents the depth trough which pollutants released near the surface are eventually mixed (Arya 2001). At mesoscale cities appear as large point sources with their plume extending many kilometres downwind (Oke 1987).

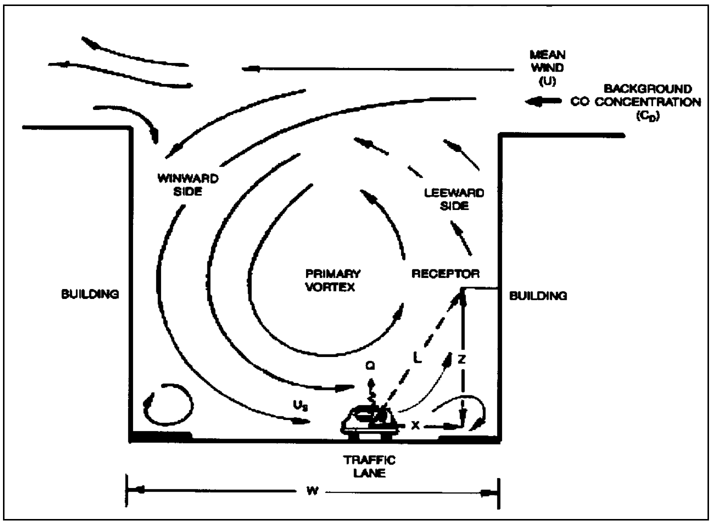


*Figure 2.15: Pollutant dispersion in a regular canyon (same building height as street width). The circulation inside canyons is generally reduced with higher pollution concentrations at the leeward side of the canyon and near the ground (Ahmad et al. 2005).*

The main atmospheric pollutants are sulphur compounds, carbon oxides (mono- and dioxide), hydrocarbons, nitrogen compounds and particles. All have natural origin but in urban areas the anthropogenic sources like combustion (burning of oil, coal, fuel) and industrial processing (iron foundaries, metal and brick work, etc.) hold the main portion (Oke 1987, Seinfeld and Pandis 2006). Besides these major air pollutants minor pollutants are released in small quantities, or are restricted to small areas, but they may be significant (toluene, hydrogen fluoride, ammonia, radioactive substances) (Oke 1987). Furthermore, secondary pollutants are created by chemical reactions between two or more pollutants, or between pollutants and natural atmospheric constituents. The most notable examples are the products of photochemical chain reactions, such as ozone ($O_3$), peroxyacetyl nitrate (PAN), and aldehydes. Pollutants might also be released by industrial accidents (Fenger 1999).

Traffic holds a relative high proportion in the emission of urban air pollutants (Stanners and Bourdeau 1995, Fenger 1999). Stanners and Bourdeau (1995) showed that more than half of the carbon monoxide, lead, nitrogen dioxide emissions and up to a half of all total suspended particles in urban areas are induced by traffic. The influence of traffic can be observed on profiles of pollution concentrations. Figure 2.16 shows the example for mean daily $PM_{10}$ concentrations (particulate matter with a diameter < 10µm) measured at three different stations in the city of Strasbourg. The profiles show typically two peaks referring to the morning and afternoon rush hours. The station close to a main road (green) shows higher concentrations than the station in the city centre that is situated in a traffic-free zone (blue).

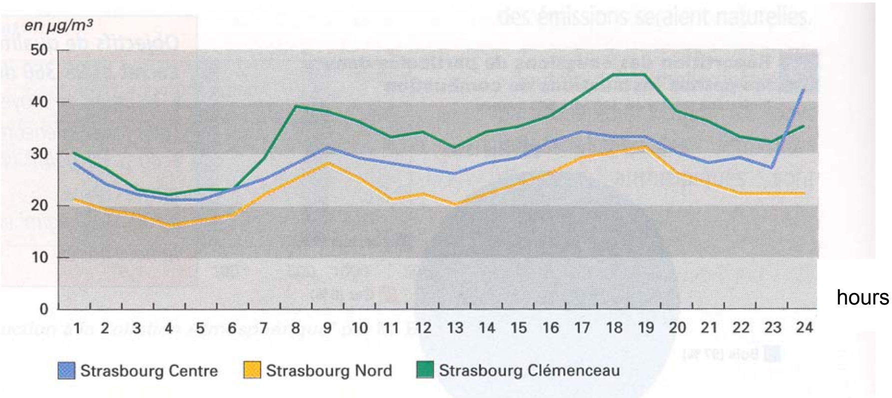


*Figure 2.16: Mean daily $PM_{10}$ concentrations measured in the city centre (blue), in a suburban site (yellow) and in a street with high traffic load (green) (DRIRE 2000).*

Another important phenomenon is smog. Smog occurs typically in urban areas and is induced by the atmospheric transformation of different oxides. Described are sulphurous smogs (London-type) due to transformation oxides of sulphur and of oxides of nitrogen and hydrocarbons which are involved in the production of photochemical smog (Los Angeles-type) (Oke 1987).

For further readings on the characteristics and chemical transformations of air pollutants and associated phenomena it is referred to Oke (1087) and Seinfeld and Pandis (2006).

### 2.2.3 Conclusions

Within this chapter, the ecosystem approach as applied by nature sciences was adopted on urban areas and the main characteristics of the urban ecosystem were presented. Main features of the urban metabolism were shown and the resulting environmental features presented. Consider cities as ecosystems underlines the impact of the ecosystem element human on the other elements that are initially natural. In the following paragraph, we want to focus on the element vegetation, its interactions and ecosystem functions.

## 2.3 The ecosystem element vegetation

Since now the ecosystem as a whole was considered. The following two paragraphs focus on the role of vegetation in the urban ecosystem. In a first step we will define the different features of urban vegetation that was used up to now as a general term but depending on the observing person or study aim each has another definition of 'urban vegetation'. In the second part, the interactions of the element are argued inside the ecosystem.

### 2.3.1 Definitions and terms

Vegetation is defined in different ways depending mainly on the observing person. It was shown that since the beginning of the last century vegetation in urban areas was intensively studied by botanists. Botanists are interested in traits of single plants or plant communities that express among others habitat conditions in urban areas (Figure 2.17). Planning considers vegetation in the form of single or multiple land use or land cover types (Figure 2.17). In the following, terms usually used by botanists and planners are defined and it is explained how each is used in the context of urban vegetation.

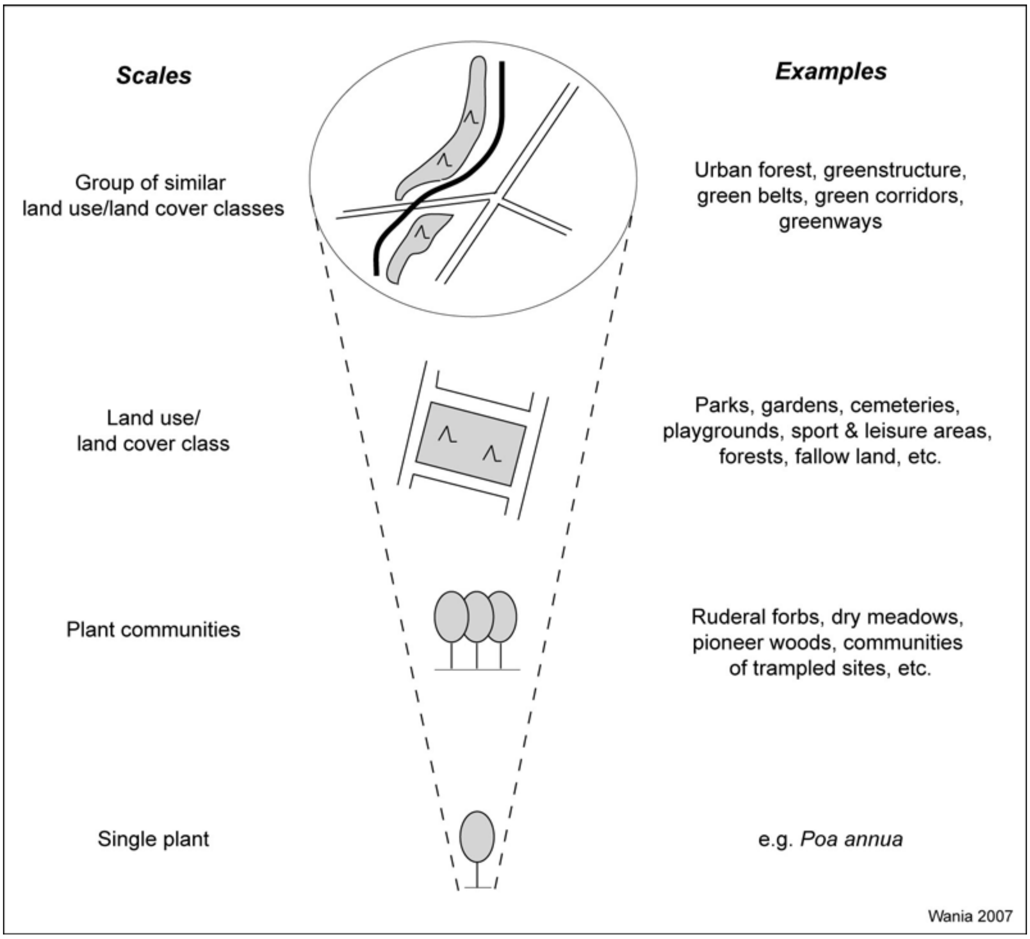


*Figure 2.17: Scales of urban vegetation. Left, common terms used by the observer (botanist, planner) and right, examples for each scale.*

#### 2.3.1.1 Botanic terms

Since the beginning the term '***vegetation***' is intentionally used as a general term. By definition vegetation is the community of plants occurring at a particular site. It is the general term for plant life of a region and does not imply anything regarding species composition, life forms, structure, spatial extent or any other specific botanical or geographic characteristics (Wittig 1998). Potentially, vegetation occupies all areas with adequate growth conditions (Sitte *et al.* 2002). The latter are determined by the conditions of the surrounding air and soil. In urban ecosystems the growth conditions are strongly modified by human activities and with increasing human influence Men may become the most important habitat factor (Wittig 1996). Without human activities central Europe would be entirely covered with plants (Sitte *et al.* 2002). Historically, cities have fought nature back to create a cultural, artificial environment as opposed to the more natural environment prevailing outside (Sukopp 2004). Nowadays, cities usually consist of a mixture of densely built areas with vegetation remnants of agro-ecosystems and even near-natural areas in urban forests, parks, and nature reserves.

To characterise urban vegetation the physiological and ecological characteristics of occurring species are analysed. It is the study of the urban ***flora***[11] a term used to designate the whole of species occurring usually in urban areas (Wittig 1996). By definition, the urban flora includes all types of spontaneous and planted species which can be found in cities. *Spontaneous flora* comprises all plants and plant communities 'naturally' occurring in some location. These are either wild plants or run wild cultivars and include all main plant groups such as algae, mushrooms, lichens, moss, fern and flowering plants (trees, shrubs and herbs). *Planted flora* concerns all intentionally planted species with preceding species selection and comprise above all flowering plants (trees, shrubs, herbs). Flowering plants seem to be the most adapted to ecological conditions in urban areas as they are the only systematic group showing a higher species number per square kilometre in the urban core than in the outskirts (Wittig 1998). Main reasons are better water balance and higher adaptability.

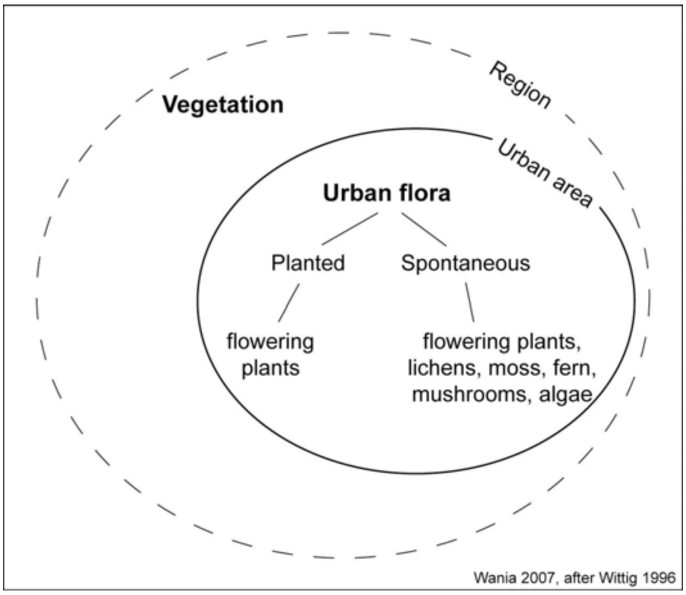


*Figure 2.18: Relation between vegetation and urban flora. Vegetation is the term used to describe all plants occurring in a region, e.g. the vegetation of central Europe. Urban flora is the term used for the whole of plants occurring usually within urban areas. Accordingly, the urban flora of central European cities differs from those of south European cities but both have typical urban features in common.*

Planted species are above all street and park trees, shrubs, wall climbing plants, herbaceous ornamental plants and cultivars in flower beds, on balconies, in gardens and front gardens (Wittig 1998). 60-70% of the urban green is planted vegetation (Gilbert 1989). Plants selection is mainly influenced by aesthetic values, functional aspects, aspects concerning costs of propagation, production, establishment, management and the adaptability to the environmental site conditions (notably the high stress level) (Tello *et al.* 2005). Aspects of biodiversity are rather seldom considered.

---

[11] Flora is the term designating the whole of species occurring in an area or biotope type (Wittig 1998). In contrast to vegetation the term necessitates the indication of an area, a biotope type or period, e.g. the flora of central Europe, of the alps, of the eutrophic lakes, tertiary flora etc.).

#### 2.3.1.2 Terms used in planning

***Land use/land cover***

The terms ‘vegetation’ or ‘flora’ are not used in urban planning to designate vegetation. Urban planning considers an urban area as a mosaic of different land uses and land covers. The object’s function is crucial in planning. Botanists and plant ecologists divide space into plant communities or analyse the city as a huge habitat and they do not account for vegetation free surfaces.

The most common terms used are ‘*green space*’, ‘*green areas*’ and ‘*urban green*’. The term ‘*urban green*’ resumes the whole of ‘green and open areas’ (Richter 1981, Klaffke 1995, Gauthiez 2003). The German dictionary of planning defines ‘green and open areas’ (Grün- und Freiflächen) as surfaces situated in settled areas, in general dominated by vegetation and used for leisure, recreation and nature experience (Klaffke 1995). ‘Green’ advances the vegetation aspect while ‘open’ underlines the land use aspect. *Open spaces* do not necessary refer to vegetation cover and can be considered as the general term including green spaces. Then, green spaces are open spaces but not every open space is a green space. The common French term is ‘espace vert’ (it is the translation of green space). It is defined as an open space dominated by green and designated to recreation, sport, games and visual amenities (Gauthiez 2003). Green and open areas can be public or private properties and are differentiated by their function, their ecological value and their belonging to other land use types (Klaffke 1995, Werquin *et al.* 2005). The most important types are:

- gardens (private balconies, terraces, front or back gardens, allotment gardens),
- ‘city green’ (private and public green and open areas, backyards, streets, squares, green corridors, fallow land),
- parks (private and public gardens, landscape parks, municipal parks),
- cemeteries,
- fragments of natural landscapes (flood planes, urban forests and woodlands, mostly non-built areas within the city area),
- nature protection areas,
- green and open areas with special functions (private or public playgrounds, sport and leisure areas, green areas in traffic infrastructure, zoos, botanical gardens, school gardens, green and open areas of public institutions).

Planning considers vegetation as a land use category. Consequently, very small areas (like balconies, terraces, front or back gardens) are assigned to the surrounding land use class that define in most cases built-up land use classes. Table 2.2 shows the urban open and green spaces defined for the city of Berlin. They are based on the analysis of aerial photographs and maps of the scale 1 : 5000.

*Table 2.2: Categories of green and open spaces identified in the Berlin Environmental Atlas (SDUD 2007).*

| Class | Description |
|---|---|
| Forest | all wooded areas of the Berlin forests, as well as those wooded stands outside the Berlin forests which appear clearly in aerial photography as self-contained forest stands. The forests include reforested former sewage farms |
| Bodies of water | all natural bodies of water - rivers, lakes, ponds - and also canals and reservoirs |
| Farmland | areas identified as being used for agricultural purposes,. difference from "Meadows and Pastures": the land is periodically sown, fertilized and harvested |
| Parks and green spaces | facilities and other city squares with a sealing level of less than 30%, and median strips used as green spaces; furthermore, playgrounds, the Botanical Garden, Zoos, public gardens, green spaces around public facilities such as hospitals |
| City squares and promenades | Serve as places of leisure for free time and recreation, as places of assembly, markets, etc.; in contrast to green spaces high degree of sealing, 30% or more; promenades also include median strips with sealing levels of over 30%, unless they are used as parking lots |
| Cemeteries | areas used for burial purposes |
| Allotment gardens | allotment garden colonies, which record the allotment gardens as defined by the Federal Allotment Garden Law, which are used as such and are on leased land |
| Vacant areas | currently not used or cared for, on which variegated stands of vegetation can develop; sand beaches and other non-vegetation-filled areas; furthermore, artificial rain catchments, ditches, landfills and wet areas are assigned to this category |
| Campgrounds | areas used for occasional residence in mobile shelters, such as tents, trailers and campers; include both tent camps and permanent campgrounds |
| Sports facilities/outdoor swimming pools | in addition to sports facilities, swimming pools and beaches, riding facilities and water sports areas; water sports areas are characterized by small dockyards, boat-hangars, club houses, parking lots, etc. |
| Tree nursery/horticulture | gardening schools, and the planting fields of private tree nurseries and market gardens, except for those areas marked as having solely greenhouse cultivation. |

### *Other terms (selection)*

Besides the official land use/land cover classes a number of more general terms are used in the context of urban vegetation. They are above all used to summarize land use/land cover classes that are dominated by vegetation cover or open spaces in general. The most common terms are green structure, green infrastructure, greenways, urban forest, green belts, green corridors, green keys. Most concepts are based on the idea to connect remnants of patches to form a network of green spaces and to connect this network to the surrounding countryside. Central to all are the objectives to conserve an ecological sound environment, promote the migration of animals and plants but also to provide recreational opportunities (Bryant 2006, Von Haaren and Reich 2006). The urban forest concept was created to provide and integrated planning concept for the whole of urban trees. These concepts are a result of the increasing interest to built networks of urban green spaces rather than to consider individual urban green elements. They offer an integrated perspective to green space planning and management. In the following, the most common concepts are briefly summarised.

The terms ***green structure, green infrastructure, green ways, green belts and green corridors*** are used often in the same line in the frame of concepts that aim to create a framework of green and open spaces. Considered are all natural, semi-natural, and artificial networks of multifunctional ecological systems within, around, and between urban areas, at all spatial scales (Tzoulas *et al.* 2007). Underlying idea of green structure/infrastructure is to consider green aspects of planning as a physical structure forming an integral part of the city and connecting the urban area to the surrounding countryside (Werquin *et al.* 2005). The concept promotes a physical green infrastructure playing a role in water management, the urban microclimate and air quality and biodiversity, and also a social infrastructure for leisure, recreation, human interaction and other social activities. It was introduced to upgrade urban green space systems as a coherent planning entity (Tzoulas *et al.* 2007). The concept of green structures/infrastructures is already established in some parts of Europe although it is not formally approved (Meeus 2000, Sandström 2002, Tjallingii 2002). The concept of green infrastructure refers much more to the functioning of green structure, which provides various services in line with other types of urban infrastructure (Walmsley 1995, Sandström *et al.* 2006a).

Werquin *et al.* (2005) defined green structure as being more than the sum of green spaces; rather it describes a network of 'green' elements. They define three layers of urban green structure. First, the basic layer goes back to the pre-urban landscape. A second layer has its origin in the development of an infrastructure network (mainly traffic). And the third layer results from deliberately creating parks, gardens, and playgrounds as a part of the urban occupation. Greenways, green belts and green corridors can be considered as elements in the network. Greenways are natural linear open spaces (corridors) set aside to connect larger areas of open space (Bryant 2006, Frischenbruder and Pellegrino 2006, Von Haaren and Reich 2006). Research on greenways was addressed in two volumes of the journal Landscape and Urban Planning[12]. A number of research studies illustrated the role of greenways in various contexts such as maintenance of biodiversity (Angold *et al.* 2006, Bryant 2006) and promotion of social and recreational cohesion (Shafer *et al.* 2000). In Germany the term "Grünzüge" (multifunctional greenways) is used as an official planning category which is mainly used at the regional level and where land uses that affect the original function are forbidden (Von Haaren and Reich 2006). Some cities already picked up the idea of green infrastructures plans. The city of Strasbourg for example initiated the conception of the 'Plan Vert' (green plan) to connect the fragments of urban green by so called 'coulées vertes' (green streams) but also blue streams 'coulées bleues' (ADEUS 1996).

***Urban forest*** is the term used for the whole of urban trees. The urban forest embraces all trees in stands and groups as well as single trees in and around urban areas and originates from the whish for more integrated concepts for the planning and management of vegetation in urban areas (Randrup *et al.* 2005). While the concept of urban forestry was already introduced in North America in the 1960s (Jorgensen 1970), it was introduced in Europe only in the 1980s (Johnston 1997a, 1997b, Konijnendijk 2003). The establishment of the concept in Europe was mainly pushed by the work done in the frame of COST Action C12 Urban Forests and Trees, a network of European greenspace researchers and the publishing of the book 'Urban forests and trees' (Konijnendijk *et al.* 2005).

[12] 1995 Vol. 33 Issues 1-3 and 2006 Vol. 76

#### 2.3.1.3 Concluding remarks

It was shown that urban vegetation is considered in different ways and while botanists focus on the scale of one single plant that forms plant communities, planning considers a limited area mainly covered by vegetation to determine classes of land use or green space. Spontaneous flora occurs every where plants can grow, even between paving stones (Figure 2.19a). However, most of the vegetated area in urban areas can be considered as planted and maintained vegetation. Figure 2.19 shows some examples of urban vegetation observed in the city of Strasbourg.

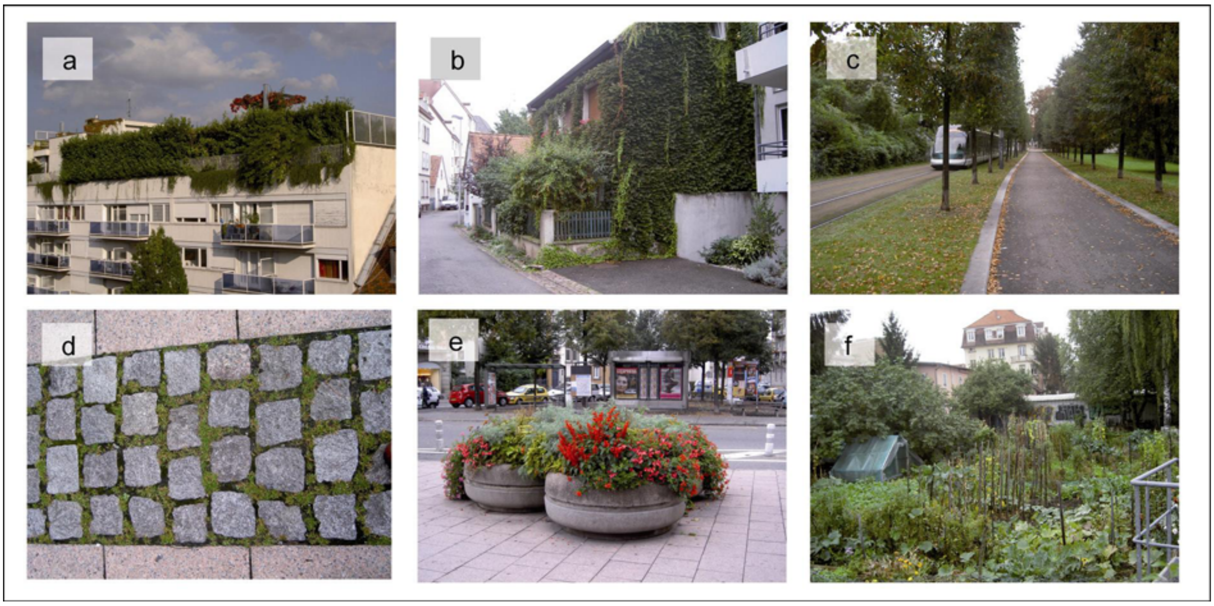


*Figure 2.19: Examples for urban vegetation in the city of Strasbourg: a) roof plantings, b) façade greening and front garden, c) greenway along a traffic infrastructure, d) spontaneous plants between paving stones, e) planted public flower beds, f) allotment garden.*

### 2.3.2 The element and its interactions

Based on the ecosystem concept we define in the following interactions putting forward the element vegetation and its interactions with the other ecosystem elements. Figure 2.20 summarizes the main interactions with the ecosystem elements. The interactions with soil, water, and atmosphere are induced by the plants metabolism (see below). Animals and plants are linked by the food cycle and plants are habitats for animals.

Indirect interactions between plants and the human being are induced by the latter that modifies the other elements. Technical elements such as buildings (all types), roads, industrial sites, other installations (infrastructure) are summarised in the element 'humans'. The influence of technical elements on plants is expressed by suppression of habitats due to constructions, pollution (air, water, soil), increased water and heat stress (mainly due to surface sealing).

Figure 2.20 evokes a direct interaction between vegetation and the human being. It is the positive influence on the human psyche and the role of parks and squares as places where people meet.

The complex of interactions with the elements atmosphere, soil, and water builds the frame for the role of vegetation for environmental quality. We will come back later to these interactions.

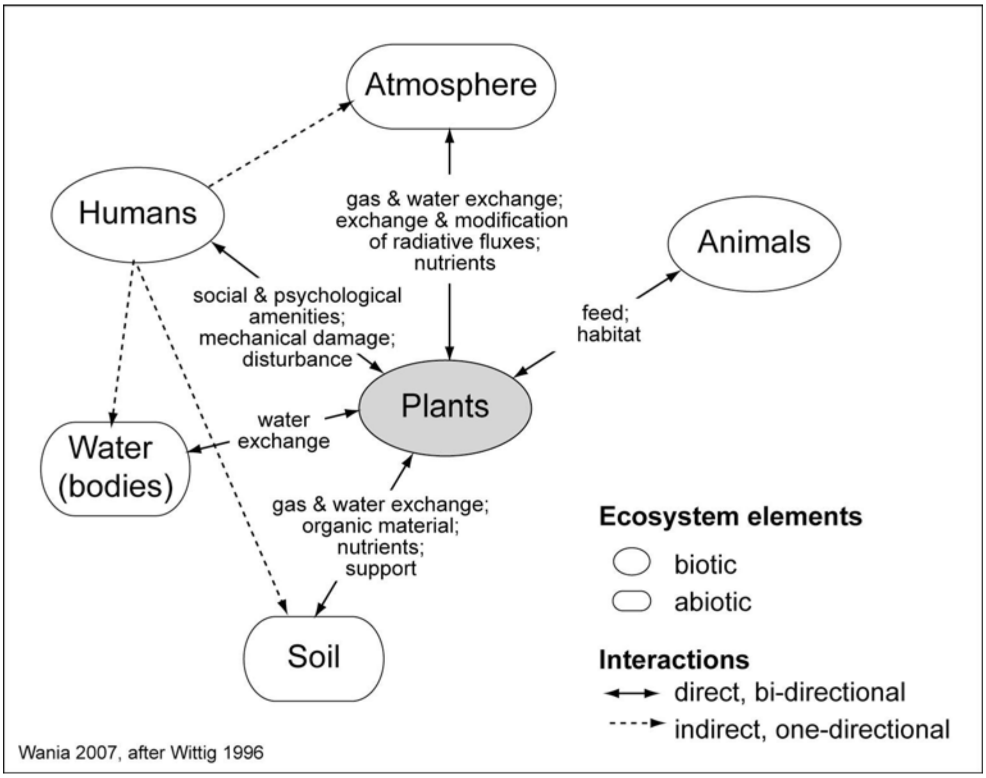


*Figure 2.20: The plant in the urban ecosystem, direct interactions of the plant with the other abiotic and biotic ecosystem elements. Represented interactions focus on vegetation; interactions between the other elements are not indicated. Technical elements are comprised in the human element. Indirect influences concern the modifications of environmental conditions that either suppress possible plant habitats (sealing, building activities) or modify the exchanges with the atmosphere, soil, and water. Direct human influences are damage and disturbance due to mechanical influence.*

#### 2.3.2.1 Interactions induced by the plant's metabolism

Plants are elements of the urban ecosystem but at the same these organisms are even functional biological systems (Duvigneaud 1980). As such they are characterised by their physiological anatomy and metabolism. Due to the metabolism as the whole of biochemical transformations within an organism, plants are open systems interacting with their environment by the exchange of substances and energy. Most plants are autotrophs: their growth depends on energy derived from the sun and uptake of water and nutrients from the environment. They are photosynthetic organisms using light energy to drive the synthesis of organic compounds (Sitte *et al.* 2002). Photosynthesis is one of the most important biochemical pathways and nearly all life depends on it. It is an assimilation process of green plants, algae, lichens and some types of bacteria transforming carbon dioxide and water into carbohydrates (chemical energy) using light energy. Photosynthesis is the only process delivering the oxygen necessary for life on earth and at the same the process is determining factor in the carbon cycle. Like all organisms plants also use oxygen to maintain life functions.

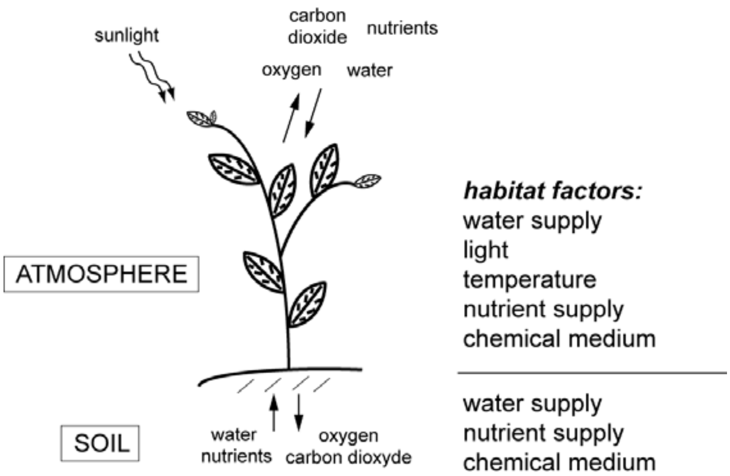


*Figure 2.21: Simplified exchange flows at the interfaces plant-atmosphere and plant-soil, on the right the most important habitat factors (after Sitte et al. 2002, Campbell and Normann 1989).*

Leaves and other photosynthetic organs on a plant serve both as solar energy collectors and as exchangers for gases. Stems and branches support these exchange surfaces in such a way that radiative and convective exchange can occur in an efficient manner (Campbell and Normann 1989). Most of the exchange of substances with the plant's environment is performed by roots and stomata on leaves. Plants take up and release nutrients, water (or water vapour), carbon dioxide and oxygen from and into the surrounding air or soil (and water in some cases). In this context transpiration has to be mentioned as an important process for water release by the plants surface. Transpiration accounts for the movement of water within a plant and the subsequent loss of water as vapour through stomata in its leaves. It is an important process for cooling the plant to avoid excessive heating by solar radiation.

The described flows happening at the interfaces plant-soil and plant-atmosphere are induced by the plants physical properties and metabolism. Consequently, plants live functions depend on soil, atmosphere conditions, and the abiotic environment of the plant. Each species tends to live within a certain environment characterised by a combination of environmental factors. Environmental or habitat factors are water and nutrient supply, oxygen, light, temperature and the chemical medium (Figure 2.21).

#### 2.3.2.2 Influence of humans on plants

In urban ecosystems the habitat factors are modified by human activities and in many respects the living conditions of plants are more unfavourable in cities than in rural areas. As for the abiotic ecosystem elements the human impact on plant communities typically increases from the outskirts to the core of urban areas (Sukopp 2004).

Very often soils, air and water supply are negatively modified exacerbating the living conditions of plants. Table 2.3 shows modifications of plants living conditions in urban ecosystems and the effects on plants. As already indicated, it is distinguished between two kinds of human influence: indirect and direct modifications. Direct human influence on plants happens by mechanical damage due to vandalism, vehicles, maintenance (pruning, mowing), construction work, by foot traffic (trampling) or intentionally plant removal for example (Gilbert 1989, Wittig 1996, Tello *et al.* 2005). As a result, the organism is damaged or weakened and may be prone to pest attacks and disasters. Indirect modifications concern above all modifications of the surrounding air, soil and water, the plants (abiotic) environment. The availability of nutrients, water, oxygen and carbon dioxide, soil conditions and surrounding temperature influence the occurrence of plants. The modified habitat conditions induce stress and disturbance and may on one hand result in physiological changes, plant damage or even disappearance (Table 2.3). On the other hand, plants may also adapt to changing habitat conditions.

*Table 2.3: Human induced modifications of plant habitats in urban areas compared to the initial natural habitat (after Sukopp and Werner 1983, Gilbert 1989, Maillet and Bourgery 1993, Wittig 1996, Sukopp and Wittig 1998, Sukopp 2004, Sieghardt et al. 2005).*

| Modification of habitats | | | Effect on plants and adaptation |
|---|---|---|---|
| **Type** | **Object** | **Effect** | |
| Indirect | Atmosphere | Warmer (urban heat island)<br>Dryer<br>Occurring strong winds (jet effects) | Excess heat (leaf and bark burn)<br>Difficulties of accessing water (necrosis, shrinkage, senescence)<br>Higher evapotranspiration<br>Longer vegetation period<br>Favours species adapted to warm and dry conditions and frost-susceptible plants, disfavours hygrophytes |
| | | Higher pollution level | Necrosis, senescence<br>Favours pollution tolerant and disfavours sensible species |
| | | Locally reduced light (shadow) | Reduced photosynthetic activity |
| | Soil | Infertile compact soils (often made of rubble)<br>Limited drainage (Excess water or dryness)<br>Higher nutrient (eutrophication) and pollutant concentration | Nutrient deficiency or overload<br>Contamination<br>Engorgement or drought<br>Small root volumes<br>Low soil aeration<br>Favours species tolerant to nutrient overload and pollution tolerant species |
| | Water | Lower ground water level<br>Higher surface water flow off<br>Waterbodies polluted (eutrophication), canalised, tubed | Difficulties of accessing water (necrosis, shrinkage, senescence)<br>Favours dryness tolerant species and deep-rooted plants<br>Disfavours hygrophytes<br>Disfavours marsh and aquatic plants (helo- and hydrophytes) |
| | Whole habitat | Disturbance, extinction, recreation | Favours species resistant to disturbance (annual , short generation cycle, high reproduction, effective reproduction mechanisms, Neophytes, etc.) |
| Direct | Plant | Growth control (abatement) | |
| | | Mechanical damage (vandalism, tree cut) | Restricted space for crown development<br>Favours species with high regeneration capability, disfavours fragile species |

### *Adaptation to limiting factors*

The tolerance to different environmental conditions varies between species; it can be rather broad for some very common species but much more tightly defined for others. Accordingly each plant shows limits of tolerance with a minimum and maximum threshold (Sitte *et al.* 2002). If a plant reaches its tolerance limits development is impossible and the metabolism is disturbed.

The majority of spontaneously occurring plant species is often prone to regular disturbance and a common characteristic of many species found in cities is the ability to tolerate stress following disturbance (Gilbert 1989). Table 2.3 depicts main features induced by disturbance and some adaptation strategies.

One way of adaptation results in morphological changes such as smaller leafs and sparse crowns (Wittig 1998)[13]. Disturbance may also result in changes in species composition. In contrast to natural ecosystems plant succession happens very quickly in the urban ecosystem, i.e. pioneer and decay phases succeed each other in short time periods and characterise thus low stability (Schulte 1995). Additionally, humans introduced species from other regions intentionally or unintentionally, namely Archaeophytes and Neophytes whereas the latter are very typical for urban areas. A high number of Neophytes are pioneer plants, what explains their high percentage in the urban flora. Generally, only those species that can adapt to the described modifications of the abiotic conditions survive in urban ecosystem. Accordingly, more light-feeders, species growing on base and nutrient rich soils and tolerating high temperatures and dryness occur in urban areas (Wittig 1998). Furthermore, life forms allowing plants to survive unfavourable seasons in the form of seeds, and completing their life-cycle during favourable seasons occur more often. Furthermore, plants in urban areas are adapted to more difficult reproduction conditions.

Spatial heterogeneity and species immigration due to human's activity are the reasons for higher species numbers in urban areas compared to surrounding rural areas (Klotz 1990, Kühn *et al.* 2004, Sukopp 2004, Wania *et al.* 2006a). Spatial heterogeneity is a major feature of urban vegetation created by the varying building densities and types, and different land uses that provide many specific ecological conditions. Cities show a mosaic of different habitats and the composition of plant communities are greatly dependent on human activities (Wittig 1996, Sukopp 2004). Disturbance and recovery during succession are key factors determining habitats and habitat composition in the urban ecosystem.

Furthermore, other biotic ecosystem elements influence the plant in the urban environment. The ecological conditions imposed to plants life and urban activities, and their specific unfavourable effects strongly influence plant development and the presence and behaviour of diseases inducing pathogens and pests affecting them (Tello *et al.* 2005). On one hand pathogens show limited attacks when environmental conditions are not favourable for them (e.g. depending on climate conditions). On the other hand, if plants are not adapted to the environment of the planting site, the environmental stress may cause them to be more prone to attacks. In their study Tello *et al.* (2005) cite fungi, insects and bacteria as the most frequently cited urban trees damaging organisms where fungi and insects hold the highest percentages (55 and 43 %).

[13] Research on the urban vegetation has been completed in many cities and in Europe research traces back to studies of the flora of the urban bombsites remaining after the Second World War (Wittig 1998). Most studies were performed on cities of western and eastern Europe (Kowarik 1990, Pyšek and Pyšek 1990, Trepl 1990, Kent *et al.* 1999, Maurer *et al.* 2000, Godefroid 2001). Nevertheless, floristic studies were also performed in American cities (Whitney 1985, Söyrinki 1991, Franceschi 1996, Schwartz *et al.* 2006). Wittig (1998) resumes characteristics of the spontaneous central European urban flora compared to flora of surrounding landscapes.

### 2.3.3 Conclusions

The present paragraph focussed on the role of vegetation in the urban ecosystem. The interactions with the elements soil, atmosphere, water, were described. The influence of humans on plants reveals the strength of the modified living conditions of plants in the urban environment. The direct influence of plants or vegetation in general on humans was briefly indicated. Additionally, plants affect the living environment of humans by the mentioned interactions that are mainly induced by the plants metabolism. We can say, plants may compensate to a certain amount the changes of the initial environmental conditions. As such they are known to contribute to environmental quality in urban areas. The most important functions of vegetation are described in the following.

## 2.4 Vegetation and urban environmental quality

Practitioners, planners, researchers and politicians increasingly deal with the contributions of the entire urban green structure to the quality of life and the environment. As already mentioned, on one hand, this role is defined by the direct influence on the human psyche. The interactions with atmosphere, soil, and water are fundamental for the influence on the quality of life that in turn is positively influenced by a healthy environment.

The following paragraphs give an overview of the functions of urban vegetation in the context of environmental quality. They are mainly summarizing research results. The functions mentioned here are mainly seen from the human point of view and his need for ecosystem health. First, plants can provide information on the environmental quality of the urban ecosystem. Second, as shown above, exchanges are induced by the metabolism of plants mainly with the atmosphere and they are the main driving force of most ecological functions considered in this context. Another ecological function focuses on biodiversity aspects and the role of vegetation as habitat in the highly ‘artificial’ ecosystem. Finally, humans profit from plants also in terms of economic, social benefits and it is shown that the presence of vegetation in the urban fabric positively influences the human psyche.

### 2.4.1 Plants as indicators of urban environmental quality

Plants show species specific tolerances to the modified environmental conditions. Like every organism, plant species and communities show an ecological tolerance or amplitude including a minimum, optimum and maximum (Duvigneaud 1980). More precisely, the existence and reproduction of living organisms is possible within a certain range of the ecological factors. According to the organisms tolerance it may adapt to and react on changing environmental conditions or not. Plants are used as indicators for certain environmental conditions (Batzias and Siontorou 2007). As bioindicators they are used to quantitatively and qualitatively evaluate the human influence on the environment. Bioindicators are based on the impairment of live functions, performance and the abundance or absence of organisms or organism communities as a consequence of modified environmental conditions (Beeby 2001, Wolterbeek 2002). Plants can be ‘used’ to indicate environmental quality namely the conditions of air, soil, and water and the degree of human influence (Figure 2.22).

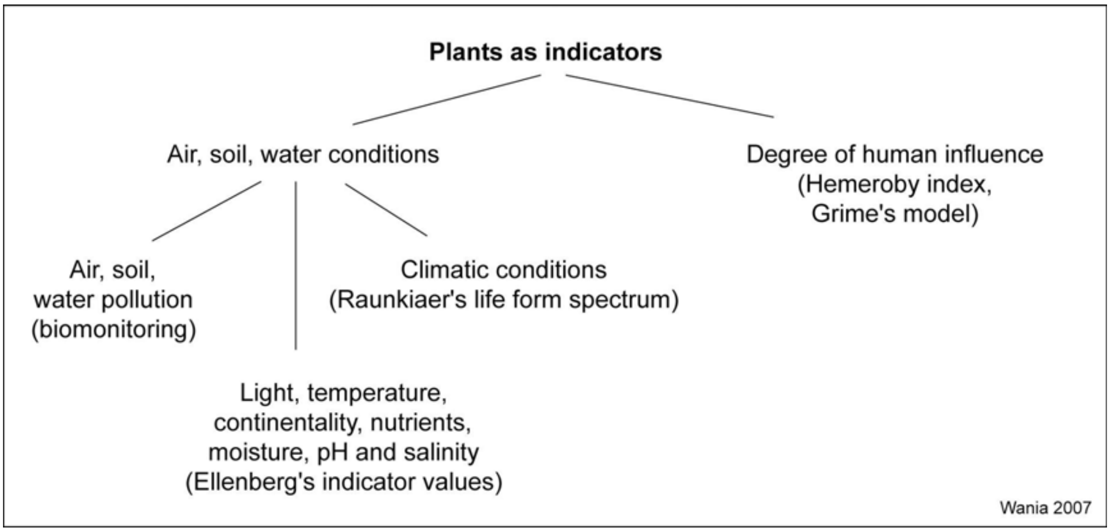


*Figure 2.22: Plants as indicators of environmental quality in urban areas.*

***Air, soil, and water conditions***

*Biomonitoring* uses bioindicators to observe temporary changes in the environment (Figure 2.22). In general, it is based on sensitive and accumulative organisms (Beeby 2001, Wolterbeek 2002). While sensitive bioindicators show specific symptoms (morphological changes, photosynthetic or respiratory activity modifications) accumulative bioindicators have the ability to store contaminants in their tissues, often without remarkable damages (bioaccumulation) (Batzias and Siontorou 2007). Consequently, the accumulated substances are available for concentration analysis. Besides animals, fungi and bacteria, plants have been employed as bioindicators in air, soil and water pollution surveys. For atmospheric pollution studies lichens were proven to be the most valuable long-term monitor (Beeby 2001, Conti and Cecchetti 2001, Batzias and Siontorou 2007). Some recent examples are (Gonzalez *et al.* 1998, Giordano *et al.* 2005, Bergamaschi *et al.* 2007, Munzi *et al.* 2007). Bergamaschi *et al.* (in Press) and Giordano *et al.* (2005) analysed the potential of different lichens transplants to detect urban trace element atmospheric pollution. Gonzalez *et al.* (1998) associated the chemical response of lichens with emission sources and the presence of trees and buildings affecting spread of pollutants. Munzi *et al.* (2007) showed significant changes in the epiphytic lichens flora of the city of Rome and a decrease in diversity over the past 20 years. But vascular plants as well can be used as bioindicators for urban atmospheric pollution as for example done in (Tarvainen et al. 2003, Klumpp et al. 2006, Berlizov et al. 2007). Tarvainen *et al.* (2003) traced back modifications in species composition along an urban gradient to long-term nitrogen-mediated changes. Klumpp *et al.* (2006) analysed the relationship between tobacco plant foliar injury degree and ozone pollution. Berlizov *et al.* (2007) found that accumulation capability of black-poplar bark is as effective as for two analysed types of lichens and consequently suites for biomonitoring. Trees and especially coniferous trees are good bioindicators of air pollution. The pine tree is particularly sensitive to air-dispersed pollutants (Lombardo *et al.* 2001).

Besides these more classical applications for pollution analyses, bioindication using plants helps also observe the urban environment in terms of temperature, soil and water conditions, disturbance and degree of human influence (Wittig 1996) (Figure 2.22). Urban flora and vegetation carries a rich information about the properties of urban ecosystems. Based on the relationship between plants and habitat factors they can be used to asses the ecological conditions of the environment, to monitor trends over time or to provide early signal of changes (Lavorel and Garnier 2002, Fanelli *et al.* 2006). In plant ecological and phytogeographical literature a long tradition in using species composition and plant traits as indicator exists. Concepts for indicators are derived from floristic characteristics of plant communities (species composition of sites). To give an idea of the basic principles the most common concept used by community ecologists are presented in the following namely Raunkiaer's forms spectrum, Ellenberg's indicator values, Grime's model of strategies and the hemeroby index.

*Raunkiaer's system* plants are categorised based on their life form (Raunkiaer 1934). Life forms are defined depending on the location of the plant's growth-point (bud) during seasons with adverse conditions (cold, dry seasons) and express the survival strategy of plants (Sitte *et al.* 2002). Life forms are thus mainly correlated with climatic conditions of the environment[14]. Therophytes are typical indicators of the difficult living conditions in urban areas as they have no perennial organs and survive in the form of seeds (Wittig 1996).

*Ellenberg's indicator values* concern light, temperature, continentality, nutrients, moisture, pH and salinity (Ellenberg 1974). The optimum of a species with respect to a given factor is expressed on a scale from 1 to 10 (e.g. a species with pH indicator value 1 is acidophilous[15], while pH 8 refers to basophilous[16] species). Using Ellenberg's indicator values it was recently proven that plant species on urban wastelands are mainly driven by soil conditions and light intensity (Godefroid *et al.* 2007). Such indicator values can be used to draw conclusions about the temporal alterations in environmental conditions as well (Godefroid 2001). Godefroid (2001) analysed the flora of Brussels between 1940 and 1994 and observed changes to more nitrophilous and shade tolerant species. No changes were observed with respect to soil moisture, reaction and temperature. For structuring the urban ecosystem of Rome (considering only parks) Fanelli *et al.* (2006) report light, temperature and continentality as being the most important indicators. Accordingly, suburban sites show higher values for light, temperature and continentality, while the moisture indicator is higher in the centre.

*Grime's triangular model* focuses on stress and disturbance and represents the range of plant strategies (CRS model) (Grime 1979). Environments with simultaneously high stress and high disturbance are inaccessible to plants while other combinations generate a suite of adaptations representing three main life strategies: competitive (C), ruderal (R) and stress-tolerant (S). Figure 2.23 shows a conversion of Grime's CRS-model to illustrate the range of habitats present in cities. The largest areas in the triangle are occupied by disturbed and productive habitats (Grime 2002). This is not unexpected due to the high level of biotic activity and the high input of materials including nutrients, a typical ecosystem feature. Fanelli *et al.* (2006) used the CSR-model to show the gradient from suburban sites toward the centre of Rome. Gilbert (1989) related typical urban plant communities to the CSR-model (Figure 2.23).

---

[14] For detailed information on the different life forms see Sitte et al. (2002).

[15] Having an affinity for or thriving in acidic conditions.

[16] Thriving in alkaline habitats.

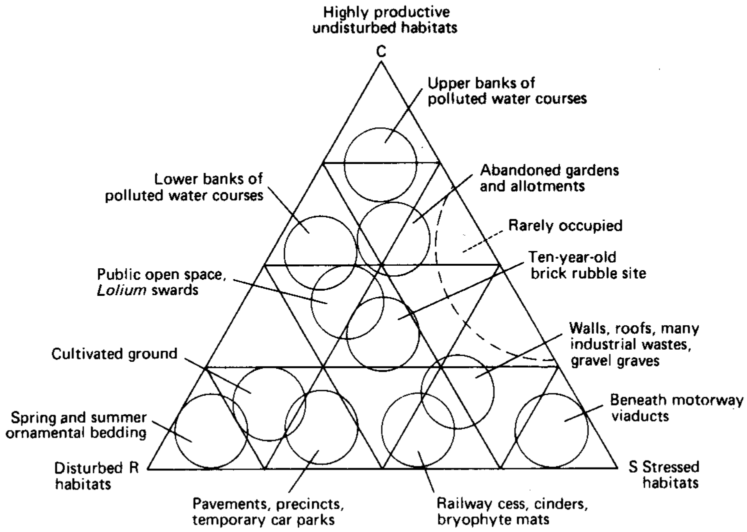


*Figure 2.23 : Grime's triangular CRS-model translated into habitats present in cities (Gilbert 1989).*

***Degree of human influence***

The degree of human influence on ecosystems can be expressed by the *Hemeroby index* on a 10 points scale. The concept was firstly promulgated by (Jalas 1955) and enlarged in works of (Sukopp 1976) and (Kowarik 1988). Table 2.4 shows the 10 points scale where increasing numbers refer to increasing human influence. Important parameters are the amount of annual species (therophytes), late immigrants (Neophytes), and the loss of naturally occurring species. Accordingly, the higher the amount of therophytes and neophytes and the less species are naturally occurring on the site the higher the human influence. The hemeroby scale is commonly applied to estimate the 'naturalness' of an area or land use (Kowarik 1990, Pyšek and Pyšek 1990, Wania *et al.* 2006a, Godefroid *et al.* 2007).

*Table 2.4: Hemeroby scale with examples of vegetation and site types (after Kowarik 1990). The arrow on the left is pointing in the direction of increasing un-naturalness.*

| | Degree of hemeroby | | Types of sites / vegetation |
|---|---|---|---|
| ↓ | H0 | ahemerobic | almost not existing in Central Europe (only in parts of high mountains |
| | H1 | oligohemerobic | virtually uninfluenced primary forests, growing flat or raised bogs, vegetation of rocks and sea-shores |
| | H2 | oligo- to mesohemerobic | extensively drained wetlands, forests with minor wood withdrawal, some wet meadows |
| | H3 | mesohemerobic | more intensively managed forests, developed undisturbed secondary forests on man-made sites, dry grassland |
| | H4 | meso- to β-euhemerobic | monocultural forests, disturbed secondary forests, skirt vegetation, less ruderalised dry grassland |
| | H5 | β-euhemerobic | Young planted forests, intensively managed meadows and pastures, ruderal vegetation of tall herbs, strongly ruderalised dry grassland on man-made sites |
| | H6 | β-eu to α-euhemerobic | traditionally managed field vegetation, trampled lawns, ruderal rough meadows |
| | H7 | α-euhemerobic | intensively managed segetal and garden vegetation |
| | H8 | α-euhemerobic to polyhemerobic | segetal vegetation affected by strong herbicide impact (e.g. maize fields), ruderal pioneer vegetation, annual trampled lawns |
| | H9 | polyhemerobic | pioneer vegetation on railway territories, rubbish places, dumps, salted motorways |
| | - | metahemerobic | no vegetation or vascular plants |

## 2.4.2 Ecological functions

### 2.4.2.1 Climate

Urban vegetation cover plays a key role in controlling the local and regional aspects of the physical environmental conditions such as radiation, wind, temperature and humidity (Givoni 1991). Thermal comfort and presence of vegetation are correlated (Gomez *et al.* 2004, Gulyas *et al.* 2006). In many studies the climatic benefits of urban vegetation were shown and only a few are mentioned here.

In general, vegetation contributes to thermal comfort in urban areas by temperature reduction trough shading (direct effect) and evapotranspiration (indirect effect). Vegetation reduces air temperature by direct shading of surfaces (causing less absorption of insulation at the underlying ground) and conversion of sensible heat (solar radiation) to latent heat through evapotranspiration (Oke 1987, Kuttler 1998). The resulting lower temperature leads to reduced long-wave reduction emitted from ground and leafs, as opposed to built surfaces. However, the efficacy of a plant cover to convert sensible to latent heat depends on the water balance and wind (Oke 1989). Higher wind and high water content in the plant favour evaporative heat suppression. The same, larger green areas or dense vegetation cover are more effective than small areas or few dense vegetation cover (Stülpnagel *et al.* 1990, Dimoudi and Nikolopoulou 2003). Larger green spaces help thus to produce cool air inside the urban area and the cooling effect extends even beyond the boundaries of green spaces and is higher downwind. The use of shade trees in streets have a significant cooling effect at noon in summer (Shashua-Bar and Hoffman 2000, Shashua-Bar and Hoffman 2003). In their study on small wooded sites in Tel-Aviv Shashua-Bar and Hoffman (2000) found out that about 80 % of the cooling effect was contributed by tree shading and perceivable up to 100 m from the site boundary. Urban greening to mitigate the urban heat island effect is especially supported in desert cities (McPherson 2001, Stabler *et al.* 2005).

### 2.4.2.2 Air pollution

The effect of vegetation on air pollution is based on two mechanisms: a) absorption due to the plants metabolism, and b) pollutant trapping on the surface of plants. The first effect is directly linked to the plants metabolism.

***Reduction of particle concentrations***

Research has shown that trees can act as biological filters, removing large quantities of particles from the urban atmosphere. Trapping of particles on leaves was proven for an urban woodland near a roadway (Freer-Smith *et al.* 1997, Ould-Dada and Baghini 2001) and on façade greenings in a residential area (Thönnessen 2002). Trees are effective in trapping pollutants and re-suspension rates are reported to be small even with increased wind speed (Ould-Dada and Baghini 2001). Freer-Smith *et al.* (1997) report higher removal rates on trees closer to motorway sources and during the growing season. Particle retention is increased if the leaf and bark surfaces are rough or sticky and coniferous trees are more efficient than broadleaved trees (Beckett *et al.* 1998, Freer-Smith *et al.* 2005). Thönessen (2002) showed that the amount of elements deposed on the plant leafs is much higher than elements taken up by plants or through stomata. As for the removal of gaseous pollutants removal rates are higher in the leave-on season (Yang *et al.* 2005). Nowak *et al.* (2006) and Yang *et al.* (2005) showed highest removal rates for $PM_{10}$ compared to nitrogen dioxide, ozone, carbon monoxide, and sulphur dioxide. Nowak *et al.* (2006) report an average daily percent air quality (all main pollutants) improvement for US cities due to trees smaller than 1 %.

***Reduction of carbon dioxide***

Retention of gaseous pollutants by penetration through skin pores was shown in chamber experiments (Hill 1971, Bennett and Hill 1973, Ould-Dada and Baghini 2001). Plants contribute to the reduction of carbon dioxide concentration by fixing it during photosynthesis and storing excess carbon as biomass (Nowak and Crane 2002, Gratani and Varone 2006). By day, plants take up carbon dioxide for photosynthesis and can thus reduce atmospheric carbon dioxide by directly storing carbon from carbon dioxide as they grow. Consequently plant canopies are considered as carbon dioxide sinks (Oke 1987).

The rate of carbon sequestration depends on plant traits and habitus (evergreen or deciduous) and accordingly the season (Johnson and Gerhold 2003, Gratani and Varone 2005, Yang *et al.* 2005). Johnson and Gerold (2003) analysed carbon storage in tree cultivars with special focus on storage in roots and showed that 16 to 41 % of the total carbon stored by urban trees was in the roots. A plane tree was reported to sequester about 117 kg per year (Gratani and Varone 2007). Based on biomass information Nowak and Crane (2002) estimated the carbon storage by urban trees in the USA to be equivalent to the amount of carbon emitted from USA population in about 5.5 months. The same authors estimate that the national annual carbon sequestration is equivalent to USA population emissions over a 5-day period.

Knowledge about carbon storage in biomass and particle deposition rates on plants were applied to estimate benefits of urban vegetation and mainly tree cover for urban areas or city districts (Jo and McPherson 1995, Yang *et al.* 2005, Nowak *et al.* 2006). Jo and McPherson (1995) calculated carbon flux of urban green spaces including carbon storage in soils and release by mowing. Accordingly, soils and woody plants were carbon sinks, while grass was a net carbon source.

Besides direct carbon dioxide reduction by the plants metabolism, vegetation and especially trees indirectly influence air quality by reducing the demand for energy through shadow (Heisler 1986, Akbari and Taha 1992, Taha *et al.* 1997, Simpson and McPherson 1998, Akbari *et al.* 2001, Jo and McPherson 2001, McPherson 2001, Nowak and Crane 2002, McPherson and Simpson 2003). Urban trees can help offset or reverse the heat-island effect by lowering temperatures and shading buildings during summer, and by blocking winds in the winter. This effect helps reducing energy consumption for cooling and heating of houses and consequently reduces carbon dioxide emissions from power plants (Heisler 1986). Based on simulations of the effects of shading, evapotranspiration and wind, it was shown that trees planted in strategic locations might increase energy conservation and finally contribute generally to carbon reduction (e.g. Akbari and Taha 1992). Heisler (1986) compared the reduction rates of irradiance for trees in leaf and without leafs. Trees in leaf showed reduction rates of 80 % and 40 % when leafless. For residential neighbourhoods in Chicago with 11-33 % tree cover Jo and McPherson (2001) reported an annual carbon emission reduction up to 4 %.

Other studies were performed to estimate the total reduction rates for cities or districts (Jo and McPherson 2001, Akbari 2002, Brack 2002). In their simulations on building prototypes in the city of Toronto Akbari and Taha (1992) found out that increasing vegetation cover by 30% and the albedo of houses by 20%, the heating energy of the city can be reduced by about 10% in urban houses and 20% in rural houses, whereas cooling energy can be reduced by 40 and 30%, respectively. Rooftop and facade greening reduce the energy needed for indoor climate control (Akbari *et al.* 1997).

***Reduction of ozone formation***

Other studies evaluated the influence of tree plantings on ozone formation by means of computer modelling (Taha 1996, Taha et al. 1997, McPherson et al. 1998, Nowak et al. 2000). Urban trees may reduce ambient air ozone concentrations, either by direct absorption of ozone or other pollutants such as nitrogen dioxide, or by reducing air temperatures which reduces hydrocarbon emissions (VOC, volatile organic compounds) from plants and ozone formation rates (Cardelino and Chameides 1990). While increasing tree cover leads to increased pollution removal rates in general it might increase ozone concentrations (Taha 1996, Taha et al. 1997). Nevertheless, vegetation induces temperature reduction what slows down the photochemical production of ozone[17]. Consequently, Taha (1996) and Taha *et al.* (1997) suggests to plant low emitters of biogenic hydrocarbons. Although, low VOC emitting species were included in the model, Nowak *et al.* (2000) report no effect on local ozone concentrations but an increase of overall regional concentrations. The physical effects of vegetation cover (reduction of wind speed) are reported to be more important for ozone concentrations than atmospheric chemical interactions with VOCs emitted from the trees.

---

[17] Ozone in the upper troposphere is a secondary pollutant and acts as a greenhouse gas. Higher concentrations were reported to cause harmful health impacts. It is a result of photochemical transformation of mainly nitrogen oxides and hydrocarbons.

#### 2.4.2.3 Water

One of the many benefits afforded by urban vegetation is the amelioration of extremes in urban water runoff regimes. Land use/land cover types with 73-96 % vegetation cover show significantly higher precipitation infiltration rates and reduced surface water runoff than land use/land cover types with lower vegetation cover (Sanders 1986, Pauleit and Duhme 2000, Tapia Silva *et al.* 2006). In their study for Munich Pauleit and Duhme (2000) could show that parks, wastelands and farmlands significantly contribute to groundwater recharge with mean infiltration rates between 30 and 38 %. Infiltration rate is reduced with increasing tree cover.

Interception values for urban forests have been reported as 1.6 % of total rainfall (Xiao and McPherson 2002). Green roofs show interception values close to urban forest sites (Carter and Jackson 2007). They serve to store water and release it into the atmosphere through evaporation or transpiration. It was shown how green roofs can be used to increase stormwater runoff storage as part of an inner city urban stormwater retrofit project in Sweden (Villarreal *et al.* 2004).

#### 2.4.2.4 Biodiversity

Although cities show significantly higher plant species numbers than the surrounding rural landscape, conservation biodiversity in urban areas is a special task (Haeupler 1974, Kühn *et al.* 2004). The high species numbers have two reasons: on one hand, more species are introduced by human activities (trade, travel) and on the other hand, urban areas offer a very heterogeneous habitat pattern what promotes plant biodiversity. Compared to the often uniform farming landscapes, urban areas can be considered as a very heterogeneous habitat island that propose various niches for species whose habitat is suppressed (Kühn and Klotz 2006, Wania *et al.* 2006a). Species numbers in urban areas are higher for both indigenous and exotic species. Although the role of exotic species is rather controversy, cities are valuable species pools. While most exotic species adapt to urban habitat conditions, indigenous species depend on remnants of nature in the city. This was proven by higher numbers of indigenous species found in semi-natural green urban areas (Kowarik 1988, Wania *et al.* 2006a). Most of the indigenous species are not used to urban habitat conditions and accordingly nature like green spaces are very important for species conservation (Wittig 1998). Cities harbour a high percentage of the whole flora from the geographical region they belong to and are therefore especially valuable for species conservation (Duhme and Pauleit 1998, Godefroid 2001, Ricotta *et al.* 2001). Parks, wasteland sites and vegetated areas in older city districts are important refuges for species and plant communities which are rare or endangered in urban areas (Maurer *et al.* 2000). Urban parks and larger green areas often reflect historical situations and act as retention sites for species that find no adequate habitat conditions elsewhere in the urban area. The same, urban and suburban forests have high biodiversity levels (Ricotta *et al.* 2001).

The role of vegetation as animal habitats in urban areas was shown in many studies and only a few are given here (Tzilkowski *et al.* 1986, Strauss and Biedermann 2005, Sandström *et al.* 2006b, Snep *et al.* 2006). It was shown that street trees are important for birds but that the attractiveness differs between species groups (Tzilkowski *et al.* 1986). Eversham *et al.* (1996) and Strauss and Biedermann (2005) showed the importance of urban-industrial habitats and fallow lands with pioneer vegetation for bugs and grasshoppers. Snep *et al.* (2006) analysed how the connection between green areas influences the occurrence of butterflies. Urban green areas are refuges for numerous animal species and animal ecologists promote the interconnection of habitats of all sizes (Sukopp and Werner 1983, Savard *et al.* 2000). However, it was shown that the quality of a green area is important for the diversity of birds for example (Tzilkowski *et al.* 1986, Sandström *et al.* 2006b).

### 2.4.3 Social, psychological, physical, and aesthetical functions

Green spaces are considered "[…] as gateways to a high quality sensory and natural world; to a non-commercialised world where children can explore, learn and play together in safety; to a good city in which people can come together and share their experiences and responsibilities." (Burgess *et al.* 1988).

#### 2.4.3.1 Psychological, and physical functions

Urban living is known to evoke increasing mental stress and stress is recognised as one factor worsening the health of the population (WHO 2007). Urban vegetation can play an important role to improve physical health and reduce the experience of stress (Ulrich *et al.* 1991). It does generate both physical and psychological health and well-being for citizens that frequent urban green spaces but also for the entire population (Grahn and Stigsdotter 2003). Greenery and access to it visually and physically are reported to be the principal keys to health in urban areas and especially at the parcel scale (Jackson 2003).

Psychologists reported the therapeutic benefits of nature and showed that the experience of nature recovers from attentional fatigue and stress (Ulrich 1984, Kaplan and Kaplan 1989). Ulrich (1984) for example showed that hospital patients recover more quickly with a view on a tree as compared with a view on a wall. The restorative function of nature experience is argued with effects like 'being away' from the urban environment, the fascination of nature (clouds, motion of the leaves in the breeze, animals), the sense of extent, and the compatibility of humans with nature (Kaplan 1995). In the urban context the contrast between nature and artificial environments is heavily expressed and urban citizens perceive green areas as life quality enhancer (Shafer *et al.* 2000, Sanesi and Chiarello 2006). On one hand, recreation contributes directly to the quality of life. On the other hand, citizens are even aware of environmental services such as mitigation of air pollution and influence on climate provided by urban green spaces (Sanesi and Chiarello 2006). Another aspect is the indirect contribution to the quality of life of the whole community using green infrastructures (greenways) for transport (Shafer *et al.* 2000).

Green spaces like parks and urban forests are used for leisure, recreation, games, and sporting activities (Oguz 2000, Roovers *et al.* 2002). Recreational activities in close contact with nature were reported to have more positive influence on psychology and physiology than those effected in 'artificial' environments (Gathright *et al.* 2006).

Besides positive effects, parks may play a negative role on people's perceptions. Some surveys have reported resident's feeling of insecurity associated with vandalism, and fear or crime in deserted places (Bixler and Floyd 1997). However, far larger is the empirical evidence of the positive functions and another study reported lower level of fear, fewer incivilities, and less aggressive and violent behaviour (Kuo and Sullivan 2001).

#### 2.4.3.2 Social functions

Besides the function for recreation, sport, and leisure green spaces like parks, squares are also considered as social capital (Walker 2004). Parks help build and strengthen ties among community residents by bringing people together, including those who are otherwise divided by race or class. Parks-like public spaces are places of social aggregation (Coley *et al.* 1997, Kweon *et al.* 1998, Germann-Chiari and Seeland 2004). Bringing people together they can reduce crime and disorder, even in very poor communities (Sampson *et al.* 1997).

The size and distance from home are factors influencing the social value of a green space. Narrow tree belts in parks are less attractive than blocks of woodland of a similar size that allow for a circuitous rather than a linear route (Coles and Bussey 2000). To achieve high social valuation of urban woodlands Cole and Bussey (2000) reported a minimum size of 2 ha and a location within 5 min walk from home. Breuste (2004) reports that residents generally ask for more and larger green spaces.

#### 2.4.3.3 Aesthetic functions

In general, all forms of vegetation contribute to visual improvement and in this context they are of aesthetic value and contribute to urban architecture (Smardon 1988, Le Coeur *et al.* 2002). Trees break up continuous building facades and provide delineation of space, shrubs anchor structures to the ground, and grass and ground cover help to define pavement edges. Vegetation offers visual, noise, and functional barrier but also links dispersed elements in the urban pattern and fills up discontinuities (Le Coeur *et al.* 2002). The aesthetic value or the beauty of a roadside also influence the safety feeling of pedestrians. Safety is related to conditions that are preferred and thus pedestrians feel safer on walking sides with trees and flowerbeds (Price 2003, Todorova *et al.* 2004).

However, public perception of the recreational function and acceptance of nature is influenced by the character of the vegetation and vegetation density (Bjerke *et al.* 2006). Users of parks and forest prefer more open structures than closed, dense tree cover for example (Coles and Bussey 2000, Breuste 2004, Bjerke *et al.* 2006, Roovers *et al.* 2006). The spontaneous vegetation on fallow sides has very few value for citizens (Millard 2004) and residents prefer much more a clean and garden like surrounding than wild, non-maintained urban nature (Breuste 2004).

### 2.4.4 Economic functions

Urban vegetation and specially larger green spaces such as parks and forests are increasingly recognised for their influence on the value of the urban neighbourhood (Walker 2004). Public surveys have shown that citizens attribute no negative effects to urban forests and relate benefits above all to nature, climate, and social values (Tyrväinen 2001). Studies found a statistically significant link between property values and proximity to green space, including neighbourhood parks and urban forests (Tyrväinen 1997, Phillips 2000, Tyrväinen and Miettinen 2000). Tyrväinen and Miettinen (2000) for example have shown that with increasing distance from the park the price decreases by about 6 %. The view onto forests leads to an increase of about 5 % in the market price of the dwelling.

Another economic benefit from vegetation is related to the influence of vegetation on local climatic conditions. As will be described later, vegetation influences the microclimate and may be used to mitigate urban heating and to reduce energy consumption for cooling in summer. In a number of studies the gain in carbon emission reduction and energy saving was calculated mainly based on computer modelling (Heisler 1986, McPherson *et al.* 1988, Akbari *et al.* 1997, McPherson *et al.* 1998, Simpson and McPherson 1998, Jo and McPherson 2001, McPherson 2001, Akbari 2002, Brack 2002, McPherson and Simpson 2002, McHale *et al.*

2007). Others evaluated the benefits from $PM_{10}$ removal (Escobedo *et al.* in press). All conclude that urban tree planting projects in specific locations may be cost effective investments. Besides energy saving McPherson and Simpson (2002) include in their cost-benefit analysis aesthetical benefits and the price of tree pruning.

The same as for energy reduction urban vegetation reduces damage due to high stormwater run-off. Interception rates are used in models to estimate the financial benefits (Brack 2002). The whole of ecological and recreational functions are considered as ecosystem services that have a substantial impact on the quality of life (Bolund and Hunhammar 1999).

The economic value of urban forests is also determined by consumptive values including market priced products such as timber, mushrooms, berries (Tyrväinen *et al.* 2005).

In North-America two tools were developed to help estimate the benefits from urban forests and trees in terms of storm water runoff, air quality, summer energy savings and carbon storage and avoidance: CITYgreen[18] and i-Tree[19]. Both are mainly based on research of G. McPherson and D. Nowak and the application of the Urban Forest Effects Model (UFORE) that was developed in the late 1990 by researchers at the USDA Forest Service's Northeastern Research Station in Syracuse New York (McPherson *et al.* 1994).

## 2.5 The need to observe and promote vegetation in cities

The aim of the present chapter was to built a perspective on urban vegetation based on the ecosystems approach. The shape of the metabolism of the urban ecosystem was presented focussing on the deteriorating environmental conditions like air pollution and urban heat island. We presented vegetation as one element of the ecosystem and showed that its definition depends on the observing person. As an ecosystem element, vegetation generates interactions with the different elements water, air, soil, and the humans. From these interactions the different functions were identified and we were focussing on the functions that help mitigating the detrimental effects of the urban ecosystem. The described functions are the starting point of the growing body of evidence on the benefits of vegetation in urban areas. Green spaces can serve as habitats for wildlife, enhance natural processes such as water infiltration, interception and flood water retention, improve air quality, and increase the quality of life by social services and psychological benefits.

Today, the role of vegetation in the urban ecosystem is widely accepted and research still goes on. Many studies have proven that vegetation can contribute to avoid or reduce environmental problems in cities and help to compensate the detrimental effects of urbanisation. It might even be an alternative to costly engineering solutions such as river engineering, rainwater retention facilities, or building air conditioning. Originally, merely decorative elements in towns and cities, urban vegetation and urban green spaces have taken on a new value and function. Today, a healthy and multifunctional urban green structure is considered as a basic service that should be provided as part of a healthy and sustainable living environment (Konijnendijk *et al.* 2004). Cities promote vegetation and the image of a green city is considered as a label for a high quality of life (Falga and Feltin 2003). The availability of accessible and attractive green spaces is an integral part of urban quality of life (Van Herzele

[18] CITYgreen can be accessed by http://www.americanforests.org/productsandpubs/citygreen/, it is a Geographic Information System (GIS) and an extension to ArcGIS and ArcView

[19] i-Tree can be accessed by www.itreetools.org

and Wiedemann 2003) and the area of and access to green spaces are commonly used to measure urban environmental quality (OFD 2002, Bonaiuto *et al.* 2006b, ICLEI 2006, CEC 2007). Vegetation is associated with living in a healthy environment, as the publicity for a new housing area in the city of Strasbourg in Figure 2.24 shows.


*Figure 2.24: Publicity for a new housing area in a city district close to the centre in the city of Strasbourg: "Living in the green close to the city centre".*

Nowadays, most of the European municipalities take care about the quality of life, environmental preservation or biodiversity assessment. In such context green space development and maintenance constitute a complex issue related to aesthetic, social, ecological factors. On the one hand vegetation is part of the urban environment and contributes to the quality of life. On the other hand, urban vegetation is exposed to extreme living conditions (dryness, missing nutrient supply, light, oxygen, space etc.) affecting tree health and shortening life duration. Consequently, regular observation of trees for example in cities is important to avoid accidental events, diseases and to maintain habitats for plants and trees.

All the more, information is needed on urban vegetation and its characteristics. Furthermore, more action is necessary to assure that research results are considered in the planning process, what is not the case everywhere (Eliasson 2000). In this context, it seems that vegetation is still considered as a design element and that ecological functions are only few considered in planning. Planning needs precise arguments and above all suitable methods and tools. As planning is a political activity which is not always based on scientific knowledge, it is necessary to improve the awareness of the public and decision-makers (Eliasson 2000).

# PART II: DETECTION OF URBAN VEGETATION

In the preceding part we focused on the role of vegetation in the urban ecosystem. The following two parts present two methods to analyse urban vegetation. First, the detection and characterisation of vegetation cover is necessary for all studies on its functions. We therefore analyse in the first part the possibility to detect urban vegetation using remote sensing techniques. In particular, we evaluate the possibility to use therefore high spatial and spectral resolution images (hyperspectral). Second, we focus on a specific ecological function of urban vegetation, namely its influence on air quality. In the second part, a microscale air quality model is used to evaluate the influence of street trees on pollution dispersion in different urban canyons and the effects on concentration levels at the height of the human respiratory tract.

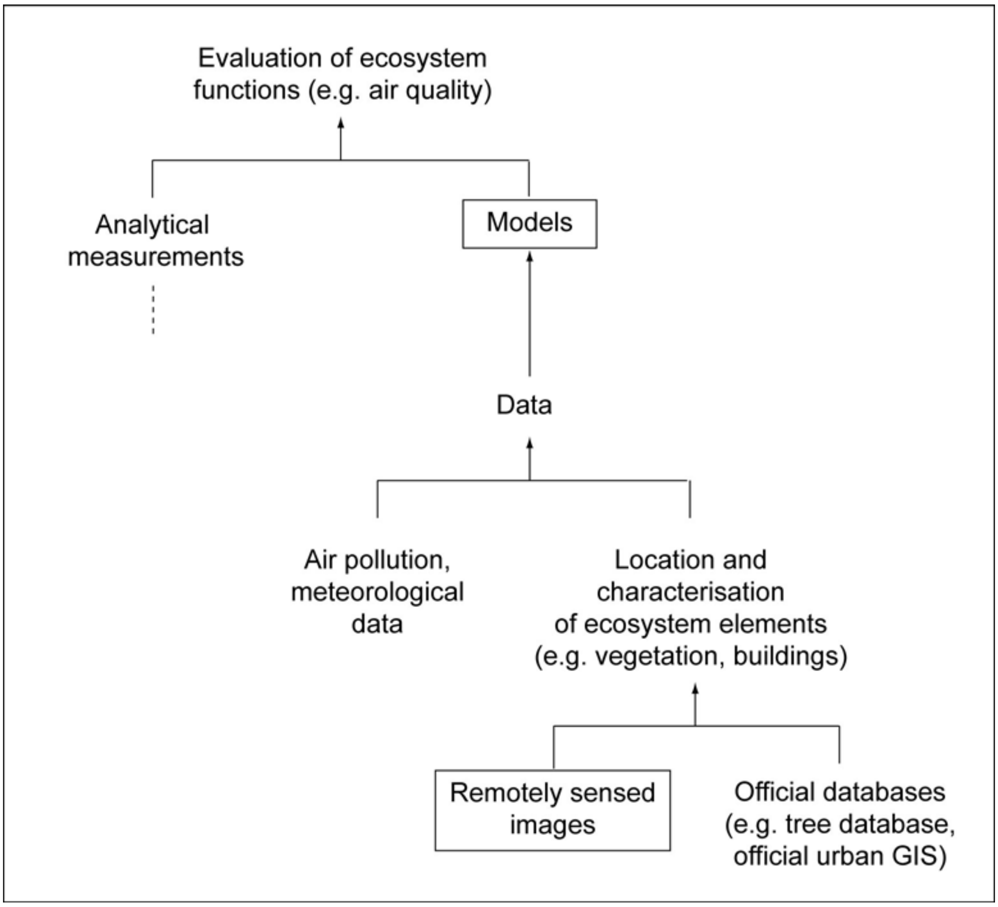


*Figure 2.25: Evaluation of the ecosystem function of urban vegetation and particularly the influence on air quality. Differentiation between two possible evaluation methods, analytical measurements and modelling. Models are an abstraction of ecosystems and consequently need among others information on the ecosystem elements, and in our case on vegetation. Such information can be derived either from official databases or remotely sensed images. This study evaluates the potential of the latter.*

The link between both parts is established in Figure 2.25. The figure depicts the place of air quality modelling and remote sensing in the context of the performed study. The overall study aim is the evaluation of an ecological function, namely air quality. We differentiate between two methods that can be used to evaluate the influence on air quality: analytical measurements or modelling. A model is used in this study. Models are an abstraction of parts of the urban ecosystem and need input data on the system elements. In our case these information concern air pollution data (emissions), meteorology and the location and characterisation of built objects and vegetation. The latter can be derived from remote sensing data or official databases. In contrast to official databases, that concern above all vegetation in public spaces (streets, parks, etc.), this information source is especially valuable as it provides data about the whole vegetation cover of an urban area. Furthermore, official databases are not available in every case and often the access to such information is restricted.

Besides the objective to provide information about urban vegetation for air quality modelling, there is a second motivation to analyse remotely sensed images. Nowadays, European municipalities take care about green space development and maintenance mainly due to the beneficial functions for life quality. Maintenance comprises the observation of vegetation also to assure the security for citizens. Extreme living conditions affect the health of plants in urban areas, shorten their life duration or make them susceptible to diseases. In this context trees are observed in particular. While healthy trees provide benefits, damaged trees might present a risk. Consequently, regular observation of trees in cities is important to avoid accidental events. Therefore, information has to be up-dated regularly what is still done mostly by field observations. However, this method is still very time consuming and expensive to assure the updating of such databases. Another aspect concerns invasive species that affect the biodiversity of the ecosystems and neighbouring ecosystems or plant diseases in general. For their detection remote sensing provides valuable information. With this study we contribute to the evaluation of this information source for such aspects.

# 3 VEGETATION DETECTION USING REMOTELY SENSED DATA

At the beginning of this part some basic principles of remote sensing are presented. Only selected aspects are presented and to more detail it is referred to the literature (Lillesand *et al.* 2004).

## 3.1 Some basic principles of remote sensing

Remote sensing is the science of obtaining information about an object, area, or phenomenon through the analysis of remotely collected data, i.e. data that are acquired by a device that is not in contact with the object, area, or phenomena under investigation (Lillesand *et al.* 2004). In the frame of this work we consider electromagnetic remote sensing. Electromagnetic sensors acquire data on the way various features on the earth's surface reflect and emit electromagnetic energy. They operate from airborne (e.g. airplanes) or spaceborne platforms (satellites).

The most obvious source of electromagnetic radiation for remote sensing is the sun (Lillesand *et al.* 2004). It is the source of energy for passive sensors that are considered in this study (for active sensors see below). The energy propagates through the atmosphere and only a small portion of the emitted energy radiation reaches the surface. Various fractions of the energy incident on the surface element are reflected, absorbed, and/or transmitted (principle of energy conservation). The nature of the object and atmospheric composition affect the energy finally received by the sensor.

In remote sensing it is most common to characterise electromagnetic waves by their wavelength location within the electromagnetic spectrum and a major characteristic of a remotely sensed image is the wavelength band it presents. Figure 3.1 shows the electromagnetic spectrum and the different regions generally referred. Passive remote sensing systems measure reflected solar radiation in the ultraviolet, visible and near to middle infrared wavelength range or the energy emitted by the earth itself (thermal infrared wavelengths) (Figure 3.1). Active remote sensing systems measure the relative return from the surface of energy emitted by the instrument itself like energy in the microwave band of wavelengths.

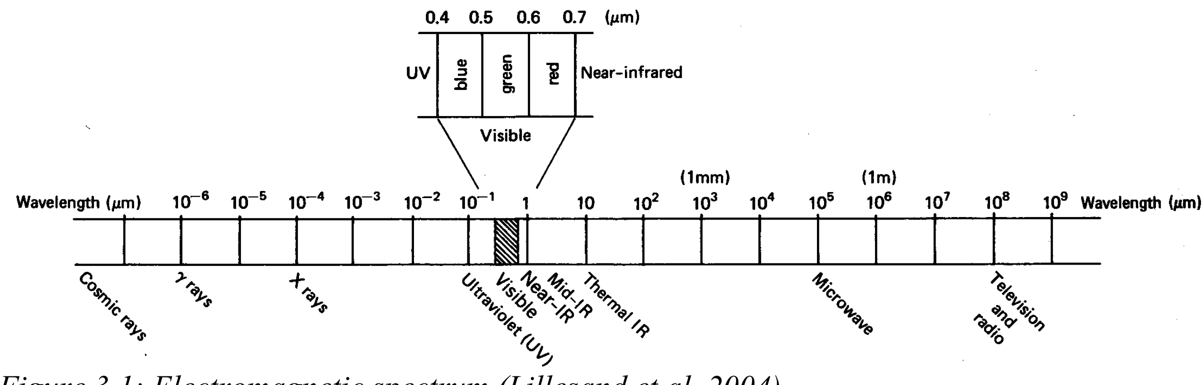


*Figure 3.1: Electromagnetic spectrum (Lillesand et al. 2004).*

The images used in this study are measurements of the spatial distribution of reflected solar radiation in the visible and near infrared range of wavelengths. The visible portion of the electromagnetic spectrum is extremely small since the spectral sensitivity of the human eye extends only from 0.4 μm to approximately 0.7 μm. The colours blue, green and red are ascribed by the approximate ranges 0.4-0.5 µm, 0.5-0.6 µm, and 0.6-0.7 µm. The infrared waves adjoin the red end of the visible portion of the electromagnetic spectrum and three different ranges of infrared energy are distinguished: near, mid and thermal infrared (Figure 3.1). In the frame of this work, only the near and mid infrared range are considered. Near infrared (NIR) covers the range from 0.7-1.3 µm, the mid infrared the range from 1.3-3 µm (Lillesand *et al.* 2004). However, there are no clear-cut dividing lines between the regions.

A graph of the spectral reflectance of an object is a function of wavelengths and is termed spectral reflectance curve (Lillesand *et al.* 2004). The configuration of the spectral reflectance curve provides insight into the spectral characteristics of the object and influences the choice of a spectral region for a given remote sensing application.

Remote sensing image data are spatially composed of discrete picture elements, or pixels, that are radiometrically quantified into discrete brightness levels (Richards and Jia 1999). The size of these pixels defines the spatial resolution of an image. The spectral range covered by a sensor and the width of spectral bands defines the spectral resolution. It is differentiated between multispectral (some large bands) and hyperspectral (many narrow bands) image data. In the present work we are mainly considering the latter.

## 3.2 Spectral characteristics of vegetation

Solar radiation impinging on the leaf's surface is reflected, absorbed or transmitted. The amount and nature of all three components depend on the wavelength, angle of incidence, surface roughness and the optical properties of leaves and biochemical contents of the leaves (Jensen 2000, Kumar *et al.* 2001). The reflectance of vegetation is a result of a very complex changing process within the leaves, the canopy and the vegetation stand. A typical reflectance spectra of healthy vegetation is shown in Figure 3.2. The characteristic sharp reflectance changes in some spectral regions are the result of the leaf optical properties that are influenced by the concentration of chlorophyll and other biochemical substances, water content and leaf structure. They reflect the interactions of incident electromagnetic energy with the pigments, water and intercellular air spaces within the plant's leaf.

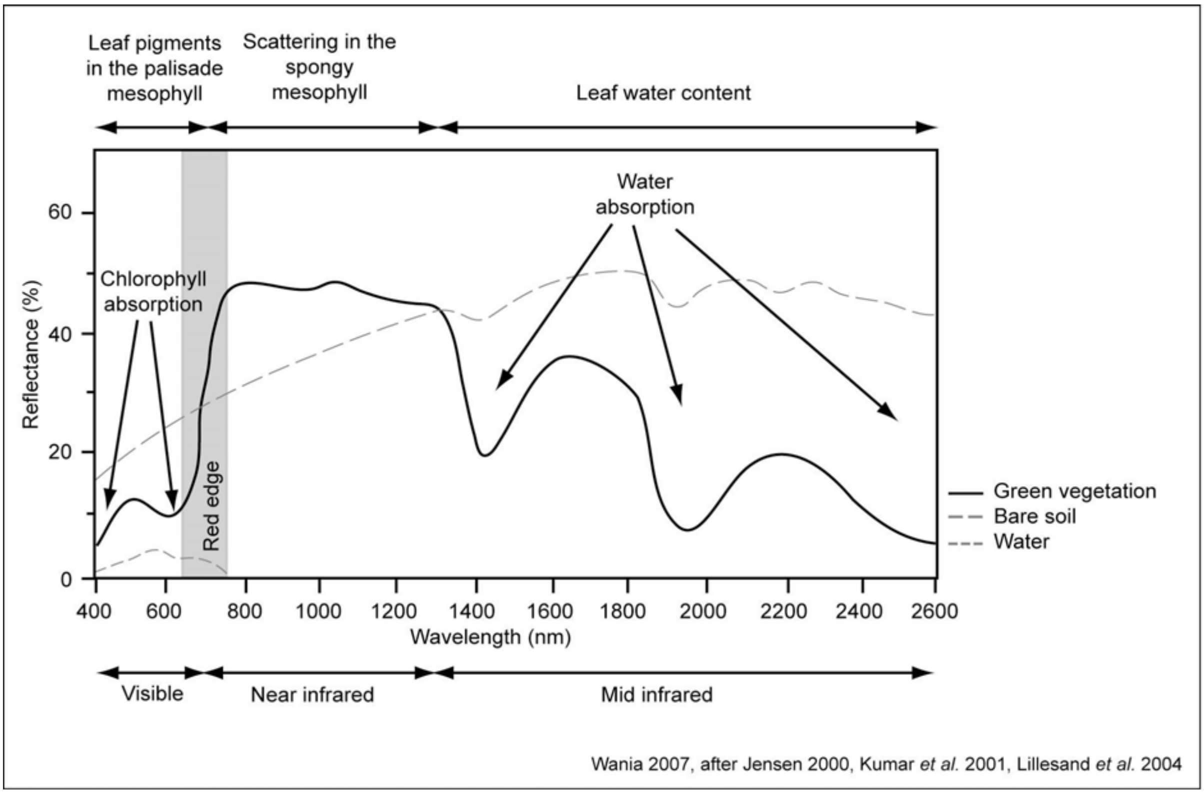


*Figure 3.2: Spectral reflectance characteristics of green vegetation in the spectral range from 400 to 2600 nm. Comparison with the standard soil and water reflectance spectra (Jensen 2000, Kumar et al. 2001, Lillesand et al. 2004). Leaf reflectance in the visible is mainly controlled by leaf pigments in the palisade mesophyll (e.g. chlorophyll a and b, and β-carotene). Dominant factor in the near infrared is the scattering of energy in the spongy mesophyll. The amount of water mainly controls leaf reflectance in the mid infrared with two dips centred at about 1400 nm and 1900 nm.*

The reflectance curve of vegetation is much more complex than that of bare soil and water (Figure 3.2). In the mid infrared range it is dominated by the water absorption bands at 1400 nm, 1900 nm and 2700 nm. Furthermore, minor absorption features occur in this region induced by other biochemical contents (lignin, cellulose, starch, proteins, nitrogen) (Kumar *et al.* 2001). The plateau between 700 nm and 1300 nm is dominated by plant cell structure while in the visible range of wavelengths the major determinant is plant pigmentation. Leaf reflection in the visible wavelengths appears to be a result of internal scattering and absorption processes within the leaf (Grant 1987). Healthy vegetation has chlorophyll absorption bands in the blue and red regions leaving only green reflection of any significance (Figure 3.2).

The most notable feature in the reflectance curve is the sharp change between 680-750 nm, termed the ***red-edge*** (Figure 3.2). This reflectance shift results from two optical properties of the plant's tissue: high internal leaf scattering causing large near infrared reflectance and chlorophyll absorption giving low red reflectance.

The relationship between red and NIR canopy reflectance has resulted in the development of numerous remote sensing vegetation indices and biomass-estimating techniques that concentrate on the visible and the NIR region. Some of them will be described later.

### 3.2.1 Influencing parameters

#### 3.2.1.1 Leaf structure

Leaf reflectance spectra are influenced by leaf structure (Leopold and Kriedemann 1975). Although the anatomical structure of leaves is highly variable depending upon species and environmental conditions, the basic elements are the same, and the variability of the leaf optical properties only results from their arrangement inside the leaf. The typical leaf structure is presented in Figure 3.3. Angiosperm leaves are thin and may be only a few cells thick (Sitte *et al.* 2002). Incoming sun radiation interacts with the leaf surface, which consists of leaf epidermis covered by the cuticule, a waxy layer of variable thickness that is sometimes covered by hairs to reduce intensity of incident radiation and to guard against excessive plant water loss.

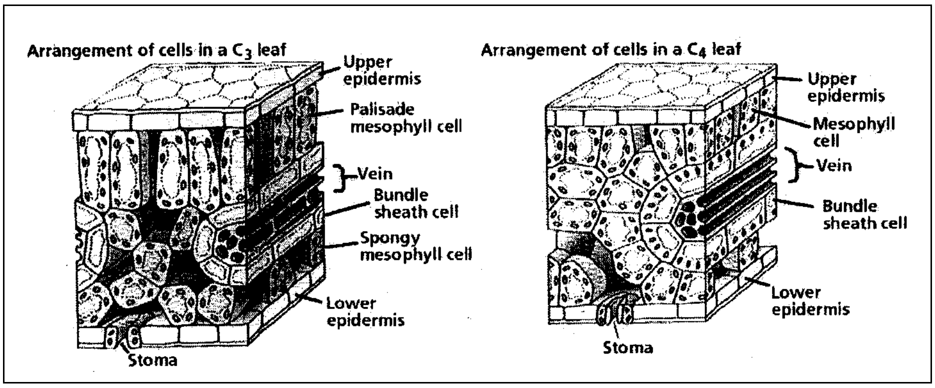


*Figure 3.3: Leaf structure of $C_3$ and $C_4$ plants. Radiance interacts with the cells of the palisade and spongy mesohyll. Pigments inside the cells reflect radiation in their respective wavelength. In contrast to $C_3$ plants $C_4$ plants have no palisade mesophyll cells what modifies the reflectance characteristics (Kumar et al. 2001).*

Much of the visible and NIR radiation is transmitted through the upper epidermis and cuticule (Jensen 2000). The transmitted radiation then interacts with cells and intercellular air spaces. Scattering is induced by the different organelles in the leaves, e.g. mitochondria, ribosomes, nuclei, starch grains, and other plastids. The internal leaf structure varies for different plant types and according to the difference in mechanisms for $CO_2$ fixation it is differentiated between $C_3$ and $C_4$[20] plants. Most plants are $C_3$ plants. $C_4$ plants show special adaptation in photosynthesis to dryness and intensive sun radiation (Sitte *et al.* 2002). The latter differs mainly due to more pronounced bundle sheaths that are particularly rich in plastids and the absence of the palisade mesophyll (Figure 3.3).

The main cell structure component considered in the context of radiation is the mesophyll that is differentiated into palisade and spongy mesophyll cells (Figure 3.3) (Sitte *et al.* 2002). In general, cellular structures in a leaf are large compared to wavelengths of light that interacts with them. Palisade cells, below the upper epidermis (Figure 3.3), are greater than wavelengths in the visible spectrum (15000 to 60000 nm) and the whole of palisade cells, the

[20] Typical $C_4$ plants are maize, sugarcane, some millet plants as well as some of Chenopodiaceae, Euphorbiaceae, Portulaceae and Amaranthaceae and halophytes (Sitte *et al.* 2002).

palisade parenchyma, consists in up to two or four dense layers (Sitte *et al.* 2002). In contrast, spongy mesophyll cells, located between the palisade cells and the lower epidermis, are smaller and less dense than the palisade cells. Intercellular air spaces account for up to 90 % of the volume of mesophyll cells (Sitte *et al.* 2002). The palisade cells contain 4/5 of the whole leaf chloroplasts with chlorophyll pigments. They are generally 5000-8000 nm in diameter and 1000 nm thick (Leopold and Kriedemann 1975). Scattering or diffraction takes place when light encounters structures whose dimensions are comparable to its wavelengths. Consequently, cellular dimensions are to large, but chloroplasts and smaller plastids are conducive to scattering.

It was reported that NIR reflectance slightly increases with increasing mesophyll thickness (Gamon and Surfus 1999). Consequently, mature or senescing older leaves tend to have a higher NIR reflectance than younger, developing leaves. Gamon and Surfus (1999) have shown that the vegetation index increases with leaf area and thickness. Accordingly, species specific characteristics such as leaf thickness influence the amount of reflected NIR as well.

#### 3.2.1.2 Leaf pigments and water content

As shown above, the spectral response of plants is linked to the content of water and pigments in the leaf cells. Water is a critical factor in plant survival and development affecting productivity, and leaf pigments are integrally related to the physiological function of leaves (Sitte *et al.* 2002). The content of the different leaf pigments can provide valuable insight into the physiological performance of leaves. Field spectroscopy[21] is commonly used to study the link between the spectral response of plants to the content of water and biochemical compounds in leafs.

Vegetation is sensitive to ultraviolet and infrared radiation and specialised to tap energy from visible radiation (between 400 and 700 nm) (Kumar *et al.* 2001, Sitte *et al.* 2002). In contrast to light in the visible region, low energy infrared light is not absorbed by plants leading to high reflectance and transmittance in the NIR.

The photosynthetic system inside a leaf cell is responsible for the fixation of carbon dioxide and tapping of the sun's radiative energy for the reduction of carbon (photosynthesis). Wavelengths of the visible spectrum are selectively absorbed mostly by chlorophylls, and other pigments, especially in the red and blue and converted to chemical energy (Gates *et al.* 1965). There exist various forms of chlorophyll and all have different properties of light absorption. Chlorophyll *a* and *b* are the most important plant pigments absorbing blue and red light (Table 3.1). Chlorophyll *a* has its absorption maxima at 490 and 660 nm and a smaller one at 420 nm, chlorophyll *b* at 435 and 643 nm (Jensen 2000). The relative lack of absorption between the main absorption maxima in the range of green light makes healthy leafs appear green to the human eye.

[21] Spectroradiometers can be both imaging and non-imaging. Non-imaging spectrometers are used for ground measurements.

*Table 3.1: Plant pigments and their absorption maxima (Kumar et al. 2001).*

| Type of pigment | Characteristic absorption maxima (nm) |
|---|---|
| Chlorophyll a | 420, 490, 660 |
| Chlorophyll b | 435, 643 |
| β-Carotene | 425, 450, 480 |
| α-Charotene | 420, 440, 470 |
| Xanthophyll | 425, 450, 475 |

The other pigments in the palisade mesophyll cells are usually masked by the abundance of chlorophyll pigments. With plant senescence the chlorophyll pigments disappear and consequently the other pigments with their representative absorption features appear and modify the signal of reflected irradiance. Changes in chlorophyll concentration produce a shift of the red-edge to shorter wavelengths. With loss of chlorophyll it shifts toward the blue part of the spectrum (Figure 3.4). The marked increase in red reflectance during senescence is due to a faster degradation of chlorophylls compared to carotenes (Sanger 1971).

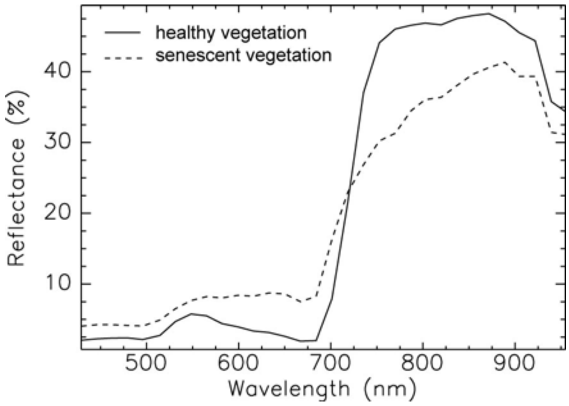


*Figure 3.4: Spectrum of a healthy tree (continuous) and a senescent tree (dashed) (spectra from CASI image).*

The main water absorption bands are centred at 2660, 2730, and 6270 nm (Jensen 2000, Kumar *et al.* 2001). The dips mainly observed at 1200, 1400, 1900 and 2500 nm are overtones. Additionally, green leaves are characterised by an intense absorption wing produced by high blue and ultraviolet absorptions. Besides the missing chlorophyll absorption feature, the reflectance spectra of dry plant material lack the intense water absorptions.

Research on leaf content of water and pigments tries to identify the wavelengths which show the best correlation between wavelengths and water and pigment content (Kumar *et al.* 2001). Besides straight correlations, different algorithms have been proposed which utilise ratios and combinations of different wavelengths. Commonly used are vegetation indices that relate the wavelengths centred on the absorption and reflectance maxima. Some are described later.

#### 3.2.1.3 Bi-directional effects

Additionally, to these internal optical leaf properties much variation in the spectral response of vegetation results from viewing geometry, characteristics of the vegetation canopy and the underlying surfaces. The geometric manner in which an object reflects energy is primarily a function of its surface roughness (Lillesand *et al.* 2004). Flat surfaces manifest mirrorlike, specular reflectance where the angle of reflectance equals the angle of incidence (Figure 3.5a,b). Diffuse or Lambertian reflectors are rough surfaces that uniformally reflect in all directions (Figure 3.5c,d). Most terrestrial surfaces are neither perfectly specular nor diffuse reflectors and remote sensing is most often interested in measuring the diffuse reflectance of objects.

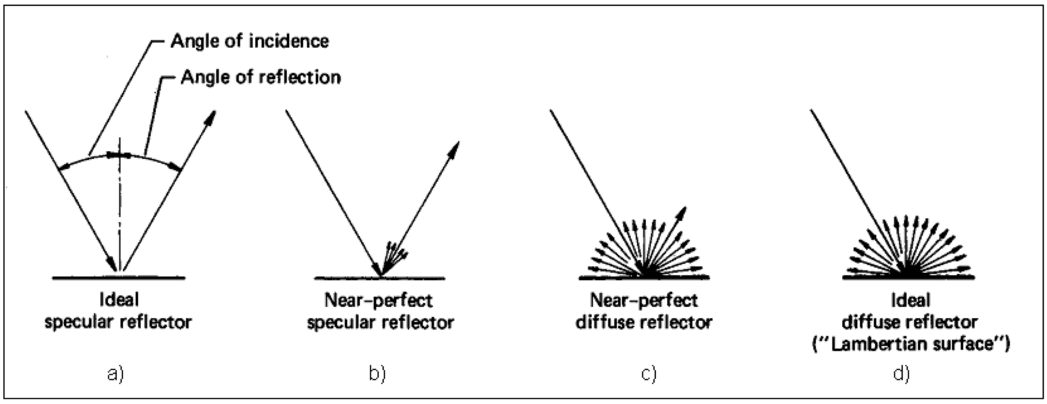


*Figure 3.5: Specular (a,b) and diffuse reflection (c,d) (Lillesand et al. 2004).*

Terrestrial surfaces have bi-directional properties (Lillesand *et al.* 2004). The term bi-directional comes from the relationship between the amount of reflected radiance with first, the geometric characteristics of the Sun's irradiance and second, the sensor viewing geometry. Depending on the specific irradiance and sensor viewing angles, most surfaces appear brighter or darker (Jensen 2000).

Research has demonstrated that vegetation canopies do not reflect incident radiant energy equally in all directions (Kimes 1983). In fact, the spectral radiant flux leaving a vegetation canopy is significantly impacted by a number of factors (Jensen 2000). Table 3.2 resumes the main factors influencing the bi-directional reflectance of a vegetation canopy. First, the illumination conditions with the angle of incidence of the incoming radiation and the azimuth are important variables. Furthermore, the wavelength range of radiation influences the reflectance from vegetation canopies. Variables linked to the sensor are its angle of view and azimuth, its sensitivity to received radiation, and its instantaneous field of view (IFOV). Besides these viewing geometry effects the characteristics of the vegetation canopy are major variables (Table 3.2). Higher vegetation objects such as trees have different spectral characteristics than herbaceous surfaces. Depending on the canopy closure the soil or surface underneath the vegetation canopy might influence the reflected irradiance. Few crown closure leads to mixed pixels. Vegetation might be arranged systematically in rows or oriented randomly. The crown shape of trees, its diameter as well as the density of trunks per area impact on the reflection of incident light toward the sensor. Another important factor is the orientation of leaves that changes throughout the day as they orient themselves toward the incident radiation. Much of the signal depends on the leaf area index (LAI) defining the area that interacts with the radiation and the surface for carbon absorption and exchange. Some canopies have substantially higher LAI than others.

*Table 3.2: Major factors influencing the bi-directional distribution function of a vegetation canopy (after Jensen 2000).*

| | |
|---|---|
| Illumination | Viewing geometry:<br>- angle of incidence of sun<br>- azimuth<br>Spectral characteristics (wavelength) |
| Sensor | Geometry:<br>- angle of view (e.g. nadir)<br>- azimuth look direction (0-360°)<br>Spectra sensitivity (wavelength)<br>Instantaneous field of view (milliradians) |
| Vegetation | Canopy :<br>- type (tree, herbaceous),<br>- closure (%)<br>- orientation (systematic, unsystematic),<br>Crown:<br>- shape (e.g. circular, conical)<br>- diameter (m)<br>Trunk or stem<br>- density (units per $m^2$)<br>- tree diameter-at-breast-height (DBH)<br>Leaf:<br>- leaf area index (LAI)<br>- leaf angle distribution (planophile, erectophile) |
| Understory | Same as vegetation |
| Soil | Texture<br>Colour<br>Moisture |

It is possible to correct such effects using the bidirectional reflectance distribution function (BRDF). It is a mathematical description of how reflectance varies for all combinations of illuminations and viewing angles at a given wavelength (Lillesand *et al.* 2004). The BRDF is extensively used in remote sensing of vegetation to model canopy brightness or radiance. The model represents how bright the canopy would appear if viewed from various directions by a sensor with a narrow field-of-view (e.g. 5°). However, most BRDF models require information about vegetation which is usually not available from remote sensing measurements (e.g. height) (Bannari *et al.* 1995).

## 3.3 Urban vegetation analysis

### 3.3.1 The use of remote sensing for urban vegetation detection

Remotely sensed images provide useful information on urban vegetation at different scales. First, regarding the typology of green spaces shown in Part I, remote sensing is valuable for the detection of land use types such us parks, cemeteries, allotment gardens. Second, besides these public green areas that are usually referenced in databases, remote sensing data allow to detect private green areas, green in courtyards, and fallow land that are not included in such databases. Consequently, it is possible to obtain information about the whole vegetation cover in an urban area what is important for environmental and ecosystem studies. A third aspect is the value for the management and maintenance of vegetation in cities. In this context, trees are of special interest. On one hand, due to their different life span compared to herbaceous plants, they are an object of long-term observations. On the other hand, their health is affected by urban environmental conditions what induces also concern about the citizen's security.

Since high spatial resolution sensors are available, remote sensing information can be used for urban vegetation analysis at fine resolution. In the following, it is shown how these data were used in the past.

### 3.3.2 Studies on urban vegetation

Urban vegetation analysis has a relatively long tradition. Colour infrared (CIR) aerial images were among the first data used to analyse the quality of urban trees and especially the vitality of trees based on colour and texture characteristics (Kenneweg 1973, Van de Garde 1976, Fuhrer *et al.* 1981). Nowadays, they are still exploited (Hermans *et al.* 2003) and CIR aerial and satellite images are still the main database used in city planning not only to delineate real estates, building objects but biotope types and trees as well.

Other research focuses on 3D reconstruction of urban vegetation and especially trees using digital elevation models (Straub and Heipke 2001, Iovan *et al.* 2007) or laser data (Haala and Brenner 1999, Hermans *et al.* 2003, Samadzadegan *et al.* 2005). In most cases they apply object-based methods to delineate tree crowns and to find tree top positions.

Besides CIR aerial and satellite images, very high spatial resolution multispectral Quickbird and Ikonos data were used to detect urban trees (Sugumaran *et al.* 2003, Ouma *et al.* 2006) or to differentiate between surface vegetation and higher vegetation (Moeller and Blaschke 2006). Other studies focused on the determination of vegetation abundance in urban areas (Small 2001, 2003, Song 2005, Buyantuyev *et al.* 2007, Nichol and Wong 2007). These studies used spectral mixture analysis to calculate vegetation cover fractions.

In more general studies on urban land use, vegetation is detected as land use or land cover class (De Genst and Canters 2004). Other studies used satellite image data for change detection of urban vegetation cover and to derive carbon storage estimates (Myeong *et al.* 2006).

The main problem concerning the detection of urban vegetation stems from the heterogeneous environment and the resolution of objects. Tree detection methods developed for forest stands perform poorly in urban environments where trees greatly vary in size and species and are rarely neighboured by the same tree (Iovan *et al.* 2007).

There exists a variety of indices, models, and algorithms developed to extract vegetation characteristics. Kumar *et al.* (2001) gives an overview of the most common methods used in airborne and field imaging spectrometry and almost all of them were developed for forest and agricultural applications. Since high spatial and spectral resolution sensors are available, research focuses also on urban areas but applications are still few compared to studies performed on forests and agricultural landscapes. Some studies used hyperspectral data to study urban vegetation and analysed land cover or biotope types (De Genst and Canters 2004, Bochow *et al.* 2007), or even identified tree species (Xiao *et al.* 2004). With this study we seek to provide a further contribution for the analysis of urban vegetation using hyperspectral images.

## 3.4 Hyperspectral data for urban vegetation analysis

### 3.4.1 Characteristics of hyperspectral data

Hyperspectral image analysis has developed in the last twenty years since the first aircraft scanners capable of recording image data in a large number of spectral bands are available (Richards and Jia 1999). The term 'hyper' refers to the high number of measured wavebands, typically hundred. For a given area imaged, the data produced by hyperspectral sensors can be viewed by a cube with two dimensions *x* an *y* that represent the spatial position and a third dimension that is defined by the wavelengths *λ* (Figure 3.6a).

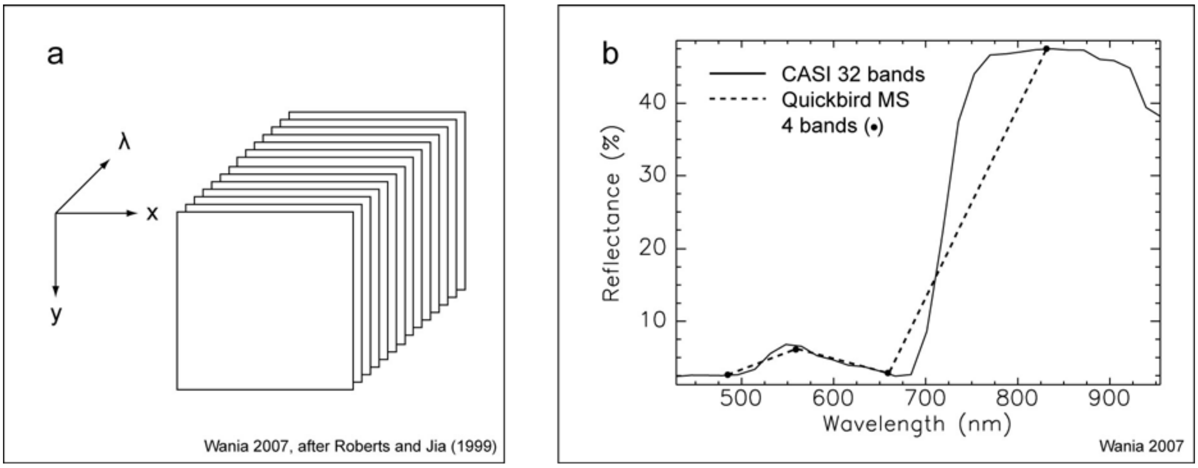


*Figure 3.6: Fine data resolution of hyperspectral image data: a) hyperspectral 'cube' of data and b) Vegetation spectrum recorded by CASI at approximately 11.5 nm spectral sampling and Quickbird MS (derived from resized CASI bands).*

Hyperspectral instruments allow a very accurate characterisation of a pixel's spectral reflectance curve. The fine spectral detail available in hyperspectral image data (or imaging spectrometer data in general) can be observed in Figure 3.6b. The figure shows the reflectance spectra of a vegetation pixel extracted from a hyperspectral and multispectral image. To derive the spectra, the hyperspectral CASI image was resized to the spectral bands of the Quickbird MS sensor (multispectral). While in the multispectral dataset the spectra is defined by four datapoints, the spectra extracted from the hyperspectral image is defined by 32 datapoints.

Currently, a number of hyperspectral sensors are available and Table 3.3 summarizes the most common of them with their spectral characteristics. Besides the numerous airborne sensors two spacecraft sensors are operative and projects are ongoing for the set up of further space-base sensors (e.g. PROBA and PRISM of the European Space Agency).

*Table 3.3: Current hyperspectral sensors and data providers (Shippert 2003). The spatial resolution is not indicated as for some sensors it depends on the chosen configuration.*

| **Satellite sensors** | **Manufacturer** | **Number of bands** | **Spectral range (in microns)** |
|---|---|---|---|
| FTHSI on MightySat II | Air Force Research Lab | 256 | 0.35-1.05 |
| Hyperion on EO-1 | NASA Goddard Space Flight Center | 220 | 0.4-2.5 |
| **Airborne sensors** | **Manufacturer** | **Number of bands** | **Spectral range (in microns)** |
| AVIRIS (Airborne Visible Infrared Imaging Spectrometer) | NASA Jet Propulsion Lab | 224 | 0.4-2.5 |
| HYDICE (Hyperspectral Digital Imagery Collection Experiment) | Naval Research Lab | 210 | 0.4-2.5 |
| PROBE-1 | Earth Search Sciences Inc. | 128 | 0.4-2.5 |
| CASI (Compact Airborne Spectrographic Imager) | ITRES Research Limited | up to 288 | 0.4-1.0 |
| HyMap | Integrated Spectronics | 100 to 200 | Visible to thermal infrared |
| EPS-H | GER-Corporation | VIS/NIR (76), SWIR1 (32), SWIR2 (32), TIR (12) | VIS/NIR (0.43-1.05), SWIR1 (1.5-1.8), SWIR2 (2.0-2.5), and TIR (8-12.5) |
| DAIS 7915 | GER Corporation | VIS/NIR (32), SWIR1 (8), SWIR2 (32), MIR (1), TIR (6) | VIS/NIR (0.43-1.05), SWIR1 (1.5-1.8), SWIR2 (2.0-2.5), MIR (3.0-5.0) and TIR (8.7-12.3) |
| DAIS 21115 | GER Corporation | VIS/NIR (76), SWIR1 (64), SWIR2 (64), MIR (1), TIR (6) | VIS/NIR (0.40-1.0), SWIR1 (1.0-1.8), SWIR2 (2.0-2.5), MIR (3.0-5.0) and TIR (8.0-12.0) |
| AISA (Airborne Imaging Spectrometer) | Spectral Imaging | up to 288 | 0.43-1.0 |

Footnotes: VIS = visible NIR = near infrared SWIR = shortwave infrared TIR = thermal infrared MIR = mid infrared

Hyperspectral sensors acquire surface information in a huge number of narrow adjacent bands. The small spectral distance between adjacent bands leads to high correlations and spectrally redundant[22] information (Richards and Jia 1999). For a particular application, much of the additional data does not add to the inherent information content even though it often helps in discovering new information. In such cases, not all of the data are necessary to characterise a pixel, but the redundancy of data is different for each application. Spectral redundancy can bee seen from the correlation matrix for an image. In Figure 3.7 grey scale levels are used to represent correlation levels in the CASI image. High correlations indicate high degrees of redundancy. The bands in the visible wavelength range are correlated; the same applies for the bands of the NIR wavelengths range. The bands covering the visible spectrum (429-514 nm) are not correlated with those covering the NIR spectrum (753-921 nm).

[22] In this context we focus only on spectral redundancy. Spatial redundancy is not considered.

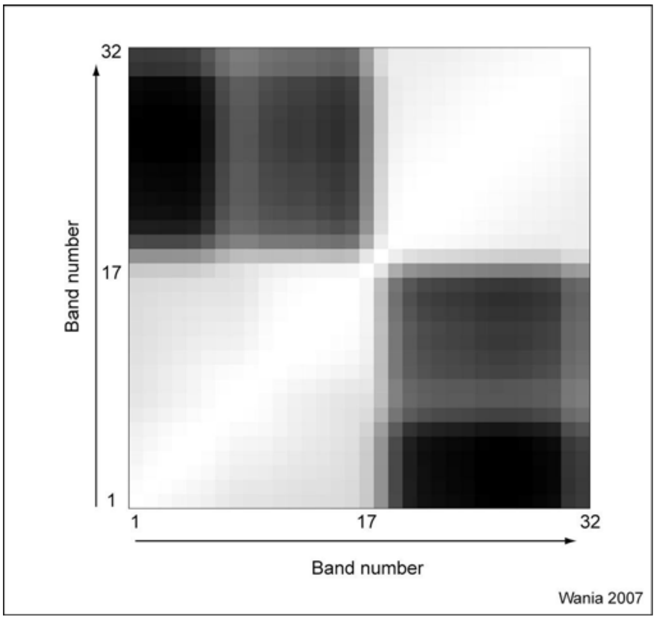


*Figure 3.7: Correlation matrix for the 32 CASI bands. White represents correlations of 1 or -1, black a correlation of 0. Band means: band 1 = 429 nm, band 17 = 701 nm, band 32 = 954 nm. The highest correlations are observed between the bands in the visible range and those in the near infrared range.*

### 3.4.2 Methods in hyperspectral data analysis

Hyperspectral images were used for different applications. Common fields are mineral mapping (Kruse 1988, Kruse *et al.* 1993b, Van der Meer 1996, Baugh *et al.* 1998) and soil mapping (Taylor *et al.* 1996, Chabrillat *et al.* 2002, Ben-Dor *et al.* 2006), vegetation mapping mainly in forests and coastal zones (De Jong *et al.* 2003, Schmidt and Skidmore 2003, Underwood *et al.* 2003, Clark *et al.* 2005), or the detection of urban objects (Saaroni *et al.* 2000, Ben-Dor *et al.* 2001, Roessner *et al.* 2001, Herold *et al.* 2003, Segl *et al.* 2003). There are many unique image analysis algorithms that have been developed to exploit the extensive information. Some of them are implemented in software programmes such as ENVI (Research Systems Inc.) or MultiSpec (Purdue Research Foundation). To map targets in images usually pixel spectra are compared with a reference spectrum. This reference spectrum is either derived from the image from one single pixel or an average of a region of interest, or they can be obtained by field measurements or spectral libraries. Common classification algorithms compare an unknown pixel with the spectral characteristics of a training sample (or reference) using statistical separation approaches (Van der Meer *et al.* 2001). The application of these methods needs special data pre-processing, as we will show later. By applying these methods, the thematic information is obtained disregarding the mostly compositional nature of surface materials. Pixel reflectance results from the spectral mixture of a number of ground spectral classes. Mixture modelling and spectral unmixing are other methods used above all in hyperspectral image analysis to map the composition of a pixel (sub-pixel).

#### 3.4.2.1 Sub-pixel mapping

Spectral unmixing offers a solution for the mixed pixel problem that remotely sensed image interpreters have to cope with (Richards and Jia 1999). It is based on the assumption that each pixel is a combination of different targets (endmembers) and sub-pixel methods are used to calculate the quantity of a target in each pixel of the image (Figure 3.8). With low spectral resolution the approach did not meet with a great deal of success because most cover types are not well differentiated in the small number of wavebands used. The approach was re-visited with the availability of hyperspectral data as they offer the possibility to uniquely characterise surface cover types by differentiating them spectroscopically. In cases of good spectral contrast between a target and its background, sub-pixel analysis can detect targets covering as little as 1-3 % of the pixel. The technique has particular relevance in minerals mapping where abundance maps for minerals of interest can be produced (Adams *et al.* 1986, Boardman 1989).

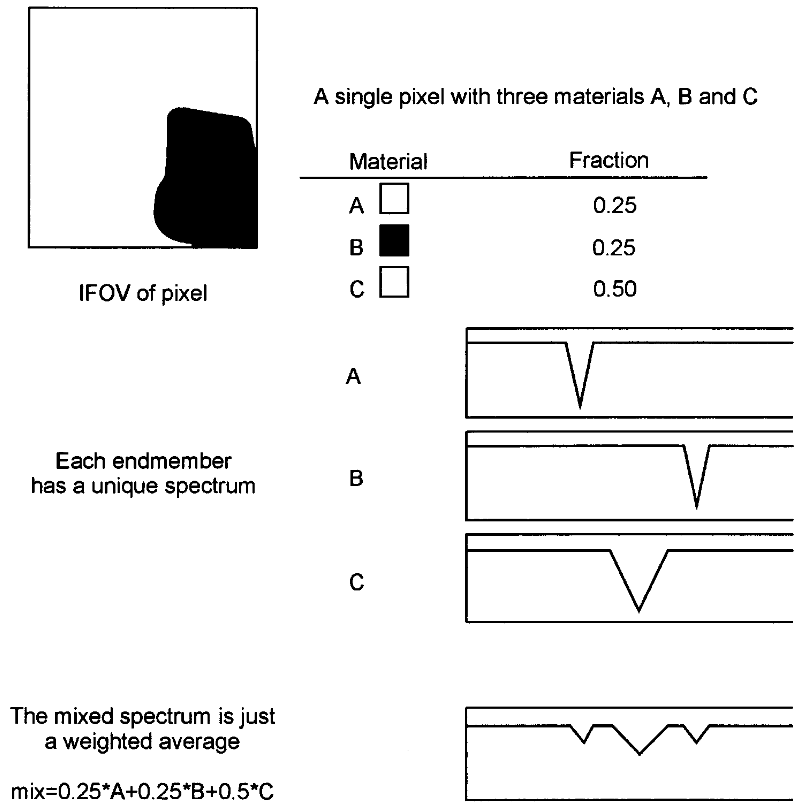


*Figure 3.8: Principle of spectral mixing and unmixing (Van der Meer et al. 2001).*

Methods for sub-pixel mapping focus either on complete or partial unmixing. The first one is based on the assumption that the reflectance spectra of a pixel is a linear combination of reflectance spectra (Adams *et al.* 1986, Boardman 1989). The second is applied when not all endmembers are known (Boardman *et al.* 1995).

### 3.4.2.2 Whole pixel mapping

Whole pixel analysis methods can be performed with the standard supervised classification algorithms or with tools developed specifically for hyperspectral image analysis such as the Spectral Angle Mapper (Kruse *et al.* 1993a). In this study, we choose to focus on the application of the Maximum Likelihood (ML) classifier that is still the most common algorithm used with remote sensing data (Richards and Jia 1999).

A serious problem with traditional supervised classification techniques that are based on the statistical approach, is the estimation of class signatures (Richards and Jia 1999). For the classification of a pixel, the ML classifier quantitatively evaluates both the variance and covariance of the class' spectral response. During data processing it is assumed that the distribution of the cloud of points forming the training data class is Gaussian (Lillesand *et al.* 2004). The spectral response pattern of a class is then described by the mean vector and the covariance matrix. Probability density functions for each class are used to classify an unidentified pixel by computing the probability (likelihood) of the pixel value belonging to each category. Finally, the pixel is assigned to the class with the highest probability value. A pixel might be labelled 'unknown' if the probability values are all below a user defined threshold.

Sufficient training samples for each spectral class must be available to allow reasonable estimates of the elements of the mean vector and the covariance matrix to be determined (Richards and Jia 1999). Additionally, the number of labelled samples for a supervised classification increases as a function of dimensionality (Landgrebe 1999). In general, for an N dimensional spectral space at least N+1 samples are required to avoid that the covariance matrix is singular (Richards and Jia 1999). A part from this condition, it is important to have as many training pixels as possible. A practical minimum of 10*N samples per spectral class is recommended (Swain and Davis 1978). This condition is particularly important as the dimensionality of the pixel vector space increases and poses clear restrictions in hyperspectral image analysis. Richards and Jia (1999) even state that 100*N samples are desirable for the training set size.

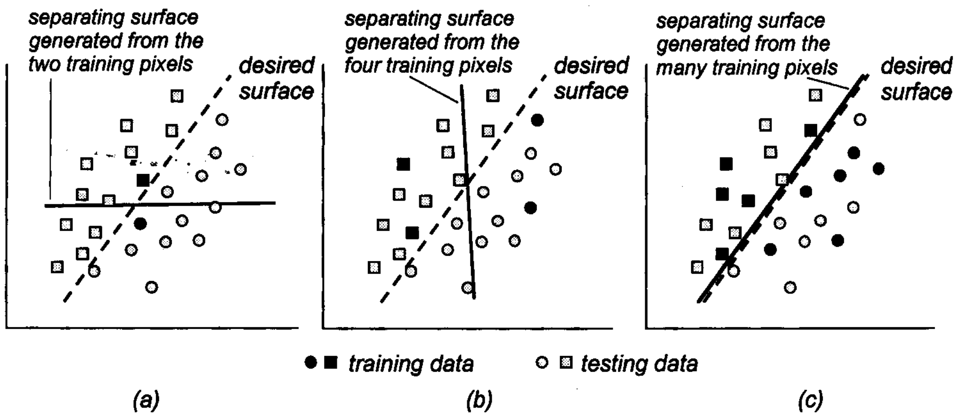


*Figure 3.9: The importance of enough training samples per class to ensure reliable estimates of class statistics for supervised classifiers such as ML. If too few pixels are used classification is possible but the training samples are not correctly classified (a). Increasing the number of samples per class improves the class separation for both training and test data (b,c) (Richards and Jia 1999).*

Figure 3.9 shows a simple example of the problem based on determining a reliable separating linear surface. Three different training sets are shown for the same two-dimensional data set. The separating surface can be found in any case but performs poorly if too few training samples are used (Figure 3.9a). The quality of the estimate increases with increased training sample size (Figure 3.9b,c).

To cope with the problem of training sample size, hyperspectral data are usually reduced in dimensionality before applying a ML classifier. Besides this reason, dimensionality reduction is also performed to cope with the 'Hughes phenomenon' that will be described in the following.

### 3.4.2.3 Dimensionality reduction

#### *3.4.2.3.1 The problem of dimensionality*

As stated above, the training of a supervised classifier needs a minimum ratio of the number of training pixels to the number of spectral bands to ensure reliable estimates of class statistics. Accordingly, with increasing band number, the size of the training set has to be increased. However, with a fixed training sample size, the accuracy of a classification increases first with increasing number of measurements (bands), but decay with measurement complexity higher than some optimum value (Figure 3.10). The performance of the classifier is compromised by the poor estimates of the training statistics beyond about ten features[23]. This phenomenon was termed 'Hughes phenomenon' since it was first described by G. Hughes in the late 1960 (Hughes 1968).

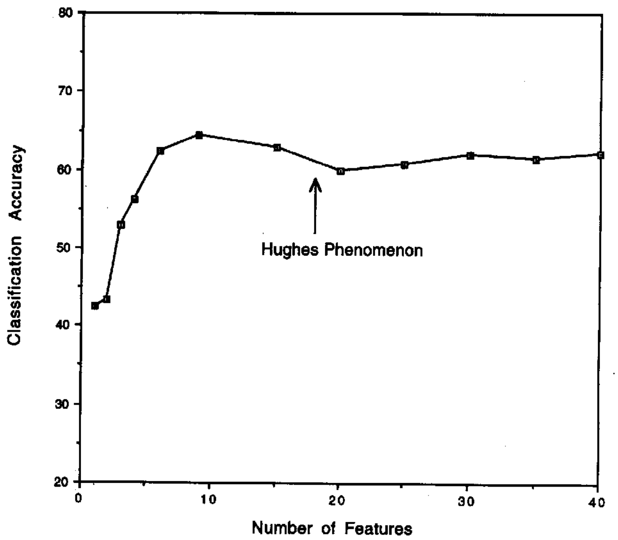


*Figure 3.10: The Hughes phenomenon: the loss in classification accuracy beyond a certain number of bands (features) (Richards and Jia 1999).*

Methods to cope with the problem of dimensionality and redundant information focus on reducing the number of features. Moreover, feature reduction reduces also further processing. There exist two main groups of processing techniques: a first group aims at feature selection and a second group at feature extraction.

#### *3.4.2.3.2 Feature selection*

Feature selection techniques evaluate the existing set of features for the pixel data concentrating on the selection of the most discriminating features (Richards and Jia 1999). In the present study, two feature selection procedures were used. The first one is based on a common class separability measure and the second one is a new unsupervised classification algorithm that was examined for band selection in hyperspectral image analysis.

[23] In the field of remote sensing features are image bands or channels.

***Bhattacharyya distance***

Typically, the Bhattacharyya selection method is used to evaluate the separability between two classes. In the multispectral remote sensing context, the Bhattacharyya distance has shown to be an appropriate predictor of classification accuracy (Landgrebe 1999) and is commonly used to predict the accuracy of a classification from the training samples of the defined classes. For the two-class case of a Gaussian data, the definition of Bhattacharyya distance is (Fukunaga 1990):

$$B=\frac{1}{8}\left(M_j-M_i\right)^T\left\{\frac{\Sigma_i+\Sigma_j}{2}\right\}^{-1}\left(M_j-M_i\right)+\frac{1}{2}\ln\left\{\frac{\left|\frac{\Sigma_1+\Sigma_2}{2}\right|}{\sqrt{\left|\Sigma_i\right|}\sqrt{\left|\Sigma_j\right|}}\right\} \qquad \text{Equation 1}$$

where $M_i$ and $M_j$ are the mean vectors[24] and $\Sigma_i$ and $\Sigma_j$ the covariance matrices of classes *i* and *j*. The first term of Equation 1 accounts for the difference between the two distributions due to the mean vector and describes the separation of the classes. The second term accounts for the difference between the two covariance shifts and measures the portion of the separation due to the differences in the covariance matrices.

The results of the Bhattacharyya selection method consist in an evaluation of pair-wise class separability and the identification of the most discriminating bands. Subsets of bands are then listed in descending order according to the minimum of the weighted interclass distance values.

In this study the Bhattacharyya distance is used to select bands based on defined training sets and to compare the selected subset with that one identified by the Modular Approach for Clustering with Local Attribute Weighting (MACLAW).

***Modular Approach for Clustering with Local Attribute Weighting***

Recently, an unsupervised classification algorithm with feature weighting was developed that might be potentially useful for feature selection in hyperspectral images (Blansché *et al.* 2006). The Modular Approach for Clustering with Local Attribute Weighting (MACLAW) is based on a new approach called Modular Approach for Clustering. This approach consists in extracting the different object classes independently. A modular classifier is composed by several extractors ($X_k$, one for each class) (Figure 3.11). Each extractor provides a class from the dataset ($C_k$). The aim of an optimisation algorithm in the modular approach is to identify extractors that provide a good clustering or classification. The MACLAW method is a specialisation of the modular approach for classification which searches for the best local feature (band) weights to extract classes (Figure 3.11). To optimise the local feature weights, it uses a co-evolutionary algorithm. The global solution then consists of different classes together with their associated weight vectors (one for each band and class).

[24] T denotes the transpose of the vector.

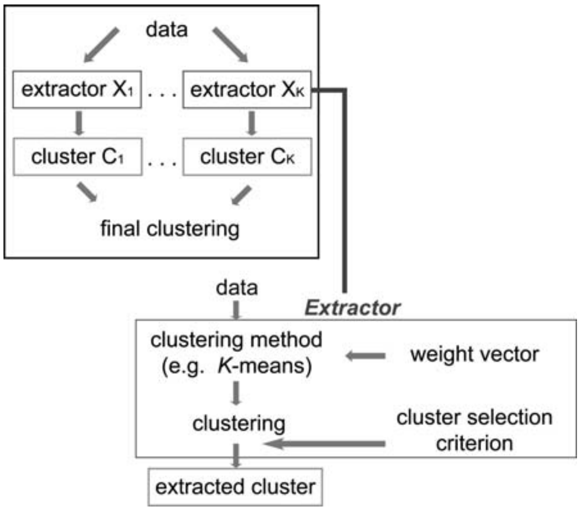


*Figure 3.11: Principle of the MACLAW algorithm. A modular classifier is composed by several extractors ($X_k$) that provide classes ($C_k$) from the dataset. The algorithm searches the best local feature weights (weight vector) to extract classes.*

MACLAW is an unsupervised method to discover classes in image data while at the same time the algorithm provides the most relevant bands what helps reducing the dimensionality. In contrast to most feature selection methods that need expert knowledge (Warner and Shank 1997, Serpico and Bruzzone 2001, Groves and Bajcsy 2003) MACLAW needs no knowledge *a priori*. As such, it can be a useful tool that helps to explore the information content in hyperspectral images and can be used to mark training areas.

The algorithm has been validated on large data sets others than images (Blansché *et al.* 2006). Recently, the algorithm was tested on a small image extract from DAIS radiance data for four classes (Gançarski *et al.* 2008). With the tests of this study the capacities for further use in hyperspectral image analysis have been evaluated on a larger image extract and on more classes. The algorithm was tested on an image extract to discover all possible land use/ land cover classes. It was not used to discover only spectrally similar classes.

#### *3.4.2.3.3 Feature extraction*

Another method to reduce the dimensionality of an image is feature extraction. It consist in a transformation of data to a new set of features in which separability is higher in a subset of the transformed features than in any subset of the original data (Richards and Jia 1999). In this study three different feature extraction algorithms were examined. They are all linear transformations, namely Minimum Noise Fraction transformation (MNF) and two class-dependent extraction methods: Discriminant Analysis Feature Extraction (DAFE) and Decision Boundary Feature Extraction (DBFE).

***Minimum Noise Fraction transformation***

The MNF transformation is a two-step principal component (PC) transformation. PC transformation is commonly used to minimise the influence of band to band correlations and to investigate variance partitioning of multiband images (e.g. Richards and Jia 1999). The transformation is based upon the global means and covariance matrix of the full set of image data.

PC transformation produces a space in which data has most variance along the first axis, the next large variance along the second mutually orthogonal axis, and so on. The low order PCs are expected to show little variance. The PC image data values are linear combinations of the original data values multiplied by the appropriate transformation coefficients that are statistical quantities known as eigenvectors or PC (Lillesand *et al.* 2004). Figure 3.12 shows a two band data example. A random undifferentiated sample of pixels is plotted on the spectral space defined by band A and B. Superimposed are two new axes I and II that are rotated with respect to the original measurement axes and that have their origin in the mean of the data distribution. These axes indicate the direction of the principal components.

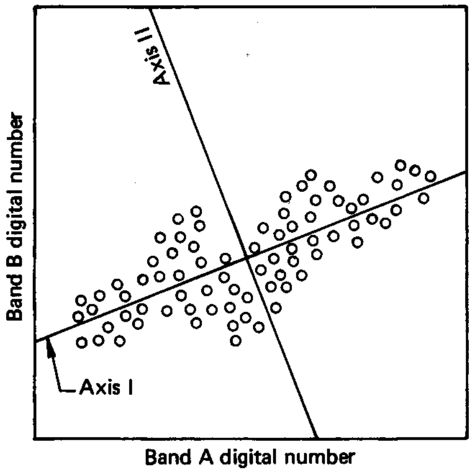


*Figure 3.12: Undifferentiated sample of pixels in a two-dimensional spectral space and position of new rotated axes that indicate the direction of two principal components (Lillesand et al. 2004).*

As PC transformation makes use of a global mean and covariance, the enhancement technique is particularly appropriate where little prior information concerning a scene is available (Lillesand *et al.* 2004). Consequently, it is not sensitive explicitly to class structure in the data. However, instead of usig the global covariance matrix, a subset with the cover types of interest can be selected in the image and used for the calculation.

The MNF transformation is based on the PC transformation. Besides the information reduction due to band correlations the noise is additionally reduced (Green *et al.* 1988). It is assumed that noise is spatially uncorrelated and that the information content is related to spatially correlated variance. The transformation seeks to diagonalise the noise covariance matrix prior to the PC transformation thereby reducing the effect of band-specific noise sources (Small 2001). The method consists in two cascaded PC transformations (RSI 2004). Accordingly, the first PC transformation decorrelates and rescales noise in the data. The second is a standard PC transformation of the noise-whitened data (RSI 2004). Like for the simple PC transformation, the inherent dimensions are reduced to only a few bands with high eigenvalues and coherent spatial information. The criterion of eigenvalue is commonly used and bands with eigenvalues below one explain no relevant variance.

The noise statistics can be estimated from sensor calibration measurements or derived from the image by defining a homogeneous area within the scene. The latter underestimates in most cases the signal-to-noise ratio since interpixel variability contributes to the noise component (Van der Meer *et al.* 2001).

The MNF transformation is implemented in the software ENVI® and was performed with the version 3.4 (Research Systems Inc. 2006).

***Discriminant Analysis Feature Extraction***

In case that information about particular features in the image are available, other feature extraction methods might be better suited, such as Discriminant Analysis Feature Extraction (DAFE). It is also referred to canonical analysis or multiple discriminant analysis (Richards and Jia 1999, Lillesand *et al.* 2004). The method aims to optimize class separation. Instead of using the global covariance matrix DAFE is based on the among-class and within-class covariance matrix. As mentioned above in the PC transformation the new axes were located on the basis of a random undifferentiated sample of pixels. In contrast, in DAFE the canonical axes have been positioned such that classes previously defined have their largest possible separation between their means (among class variance) when projected to an axis, while at the same time they should appear as small as possible in their individual spreads (within class variance). Accordingly, a canonical axis has to be defined to maximize the ratio

$$\frac{\sigma_A^2}{\sigma_W^2} = \frac{among \quad class \quad \text{var}iance}{within \quad class \quad \text{var}iance} \qquad \text{Equation 2}$$

where σ is the standard deviation (Richards and Jia 1999). Figure 3.13 shows a simplified two-class example. Illustrated is the lack in separability in either original bands or few separability in a principal component (Figure 3.13a). The new canonical axis is calculated such that the classes have the largest possible separation between their means when projected onto the axis ($\sigma_A^2$) while at the same time they should appear as small as possible in their within class spread ($\sigma_W^2$) (Figure 3.13b).

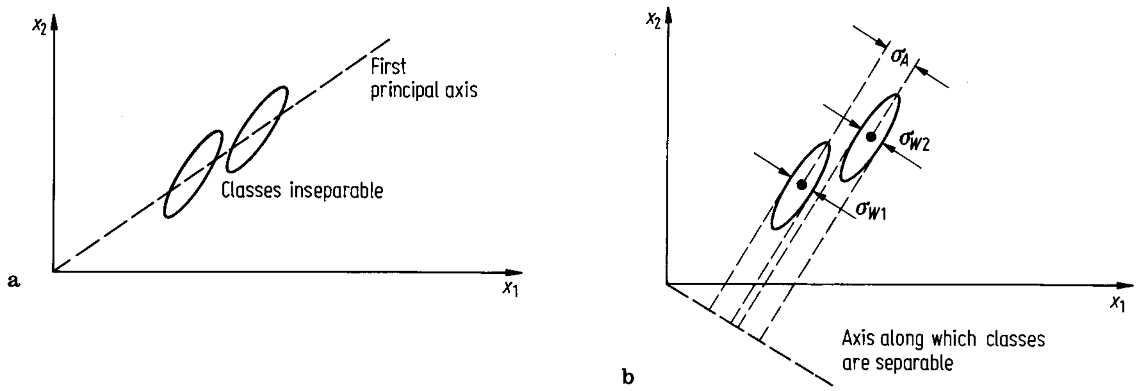


*Figure 3.13: Differentiated classes in a two-dimensional space: a) lack of separability in either original bands or in a principal component, and b) new canonical axis along which classes are separable (Richards and Jia 1999).*

As for the PC transformation, the first canonical axis will have the largest ratio of variances and the classes will have maximum separation. The second axis corresponding to the next largest ratio of variances will provide the next best degree of separation, and so on.

DAFE provides the best results to achieve satisfactory classification if the number of features to achieve satisfactory classification is less than the number of classes (Landgrebe 1999). This implies that in any case the dimensionality of the transformed feature space will be less than that of the original data (Richards and Jia 1999). Consequently, canonical analysis provides class separability with reduced dimensionality.

The method has two significant limitations (Landgrebe 1999). First, DAFE becomes ineffective if the classes involved have very little difference in mean values. Remember that classes, especially high dimensional ones, can be better separated based on their covariance matrices alone. From the ratio of variances it is apparent that in the case where class means have small differences but the classes can be substantially separated based on their covariances, this would affect the efficacy of the transformation. The second limitation stems from the above mentioned condition that the transformation provides reliable features up to one less than the number of classes what poses problems in applications with a low number of classes.

DAFE is implemented in the freeware software MultiSpec© (version 5.2001, Purdue Research Foundation, West Lafayette, Indiana).

***Decision Boundary Feature Extraction***

Like DAFE the Decision Boundary Feature Extraction (DBFE) is a class-dependent linear transformation (Lee and Landgrebe 1993). In contrast to DAFE, where the transformation was based on the mean vector and covariance matrix, the transformation is directly based upon the training samples. Consequently, DBFE has not the limitations mentioned for DAFE and a major advantage is that the transformation does not deteriorate when the mean or covariance differences are small. The algorithm predicts the minimum number of features needed to achieve the same classification accuracy as in the original space.

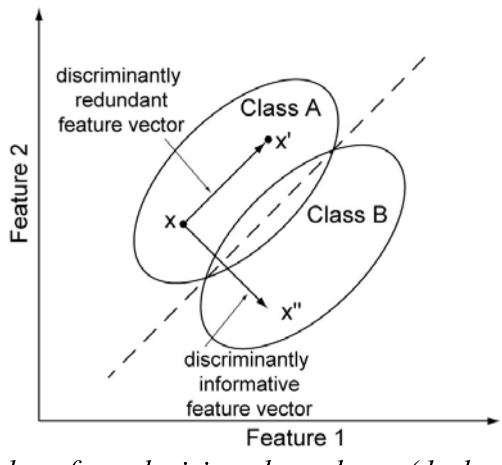


*Figure 3.14: The principle of a decision boundary (dashed) with an example of a discriminantly redundant and a discriminantly informative feature vector. As the observation X moves along the direction of the redundant feature vector (X'), the decision will be the same. In contrast, as X moves along the direction of the informative feature vector (X''), the classification result of the observation is changed. The effective decision boundary is the intersection of the boundary and the regions where most of the data are located (Lee and Landgrebe 1993).*

Decision boundaries are placed directly on the training samples using a definition for discriminantly informative and discriminantly redundant features (Figure 3.14). Then, with the effective portion of that decision boundary, an intrinsic dimensionality for the problem is determined[25]. A transformation is then defined which enables the calculation of the optimal features. The eigenvalues of the transformed features give a direct indication of how valuable each new feature will be.

The calculation of DBFE is longer than for DAFE, especially if the training set has many samples (Landgrebe 1999). In contrast to DAFE, DBFE provides satisfactory classification results if the number of features is greater than the number of classes (Landgrebe 1999). However, there is one limitation. As DAFE directly operates on the training sets, it tends to be ineffective when the training set is small (Landgrebe 1999).

Like DAFE, DBFE is implemented in the freeware software MultiSpec© (version 5.2001, Purdue Research Foundation, West Lafayette, Indiana).

#### 3.4.2.4 Summary on performed dimensionality reduction methods

In the present study, the relevance of the different feature selection and extraction algorithms for the detection of spectrally similar vegetation classes and urban vegetation in general is examined. We compare one a feature selection and two feature extraction methods that are based on class specific information with an extraction and a selection method that are based on the global dataset (Table 3.4). While MNF, DAFE, and DBFE are used for the extraction of vegetation objects (cf. 3.5), the two feature selection algorithms are used for the analysis performed to extract all possible land use/ land cover classes (built and non-built) (cf. 3.6) (Table 3.4).

*Table 3.4: Comparison of the examined feature selection and extraction methods and their application in the present work.*

| | **Bhattacharyya distance** | **MACLAW** | **MNF** | **DAFE** | **DBFE** |
|---|---|---|---|---|---|
| Training sample | Class means and covariances | Independent | Independent | Class means and covariances | Class means |
| Training sample characteristics | Ineffective when little differences between samples | Independent | Independent | Ineffective when little difference in means | Ineffective for small training sets |
| Number of features | User dependent, the best subset depends on the distance measure chosen for the selection (e.g. minimum, maximum or average) | User dependent | Eigenvalues | Eigenvalues, ideally feature nb < nb classes | Eigenvalues, ideally feature nb > nb classes |
| Application within this work | 1) Extraction of different land use/ land cover classes | 1) Extraction of different land use/ land cover classes | 1) Extraction of vegetation classes 2) Extraction of different land use/ land cover classes | 1) Extraction of vegetation classes 2) Extraction of different land use/ land cover classes | 1) Extraction of vegetation classes 2) Extraction of different land use/ land cover classes |

MACLAW Modular Approach for Clustering with Local Attribute Weighting, MNF Minimum Noise Fraction transformation, DAFE Discriminant Analysis Feature Extraction, DBFE Decision Boundary Feature Extraction

[25] Intrinsic discriminant dimensions can be seen as the smallest dimensional subspace wherein the same classification accuracy as in the original space can be obtained (Lee and Landgrebe 1999).

The motivation to test both class dependent feature extraction methods (DAFE and DBFE) for the vegetation analysis mainly stems from the problems encountered with the training sample definition (cf. 3.5.4.1). Vegetation objects are a priori spectrally similar what might affect on one hand the efficacy of DAFE, but on the other hand DBFE is ineffective for small training sets. As will be described later, the size of the training samples that could be defined is rather small.

## 3.5 Urban vegetation analysis with CASI data

In the frame of this study we evaluate the potential to identify discriminating features of urban vegetation cover from hyperspectral imagery. The analysis is performed using an image acquired with the Compact Airborne Spectrographic Imager (CASI) in 32 spectral bands. We hypothesise that these high spectral resolution data provide valuable information on urban vegetation and even more than multispectral data. A two-class differentiation between herbaceous and tree/shrub vegetation objects is usually possible with multispectral data using texture information. In such cases high spectral resolution data are not necessarily needed. In contrast, with their fine spectral resolution hyperspectral data potentially should allow to discriminate between different vegetation objects of the same class such as different tree or shrub species. Figure 3.15 illustrates this potential at the example of trees. The spectral signatures of three different species are compared in the hyperspectral CASI data used in this study (Figure 3.15a) and multispectral data derived from these data (Figure 3.15b, for band definition of the multispectral data see 3.5.4.4). Two trees are healthy (points and continuous), the third one is a senescing tree that shows generally lower reflectance values (dashed). The comparison of both figures reflects the potential of high spectral resolution data. The hyperspectral data show much more detail than the low spectral resolution data and reveal differences between species that are less evident in the multispectral data set. Furthermore, although in the multispectral data set it is possible to differentiate between the senescing and healthy trees, the difference between the two healthy ones is less evident.

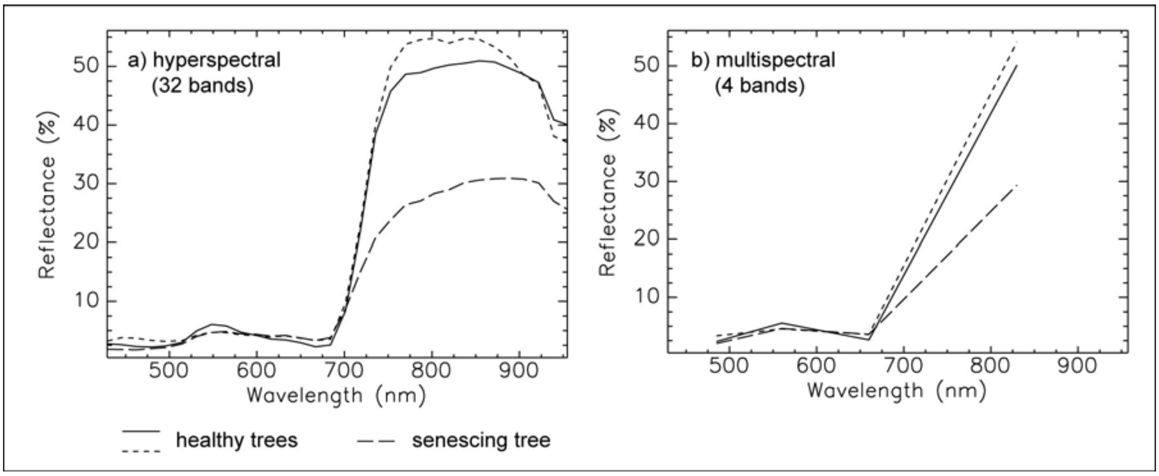


*Figure 3.15: Comparison of reflectance spectra for three different trees in (a) hyperspectral and (b) multispectral image data (multispectral data resized from hyperspectral data): two healthy trees (continuous and points) and one senescing tree (dashed).*

Since some decades researchers try to detect urban trees and their health status. Although hyperspectral images do not (yet) show the same very high spatial resolution like multispectral airborne images, they are potentially interesting to provide information on species types and health. They could, for example, provide valuable information for the creation and updating of tree databases that still needs extensive fieldwork.

The literature review has shown that until now very few studies have focussed on urban applications using hyperspectral data. Outside urban areas studies on the discrimination of vegetation types and species with high spectral resolution data yielded promising results (Schmidt and Skidmore 2003, Underwood *et al.* 2003, Clark *et al.* 2005). To our knowledge, the only study performed in urban areas to discriminate plant species was performed by Xiao *et al.* (2004).

Despite the advantage of high spectral resolution it is important to underline that we are dealing with spectrally similar objects whose discrimination is a special challenge in remote sensing. Nevertheless, some studies have shown that discrimination is possible (e.g. Schmidt and Skidmore 2003). In contrast to minerals that show different absorption peaks, healthy vegetation objects have all nearly the same absorption features as described in the beginning. Additionally, most methods developed for high spectral resolution data analysis (imaging and field spectrometry) were intended for applications others than vegetation analysis like mineral mapping where most pioneer work was done (e.g. Kruse 1988).

In the following, the results of a study on urban vegetation using hyperspectral image data are presented. The main objective is to evaluate the possibility to detect urban vegetation with the available dataset, to identify discriminanting features and to compare the performance with that one of multispectral image data.

### 3.5.1 Data

The following analysis was performed on a subset of a CASI-2 image acquired during a hyperspectral flight campaign in September 2005 on the city of Strasbourg (France). The sensor was provided by the company Actimar (Brest, France). Field measurements were performed during the flight campaign. The 220 acquired field spectra cover built and non-built surfaces. They were analysed and organised to built a database for multistrategic and multiscale image analysis and are not presented any further in the frame of this work (Wania *et al.* 2006b see Annex).

The image was acquired in 32 bands covering the spectral range between 429 and 954 nm (Table 3.5). The bandwidth varies between 11.4 and 11.8 nm (FWHM Table 3.5). The spatial resolution of the image is 2 m. The very high spatial resolution of the image was defined as a priority for the configuration of the sensor.

*Table 3.5: Definition of the 32 spectral bands in the CASI-2 image (FWHM = full width half mean expresses the band width) (Thomas and Lennon 2005).*

| | **Band N°** | **Wavelength (nm)** | **FWHM (nm)** | | **Band N°** | **Wavelength (nm)** | **FWHM (nm)** |
|---|---|---|---|---|---|---|---|
| UV | 1 | 429.10 | 11.4 | Near Infrared | 17 | 701.20 | 11.8 |
| Blue | 2 | 445.70 | 11.4 | | 18 | 718.40 | 11.8 |
| | 3 | 462.40 | 11.4 | | 19 | 735.50 | 11.8 |
| | 4 | 479.10 | 11.4 | | 20 | 752.70 | 11.8 |
| | 5 | 495.90 | 11.6 | | 21 | 769.90 | 11.8 |
| Green | 6 | 514.50 | 11.6 | | 22 | 787.20 | 11.8 |
| | 7 | 531.30 | 11.6 | | 23 | 802.50 | 11.8 |
| | 8 | 548.20 | 11.6 | | 24 | 819.80 | 11.8 |
| | 9 | 565.10 | 11.6 | | 25 | 837.10 | 11.8 |
| | 10 | 582.00 | 11.6 | | 26 | 854.40 | 11.8 |
| Yellow | 11 | 599.00 | 11.6 | | 27 | 871.70 | 11.8 |
| Red | 12 | 615.90 | 11.6 | | 28 | 889.00 | 11.8 |
| | 13 | 632.90 | 11.6 | | 29 | 904.50 | 11.8 |
| | 14 | 650.00 | 11.6 | | 30 | 921.90 | 11.8 |
| | 15 | 667.00 | 11.6 | | 31 | 939.30 | 11.8 |
| | 16 | 684.10 | 11.8 | | 32 | 954.70 | 11.8 |

The whole of the acquired image covers 143 km². In the centre of the image is the city of Strasbourg and the boarders reach its outskirts and partly the rural areas. For the vegetation analysis the image was subset to an area of 1825 x 1438 pixels covering half of the densely built city centre and two city districts. Figure 3.16 shows the image subset and the whole CASI image. The image data was provided by Actimar in apparent reflectance with atmospheric correction.

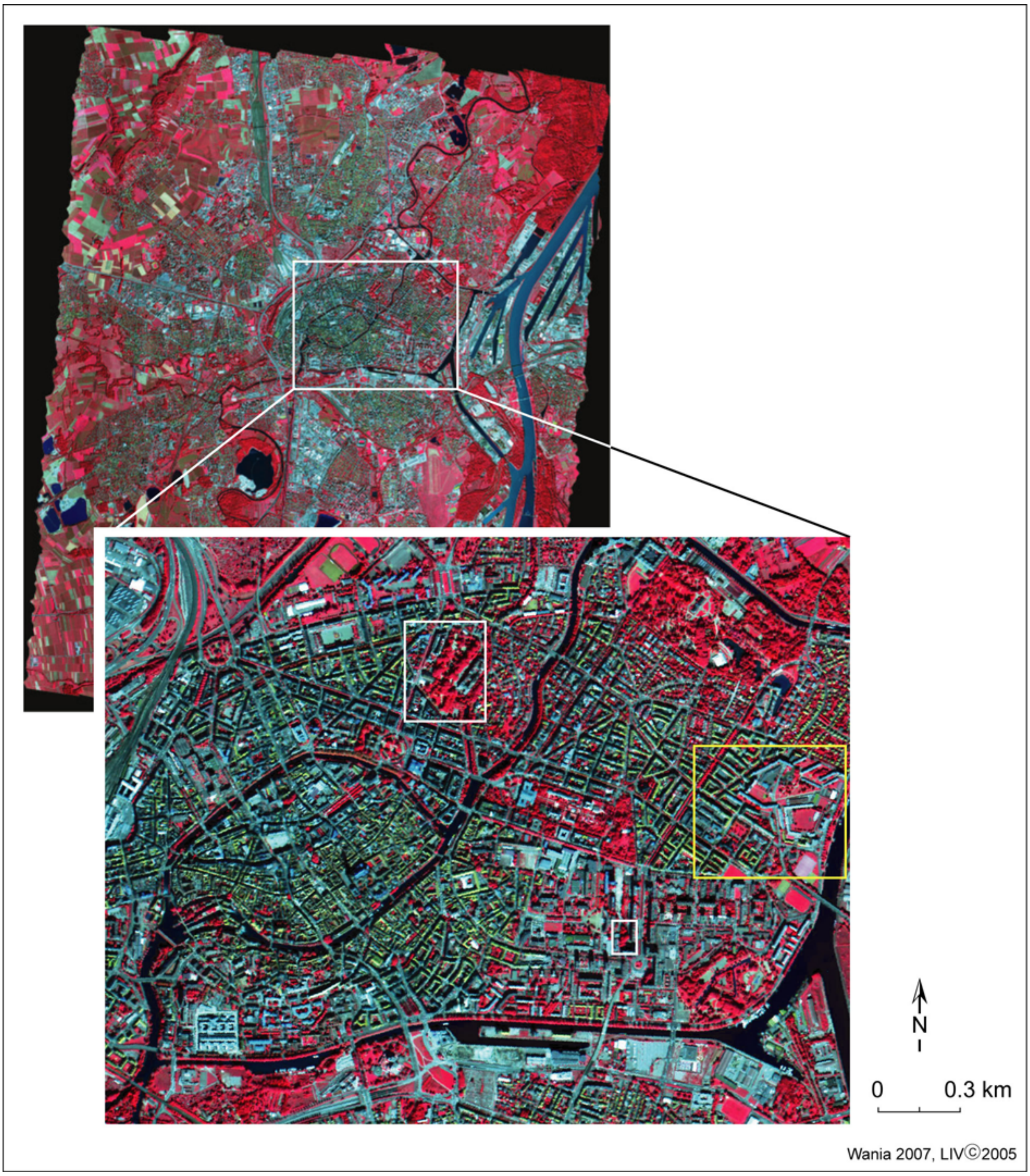


*Figure 3.16: Extract from the analysed CASI-2 image. It covers mainly the city centre surrounded by the river Ill and the old city districts in the north, northeast, and south as well as a new district in the east. The two smaller white rectangles show extracts that were used for the presentation of results from the vegetation analysis. The yellow rectangle indicates the location of the extract used for the validation of the unsupervised feature selection algorithm MACLAW (see 3.6).*

### 3.5.2 Spectral properties of urban vegetation cover

In the following paragraph characteristics of urban vegetation as observed in the CASI image are examined. The focus is on the differences between different vegetation objects (e.g. small or big tree, lawn or tree) and species, as well as the underlying soil. In a first step, considerations about the basic perturbations occurring in urban areas are described. They are important for the understanding of the radiometric characteristics of urban vegetation.

#### 3.5.2.1 Specific radiative features of urban areas

Image acquisition over urban areas is characterised by specific features that affect incoming and reflected radiation. The amount of total radiation impinging on the surface is the sum of direct, diffuse, and reflected radiation, as well as reflections induced by the environment (Figure 3.17) (Lhomme 2005).

The amount of direct radiation (Figure 3.17a) is a function of the zenith angle of the sun, the inclination of the object and the atmospheric transmission (Lhomme 2005). The solar angle depends on the time of image acquisition and directly influences radiation (Lillesand *et al.* 2004). Accordingly, higher sun elevation leads to higher illumination of the target. The inclination of an object is defined by the angle between the surface's normal and the direction of the sun. Besides global effects of atmospheric transmission the urban atmosphere is disturbed by urban air pollution. The different gases and aerosols contribute additionally to atmospheric scattering and absorption and in general, air pollution leads to a general reduction of incoming solar radiation (Oke 1987). Diffuse radiation is induced by gases and aerosols and depends on solar radiation, the density of the atmosphere and the angle of irradiance (angle defining that part of the sky that is visible from the target's objective) (Figure 3.17b). The urban roughness reduces the angle of irradiance.

Reflections from surrounding areas and diffusion from the atmosphere are effects induced by the environment of an illuminated target (Figure 3.17c) (Lhomme 2005). They depend on the atmospheric diffusion and the characteristics and topography of the target's environment. Increased roughness in the urban environment contributes to such effects. Radiation received by a target might also be a result of reflections from neighbouring high rising objects (canyon effect, Figure 3.17d). Finally, shadow affects the quantity of radiation received at the surface and the consequence is total or partial absence of solar irradiation (Figure 3.17e). Shadow depends on the height of the relief, the angles of solar irradiance and the composition of the atmosphere. It can be induced by clouds or increased roughness and the latter is especially high in urban areas. Shadow contributes to the spectral signature of a pixel and affects the interpretation (Takashi *et al.* 2002, Dare 2005, Lhomme 2005). In very high spatial resolution images shadow appears as a distinct class.

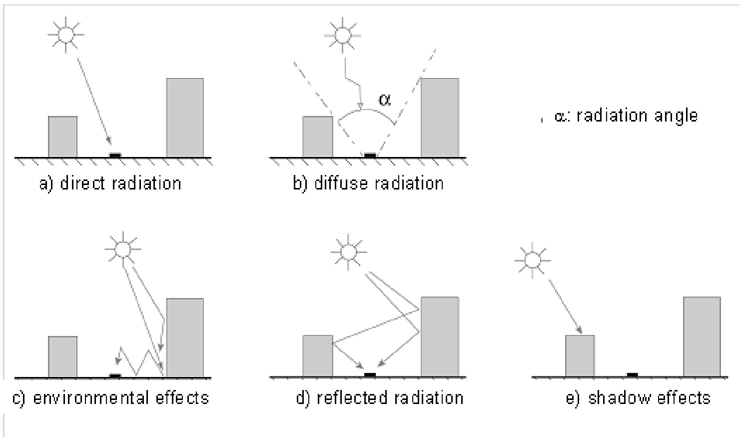


*Figure 3.17: The different elements of radiation in urban areas (Lhomme 2005).*

In the case of very high spatial resolution images, the urban roughness, geometry, topography, and the heterogeneity of materials induce a high frequency of local variations, resulting in geometric and radiometric errors that might lead to thematic errors (Lhomme 2005).

#### 3.5.2.2 Vegetation specific features

Besides these influences, the reflectance spectrum of an object is influenced by the relationship between the object's size and the spatial resolution of the image. If an object is larger than the pixel's size it is decomposed into several pixels (Figure 3.18c). Objects or portions of objects smaller than the pixel's size are represented as mixed pixels what modifies the initial spectrum. To illustrate the relationship between object's size and spatial resolution of the image, an extract from the CASI image (2 m) in Figure 3.18a is compared with the same extract taken from an aerial photograph with 0.5 m resolution in Figure 3.18b. The extract shows a double row of street trees with closed crowns and two parallel tree rows of smaller trees beside. In the aerial photograph the small trees appear as circular objects while in the CASI image a pixelisation of the object can be observed.

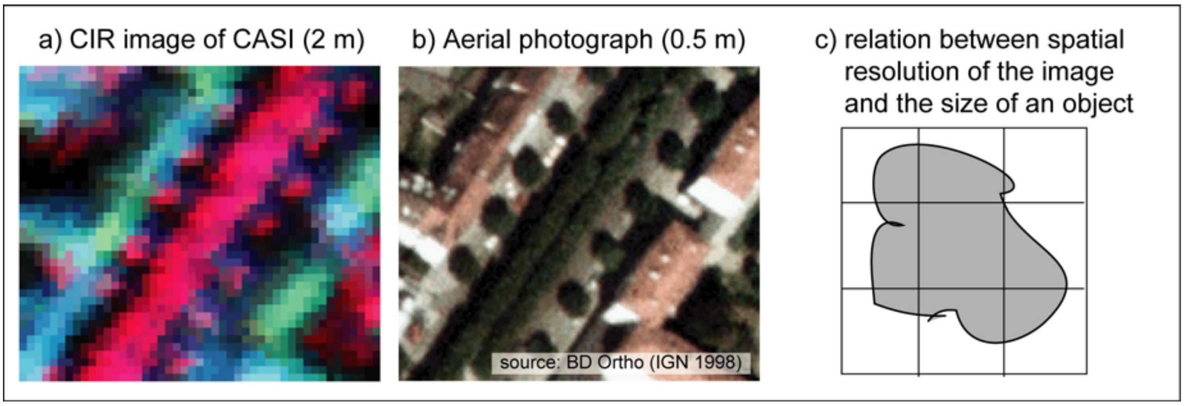


*Figure 3.18: Appearance of street trees in the CASI image (a) and an aerial photograph (b). The spectral signature of an object is influenced by the relationship between the object's size and the spatial resolution of the image (c). To obtain a pure spectrum from an object, it has to cover at least one pixel. Small objects or portions of objects overlapping with neighboured objects form a mixed pixel.*

Besides the size and shape (x, y) of the object its height (z) and underlying objects or surfaces influence the reflectance spectrum. In the following, we focus on spectral features of trees and herbaceous areas. They are considered as the basic features (or smallest units) of urban vegetation and show *a priori* different spectral responses. In general, trees show a higher intra-object variance than herbaceous areas. The main reason for that is their increased vertical extension resulting in varying illumination conditions (compare Figure 3.19 and Figure 3.21). Depending on the shape of the crown, its density, depth and underlying surface the spectral signature of individuals of the same species may vary. Examples are given in Figure 3.19. It shows the spectral signature of four London plane trees on different grounds and of different sizes. The samples were taken from the CASI image on the whole tree crown and in case of the smaller, pruned trees (c and d, compact crowns) the sample covers more than one tree. Nevertheless, the intra-object variance is higher for the large, unpruned trees (Figure 3.19a,b). The higher variance can be explained by the differences between fully exposed and shaded areas inside the canopy. Theoretically, the illumination conditions inside tall trees vary more than in small, compact trees. But it is not excluded, that the underlying asphalt in Figure 3.19b has an important influence on the signal as well. Furthermore, the tree height is half that one in the urban park and for the latter other vegetation layers occur underneath the crown. The way how surrounding objects influence the signal is more evident for smaller trees as Figure 3.19c shows. In this case the reflectance plateau in the NIR is modified with reflectance values decreasing toward higher wavelengths. Obviously, the surrounding built areas lead to a mixed reflectance. Furthermore, the difference between the green reflectance peak and the red absorption dip is smaller. In Figure 3.19d the spectrum of the same tree (same shape due to pruning) but continuously lined up in a double tree row is presented. This tree sample shows the highest reflectance values. The same, if the two pruned trees (Figure 3.18c,d) are compared with the unpruned large trees (a,b) it seems that the first have always higher reflectance values. Again, this can be explained by the highly varying illumination conditions inside large trees.

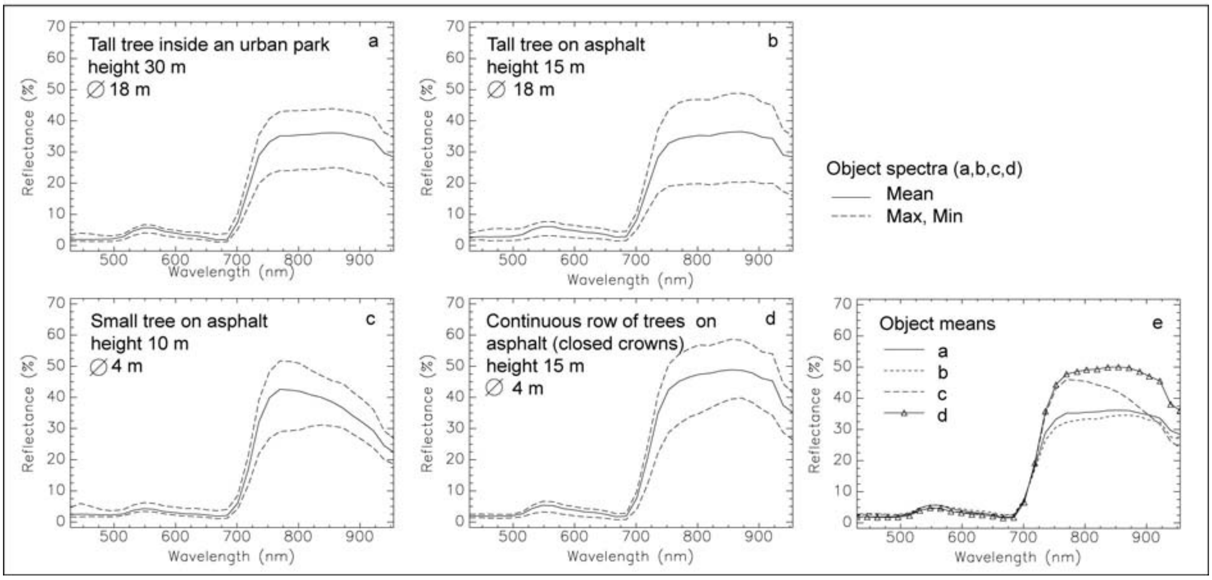


*Figure 3.19: Comparison of spectra of four different London Plane trees (CASI image): a) and b) spectral signature of two tall trees with large crowns (not pruned), c) and d) two smaller, pruned trees with compact crowns (samples are taken on more than one tree). The shape of the mean spectra (e) of a and b is similar, the spectra of the small, isolated tree (c) differs significantly from the other trees and even from the similarly pruned tree in continuous rows (d).*

Figure 3.20 shows some photographs of typical urban trees in the city of Strasbourg. Figure 3.20a shows an example of the strongly pruned London plane tree from which the spectrum in Figure 3.19c was derived. In contrast, the London Plane in Figure 3.20b has a much larger (diameter and vertical height) and less dense crown. While the smaller tree (a) grows inside a densely built housing district, the large tree (b) is planted along a road and beside a river bank. Trees, covering only a small area on the ground such as shown in Figure 3.20c,e,f can not be detected in an image with 2 m spatial resolution, at least not if they are single trees. Furthermore, differences in crown density can be observed in the photographs. Figure 3.20 c, d and g are sparsely foliated trees where the contribution of the underlying soil is potentially high. In contrast, the Thuya in Figure 3.20e is expected to have only a reduced soil signal (dense crown) but the probability to observe the signal of a mixed pixel in the CASI image is higher for this case due to its small crown diameter.


*Figure 3.20: Example of different urban trees: two London Planetrees as street trees a) strongly pruned, small tree and b) relatively few pruned, larger tree. c) small pruned Crimean Linden tree, d) Black poplars aligned, e) Thuya, f) pruned Sycamore Maple, g) Japanese Pagodatree, h) Large-leaved Linden surrounded by small London Planetrees, i) again a Sycamore Maple in a front house garden with a large, less compact crown.*

Figure 3.21 shows three reflectance spectra for herbaceous vegetation objects. In general, they show the typical lower intra-object variances despite the large sample size that was even larger than that for the tree canopies. One main reason is the height of the object that induces few effects due to the three-dimensional geometry. Nevertheless, the mixture of a flowerbed and lawn (Figure 3.21b) differs from the signature of the dense lawn (a) in the NIR plateau were small peaks occur. Similar peaks appear in the spectrum of the dry lawn that shows the typical increase in red reflectance (Figure 3.21c).

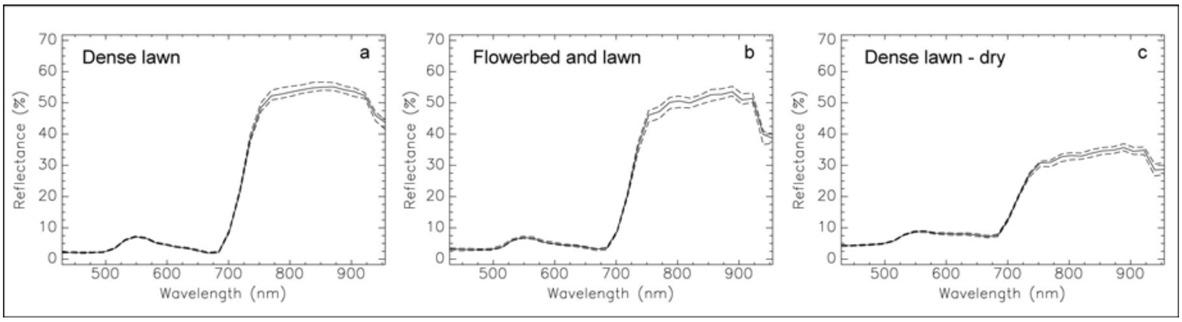


*Figure 3.21: Comparison of three herbaceous vegetation canopies. In general, the intra-object variances are smaller than those of trees. The dense lawn (a) and the mixture of flowerbed and lawn (b) show the typical spectra of healthy vegetation while the dry lawn (c) shows increased red reflectance and reduced NIR reflectance referring the reduced chlorophyll content.*

However, it is difficult to estimate the part of each of the influencing factors on vegetation canopy reflectance. In particular for small trees, showing a signal comparable to that of senescing vegetation it is difficult to estimate if the modified reflectance is induced by the fact that the pixel is mixed or by the vegetation's health. This observation corresponds to Horler *et al.* (1983) who stated that the assessment of stress conditions in vegetation can be confounded with ground cover variations.

***Shadow on vegetation***

Variations of reflectance increase when shadow is present. In the urban environment shadow is a component that plays an important role in many environmental applications (Gwinner and Schaale 1997). It can be found over different surface materials, which can affect the final spectrum. Shadow reduces the overall reflectance values. Figure 3.22a shows the reflectance spectra of the same tree species in two illumination conditions (for the appearance in the image see Figure 3.22b and c). The shaded tree has much smaller reflectance values than the tree in full illumination.

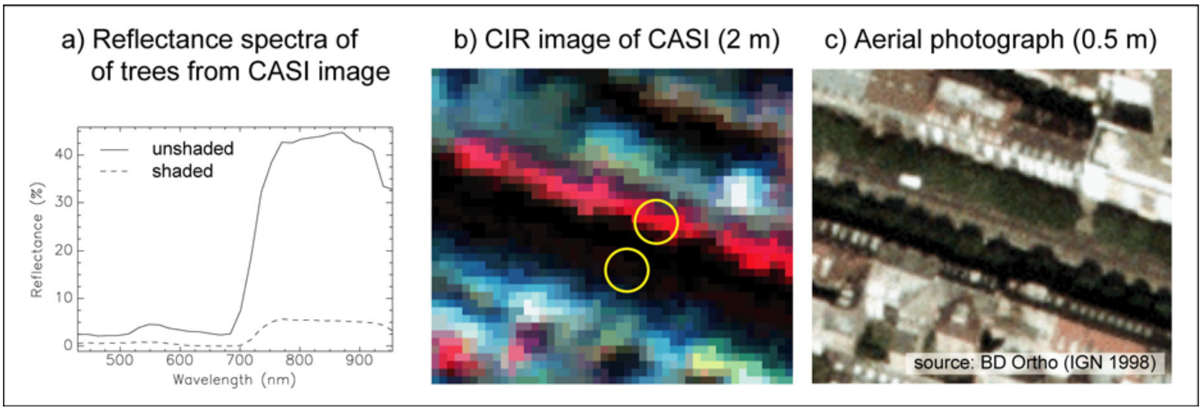


*Figure 3.22: The influence of shadow on the reflectance spectra of vegetation objects, example of trees under full illumination and in the shadow of buildings. Reflectance spectra (a) and appearance in the CASI image (b) and the aerial photograph (c). The tree under full illumination (a, continuous) shows much higher reflectance values than the shaded tree (a, dashed) (one pixel each, same tree species, location is indicated by the yellow circles in b).*

## 3.5.3 Vegetation indices and variations in red-edge inflection point

### 3.5.3.1 Vegetation indices

#### *3.5.3.1.1 Description of the used indices*

A common tool for vegetation characterisation is the vegetation index. Vegetation indices have been widely used as measures of absorbed photosynthetic active radiation and green vegetation cover (Bariou *et al.* 1985, Bannari *et al.* 1995). They are one way to estimate biophysical variables from reflectance data such as Leaf Area Index (LAI), vegetation cover, biomass and other important variables for ecosystem studies. Vegetation indices are designed to provide a measure of the overall amount and quality of photosynthetic material in vegetation, which is essential for understanding the health status of vegetation.

In remote sensing, vegetation indices are normally derived from broad red and near-infrared wavebands. However, experiments at the leaf scale have shown that broadband vegetation indices can be improved by using a narrow waveband at the edge of the chlorophyll absorption feature rather than the middle, which results in a more linear relationship between the index and chlorophyll content (Gitelson and Merzlyak 2003). To capture the effect of varying chlorophyll contents, Gitelson and Merzlyak (1994) replaced the red band in the Normalized Difference Vegetation Index (NDVI) by a band at the edge of the chlorophyll absorbance region (705 nm). Other narrowband indices were developed to detect changes in leaf pigment, nitrogen, carbon, water content, etc.

Commonly, the NDVI (Rouse *et al.* 1974) is used to differentiate between vegetation and non-vegetation and to built vegetation masks (Underwood *et al.* 2003, Xiao *et al.* 2004). However, most of these studies are performed outside urban areas and it was supposed that a normal NDVI performs not well in heterogeneous urban areas where the influence of the soil and atmospheric scattering due to high aerosol concentration on the signal is considerably high. Furthermore, Bannari *et al.* (1994) have shown the utility of hybrid indices that lead to improved results in areas with heterogeneous vegetation density cover. Consequently, we compared NDVI with two hybrid indices accounting for the influence of soil: the Transformed Soil Adjusted Vegetation Index (TSAVI) and the Transformed Soil

Atmospherically Resistant Vegetation Index (TSARVI). All indices were initially developed for multispectral data.

The objective of the following analysis is thus two-fold. On one hand, the influence of using bands at the red-edge for the calculation of vegetation indices should be evaluated. On the other hand, besides the commonly used NDVI other indices should be examined in order to evaluate the relevance of each for detecting urban vegetation.

***Normalized Difference Vegetation Index***

The performance of NDVI, which is typically used for multispectral image analysis, was compared to an NDVI based on the chlorophyll index (Gitelson and Merzlyak 1994). Several studies on the leaf-scale could show that chlorophyll content was best correlated with bands at the edge of the red-edge shift and only weakly correlated with those centred at bands of multispectral images (Gamon and Surfus 1999, Sims and Gamon 2002). In the latter the red channel is usually centred at 680 nm and the NIR band at 800 nm to focus on the main absorption and reflectance peaks. Gitelson and Merzlyak (1994) noted that for leaf-scale assessment of chlorophyll content, the NDVI can be improved using a narrow waveband at the edge of the chlorophyll absorption feature rather than at the middle, which results in a more linear relationship between the index and the chlorophyll content. They proposed to use the set of 705 nm and 750 nm for the NDVI. However, these relationships were described on the leaf scale and we wanted to find out if they are valuable for urban vegetation detection from hyperspectral image data. Consequently, a red-edge NDVI (Equation 4) was compared to a NDVI using the centre wavelengths of the red and NIR bands in multispectral images referred in the following as broadband NDVI (Equation 3). The formulas are as follows:

$$NDVI_{667} = \frac{R_{802} - R_{667}}{R_{802} + R_{667}}$$ Equation 3

$$NDVI_{701} = \frac{R_{753} - R_{701}}{R_{753} + R_{701}}$$ Equation 4

where $R$ is used for the reflectance in the respective bands. As modification of the red-edge $NDVI_{701}$ the Modified Red Edge Normalized Difference Vegetation Index (mNDVI) was examined (Sims and Gamon 2002). The mNDVI is an improved version of the NDVI incorporating a correction for leaf specular reflection. High leaf surface (specular) reflectance tends to increase the reflectance across the whole visible wavelength range. Adding a constant to all reflectance values reduces the NDVI even when there is no change in the absorption of tissues below the epidermis. The effect is removed by including reflectance at 445 nm as a measure of surface reflectance (combined absorption of chlorophyll and carotenoids results in minimal reflectance in this spectral region). Sims and Gamon (2002) showed that this wavelength is insensitive to chlorophyll content until it drops below 4 % of maximal content. The mNDVI is calculated by:

$$mNDVI_{701} = \frac{R_{753} - R_{701}}{R_{753} - R_{701} - 2 * R_{445}}$$ Equation 5

***Transformed Soil Adjusted Vegetation Index***

The TSAVI is a hybrid index that integrates the slope and origin of the soil line to account for the effect of soil brightness and colour (Baret *et al.* 1989). It is a transformation of the Soil Adjusted Vegetation Index (SAVI) (Huete 1988) that is a compromise between ratio indices like NDVI and orthogonal indices like the Perpendicular Vegetation Index PVI (Richardson and Wiegand 1977) that were the first indices integrating the concept of the soil line (Bannari *et al.* 1995). The slope and origin of the soil line are introduced in the calculation of this index. The slope *a* and origin *b* of the soil line are calculated using Equation 7. The first version was readjusted to minimize the effects of soil brightness by adding a value *X* equal to 0.08 (Baret and Guyot 1991). The improved version of the TSAVI is calculated as follows:

$$TSAVI_{701} = \frac{[a(R_{753} - aR_{701} - b)]}{[(R_{701} + aR_{753} - ab + X(1 + a^2))]} \qquad \text{Equation 6}$$

$$R_{753} = aR_{701} + b \qquad \text{Equation 7}$$

As for the NDVI we compared the performance of $TSAVI_{667}$ to the red-edge $TSAVI_{701}$. The only difference is the red band used in the calculation ($R_{667}$ instead of $R_{701}$).

***Transformed Soil Atmospherically Resistant Vegetation Index***

The Transformed Soil Atmospherically Resistant Vegetation Index (TSARVI) was examined (Equation 8) (Bannari *et al.* 1994). It is an improvement of the TSAVI that has proven utility in urban applications (Bannari *et al.* 1994, Bannari *et al.* 1998). The main difference to TSAVI is the use of a hybrid channel in the index formula and the formula used to calculate the soil line. The difference in reflection between the blue and red channel gives a new red-blue channel (Equation 9). The hybrid channel minimizes the effects of atmospheric scattering caused by aerosols in the red channel and was first used instead of the red channel in the Atmospherically Resistant Vegetation Index (ARVI) developed by Kaufman and Tanre (Kaufman and Tanre 1992). Bannari *et al.* (1994) introduced the hybrid channel in the calculation of the soil line as well to correct for atmospheric effects and termed it Soil Line Resistant to Atmospheric effects (SLRA) (Equation 10). Bannari *et al.* (1994) showed that TSARVI shows insignificant sensitivity to bare soils and their colour (+/- 2 %).

To summarise, the effects of the atmosphere, soil brightness, and soil colour on the calculation of vegetation cover are minimised in TSARVI by integrating the slope and the origin of the SLRA and a hybrid channel.

As for the NDVI we compared the performance of $TSARVI_{667}$ to the red-edge $TSARVI_{701}$. The only difference is the red band used in the calculation ($R_{667}$ instead of $R_{701}$). The formula of $TSARVI_{701}$ is as follows:

$$TSARVI_{701} = \frac{[a(R_{753} - aR_{445} - b)]}{[(R_{445} + aR_{753} - ab + X(1 + a^2))]} \qquad \text{Equation 8}$$

$$\text{Hybrid channel } RB = R_{701} - \gamma(R_{701} - R_{445}) \Rightarrow RB = R_{445} \qquad \text{Equation 9}$$

SLRA $R_{753} = aR_{445} + b$ Equation 10

Bare soil pixels for the calculation of slope *a* and ordinate *b* of the soil line used in TSAVI and TSARVI were detected within several 2D-Scatterplots of the red and NIR (for TSAVI) and the hybrid and NIR band (for TSARVI). The regions used for the scatterplots were chosen to reflect the different soil conditions in the image extract (bare soils and sealed surfaces). $\gamma$ is an atmospheric self-correcting factor, which depends on aerosol types (Bannari *et al.* 1995). According to Bannari *et al.* (1995) $\gamma$ was set to 1. In case that the aerosol model is unknown a value of 1 has proven to be the best adjustment for most remote sensing applications. Consequently, the hybrid channel equals the blue band ($R_{445}$).

The main motivation to examine TSARVI was that vegetation in urban areas often covers bare soils or artificial surfaces (asphalt, pavement). Furthermore, the urban atmosphere shows high aerosol concentrations mainly due to combustion. While most of the existing vegetation indices were developed for forest and agricultural applications TSARVI seems to be an index useful for applications in urban areas.

#### *3.5.3.1.2 Comparison of results*

Figure 3.23 shows the example of a tree group surrounded by built surfaces and the results of each vegetation index. All NDVI and TSAVI show the tendency to report higher values in the shaded parts of the tree canopies (Figure 3.23b,c,e,f). The TSARVI is not affected by such effects (Figure 3.23h,i). The region between both tree groups is shaded by the tree group below and in reality it consists of a mixture of lawn, small shrubs and bare soil (small park). While both NDVI and TSAVI report high values in this shaded zone the TSARVI reflect low vegetation cover. Furthermore, both NDVI and TSAVI report false cover estimates in the shadow of the high rise building on the right of the tree groups (Figure 3.23b,c,e,f) while the aerial photograph and the colour infrared image show no vegetation cover in this area (Figure 3.23a,d). It seems that the correction for the effect of soil in TSAVI leads to no significant changes in the signal. In contrast, adding a correction for atmospheric effects leads to correct detection in the case of TSARVI (Figure 3.23h,i). The correction for leaf specular reflectance in the $mNDVI_{701}$ led to no relevant results. Although false cover estimates in shaded zones are generally reduced the result is affected by a speckling effect and locally high values in shaded zones.

For NDVI and TSAVI the differences between the red-edge and the broadband indices are small. However, the latter give false estimates for vegetation covered by shadow, more than the narrowband indices. The values of the red-edge NDVI and TSAVI are lower than those of the broadband indices mainly because the used red band is placed besides the absorption peak in the red wavelengths. In contrast, the red-edge TSARVI shows slightly higher values than the broadband TSARVI but these differences are much smaller than for the NDVI and TSAVI.

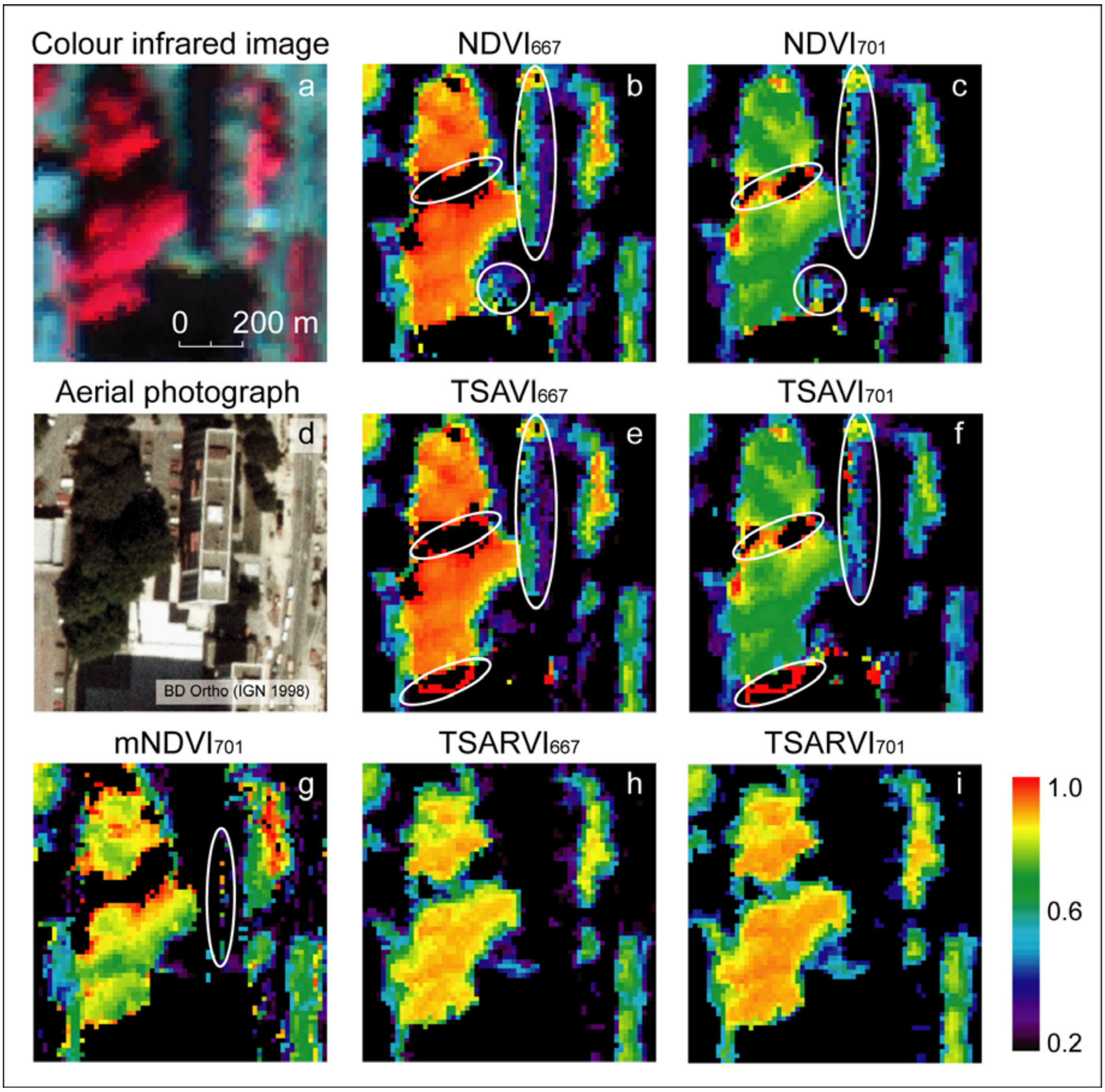


*Figure 3.23: Comparison of broadband and narrowband NDVI, TSAVI, TSARVI and mNDVI (values below 0.2 and equal to 1.0 are masked). All NDVI and TSAVI are affected by shadow leading to smaller values on the shaded canopy side and higher ones on the side exposed to the sun. Furthermore, they report false cover estimates for shaded areas.*

### 3.5.3.2 Variations in red-edge inflection point

#### *3.5.3.2.1 Calculation of the red-edge*

The analysis of the image bands at the red-edge is an alternative method to vegetation indices. The information contained in the first derivative of red-edge reflectance values (nominally 680-750 nm) has been shown to be useful for the discrimination of vegetation (Portigal *et al.* 1997). In particular, identification of the maximum inflection point contains potentially useful information. Its location in the upper part of the red-edge refers to high chlorophyll content. A shift to the red wavelengths refers to senescence.

The derivative of a spectrum is its rate of change with respect to wavelength. The technique of derivatives tackles many of the problems of quantitative analysis in a better way than ratios and differences (Demetriades-Shah *et al.* 1990). In remote sensing above all the first derivative has been used to facilitate the location of critical wavelengths such as the red-edge. The first derivative of leaf reflectance spectra is for example used to locate the red-edge inflection point (Horler *et al.* 1983). We computed the first derivatives of the image reflectance spectra according to Danson *et al.* 1992 using the first order difference as an approximation of the differential in each spectral waveband of the red-edge:

$$\frac{dR_i}{d\lambda} = \frac{R_{i+1} - R_i}{\lambda_{i+1} - \lambda_i} \qquad \text{Equation 11}$$

where $R_i$ is the reflectance and $\lambda_i$ the wavelength (mean) of band $i$. The derivative of the reflectance spectra was calculated over the bands with the means 684, 701, 718, 735, and 753 nm.

### *3.5.3.2.2 Results*

The first derivative helps identifying above all senescent vegetation. Figure 3.24 shows an example for two vegetation pixels, one with high and the other one with low chlorophyll content. While the object with high chlorophyll content (continuous line) shows the typical peak in the green followed by the absorption maximum in the red wavelengths and the typical plateau in the NIR, the other (dashed) shows increased red reflectance referring to lower chlorophyll pigments that are overtoned by other pigments (Figure 3.24a).

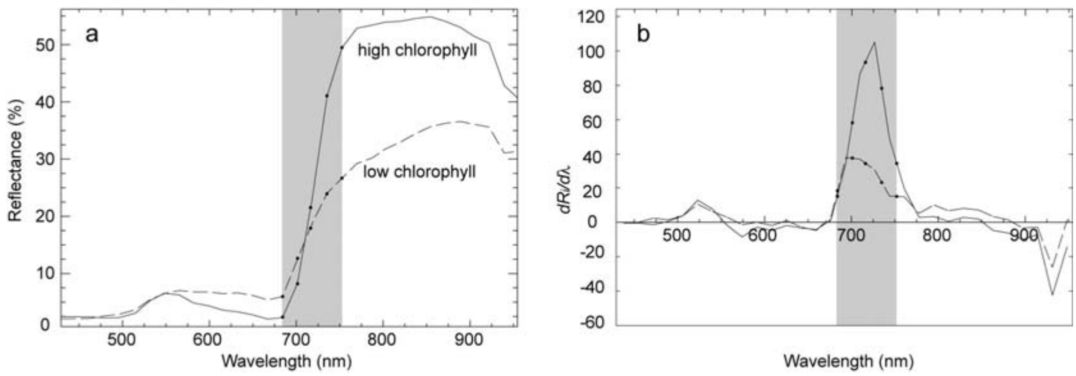


*Figure 3.24: Comparison of reflectance spectra (a) and their first derivative (b). The continuous line shows the reflectance spectrum of vegetation with high chlorophyll content, the dashed line vegetation with low amount of chlorophyll due to senescence. In gray the red-edge zone that covers five bands in the CASI image with points indicating the band means situated at 684 nm, 701 nm, 718 nm, 735 nm, and 753 nm.*

The shift of the red-edge inflection point to smaller wavelengths can be observed in the first derivative curve in Figure 3.24b. While the red-edge inflection point of green vegetation is situated between the bands at 718 nm and 735 nm the inflection point of senescent vegetation already occurs between 684 and 701 nm. The shift to shorter wavelengths is typical for a loss in chlorophyll leading to a reduction of the red absorption peak.

The display of the three first points of the red-edge reveals at least two distinct classes (Figure 3.25). The steep slope of the red-edge (red-edge inflection point = highest value of the derivative) occurs in the shorter wavelengths when chlorophyll concentration is low while for high chlorophyll concentration it occurs in the higher wavelengths of the red-edge. This information is related to the vegetation index but the appearance of senescent vegetation is more obvious from the first derivative (compare Figure 3.25b and c). The pixels with the red-edge inflection point in the shorter wavelengths show low TSARVI values and the other way round. In contrast, low TSARVI values refer also to shaded areas and indicate not necessarily senescent vegetation.

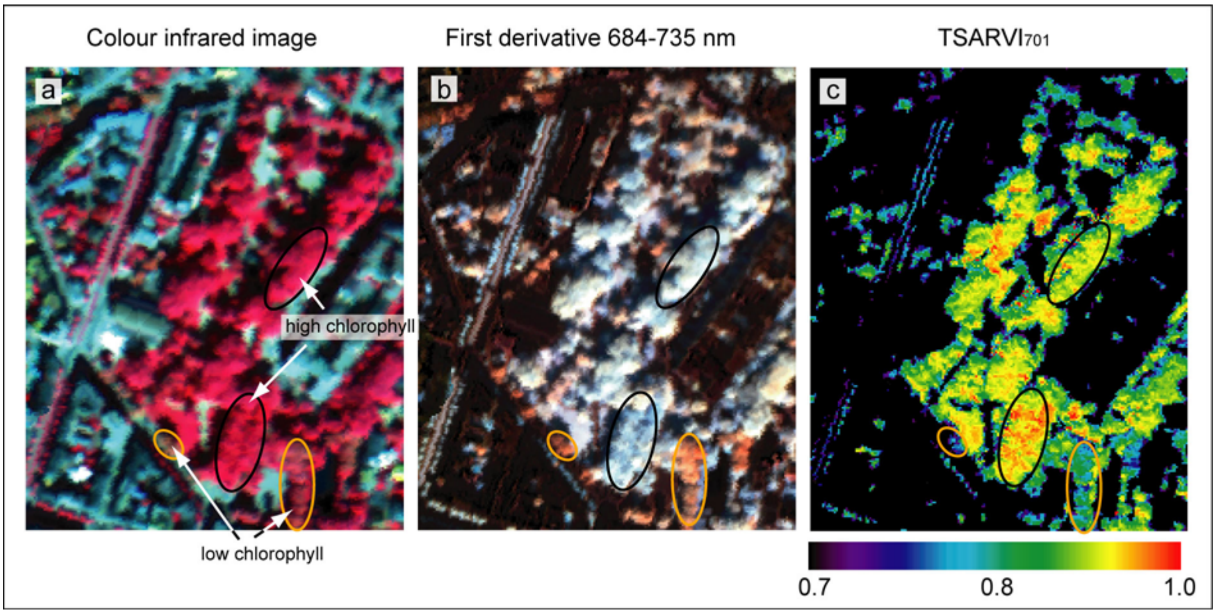


*Figure 3.25: Detection of senescent vegetation based on the first derivative at the red-edge (b) and comparison with TSARVI values (c). Display of the first three derived channels (b) (derivative values between 684 and 735 nm). The different colours refer to different locations of the red-edge shift. Maroon colours indicate a shift lying between 684-701 nm (towards the shorter wavelength), more blue colours indicate the location of the shift between 718-735 nm (towards longer wavelengths). The shift towards shorter wavelengths corresponds to lower chlorophyll concentration (compare with TSARVI, blue and green colours) and indicates senescence.*

Besides the general distinction between senescent and healthy vegetation the derivative of the red-edge bands shows small variances that indicate further differentiation of intermediate classes.

#### 3.5.3.3 Summary

The performance of different vegetation indices was examined with the aim to distinguish between vegetation and non-vegetation. Commonly used vegetation indices like the NDVI are not suited to urban areas as they overestimate shaded areas. We could show that including both the influence of the underlying soil and atmospheric effects in the calculation of a vegetation index significantly improves the performance of the index, as shown for the case of TSARVI. We showed the difference between indices using the red and infrared bands of broadband images and those using narrow bands at the red-edge. However, as no data on chlorophyll estimations are available, we cannot compare the performance of broadband and red-edge vegetation indices for urban vegetation cover estimation. Nevertheless, the narrowband indices perform slightly better in shaded areas.

Furthermore, it was shown that the identification of the red-edge inflection point using the first derivative is a simple method to identify senescent vegetation. From the point of view of tree management, this method can be used to detect trees that are affected by diseases.

### 3.5.4 Supervised classification to detect tree species

The following analysis was performed to examine if tree species can be selectively detected in the CASI image with 32 bands. The choice to detect trees was influenced by the following reasons. First, with the spatial resolution of the image, tree detection is possible and theoretically allows defining a sufficient number of training samples. Furthermore, different tree species occur inside the image extract. In contrast, herbaceous areas can be differentiated more or less only in lawn (different densities) and flower beds whereas tests have shown that both are often mixed due to the spatial resolution. Furthermore, in case that the latter are not mixed with lawn, they often cover areas smaller than the pixel size and are not properly detectable. The second reason is linked to the level of spectral detail provided by the CASI image data. For the distinction between different land cover types such as parks, allotment gardens, or fallow land, very high resolution spectral data are not necessarily needed. It is assumed that the potential of high spectral resolution data is above all to distinguish between species or to detect the health status of trees.

We performed supervised classification on transformed features (bands). Figure 3.26 depicts the scheme of processing. In a first step, a vegetation mask was created to limit further processing. The mask was created on the vegetation index TSARVI, which was the only index providing correct cover estimates. The mask was created on values > 0.7. This relatively high value was chosen to reduce the number of mixed pixels that dominate low TSARVI values. Consequently, the area covered by vegetation amounts 20 % of the image extract. In a second step, feature extraction was performed on the masked image using Minimum Noise Fraction transformation (MNF), Discriminant Analysis Feature Extraction (DAFE), and Decision Boundary Feature extraction (DBFE). Finally, supervised classification using Maximum Likelihood was performed on a subset of the transformed bands.

The best classification result is compared with a classification on multispectral data. Therefore Quickbird spectral bands were derived from the CASI image. The aim was to evaluate if the precise information in hyperspectral data leads to better results than the less complex multispectral data.

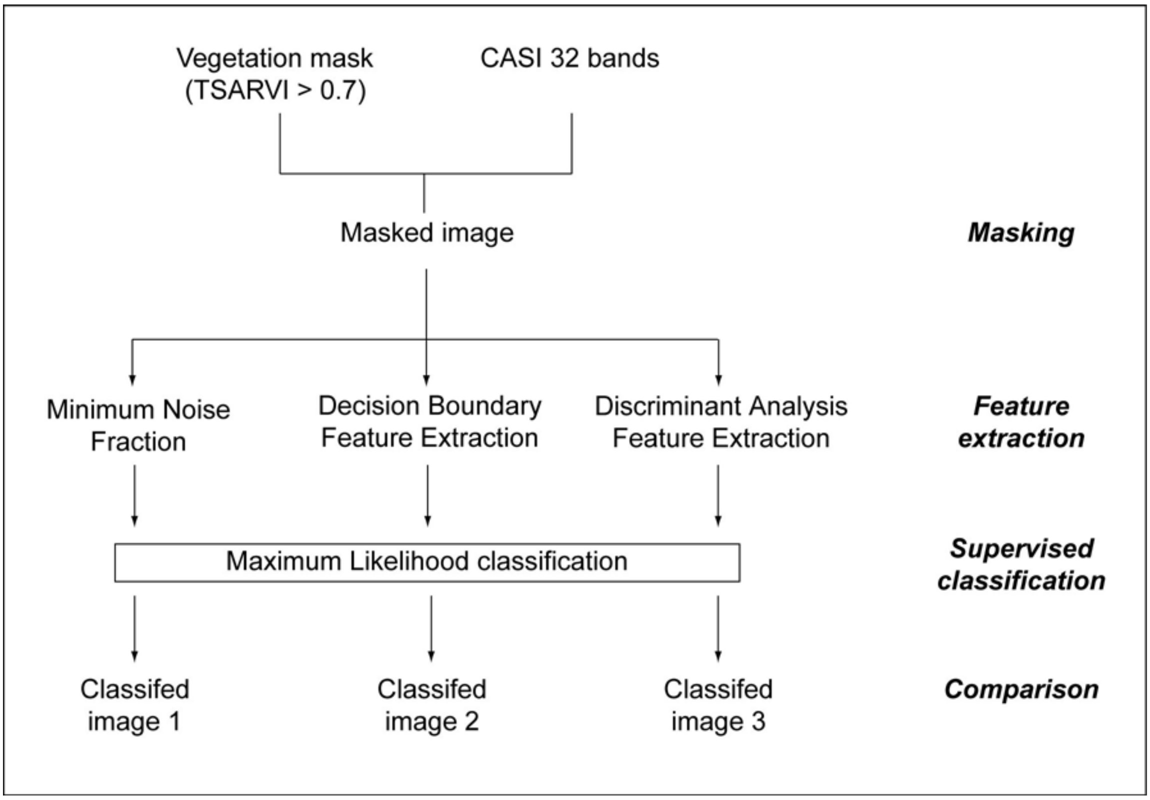


*Figure 3.26: Processing of CASI image with different feature extraction methods. Supervised classification on the transformed images was performed using the Maximum Likelihood classifier.*

### 3.5.4.1 Definition of training sets

Training sets were defined in the image using the tree database of the city of Strasbourg and own field data collection. As described before the application of the ML classifier requires a minimum training sample size. This restriction had an impact on the size of the analysed image extract and the selection of identifiable tree species. In the following, we present the main influencing factors for the selection of training samples.

According to the municipality of Strasbourg 544 tree species are referenced within the whole urban community. Not all of these species can be identified in the image. The main reason is the spatial resolution of the image that, although being already high, led to a reduction of possible training samples. Small trees with diameters close to the pixel size are probably mixed up with neighbouring objects and consequently, we decided to consider only trees with a diameter of at least four meters.

Another criterion was the spatial frequency of a tree species inside the area that was mainly influencing the selection of the image extract but that limited the selection of potential tree species as well. Some species occur more often than others. For example, the London Plane (*Platanus x acerifolia*) is a very frequently planted tree in Strasbourg. In central European cities this tree is known for its resistance to stress and often planted along streets and in parks. Besides the frequency the size of crowns excluded *a priori* species. Birches for example have small crowns and single trees are nearly unidentifiable in the CASI image. Such trees with small crowns (e.g. column shape) cover almost always only one or two pixels. To identify them in the image it is necessary to identify a dense tree group.

Finally, shadow ads to the problems mentioned before. In some cases potential trees or lawn are covered by shadow. Combining a shaded and not shaded tree of the same species in one training class increases the inter-class spectral variability.

To summarise, the definition of training sets was influenced by the possibility to identify objects affected by the following factors:

- limited spatial extension of objects and consequently overlapping with neighbouring objects (e.g. single trees, bushes),
- spatial frequency of target objects,
- shadow.

Consequently, trees with a diameter smaller than 4 $m^2$ and species with a small spatial frequency were discarded from the definition of training areas. Furthermore, shaded crowns or portions of crowns, and shaded herbaceous surfaces were not included as they would increase the within-class variance. For these areas a shadow class was defined. The definition of different tree classes was constrained by the mentioned factors what finally led to a limited number of trees among the possible 544 species occurring in Strasbourg. Finally, twelve classes were defined (Table 3.6). Among them nine tree classes, two herbaceous classes and a shadow class.

The samples were separated in training and test sites. The latter serves for additional accuracy assessment (Table 3.6). Test sites should allow evaluating the performance of the classification based on independent samples, i.e. samples that were not included to calculate classification statistics. The size of the training samples for the different classes varies due to the above mentioned conditions. For the Common Ash tree class only few training samples could be defined.

*Table 3.6: Defined classes and size of the training and test samples.*

| | | | | **Sample size (nb pixels)** | |
|---|---|---|---|---|---|
| **Groups of classes** | **Class** | **Botanical name** | **Code** | **Training** | **Test** |
| Herbaceous areas | Low chlorophyll | | HerbL | 757 | 302 |
| | High chlorophyll | | HerbH | 891 | 312 |
| Trees/shrubs | London Planetree | *Platanus x acerifolia* | PA | 498 | 117 |
| | Japanese Pagodatree | *Sophora japonica* | SJ | 108 | 98 |
| | Large-leaved Linden | *Tilia platyphyllos* | TP | 128 | 128 |
| | Crimean Linden | *Tilia euchlora* | TE | 137 | 100 |
| | Common Horsechestnut | *Aesculus hippocastanum* | AH | 262 | 133 |
| | Sycamore Maple | *Acer pseudoplatanus* | AP | 112 | 101 |
| | European beech | *Fagus sylvatica* | FS | 115 | 65 |
| | Common Ash | *Fraxinus excelsior* | FE | 78 | 36 |
| | Common Locust | *Robinia pseudoaccacia* | RP | 123 | 38 |
| Shadow | Shadow | | shadow | 305 | 108 |

The mean spectra of all classes are shown in Figure 3.27. Differences in the red-edge inflection point can be observed. The chestnut class is distinct, showing lower reflectance values in general, a red-edge shift to the lower wavelengths, and a typical spectrum for senescent vegetation with increased reflectance in the red wavelengths. At the time of image acquisition this species was already senescing mainly induced by the parasitic animal the horse chestnut leaf miner (*Cameraria ohridella*) that also leads to reduced leaf density (Figure 3.27b). The low chlorophyll herbaceous class shows lower NIR reflectance, a green peak in the green wavelengths, but increased reflectance in the red range. Nevertheless, the plateau in the NIR is still present. The tree classes show similar spectra. However, they have lower green and NIR reflectance than the high chlorophyll class.

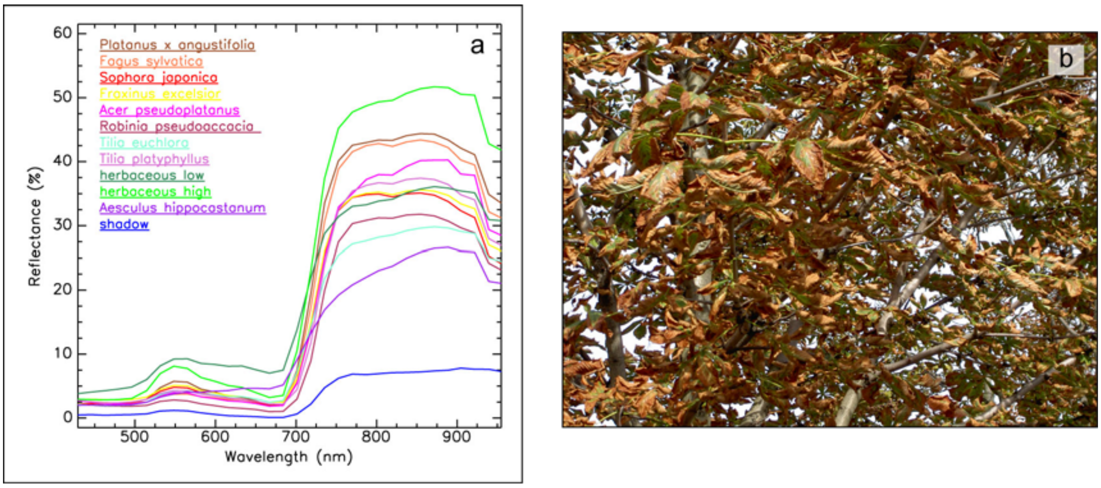


*Figure 3.27: Mean spectra of training classes (a) and leaves of a chestnut tree in mid September (b) inducing the specific reflectance spectrum of the Horsechestnut class. The leaves are still slightly green but nevertheless heavily affected by senescence probably induced by environmental stress (dryness, pollution) and the parasite horse chestnut leaf miner.*

Figure 3.28 shows the position of the class mean vectors in the three-dimensional sub-space defined by a green, red, and infrared channel. Only vegetation pixels are presented. The vegetation classes spread along a bulge pointing in the direction of the NIR axis. Compared to the whole extent of the point cloud, the space covered by the vector means of the vegetation objects is rather small. The means of *Sophora japonica* and *Fraxinus excelsior* for example are very close. The classes with low reflectance values are rather distinct, namely the shadow, *Aesculus hippocastanum*, low chlorophyll herbaceous, and the *Tilia euchlora* class.

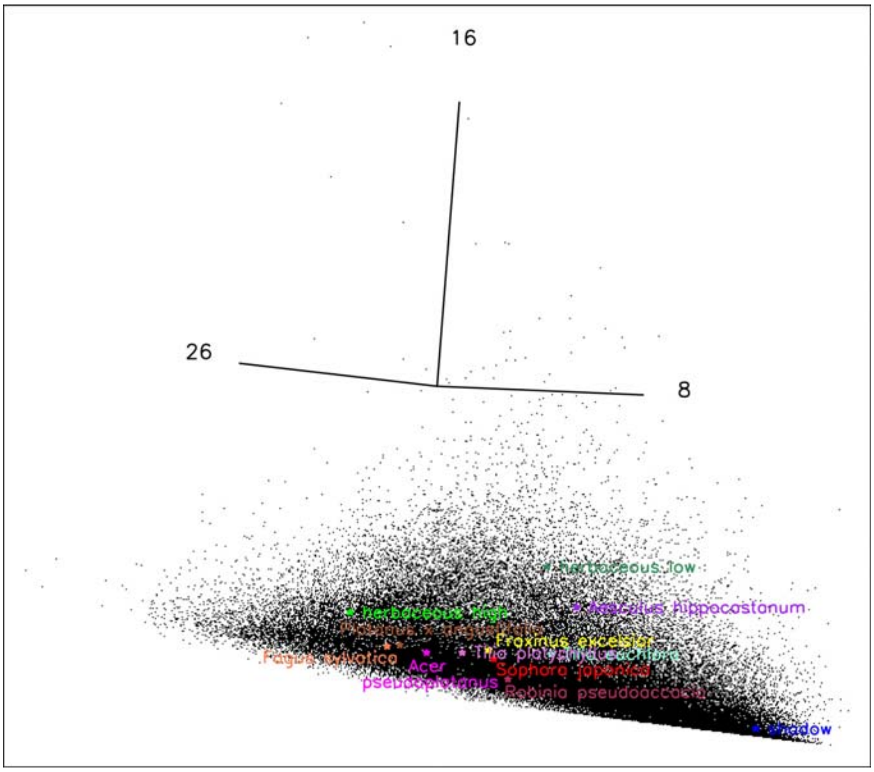


*Figure 3.28: Class mean vectors in the original feature space of CASI (image subset, only vegetation pixels are presented), class vectors in the cloud of a 3D-subspace (means of displayed bands CIR: band 8 548 nm, band 16 684 nm, band 26 854 nm).*

#### 3.5.4.2 Feature reduction

From the mean spectra and the position of the mean vectors in the 3D sub-space it is evident that the defined classes are spectrally very similar. Accordingly, different feature extraction algorithms were evaluated. As mentioned before, DBFE and DAFE are class dependent and they were examined in this context to improve the separability between similar classes for the subsequent classification. They were compared to the class independent extraction method MNF. Each transformation was performed on the pixels inside the vegetation mask.

For the MNF transformation noise was estimated from a spatial subset with homogeneous spectral characteristics (built area). This method is critical as inter-pixel variability contributes to the noise component. Nevertheless, it was applied because no information about noise from the sensor was available. One criterion for the selection of transformed MNF bands was their eigenvalue. A common criterion is to choose bands with eigenvalues higher than one. Bands with eigenvalues below one contain no relevant variance. A second criterion was the spatial coherency of information in the transformed images. Based on both criteria nine MNF bands were selected for the further analysis.

Despite their high eigenvalues, two of the high order MNF bands were excluded from the subsequent analysis as they were reflecting varying illumination conditions inside a flight line. Figure 3.29 shows the noise at the example of band 7 compared to the first MNF band that shows not this phenomenon. During the transformation this noise is detected as significant information. None of the initial bands shows this phenomena and it is considered to be nevertheless small for an airborne image. The occurrence in the concerned MNF images reflects the movement of the airplane and is due to the anisotropy of the solar radiation between the nadir and the borders of the flight lines (Thomas and Lennon 2005). Both bands were removed and accordingly MNF bands 1-6 and 9-11 were retained for further analysis.

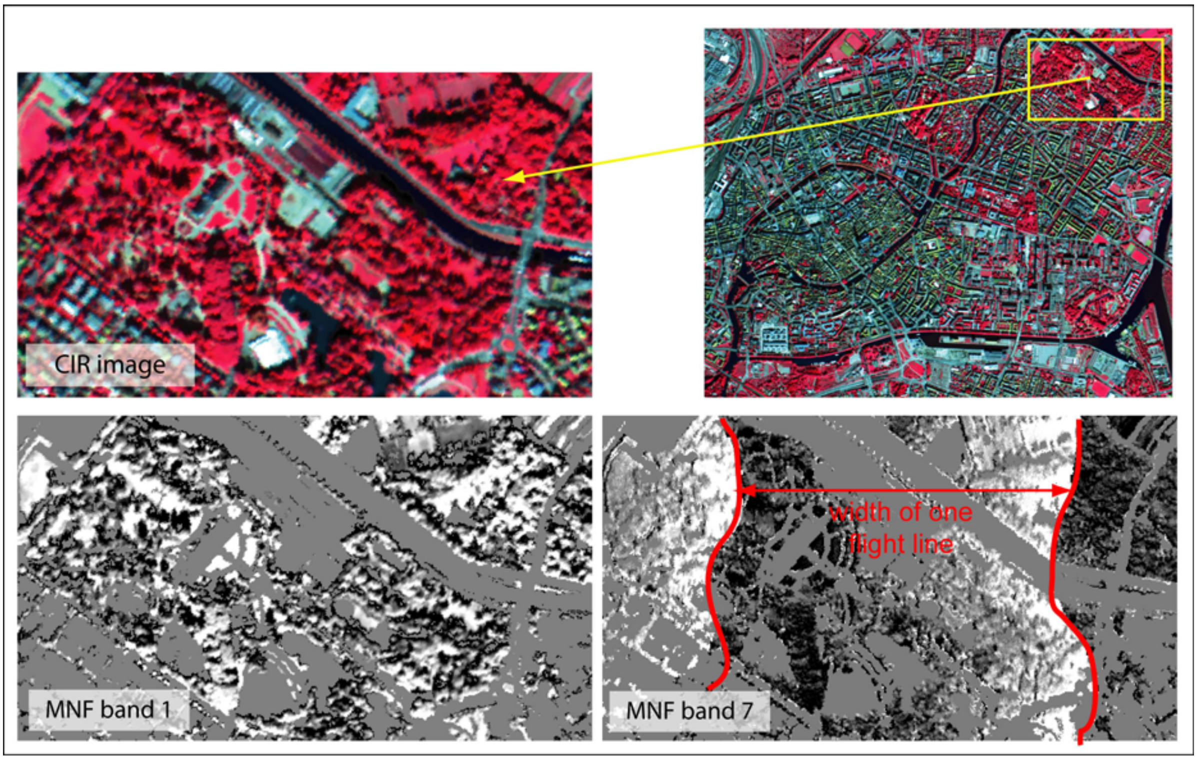


*Figure 3.29: Noise detection in two high order MNF bands. Example of the CIR image extract, the first MNF band with spatially coherent information and the seventh MNF band where the noise was observed. The noise reflects the movement of the airplane (see width of indicated flight line) and is due to the anisotropy of the solar radiation between the nadir and the borders of the flight lines.*

For the other transformations, six of the features transformed with DAFE have eigenvalues higher than one. DBFE led to eleven features with eigenvalues higher than one. The subsets were used in the following supervised classification.

### 3.5.4.3 Supervised classification

Supervised classification was performed on all three subsets of transformed bands. Table 3.7 shows the accuracies and Kappa coefficients for each classification (for confusion matrices see Annex Tables AC3-1, AC3-3, AC3-4). The highest accuracy is obtained with the eleven DBFE bands. Nevertheless, six bands extracted by DAFE reach higher accuracies than the nine bands from the MNF transformation. In general, the two class related feature extraction methods perform better than the MNF transformation.

*Table 3.7: Overall accuracy and Kappa for training and test samples for the ML classifications on 9 MNF, 6 DAFE, and 11 DBFE bands.*

| | **Overall accuracy (%)** | **Kappa** |
|---|---|---|
| MNF 9 bands | 95.3 / 66.8 | 0.94 / 0.62 |
| DAFE 6 bands | 95.7 / 79.8 | 0.95 / 0.77 |
| DBFE 11 bands | 97.9 / 71.2 | 0.97 / 0.67 |

However, the evaluation of accuracies for each class shows a differentiated picture (Table 3.8). The highest accuracies are achieved for the spectrally distinct classes shadow, the *Aesculus hippocastanum* class and the two herbaceous classes. However, the herbaceous high chlorophyll class performs rather poor on the test samples. Relative high accuracies are achieved for the *Platanus x acerifolia* and the *Fagus sylvatica* class as well. The *Fraxinus excelsior* class fails mainly regarding the test sites. Remember, that this class covered the smallest training sample set. Problems occur mainly with the detection of the *Robinia pseudoaccacia* and *Tilia* classes. Although the training set evaluation showed that the *Acer pseudoplatanus* class is correctly classified, its test site evaluation is rather poor.

*Table 3.8: User accuracies for each class in the ML classifications on 9 MNF, 6 DAFE, and 11 DBFE bands.*

| **Class** | | **User accuracy training / test (%)** | | |
|---|---|---|---|---|
| **Code** | **Name** | **9 MNF** | **DAFE 6 bands** | **DBFE 11 bands** |
| HerbL | Herbaceous low chlorophyll | 100.0 / 100.0 | 99.9 / 100.0 | 100.0 / 100.0 |
| HerbH | Herbceous high chlorophyll | 99.9 / 57.83 | 99.9 / 77.2 | 100.0 / 57.8 |
| PA | *Platanus x acerifolia* | 96.7 / 67.7 | 98.5 / 90.7 | 98.8 / 84.1 |
| SJ | *Sophora japonica* | 75.9 / 69.9 | 95.2 / 91.8 | 98.1 / 87.1 |
| TP | *Tilia platyphyllos* | 86.6 / 61.8 | 80.9 / 67.3 | 94.7 / 68.8 |
| TE | *Tilia euchlora* | 80.7 / 53.3 | 74.7 / 72.0 | 78.3 / 66.7 |
| AH | *Aesculus hippocastanum* | 96.1 / 69.3 | 97.2 / 82.9 | 96.9 / 81.2 |
| AP | *Acer pseudoplatanus* | 88.5 / 79.0 | 88.3 / 66.3 | 97.4 / 51.3 |
| FS | *Fagus sylvatica* | 94.9 / 96.5 | 91.4 / 87.7 | 99.1 / 79.4 |
| FE | *Fraxinus excelsior* | 68.7 / 11.5 | 77.5 / 22.2 | 94.9 / 31.6 |
| RP | *Robinia pseudoaccacia* | 86.8 / 65.4 | 86.4 / 33.3 | 95.2 / 51.3 |
| shadow | Shadow | 100.0 / 91.4 | 99.3 / 96.4 | 100.0 / 96.4 |

The detection of species was additionally evaluated based on the image result. Figure 3.30 shows an extract of the image and the result of an evaluation based on the tree database and verifications in the field. This figure reveals the mentioned problems with species detection and shows furthermore that false detections occur above all in the case of very small objects like small street trees (black circles). From the same figure it is evident that some classes are properly detected while others mix up with other classes. Properly detected classes are *Platanus x angustifolia, Fagus sylvatica, Aesculus hippocastanum, Acer pseudoplatanus* and the two herbaceous classes. The classes *Sophora japonica*, the two *Tilia* classes, and the *Fraxinus excelsior* class occur also in areas where none of the properly detected species occur in reality. The best example is the *Tilia euchlora* class that shows low accuracies but is often identified in the classified image (Figure 3.30).

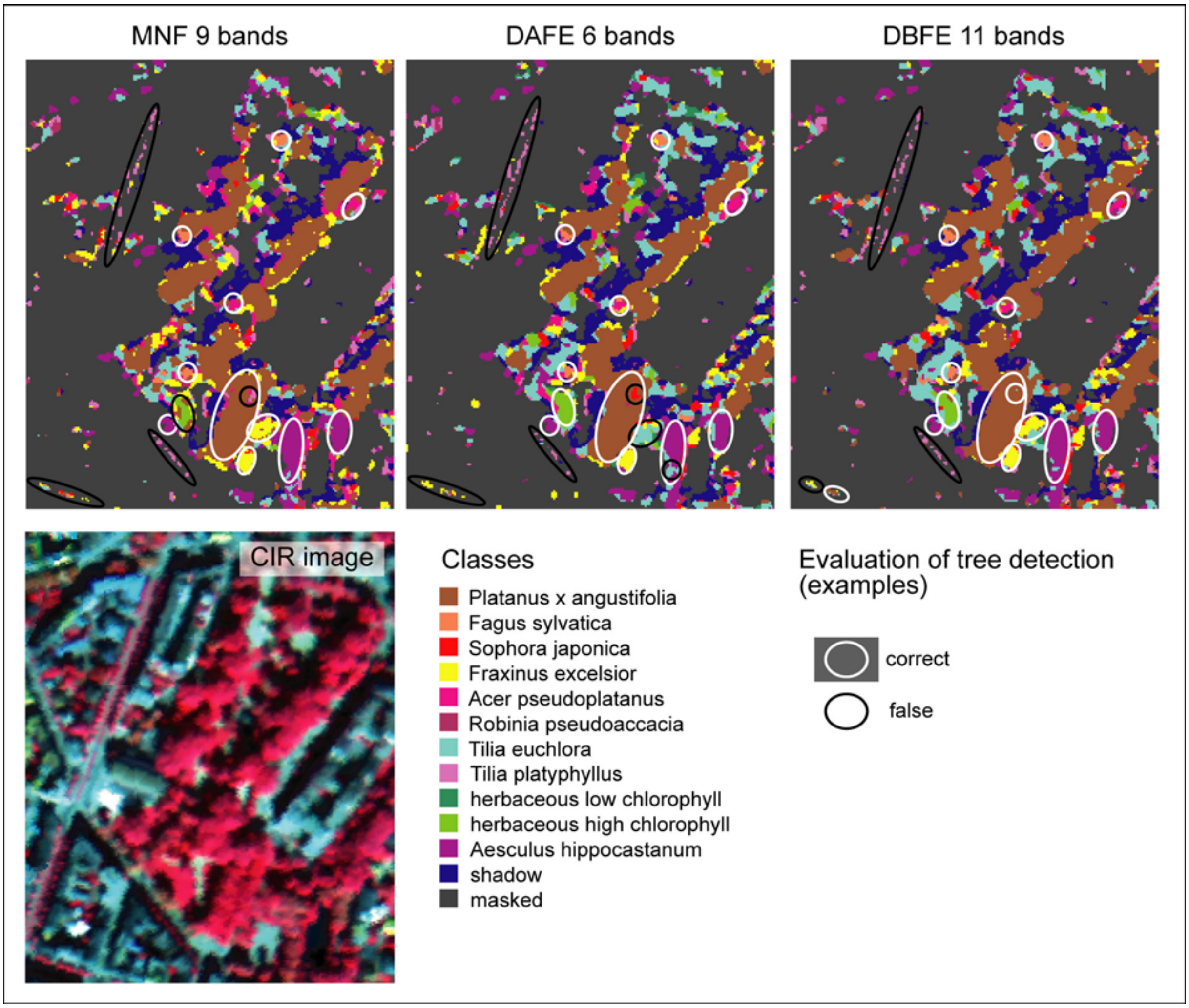


*Figure 3.30: Result of ML classification on 9 MNF, 6 DAFE, and 11 DBFE bands. The classification results are filtered with a majority filter 3x3. In general, Platanus x angustifolia, Aesculus hippocastanum, Fagus sylvatica, and Acer pseudoplatanus are correctly identified.*

***Further remarks on performed tests***

Several tests were run to evaluate if the distinction between the classes can be improved first, using a texture layer, and second, using different class weights in the class dependent feature extractions. A texture layer was introduced to improve the differentiation between the herbaceous and the tree classes. Herbaceous objects like maintained lawn, fallow land, or other herbaceous plant cover are usually more homogeneous in texture (grey level) than shrub and tree cover that is affected by much higher leaf scattering and differences induced by the uneven surface. Tests have shown that the reflectance spectra of lawn equal those of some trees. The texture layer was created based on the NIR band at 753 nm (the same as for the vegetation index calculations). Homogeneity (co-occurrence) was calculated using a mobile window of 7x7 pixels according to Puissant *et al.* 2003. While increasing the global accuracy the inclusion of the texture layer does not improve the distinction between herbaceous and tree classes but the distinction between tree classes (see confusion matrix Annex Table AC3-2). However, these changes seemed to be artificially. Furthermore, the lawn classes are correctly detected in the classifications without the texture layer. It was finally decided to omit texture information from classification.

Other tests concerned the two class specific transformations DBFE and DAFE. To limit the feature transformation to spectrally similar classes, it was tested first, to omit spectrally distinct classes from the feature extraction and second, to affect the same with lower weights. These classes were shadow, the two herbaceous classes and the *Aesculus hippocastanum* class. The results led to no significant modifications.

#### 3.5.4.4 Performance of hyperspectral data compared with multispectral data

In order to evaluate if hyperspectral data improves the detection of urban trees, the results of the classification on 11 bands from DBFE transformation were compared with a classification on low spectral resolution Quickbird MS (multispectral) data. We decided to resize the 32 CASI bands to the four Quickbird bands (referred as Quickbird data in the following, band definition see Table 3.9) in order to assure comparability. Supervised classification was performed with the same training samples and accuracy assessment was performed on both training and test samples.

*Table 3.9: Band definition of Quickbird MS data (Lillesand et al. 2004).*

| Band N° | Spectral range |
|---|---|
| 1 | 0.45-0.52 |
| 2 | 0.52-0.60 |
| 3 | 0.63-0.69 |
| 4 | 0.76-0.90 |

Table 3.10 shows the overall accuracies for both classifications (for confusion matrices see Annex Tables AC3-4 and AC3-5). The accuracy for the training samples is about 14 % higher in the classification on transformed hyperspectral data; the difference between the accuracy for the test samples reaches only approximately 4 %. However, this difference might be above all induced by the higher number of bands included in the classification on DBFE features. For further evaluation the user accuracies of each class and the thematic maps are evaluated.

*Table 3.10: Overall accuracies and Kappa for the classification on transformed hyperspectral CASI data (DBFE) and multispectral Quickbird MS data (resized from CASI).*

| | Overall accuracy (%) | Kappa |
|---|---|---|
| DBFE 11 bands (CASI) | 97.9 / 71.2 | 0.97 / 0.67 |
| Quickbird MS (resized from CASI) | 83.5 / 66.8 | 0.81 / 0.63 |

The user accuracy for each class on training and test samples confirms the differences between both classifications (Table 3.11). Classes that were properly defined in the transformed hyperspectral data set like *Platanaus x acerifolia* and *Fagus sylvatica* show rather poor accuracies. The accuracy for *Aesculus hippocastanum* is rather high. Classes that performed relatively poorly in the hyperspectral data like the two *Tilia* classes, *Sophora japonica*, and the *Fraxinus excelsior* classes have very low accuracies. The latter even fails completely in the evaluation of the test sample.

*Table 3.11: User accuracy of ML classification on 11 DBFE bands and the four Quickbird bands.*

| Class | | User accuracy training / test (%) | |
|---|---|---|---|
| **Code** | **Name** | **DBFE 11 bands** | **Quickbird MS** |
| HerbL | Herbaceous low chlorophyll | 100.0 / 100.0 | 100.0 / 96.9 |
| HerbH | Herbceous high chlorophyll | 100.0 / 57.8 | 94.36 / 83.6 |
| PA | *Platanus x acerifolia* | 98.8 / 84.1 | 79.5 / 53.2 |
| SJ | *Sophora japonica* | 98.1 / 87.1 | 48.1 / 51.5 |
| TP | *Tilia platyphyllos* | 94.7 / 68.8 | 36.7 / 34.0 |
| TE | *Tilia euchlora* | 78.3 / 66.7 | 61.2 / 35.0 |
| AH | *Aesculus hippocastanum* | 96.9 / 81.2 | 92.9 / 86.2 |
| AP | *Acer pseudoplatanus* | 97.4 / 51.3 | 42.2 / 50.6 |
| FS | *Fagus sylvatica* | 99.1 / 79.4 | 64.5 / 64.5 |
| FE | *Fraxinus excelsior* | 94.9 / 31.6 | 50.0 / 0 |
| RP | *Robinia pseudoaccacia* | 95.2 / 51.3 | 70.0 / 59.5 |
| shadow | | 100.0 / 96.4 | 99.7 / 88.5 |

The thematic map in Figure 3.31 confirms the observations made on the accuracies. In general, more false or improper detections occur. Even the spectrally distinct *Aesculus hippocastanum* class is improperly detected. *Platanus x acerifolia* objects are less homogeneous. *Fagus sylvatica* is improperly detected; however, small object seedlings appear.

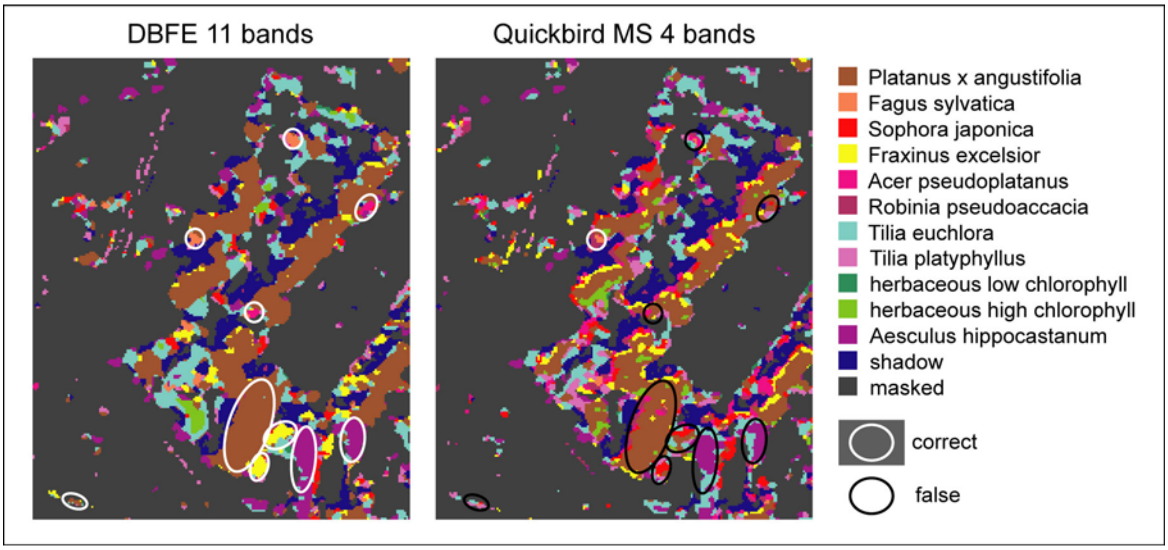


*Figure 3.31: Comparison of ML classification on 11 bands extracted from hyperspectral CASI data (DBFE) and on four Quickbird MS bands (resized from CASI) (majority filter 3x3). The circles indicate trees that were correctly identified in the classification on 11 DBFE bands and the evaluation of their detection in the Quickbird MS image.*

### 3.5.4.5 Conclusions

Class related feature extraction methods performed better than transformations performed on the global data set. For spectrally similar classes the DBFE extraction led to better classification results. It seems that the algorithm is less influenced by the small differences between the class means. It was possible to detect different tree species. However, some classes seem to be unstable. Isolated vegetation pixels are improperly identified in general referring to the mixed pixels problem.

The differences observed in the classifications on the multispectral and hyperspectral datasets are poor in terms of accuracy. Nevertheless, the classification on multispectral data shows false detections inside correctly identified objects. These results emphasise the relevance of the high information content provided by hyperspectral image data.

## 3.6 Test of a new algorithm for feature selection in hyperspectral images

In the following paragraph results of tests performed to evaluate the potential to use the unsupervised classification algorithm MACLAW for feature selection in hyperspectral images are presented (for the description of the algorithm see 3.4.2.3.2). As we have shown in the beginning, the dimensionality of hyperspectral images is problematic for the extraction of object or land use/land cover classes. The application of supervised classification algorithms needs a feature reduction that can be performed either by feature extraction and the creation of neo-bands (feature extraction) or the selection of discriminating bands from the original image (feature selection).

Blansché *et al.* (2006) proposed this new unsupervised algorithm among others for feature selection in hyperspectral images. The algorithm might be useful in helping the image analyst to discover relevant training samples and to perform a first feature reduction.

#### 3.6.1.1 Data and methods

The tests were performed on an image extract from the CASI image covering 369 x 312 pixels (Figure 3.32). The image extract was chosen regarding the variability of objects. Consequently, besides vegetation objects, water, different roof and built surfaces are present. The algorithm should be tested to discover spectrally different object classes, thus different built and vegetation objects.

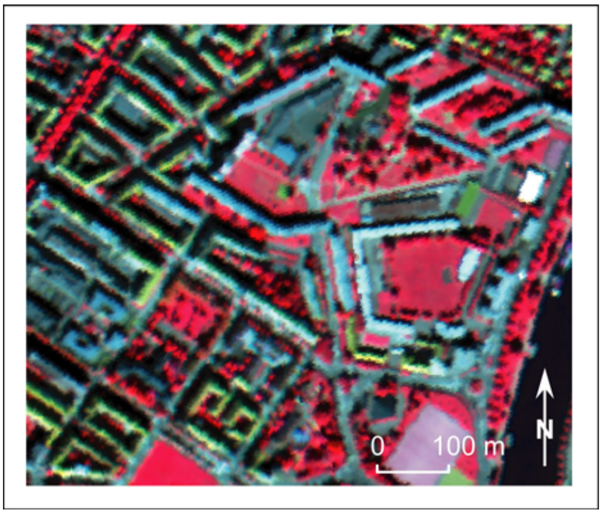


*Figure 3.32: CIR image of the CASI extract used for the validation of MACLAW. In the image occur mainly buildings built at the end of the 19th century (mainly red tile roofs), high rise buildings built in the 1970 with flat bitumen roofs, sports fields (artificial surfaces and lawn) and part of the channel on the right image border.*

The image extract covers a city district in the east of Strasbourg close to the Rhine harbour. It is located at the transition from an old city district built at the end of the 19th century to a city district from the 1970. The latter is characterised by high rise, widely spaced buildings (Figure 3.23). Buildings in the older part are organised in blocks.

Parallel to the unsupervised algorithm a supervised classification (Maximum Likelihood) on bands extracted by the three feature extraction algorithms was applied (Figure 3.33). The idea was to examine first, which classes the MACLAW algorithm discovers and second, how bands which are mainly used to extract these classes perform in a supervised classification (on the same training samples).

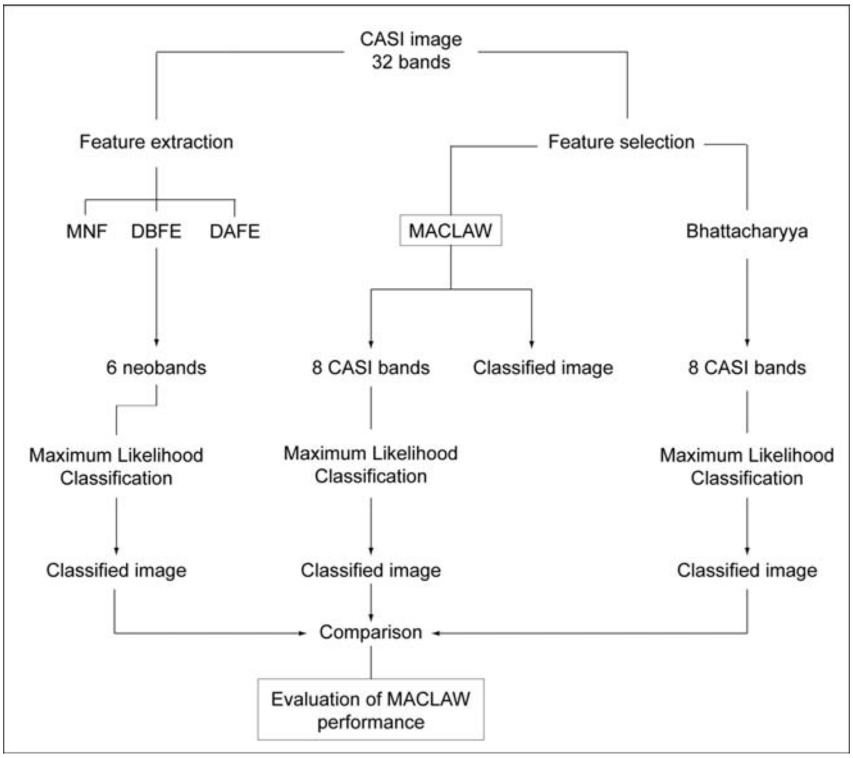


*Figure 3.33: Processing scheme for the validation of MACLAW. Feature selection was performed with MACLAW and based on Bhattacharyya distance. At the same time, feature extraction was carried out with MNF, DAFE and DBFE. Supervised classification was performed on the extracted features and the bands selected by MACLAW and Bhattacharyya. Among the feature extraction methods the best result was selected (6 DBFE bands). The results obtained with the ML classifier on 6 neobands and 8 bands selected by MACLAW and the Bhattacharyya distance are compared in order to evaluate the performance of MACLAW.*

#### 3.6.1.2 Supervised classification on transformed features

A supervised classification was carried out to obtain a map with target classes. As for the analysis on vegetation objects, features were extracted from the CASI image using the Minimum Noise Fraction Transformation (MNF), the Discriminant Feature Extraction (DAFE), and Decision Boundary Feature Extraction (DBFE). Noise statistics for the MNF were used from the large image extract. Based on the evaluation of the noise level and the eigenvalues the first eight MNF bands were selected for further use.

The definition of target classes was performed with the aim to extract all main built-up and non-built-up object classes. The training samples cover 2936 pixels in total; additionally, 1543 test pixels were defined. The number of classes was influenced by the results of first tests performed with MACLAW that showed reduced performance of the algorithm with increasing class number. Consequently, we decided to perform the comparison with seven classes that were based on merged original classes. Two vegetation and several built-up classes were identified. A shadow and water class were additionally defined.

We compared the performance of the different feature extraction algorithms. The results of the classification on eight MNF and six DBFE bands are similar although the accuracy is slightly higher in the classification on eight MNF bands (Table 3.12).

*Table 3.12: Overall accuracies and Kappa (training/test) for the ML classification on bands extracted by MNF, DBFE and DAFE.*

| | **Overall accuracy (%)** | **Kappa** |
|---|---|---|
| MNF (8 bands) | 98.0 / 92.3 | 0.98 / 0.91 |
| DAFE (4 bands) | 98.0 / 90.4 | 0.98 / 0.88 |
| DBFE (6 bands) | 98.1 / 92.3 | 0.98 / 0.91 |

The classified images are shown in Figure 3.34. Confusion between classes is observed above all between the asphalt class and the bitumen roof class (see confusion matrices Annex Tables AC3-6, AC3-7, AC3-8). It is noteworthy that for MNF and DBFE pixels of the red tile roof class are often occurring instead of vegetation. Tests have shown that concerned are above all vegetation objects close to asphalt thus mixed pixels whose spectral signature is too different from the signature of the vegetation class. In contrast, DAFE underestimates the abundance of bitumen roofs, and overestimates the occurrence of asphalt. Despite correct accuracies for the training and test sites, the image result shows false estimates for the asphalt class. The result obtained in the classification on the DBFE band subset was finally chosen for the comparison with MACLAW.


*Figure 3.34: Comparison of ML classification on band subsets obtained with three feature extraction methods a) class independent MNF, b) class dependent DAFE, and c) class dependent DBFE.*

### 3.6.1.3 Unsupervised classification and feature selection with MACLAW

The MACLAW algorithm was parameterised to discover seven classes. Figure 3.35 shows the classification (a) and the result of the supervised classification for comparison (b). The reflectance spectra in Figure 3.35c give an idea of the classes defined by MACLAW. For comparison the mean spectra of the training sample sets are shown in Figure 3.35d. MACLAW identified one vegetation class, one class combining shadow and water pixels, and six built-up classes. In the case of the latter MACLAW identifies two asphalt classes and a class combining the painted asphalt class from the supervised classification with the red tile roofs and the mixed vegetation pixels (asphalt and vegetation). The unsupervised algorithm detects a class of high reflecting buildings that was not explicitly defined in the supervised classification.

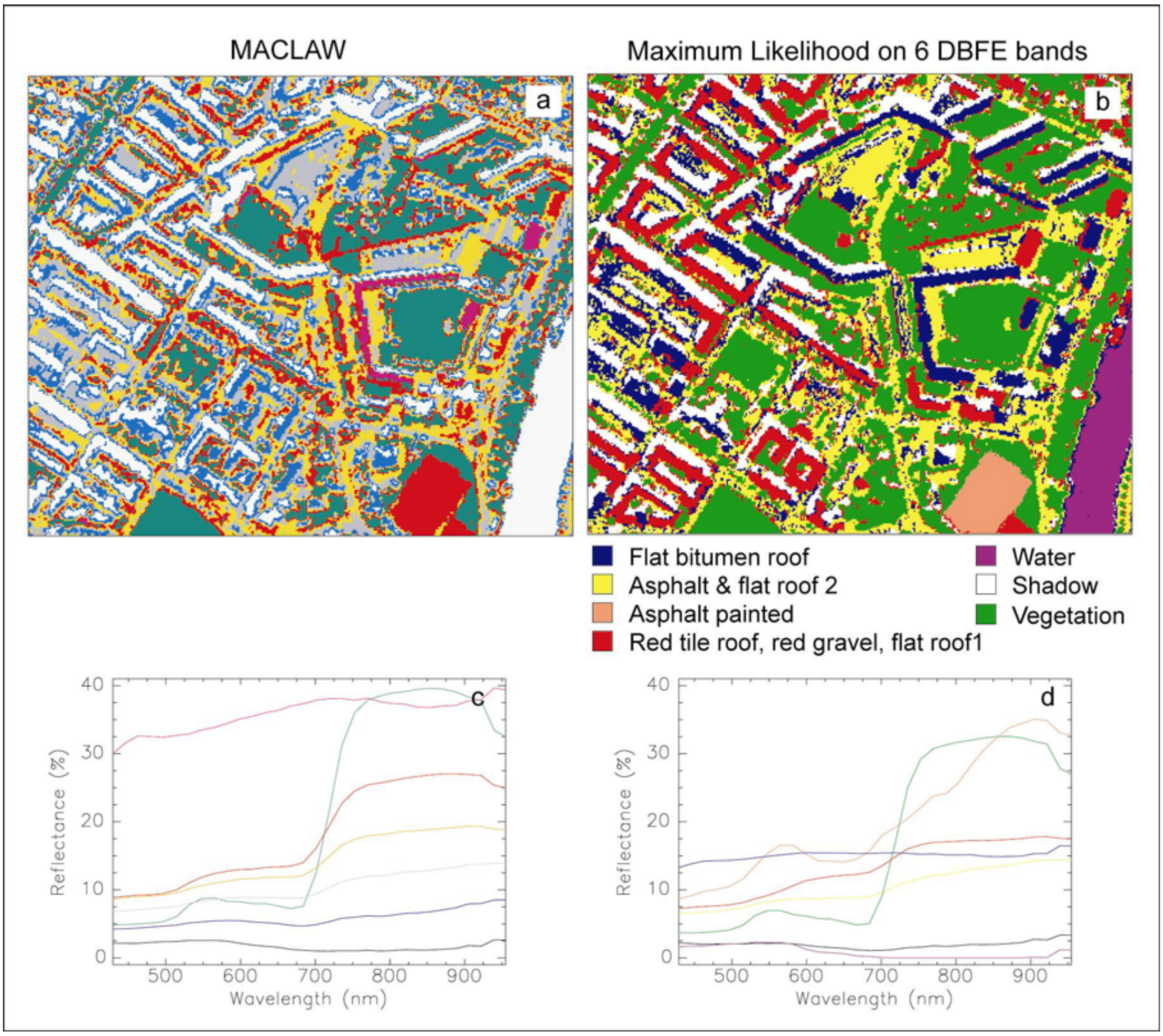


*Figure 3.35: Comparison of the classification result obtained with MACLAW (a) and with the ML classifier on 6 DBFE bands (b). The plots show the class means for c) the MACLAW classification (statistics of all pixels), and d) supervised ML classification (statistics of training set). The colours used for both classifications are intentionally not the same. The classes extracted by MACLAW were interpreted as follows: green= vegetation (class 1), red=red surfaces & painted asphalt (class 2), white=water & shadow (class 3) (black colour for the spectra in c), yellow=asphalt (class 4), blue=flat bitumen roof (class 5), magenta=highly reflective roofs (class 6), grey=asphalt (class 7).*

The MACLAW algorithm was set to identify the eight most relevant bands. The bands with their local and global weights are listed in Table 3.13. The highest weights were identified for five bands in the NIR and three in the blue wavelength range. The extracted classes were interpreted and the relevance of the bands for each was consequently examined based in the local weights. Accordingly, Class 1 covers vegetation pixels and MACLAW used above all a blue band and an infrared band (smaller weight) for their extraction. Class 2 comprises the red surfaces (red tile roofs, red gravel) and the class previously identified as painted asphalt. For the extraction of this class MACLAW used one single infrared band. Class 3 is identified as shadow and water that was extracted using again only one infrared band. Class 4 and 7 are two asphalt classes and for their identification MACLAW used two different infrared bands. In the mean plots in Figure 3.35c class 4 shows higher reflectance values in the NIR than class 7. Class 5 is interpreted as flat bitumen roofs; the same infrared band as for class 7 was used for its extraction. For the extraction of Class 6 (highly reflective roofs) the algorithm used two neighboured bands in the blue wavelength range where the difference to the other classes is the highest.

*Table 3.13: Local weights and global weights for the eight MACLAW bands. The higher the value the more the band is relevant for the extraction of the class.*

| | Band mean (nm) | Class 1 | Class 2 | Class 3 | Class 4 | Class 5 | Class 6 | Class 7 | Global |
|---|---|---|---|---|---|---|---|---|---|
| Blue | 462.4 | **1.0** | 0.0 | 0.0 | 0.0 | 0.0 | 0.0 | 0.0 | **0.7** |
| | 479.1 | 0.0 | 0.0 | 0.0 | 0.0 | 0.0 | **0.2** | 0.0 | **0.2** |
| | 495.9 | 0.0 | 0.0 | 0.0 | 0.0 | 0.0 | **1.0** | 0.0 | **0.8** |
| NIR | 752.7 | 0.0 | 0.0 | 0.0 | **1.0** | 0.0 | 0.0 | 0.0 | **1.0** |
| | 769.9 | 0.0 | **1.0** | 0.0 | 0.0 | 0.0 | 0.0 | 0.0 | **1.0** |
| | 787.2 | 0.0 | 0.0 | 0.0 | 0.0 | **1.0** | 0.0 | **1.0** | **1.0** |
| | 819.8 | 0.0 | 0.0 | **1.0** | 0.0 | 0.0 | 0.0 | 0.0 | **1.0** |
| | 837.1 | **0.3** | 0.0 | 0.0 | 0.0 | 0.0 | 0.0 | 0.0 | **0.3** |

Interpretation of classes: Class 1=vegetation, Class 2=red surfaces & painted asphalt, Class3=water & shadow, Class4=asphalt, Class5=flat bitumen roofs, Class6=highly reflective roofs, Class7=asphalt.

#### 3.6.1.4 Evaluation of the performance of MACLAW band selection

The bands identified by MACLAW were consequently used in the supervised classification with the ML classifier and compared with the results obtained on the six DBFE bands. Table 3.14 shows the accuracies and Kappa for both supervised classifications (see also confusion matrices Annex Tables AC3-8 and AC3-9). The accuracy for the classification on the MACLAW band subset is lower than for the one on the DBFE band subset.

*Table 3.14: Overall accuracies and Kappa for the ML classification on the subset of six DBFE bands, eight MACLAW and eight Bhattacharyya bands.*

| | Overall accuracy (%) | Kappa |
|---|---|---|
| DBFE (6 bands) | 98.1 / 92.3 | 0.98 / 0.91 |
| MACLAW (8 bands) | 95.7 / 89.6 | 0.95 / 0.87 |
| Bhattacharyya (8 bands) | 98.1 / 93.1 | 0.98 / 0.92 |

Another subset of eight bands was selected based on the Bhattacharyya distance. In contrast to the MACLAW subset that was composed only of bands in the blue and near infrared wavelength range, the bands selected based on the Bhattacharyya distance cover also green, yellow and red wavelengths. The means of the bands are 429, 514, 599, 684, and 701, 753, 770 and 889 nm for the four near infrared bands. The performance of this subset in the supervised classification is better than that one of the subset selected by MACLAW (Table 3.14 and Annex Tables AC3-9 and AC3-10).

The three classified images are shown in Figure 3.36. The comparison reveals a speckling effect that is more dominant in the classification on bands selected by MACLAW (compare Figure 3.36a and b). The detection of the flat bitumen roofs that posed already problems with the extracted DBFE features (Figure 3.36b) is even worst. Furthermore, more confusion can be observed between the vegetation class and the class of red surfaces (compare also Annex Tables AC3-9 and AC3-10). The classification on the Bhattacharyya band subset is less affected by the described improper class detection and the result is generally better than that of the classification on the MACLAW band subset.

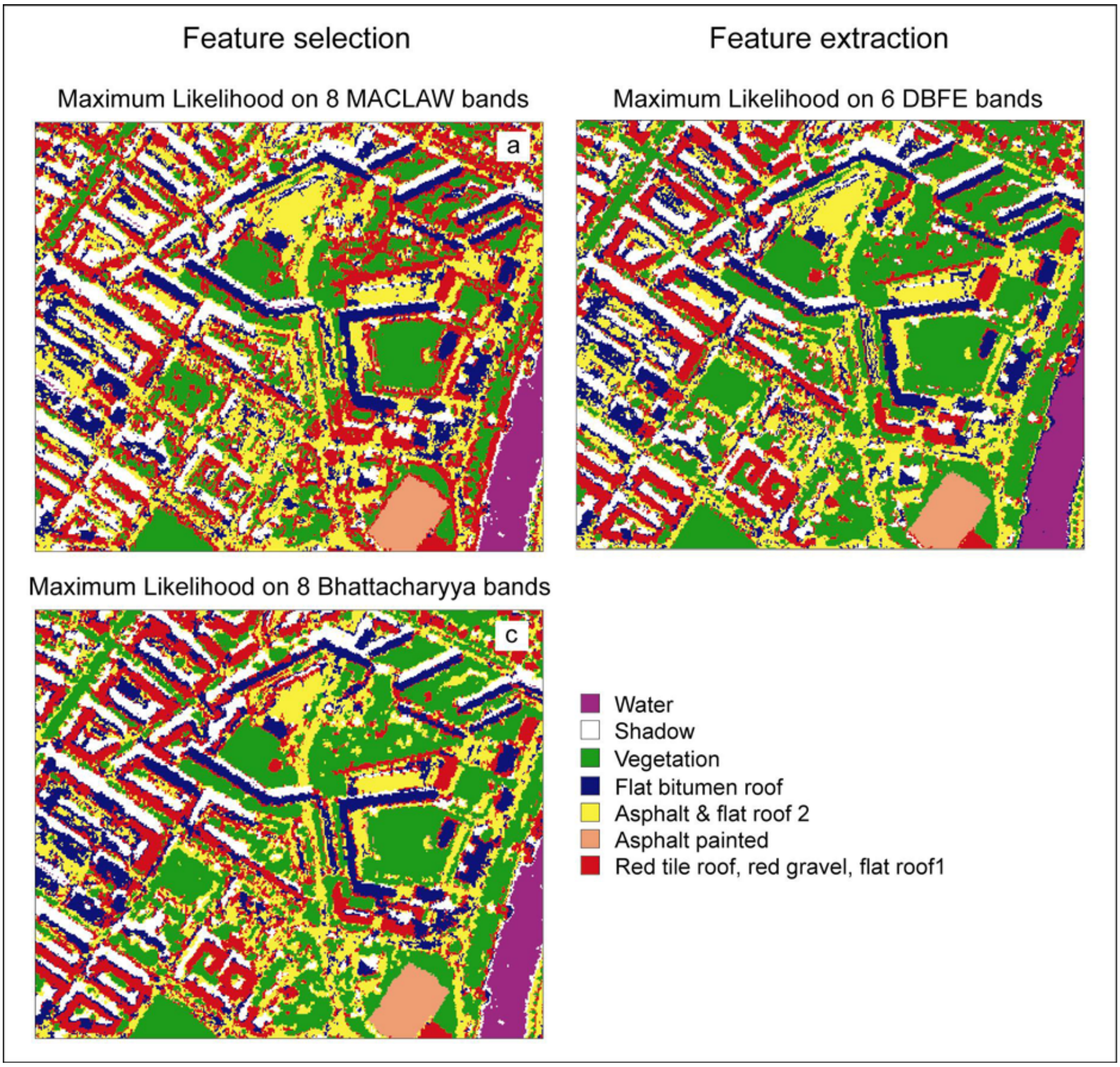


*Figure 3.36: Comparison of ML classification on eight MACLAW bands (a), six DBFE bands (b), and eight bands selected based on the Bhattacharyya distance (c).*

### 3.6.2 Conclusions

The results of this test series show that the performance of MACLAW is relatively good. The subset of selected bands performs poorer in the supervised classification than bands selected based on the class statistics (Bhattacharyya distance, user defined classes). Nevertheless, the latter needs knowledge *a priori* on possible classes and the motivation to test the MACLAW algorithm was to evaluate its ability to facilitate the detection of classes in hyperspectral images. The less better result of the supervised classification on the MACLAW band subset is certainly induced by the fact that the classes detected by the algorithm are different from those defined by the expert. Shadow and water for example were not distinguished by MACLAW but by the expert. Consequently, the selected bands perform poorer when they are used for the classification of different classes.

Other tests were performed to detect spectrally similar classes (only vegetation). The performance of MACLAW was rather poor and further development is ongoing to improve the algorithm.

## 3.7 Discussion

The presented work gives first insights in the specific features of urban vegetation in hyperspectral image data, the problems encountered, and presents results of one approach to analyse hyperspectral data. We could show how the specific radiation conditions in urban areas affect the spectral signature of vegetation objects and complicates the identification of spectrally unique features.

***Utility of vegetation indices***

Vegetation analysis commonly uses masking methods to reduce processing and the influence of information that is not relevant for the study (Underwood *et al.* 2003, Xiao *et al.* 2004). For the creation of such a mask, different vegetation indices were examined. We could show, that including corrections on the atmosphere and the underlying soil improves the detection of urban vegetation. Commonly used indices like the NDVI even give false estimates. Our results confirm the findings of Bannari *et al.* (1998) for very high resolution data that have shown the advantage of TSARVI compared to NDVI for the estimation of vegetation cover in urban areas for classes with high mixture of bare soil and vegetation.

We calculated broadband and narrowband indices that showed differences in the values but it was not possible to evaluate if one provides better estimates of urban vegetation cover than the other. We assume that they are proportional but it would be interesting to compare the index values with chlorophyll or LAI measurements. Eventually, this information can be used to evaluate the influence of the underlying soil on the signal.

***Utility of the used methods***

All in all, the results of the tree species detection are only partly satisfying. They indicate the possibility to distinguish between tree species but however, despite the definition of several species, the number of those that can be clearly distinguished, is limited to only a few. One reason might be the small number of classes and the significance of their characteristics. Some classes are probably more influenced by the underlying soil than others due to generally lower leaf area density observed in the field. However, the unique character of this influence leads obviously to a spectral difference.

Another reason is the chosen method and the size of the training sets that reaches the minimum necessary size (ten times the band number). In order to reduce the influence of the Hughes phenomenon on the Maximum Likelihood classifier we reduced the initial dimension of the image applying different feature extraction methods. The class related ones perform better than the transformation performed on the whole dataset. However, the efficacy of the Maximum Likelihood classifier depends on the class statistics and we cannot exclude that it is affected by the spectral similarity of the classes that persists even after the feature transformation. Other supervised classifiers like the minimum distance, that evaluates only class means, were tested but performed very poor on the data.

Vegetation is a highly rough surface with regions characterised by different illumination conditions (fully exposed, shaded, and intermediate states). Clark *et al.* (2005) suggest that for within-species diversity a classification based on a single distance metric would be ineffective. He suggests that methods like the Spectral Angle Mapper (SAM) would be more promising since it evaluates the similarity between two spectra in an n-dimensional space without using second-order statistics. This method is especially useful when the strength of illumination is not important (Kruse *et al.* 1993a). Usually, SAM is used to repress the influence of shading to accentuate the target reflectance characteristics (De Lange *et al.* 2004). However, it seems that the spectral signature of urban vegetation is not only a result of different illumination levels and many other factors influence the spectral shape. Until now, the SAM classifier was very few used for vegetation detection what might refer to its limited performance on these objects (Clark *et al.* 2005). In the analysis on forest species of Clark *et al.* (2005) the SAM classifier failed. SAM needs unique spectral signatures or endmembers that are compared with image spectra. However, to account for the intraspecies variability, more than one or two spectral signatures have to be used (Price 1994). The SAM classifier was tested on the analysed data but lead to no relevant result what is probably mainly linked to the defined reference spectra that are calculated based on the class means (Wania and Weber 2007). We defined some unique spectra in the image based on only a few and above all very similar pixels. The abundance map calculated by SAM then may at least provide object seeds. To obtain the whole of an object, one has to define several signatures that account all for the whole within-object variance.

Future work should focus on the combination of object-based and spectral classification approaches. Feature extraction might be included in this process as it is a valuable method to handle the high information content in hyperspectral images. However, the main problem is still the identification of spectral signatures that represent all intra-species variations.

Another option is to test other supervised classifiers that might perform better and should be tested in the future. An example is the Support Vector Machine that has proven good performance in a rural application (Lennon *et al.* 2002).

***Spectral similarity of vegetation objects***

Spectral signatures of vegetation objects may not be unique (Cochrane 2000). The unique identification of materials is difficult due to the numerous problems present in real world measurements, such as angle of view, atmospheric properties, spectral mixture, moisture content, and illumination angle and quantity, to name only a few. The complexity of the urban environment additionally modifies the spectral signature of objects what makes the identification of a unique signature very difficult. Additionally, stress factors and leaf age can change the spectral properties of foliage. Studies showed that the influence of shadow in-between the trees is very small for a spatial resolution of 1 m (Sugumaran *et al.* 2003).

The spectral separability of vegetation provides special difficulties because its spectral behaviour is described by a small number of independent variables (Price 1992). We have shown that in the visible wavelengths it is primarily determined by the concentration and composition of chlorophyll *a* and *b* and other pigments. Conversely, the reflectance in the NIR is a function of the internal leaf structure. In general, the reflectance of vegetation from different species is highly correlated due to their common chemical composition (Portigal *et al.* 1997).

Nevertheless, some studies have shown the possibility to discriminate different species (Cochrane 2000, Schmidt and Skidmore 2003, Xiao *et al.* 2004). However, most of them use reflectance spectra acquired using field or laboratory spectrometry what excludes some of the above mentioned factors. Xiao *et al.* (2004) differentiated between tree types (coniferous and deciduous) and deciduous tree species in an urban area using spectral mixture analysis and vegetation masking. Deciduous and coniferous trees show distinct spectral signatures.

However, in our study, coniferous trees could not be defined as training classes as they are too small and show low frequencies in the image. Xiao *et al.* (2004) state also that the overlapping of objects and reduced object size affect the detection of deciduous species and negatively influence their classification accuracy. The differences in our results and those of Xiao *et al.* (2004) might also be induced by the differences in the analysed spectral range. We used image data covering the visible and near infrared range. The image data used by Xiao *et al.* (2004) cover also the range of the mid infrared wavelengths where spectral features are additionally influenced by water content and lignin.

***Feature reduction methods***

We compared different feature extraction algorithms. Class dependent transformations perform better than the MNF transformation on the global dataset. This is not surprising. However, the selection of a specific feature extraction method depends on the training sets and the sample size. DBFE performs better than DAFE for the discrimination between spectrally similar classes.

In general, combined with the ML classifier, feature extraction methods perform better than feature selection algorithms. While the first theoretically includes all information of an object, the second one chooses among the initial bands excluding *a priori* information that might be discriminating to a smaller degree but that the algorithm considers being insignificantly. However, the new algorithm MACLAW might be useful in detecting classes in hyperspectral image data and help the interpreter in the preparation of further classification or extraction of endmembers.

# PART III: EVALUATION OF THE FUNCTION FOR AIR QUALITY

## 4 MICROSCALE AIR QUALITY SIMULATIONS

Traffic-induced emissions are major sources of air pollutants in urban areas (Fenger 1999, Colvile *et al.* 2001, Ketzel and Berkowicz 2004). Despite significant reduction of emissions due to technological improvements, motorized transport has lead to problems of higher vehicular exhaust emissions and traffic-induced emissions account for up to half of the main urban pollutants (Stanners and Bourdeau 1995, Fenger 1999). Many of the substances that are directly emitted by vehicles or indirectly produced through photochemical reactions represent a serious hazard for human health (Hoek *et al.* 2000, Dab *et al.* 2001). In France and Switzerland, for example, the traffic-related proportion of the total health cases attributable to air pollution amounts to more than the half (Künzli *et al.* 2000). Urban inhabitants are the most affected group most particularly those residents living in close vicinity to urban roadways and the pedestrians.

Urban areas are a focus of air quality assessment studies that are performed with empirical measurements or modelling techniques. The latter are useful to study present phenomena, as well as to provide predictions for future trends. In general, models use abstraction to help us understand reality. Air quality modelling techniques help to describe and interpret spatial phenomena, a difficult task when only a number of point measurements are available. Numerical codes have often been applied in combination with wind tunnels[26] (Johnson and Hunter 1999, Sagrado *et al.* 2002) or field data (Hassan and Crowther 1998, Riain *et al.* 1998, Mensink *et al.* 2006, Berkowicz *et al.* 2007) to simulate small-scale dispersion of pollutants within the urban canopy. These studies contribute to the understanding of local air flows and the resulting pollution dispersion.

Vegetation has an influence on air quality. As shown in Part I, the effect is two-fold: first, through vegetation's influence on climatic conditions such as humidity, temperature, etc. and second, through its interception and absorption of certain air pollutants. Little knowledge exists about the second effect, whereas the first impact is well-known and described. Methods that can be used to study the effect of vegetation on air pollution are generally those that are applied in air quality assessment studies. The climatic benefits from planted areas was shown using microclimatic measurements and modelling (Shashua-Bar and Hoffman 2000, Dimoudi and Nikolopoulou 2003, Shashua-Bar and Hoffman 2003). The retention of particles on plant leaves was demonstrated with chemical analysis (i.e. analysis of the type and quantity of substances on plant leaves) (Freer-Smith *et al.* 1997, Beckett *et al.* 1998, Ould-Dada and Baghini 2001, Thönnessen 2002, Freer-Smith *et al.* 2005). The absorption of gaseous pollutants into the plant tissue has been quantified in chamber experiments (Hill 1971, Bennett and Hill 1973).

Besides its effects on climatic conditions and air pollution, vegetation also influences the air flow by contributing to aerodynamic resistance. In studies focusing on the dynamics of flows in built environments, the influence of street trees on ventilation - particularly wind speed

[26] Wind tunnel studies are considered as a modeling technique here. Such experiments are used to simulate flow processes in street canyons. In most cases, the street canyon is reconstructed as two parallel walls (Gayev and Savory 1999; Gerdes and Olivari 1999; Gomes *et al.* 2007).

reduction - was shown to be important (Ries and Eichhorn 2001). Modifications of the flow field inside canyons by obstacles in general with increased turbulence were shown among others in Gayev and Savory (1999). Trees can be considered to be obstacles but, in contrast to cars, buildings and other obstacles, they are permeable, i.e. air flows can penetrate into the tree canopy. Although this effect has been described in the literature, little knowledge exists about its consequences in built environments and especially the main parameters that influence such flows.

Combining all of these points leads to the following conclusion: from one perspective, the ability of vegetation to remove pollutants positively influences air quality, but from another, trees and bushes might inhibit street ventilation and locally deteriorate air quality. Based on this knowledge, this study aims to evaluate the role of urban vegetation objects such as trees and bushes for pollution dispersion in built environments, with specific attention to its role in the removal of pollutants and its influence on ventilation. The evaluation is performed using computational modelling. This method has the advantage that the influence of governing parameters can be better evaluated individually, while in field measurements all governing parameters are simultaneously operating and it is consequently difficult to determine which parameters are significant or insignificant. It is nearly impossible to identify similar model areas with the same base conditions (wind flow, thermal stratification, solar radiation conditions, building geometry, and street configuration) and different vegetation conditions in complex environments like urban areas.

## 4.1 Definition of a spatial scale

The selection of an adequate computational model depends on the scale of the study. Atmospheric processes are the main driving factor of the relationships to be analysed and generally, they can be classified into three rough categories. At the microscale, phenomena occur on scales in the order of 0-100 m, at the mesoscale on scales of tens to hundreds of kilometres, and at the macroscale[27] at scales larger than hundreds of kilometres (Seinfeld and Pandis 2006). The microscale of urban air pollution overlaps with the mesoscale of regional air pollution.

Urban geometry affects the capacity of the environment to disperse pollutants in a city at the micro- and mesoscales (Oke 1988). At the mesoscale, the whole of urban roughness elements affects the production of mechanical turbulence, the vertical wind profile, and the depth of the urban mixing layer. At the microscale, effects are produced by each building’s wakeshed and both the circulation and turbulence associated with street canyons. The present study focuses on microscale effects that influence short-range dispersion and human exposure.

A large proportions the vehicular exhaust emissions in urban areas are released in street canyons and beside buildings - thus in very close proximity to human receptors. In most city centres, the concentration of pollutants is significantly enhanced by the fact that many roads have buildings alongside them (Oke 1988, ADEME 2002). Pollutant dispersion is mainly influenced by the configuration of street canyons, buildings and other obstacles such as vegetation. Vegetation ‘removes’ particles from the ambient air by dry deposition and by absorption of gases. It is a part of the urban ecosystem, and occupies above all non-built-up, open spaces.

[27] We summarise the synoptic and global scales that are usually distinguished in studies on atmospheric processes as the macroscale.

At the mesoscale, pollution removal by urban forests (i.e. all urban trees) was quantified for different cities (McPherson *et al.* 1994, Nowak *et al.* 2006). These studies revealed the quantitative effect per unit of area and provided important information for both current city planning and potential future urban development. Microscale studies investigated the retention of pollutants on or in plant leaves and described the aerodynamical resistance of vegetation objects (Hill 1971, Bennett and Hill 1973, Rauner 1976, Freer-Smith *et al.* 1997, Beckett *et al.* 1998, Ould-Dada and Baghini 2001, Thönnessen 2002, Freer-Smith *et al.* 2005). The trapping of pollutants promotes plantings but also induces other negative effects, such as ventilation inhibition (Ries and Eichhorn 2001). However, microscale air quality assessment with a focus on urban vegetation has not been completed. Microscale studies allow investigation of the effects of vegetation on pollutant dispersion. Ideally, microscale studies will draw upon existing knowledge and will be focused on the interactions of pollutants with the built environment.

In this study, the three-dimensional micro climate model ENVI-met (Bruse and Fleer 1998, Bruse 1999) is applied to study the microscale effects of vegetation on particle dispersion in the built environment. The model was chosen for the following reasons. A first important criterion was the integration of vegetation in the model. It was especially important that processes at the atmosphere-plant interface are taken into account by the model (e.g. processes related to the metabolism of the plant, dry deposition). In order to test different vegetation objects it was furthermore important that physical characteristics of vegetation objects could be modified. Finally, it was necessary to be able to represent the complexity of an urban environment in order to account for its influence on atmospheric processes. Consequently, the spatial resolution should be high and the model should account for relevant processes.

## 4.2 The ENVI-met model

ENVI-met is a freeware programme designed for simulations of plant-air-surface interactions in the urban environment at the microscale, i.e. for simulations at the level of a street or building block, or small city districts (Bruse 2007). The first version of the model was developed in the 1990 at the University of Bochum (Germany) by M. Bruse. The present study used version 3.0.

The following description aims to give a general idea of the model's design and functionality. Special focus is on functions that are important for the study aim, particularly relevant features for modelling the influence of vegetation on atmospheric processes. The model description is based on the documentation provided on the model website (www.envi-met.com). For more information on the parameters and equations, refer to Bruse & Fleer (1998), Bruse (1999), and the online manual with scientific documentation.

### 4.2.1 Model description

#### 4.2.1.1 General model design

Figure 4.1a gives an impression of the basic structure of ENVI-met. Basically, the model consists of a three-dimensional ***main model*** that is encapsulated within a one-dimensional model. The model area is subdivided into grid cells (x, y, z) and the size of each dimension defines the resolution of the model. In vertical direction, all grids, except the lowest five have an identical vertical extension (Figure 4.1b). The lowest five grid cells have the size

$\Delta z_g=0.2\Delta z$, increasing the accuracy in calculating surface processes. This equidistant grid type is useful for simulations focusing on processes near the surface.

The ***1D model*** provides the boundary conditions. It runs in an initialisation phase to provide the vertical profiles of all model variables for the inflow boundary of the 3D model (model initialisation) and runs parallel to the main model to provide the boundary conditions (Figure 4.1a). The 1D model allows an accurate simulation of the atmospheric processes within the boundary layer that reaches up to 2500 m in the case of ENVI-met (fixed). The simplified 1D model is introduced to reduce calculation time and at the same time to guarantee accurate calculation of atmospheric processes. Generally, microscale studies focus on processes occurring within the first hundreds of meters, but in turn, they also depend on atmospheric processes occurring in the upper heights of the boundary layer. Consequently, the 1D model takes over the calculation from the top of the 3D model, which is user defined.

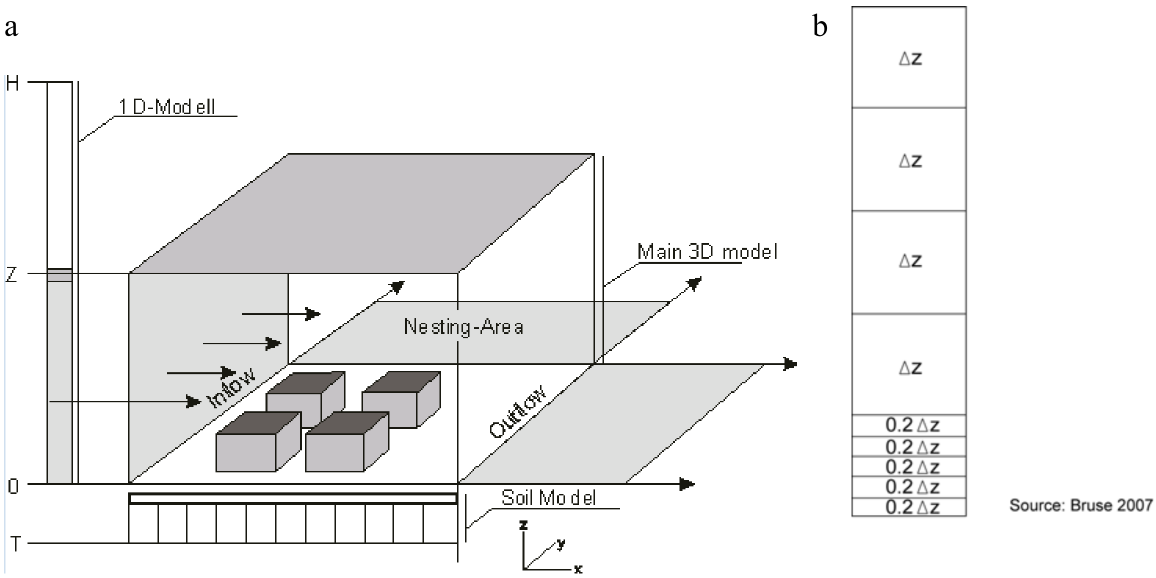


*Figure 4.1: Schematic overview over the ENVI-met model layout (a). The 3D model is the main model. Inflow variables and boundary layer processes are simulated in the 1D model. The vertical grid layout is equidistant with identical vertical extension of all grids except the first grid that is split in five sub-boxes with $\Delta z_g=0.2\Delta z$ (Bruse 2007). Nesting grids are added to avoid calculation errors at the model boarder. Soil properties are also modelled, using a soil model. (b) shows the vertical grid layout of the main model (equidistant).*

A ***nesting area*** is added around the main model to increase the distance of the model border to the core area. It consists of a band of grid cells that increase in horizontal resolution to the border. Nesting grid cells are added to avoid numerical errors at the model borders. No objects (buildings, sources, etc.) can be defined in these grid cells, which only allow the application of predefined soil profiles (see soil section below).

Finally, a ***soil model*** calculates the heat transfer from the surfaces into the ground and vice versa. Except the uppermost soil layer, in which the heat transfer is calculated in three dimensions, soils are treated as a one-dimensional vertical column. The soil model also provides information about the available water inside the soil, an important parameter for the calculations performed on the vegetation influence.

#### 4.2.1.2 Model configuration and model area definition

Two simulation files are necessary to run the model (Figure 4.2). They comprise the definition of the basic settings and the definition of the main model area. The basic settings are defined in the configuration file (Figure 4.2), which includes specifications on which files to use and generate, the input area file, the output names, simulation timing, etc., and defines the meteorological settings. Furthermore, special sections can be added to define model parameters such as receptors, the geographic position, the internal turbulence model, lateral boundary condition types, time steps, thermal properties of buildings, thermal and humidity profiles of soils, the model to calculate stomata resistance, etc.

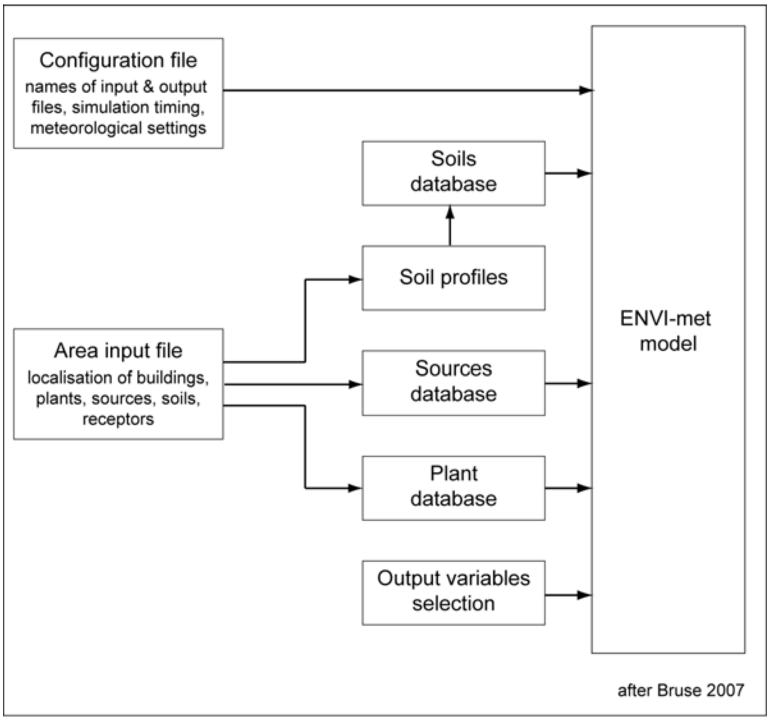


*Figure 4.2: Necessary input information for the ENVI-met model. The configuration file sets up the general configuration. The model area is defined in the area input file, where different objects are placed. Plant and source characteristics that can be adapted to the simulation task are accessed through their respective databases. The soil profiles placed in the area input file refer to soils defined in a special database (soils database). Output variables have to be defined for each simulation.*

The model environment is specified in detail in the area input file (Figure 4.2). Objects such as buildings, plants, emission sources, receptors are placed in the model and their characteristics are defined in specific databases (content is modifiable notably in the plant and sources database) (Figure 4.2).

***Buildings*** are defined in the area input file (Figure 4.1) by a height. All roofs are flat but other roof types such as saddle roofs can be simulated in the form of staircases. The thermal complex of the building system is defined in the configuration file with the indoor temperature and the heat transmission through the walls and the roof. Additionally, the albedo of walls and the roof is defined.

Four ***source*** types can be defined in ENVI-met: linear, point, volume, or area source. They can be simulated with time dependent emission rates where each source is defined by 24 values representing the emission rates for each hour of the day. The model can handle sources of gases as well as particles, but for each simulation, only one component can be emitted. Chemical transformations are not calculated by the model. The type of emitted gas or particle is defined in the configuration file by its diameter and density. Emission rate and source height are defined in the sources database (Figure 4.1).

***Vegetation*** is placed in the area input file and defined in the plant database (Figure 4.1) where the following parameters are defined: height, plant type regarding $CO_2$ fixation (C3 or C4 plant), plant type with respect to leaf diameter and aerodynamic properties (deciduous or coniferous), minimum stomata resistance, and short-wave albedo. Furthermore, each plant or area covered by lawn is treated as a one-dimensional, permeable column that is subdivided into layers (one layer per box). Above the ground, each is described by a profile of leaf area density (LAD) and under the surface, a profile of root area density is specified (RAD). Both profiles are defined by ten data points (LAD1 to LAD10 and RAD1 to RAD10) and normalized from z/H=0.1 to z/H=1 where z is the height of the LAD/RAD entry and H is the total height of the plant or the depth of the root zone. A model for the calculation of the stomata resistance is specified in the configuration file. It is used to calculate the transpiration of plants and depends on environmental parameters such as solar radiation, air temperature, and soil water content.

A ***soil*** type is assigned to each grid cell and is characterised in the soils database where parameters for the simulation of heat transfer are defined (heat conductivity and capacity, water content). Different soil materials can be selected and each soil type refers to a soil profile in the profiles database (Figure 4.1). Together, both form a relational database. In the profiles database, each of the soils is subdivided into vertical grid boxes defined by a soil referenced in the soils database (sand, loam, etc.). For the uppermost soil layer of each profile, roughness length, short-wave albedo and long-wave emissivity are defined. Finally, the initial temperature and humidity of the soil is set in the configuration file. Both represent the general surface values at the model start for calculating the vertical temperature profile (0-2500 m).

#### 4.2.1.3 Some basic modelling principles

This section aims to give an overview of the basic mathematical principles and of the parameters used to simulate the influence of vegetation on atmospheric processes. Formulas are omitted.

***Model type and modeling approach***

The ENVI-met model is based on the fundamental laws of fluid- and thermo-dynamics. It is part of the group of Computational Fluid Dynamics (CFD) models. In general, CFD modelling is based on the numerical solution of the governing fluid flow and dispersion equations, which are derived from basic conservation and transport principles (Vardoulakis *et al.* 2003). Atmospheric motions are governed by three fundamental physical principles: conservation of mass, conservation of momentum, and conservation of energy (Holton 1992). The mathematical relations that express these laws are derived by considering the budgets of mass, momentum, and energy for a control volume in the fluid.

The control volume of Eulerian models - such as ENVI-met - consists of a parallelepiped (Holton 1992). The position of the volume is fixed relative to the coordinate axes x, y, z.

Mass, momentum and energy budgets are calculated using fluxes caused by the flow of fluid through the boundaries of the control volume[28]. Consequently, the investigated three-dimensional spatial domain is decomposed into elementary volumes (grid cells) and the mathematical equations are solved for each cell.

### *Calculation of atmospheric processes*

The physical relations used to calculate the main atmospheric processes are summarised in an atmospheric model. It is linked with a soil and vegetation model that calculates the influences of soil and plants on atmospheric processes. The atmospheric scheme is based on equations that describe the evolution of the main forecasting variables: wind flow, temperature, and humidity. The turbulence is described using a E-ε model[29]. To account for vegetation's influence on atmospheric processes, all prognostic equations are extended into the vegetation layers using source/sink terms describing heat, humidity and momentum exchanges. Source/sink terms are mainly solved by the vegetation model. They are calculated using the LAD and the gradient of wind, temperature, and humidity. Below, the main relevant features are briefly summarised.

1) ***Influence on wind flow and turbulence***. The loss of wind speed due to vegetation friction is parameterised in the equations for the calculation of air flow. Besides the LAD value at different heights a mechanical drag coefficient (unique value) is added in the calculation of local source/sink terms. Two additional source terms are integrated in the equations for turbulence calculation in order to account for additional turbulence and dissipation due to the vegetation .

2) ***Influence on temperature and humidity***. Plant-specific fluxes of heat and vapour, the energy balance of the leaf, and the water balance (plant-soil) are calculated in the vegetation model that is linked by source/sink terms with the atmospheric and soil model. The vegetation model mainly accounts for the interactions between leaves and the surrounding air, expressed in terms of sensible heat flux, evaporation flux of liquid water on leaves, and transpiration flux. Furthermore, the model also simulates feedback mechanisms between transpiration and water supply by the soil. A photosynthesis model is used to simulate the gas exchange and transpiration that are controlled by stomata resistance. The influence of vegetation on short-wave and longwave radiation is calculated using different reduction coefficients. The main parameter is the leaf area index (LAI, leaf area per surface unit) that is derived from the LAD profile.

### *Calculation of gas/particle dispersion and deposition*

The model includes a dispersion and deposition model to simulate the dynamic behaviour of gases and particles. The concentration of a component (gas or particle) is calculated with the standard atmospheric diffusion equations (i.e. the Eulerian approach). Processes that induce a

---

[28] Another type of atmospheric dispersion models applies the Lagrangian method where the control volume consists of a mass of 'tagged' fluid particles (Holton 1992). This method considers the control volume as it moves, following the motion of the fluid, which always contains the same fluid particles. As opposed to the Eulerian method, the Lagrangian method needs to follow the time evolution of the fields for various individual fluid parcels ($x_0$, $y_0$, $z_0$ designate the position that a particular parcel passed through at a reference time $t_0$).

[29] In the E-ε model the equation for energy dissipation (dissipation rate ε) is added to the equation of turbulent kinetic energy (TKE, local turbulence E).

local decrease or increase in the concentration of a component are considered by adding source and sink terms in the atmospheric diffusion equation. The source term calculates the concentration with respect to the cell size in which the source is located (point, area, line or volume sources can be defined). A sink term accounts for concentration changes in the component due to sedimentation and deposition. The main forcing factors are gravitational settling and deposition at surfaces (soil, buildings, plants)[30]. The sink term is composed of the downward flux of the component, the flux received from above, and in the case of surfaces, the amount of deposed gases or particles. The main parameters for these fluxes are sedimentation and deposition velocity. Deposition velocity is calculated if the grid cell below is covered by a surface (soil surface, building, plant). In the other cases, sedimentation or settlement velocity is calculated. The latter depends on the diameter and density of the particle and the turbulence characteristics of the air flow. Deposition velocity for particles is a function of aerodynamic resistance of the surface and the sublayer resistance[31]. The resistances are inversely related to the deposition velocity. Aerodynamic resistance of plants is a function of two plant specific parameters: leaf diameter for deciduous and coniferous trees and wind speed at the surface. Sublayer particle resistance is expressed by Brownian diffusivity, which is size-dependent. Large particles experience higher sublayer resistance because they experience slower Brownian motion. Re-suspension is not taken into account by the model.

Accordingly, surface vegetation influences the deposition of particles and gases in the simulation of atmospheric dispersion. The influence is parameterised by introducing the LAD, leaf diameter and another plant type-specific parameter to calculate deposition velocity. The LAD is an important parameter in the calculation of the mass of deposed particles. An additional surface resistance for gases is added as plants actively regulate the gas exchange with the ambient air. It is mainly parameterised by the stomata resistance and the wet leaf fraction. Both are provided by the plant model. Finally, $CO_2$ is specially handled as it influences the stomata resistance of plants.

The model exclusively accounts for dry deposition of atmospheric species. Dry deposition denotes the direct transfer of gaseous and particulate species to the Earth's surface and proceeds without the aid of precipitation[32] (Seinfeld and Pandis 2006).

### *Considered pollutant*

This study focuses on particles with an aerodynamic diameter of exclusively 10 µm. The ENVI-met model can simulate the emission of only one species (pollutant) per simulation. The two parameters defining the species are its diameter and its density. The diameter is a unique value (no range). Usually, particles with a diameter of up to 10 µm are considered to be $PM_{10}$, a measure which normally includes smaller particles too.

---

[30] Usually, chemical transformations are another component of the sink term but calculations are restricted to inert gases.

[31] The quasi-laminar or sublayer is the layer adjacent to the surface. The resistance to transfer depends on the properties of the substance and surface characteristics (Seinfeld & Pandis 2006). On plant leaves the layer exists only intermittently as they are often in continuous motion.

[32] Wet deposition encompasses all processes by which airborne species are transferred to the Earth's surface in aqueous form (Seinfeld & Pandis 2006). Three processes are described: 1) dissolution of atmospheric gases in airborne droplets (e.g. cloud droplets, rain, fog, etc.). 2) removal of atmospheric particles when they serve as nuclei for the condensation of atmospheric water to form a cloud or fog droplet and are subsequently incorporated in the droplet, and 3) removal of particles when they collide with a droplet either below and or within clouds.

Particles refer to any substance, except pure water, that exists as a liquid or solid in the atmosphere under normal conditions (Seinfeld and Pandis 2006). They consist of a single continuous unit of solid or liquid containing many molecules held together by intermolecular forces, and they are of microscopic or submicroscopic size but are primarily larger than molecular dimensions (> 0.0001 µm). Particles arise from natural sources (windborne dust, seaspray, volcanoes) and from anthropogenic sources, such as combustion of fuels. If their size is less than 2.5 µm in diameter they are generally referred to as 'fine' particles while those greater than 2.5 µm are considered to be 'coarse' particles. The distinction between coarse and fine particles is made because they originate separately, they are affected by different mechanisms of transformation, removal, and deposition, they have different chemical composition and optical properties, and they differ significantly in their deposition patterns within the respiratory tract. The finer the particle, the higher the probability of its deposition in the lower parts of the human respiratory system (Seinfeld and Pandis 2006). Consequently, fine particles and especially ultrafine particles (UFP, ultra-fine particles, the diameter is < 0.1 µm) have larger impacts on health than the coarse fraction. Particles can be directly emitted (primary) or formed in the atmosphere by gas-to-particle conversion processes (secondary). Once airborne, they can change their size and composition by condensation of vapour species or evaporation, by coagulating with other particles, by chemical reaction, or by activation in the presence of water supersaturation to become fog and cloud droplets. While precipitation scavenging is the predominant removal mechanism for particles at altitudes above 100 m, particles near the ground are removed by settling and dry deposition on surfaces. As previously mentioned, this study focuses on the latter. Consequently, only a fraction of the coarse particles and only the anthropogenically-generated part arising from traffic is considered.

### 4.2.2 Model validation

The ENVI-met model was few validated. A general validation of ENVI-met was performed within the framework of the European research project 'Benefits of Urban Green Spaces' (BUGS 2001-2004, Bruse *et al.* 2002). Model results were compared to field measurements of wind speed, wind direction, temperature and humidity. Results for wind speed were satisfactory, given the relatively coarse resolution of the model used and the complex environment. Temperature and humidity were shown to correctly reflect the trends induced by modifications of the environment – especially when vegetation is present in street canyons.

Recently, the simulation of long- and shortwave radiative transfers through crop canopies were compared to two other validated models (Samaali *et al.* 2007). The results showed good agreement for the downward fluxes to the soil surface, as well as the soil and vegetation budgets. The non-attenuation of diffuse radiation assumed in the model for balancing the scattering occurring in vegetation was shown to lead to few agreements with the validated model.

Concerning pollutant concentrations no validation was performed. For such validation the contribution from sources outside the model area has to be considered. Local pollution concentrations are influenced by the local emissions but also by the pollution transport from neighbouring areas. Background pollution varies only minorly over large areas and does not differ much over microscale distances. The estimation of how neighbouring pollution sources contribute to local concentrations is much more difficult. Accordingly, local concentrations are above all a result of dispersion that depends on the environment and it is much more important to validate the general flow regime than absolute concentration values.

Such a validation could be done by coupling the model with models on larger scales. However, this study focuses on theoretical case studies with standardized scenarios where the tendency of a phenomenon interests above all. Nevertheless, it would be interesting to perform such a validation in the future. From that point of view, the ENVI-met model has been proven to be able to predict processes in urban street canyons and differences induced by modifications (Bruse *et al.* 2002). We decided that the above-reported validations were sufficient for the purpose of this study, and hence we have not performed our own validations.

## 4.3 Simulation of the influence of vegetation on particle dispersion in standard scenarios

The effect of vegetation on the dispersion of traffic-induced particles is evaluated using computer-based simulations. The focus is on vegetation objects close to traffic emission sources. As already mentioned, ventilation is especially disturbed in densely built structures. Several studies identified problems with ventilation and pollutant dispersion in narrow streets (Oke 1988, Gerdes and Olivari 1999). Some studies cited the influence of obstacles like trees, kiosks and cars on the flow (Gayev and Savory 1999). City planning promotes tree plantings in general, even in narrow streets, arguing for the positive effect of urban vegetation in general, but mainly based on the thermal benefits. However, little is known about the influence of the same trees on the air pollution load in the street. In reality, no official recommendations exist on reasonable tree plantings and consequently the choice is mainly influenced by landscape architectural and horticultural aspects and arguing for the climatic benefits. Some documents exist that evaluate the adaptability of tree species to urban living conditions and as well as some information on aesthetical aspects[33] (GALK 2006). Such lists do not provide information on possible ecological benefits, but it is important to include such information in order to optimise the function of urban vegetation. However, evidence is still missing about the relation between trees and pollution in urban streets. With the present study, we contribute to the description and understanding of this relationship in order to encourage the implementation of concrete recommendations city planners can use.

The following questions are addressed:

- How do trees and bushes influence the ventilation in streets?
- Which are the influencing factors?

To answer these questions, the influence of vegetation cover on the dispersion of traffic-induced particles was simulated in standard scenarios. The aim of the standard scenarios is the evaluation of the influence of vegetation on pollution dispersion in different urban street canyons.

[33] A list of 'adequate' street trees was set up by an association of the heads of the German horticulture institutions, for example.

### 4.3.1 Model configuration

#### 4.3.1.1 Basic parameters

The definition of standard scenarios was influenced by the following considerations. The local concentration of air pollutants is determined by the quantity of pollutants emitted in a certain area, dispersion mechanisms, and the background level. Dispersion at the microscale depends on the local flow between buildings and other obstacles, such as trees and parking cars. Flow direction and velocity are a result of interactions between the outer or main airflow and the spatial distribution and characteristics of buildings in the area of investigation. Background concentrations vary only a little at the scale of investigation and are considered to be less not important for understanding microscale effects.

Different model areas were defined to run simulations. A unique model area size and resolution was defined. The following parameters were defined to simulate different situations:

- different building structures and consequently street configurations including linear emission sources,
- two different wind speeds and inflow directions.

***Model area size and resolution***

The study focused on traffic emissions in streets between buildings that line up continuously along both sides. The basic model design is characterised by two intersecting streets with buildings aligned on both sides (Figure 4.3a,c). The buildings are placed in a model with constant main characteristics. The area and height of the model as well as the size of grid cells is the same for all simulation runs. The area covers 180x180 m and reaches a vertical height of 72 m. The size of the grid cells was set to 3 m. Consequently, each model area covers 60x60x24 grid cells (or 180x180x72m, Figure 4.4a,b). The equidistant grid layout was chosen for the vertical resolution. This means that the first vertical grid cell is subdivided into five cells of 0.6 m height (see detailed view in Figure 4.3b). To increase the distance of the model borders from the area of interest, we added seven nesting grids. This model area, height and grid cell size was applied for all simulations.

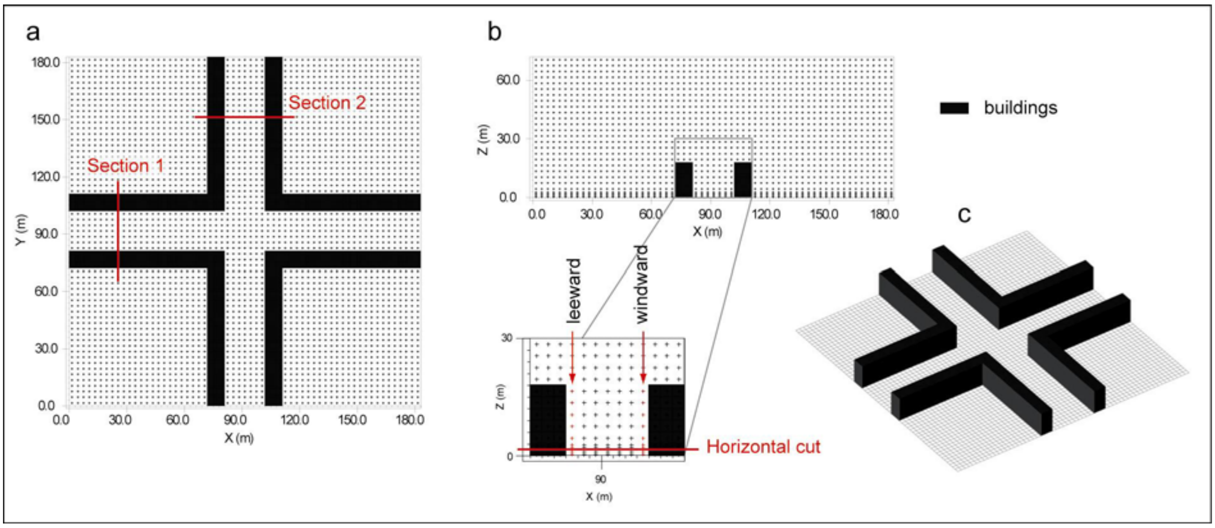


*Figure 4.3: Configuration of basic model area: a) horizontal cut, b) vertical cut with detailed view into the canyon, and c) 3D view. Note the smaller size of the lower first five grid cells in the vertical cut. The cuts used for the presentation of results are shown in red: a) vertical cuts referred to as section 1 and section 2, and b) the height of the horizontal cut and grid cells on lee- and windward canyons sides used for vertical profiles. Horizontal cuts are located between heights of 1.2 - 1.8 m (third grid cell above bottom). The building configuration shown is only an example.*

In general, the results presented here focus on the bottom of the canyon. Results are presented in three different ways. The first type of presentation is in horizontal cuts (Figure 4.3a). They cover heights between 1.2 and 1.8 m (third grid cell above the bottom, Figure 4.3b), which are considered to be the principal heights of human exposure (the height of the respiratory tract). When horizontal cuts are shown at other heights, the respective z-value is indicated. A second type of presentation is in vertical cuts (Figure 4.3b). They are placed at two positions, one parallel to the x-axis (section 1 at x=30 m) and a second parallel to the y-axis (section 2 at y=150 m). Both have nearly the same distance to the centre of the intersection. Results for the other parts of the intersection are not shown as they show the tendency of the flow and dispersion pattern like either section 1 or 2 (depending on the inflow direction). Third, in some cases, results are shown as data profiles in the z-direction only for the walking sides, i.e. profiles from the bottom of the canyon to the top. They consider the first grid cell beside the building wall that covers the walking side on both sides of the street (leeward and windward see Figure 4.3b).

### *Buildings*

Different building configurations were defined. The main parameter that we used for defining configurations is the distance between the buildings (i.e. the width if the street). In the following, the term 'street canyon' or 'canyon' is used instead of 'street', although the term refers to rather narrow streets. An important characteristic of canyons in general is their aspect or H/W ratio, where *H* is the height of the canyon walls (building height) and *W* is the canyon width. We chose to analyse the situation in one shallow or 'avenue' canyon (aspect ratio 0.5) and two deeper canyons (aspect ratios 0.9 and 1.2). Figure 4.4 shows the vertical (a) and horizontal (b) cuts of the three canyons. The geometric parameters are listed in table Table 4.1.

The selection of these aspect ratios was inspired by research findings on flow fields in street canyons and real street characteristics. Ahmed *et al.* (2005) summarize findings of several studies and report aspect ratio 0.65 as being the limit between two different major flow regimes. Furthermore, the selected aspect ratios are representative for street configurations in the city of Strasbourg. The analysis of spatial occurrence of aspect ratios showed that streets in densely built-up city districts show a tendency towards higher aspect ratios and closed façades (for detailed summary see Annex Chapter 4). Wide streets (aspect lower than 0.5) are usually flanked by only a few buildings. In contrast, higher aspect ratios tend to be flanked by continuously built-up façades. The highest aspect ratio found in Strasbourg is 1.0. This aspect ratio is present in ten percent of the streets. It occurs mainly in areas where most of the population concentrates like city centres and the residential districts close to the centre.

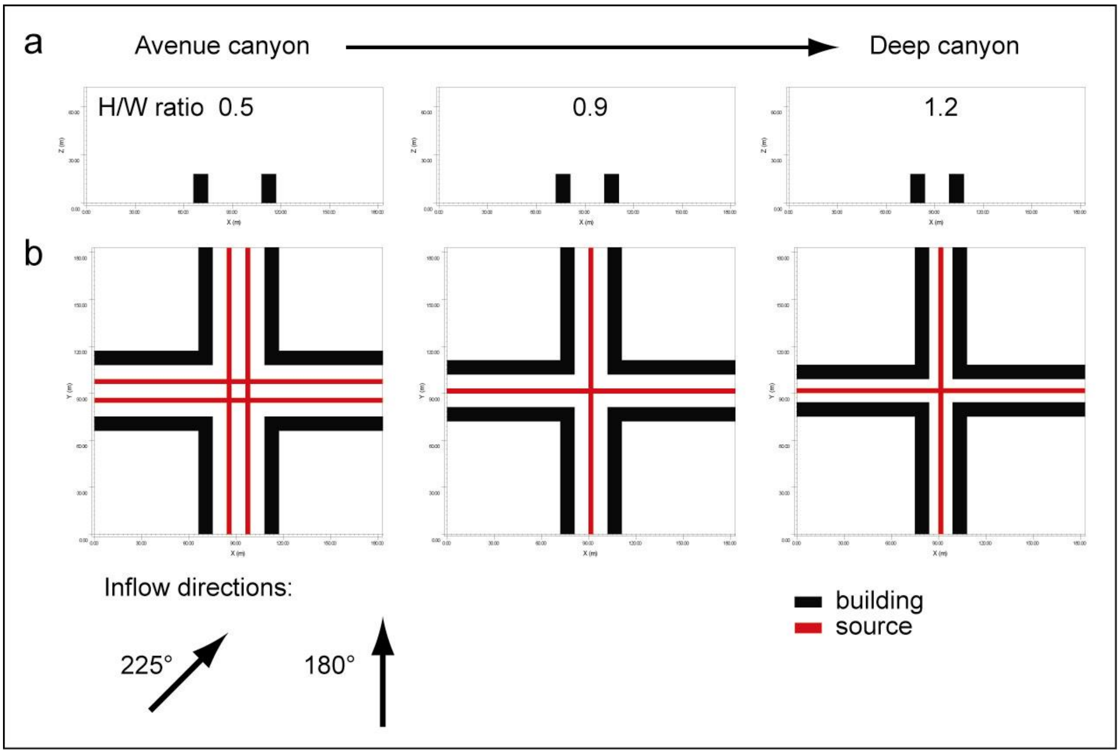


*Figure 4.4: Configuration of canyons (aspect ratios) with location of the source: a) vertical and b) horizontal cuts. Inflow directions are indicated with respect to the horizontal cuts. Street width decreases with aspect ratio while the building height remains constant.*

Grid cells that are not covered by buildings were defined as asphalt covered soils. For the nesting grids, we applied the profiles of loamy and asphalt soils.

***Emission source***

A linear source is situated in the centre or, in the case of the avenue canyon, parallel to the centreline of the canyon. Except from the avenue canyon, the source in each model area consists of one single line. The source emits $PM_{10}$ (particulate matter with a diameter of 10 µm) at 0.3 m height with a constant rate of 11.3 µg/s*m in all simulation runs. The emission value was taken from the STREET[34] database (provided by ASPA, 2000) and corresponds to

[34] The database mainly consists in emission and concentration data (STREET model, version 3.1, Pfeifer *et al.* 1996) calculated based on traffic data for 2000. Streets and intersections are those referenced in the BD Topo of IGN® (1989). Information source ASPA 05052302-ID.

the emission rate at the morning rush hour (7-8 am) for a street with medium traffic flow (10000 vehicles per day, 4 % heavy vehicles). For the avenue canyon, the emission value of each of the two lines was accordingly set to half of the total emission rate.

*Table 4.1: Characteristics of the three basic model areas (different aspect ratios): built objects, source configuration, general model area parameters and the model version used for the simulations. The model version corresponds to the model used to run the simulations.*

| N° | Street width (m) | Building height (m) | Aspect ratio (H/W) | Source | Size of grid cells (m) | Model height (m) | Area (m) |
|---|---|---|---|---|---|---|---|
| 1 | 33 | 18 | 0.5 | Double line | 3 | 72 | 180x180 |
| 2 | 21 | 18 | 0.9 | Single line | 3 | 72 | 180x180 |
| 3 | 15 | 18 | 1.2 | Single line | 3 | 72 | 180x180 |

***Wind speed and direction***

Most of air quality simulations in street canyons focus on one single street with two building rows. As the dispersion is highly dependent upon the angle between the orientation of the buildings and the approach flow direction, usually a high number of simulations have to be run to test different wind directions[35]. We decided to use a symmetric street canyon and intersection (all buildings have the same height) in order to reduce the number of necessary simulations. Accordingly, only two wind directions were analysed: 180° and 225°. Figure 4.4 shows the approaching inflow directions and their angle to the buildings. Accordingly, the 180° direction simulates wind flows blowing along-street and perpendicular to the canyon, while in the 225° direction, the wind blows in an oblique direction. The wind speed at 10 m was set to 1 and 3 m/s to simulate a calm situation and a situation with a distinct wind.

Each simulation was run for one hour. Parameters for the model initialisation (temperature, relative and absolute humidity) were set to the same values for all simulations, except the mentioned wind parameters. Consequently, the only varying parameters are the two wind directions and the building configuration, which is defined by the street canyon width. All simulations were run with the same model version.

#### 4.3.1.2 Vegetation scenarios

Trees are primarily used as vegetation objects to set up vegetation scenarios. Trees can take up more pollution than shorter vegetation due to their higher leaf areas and the turbulent air movement created by their structure (Fowler *et al.* 1989). The plants used for the scenarios were selected from the ENVI-met plant database and are listed in Table 4.2. The only parameters that vary are the height and the leaf area density (LAD). We used a 1.5 m high hedge and two different trees with a height of 10 m. Two types of trees were included: a tree with no distinctive crown and sparse leaves (T1) and a very densely foliated tree with a distinct crown (T2). Note that all objects are defined as blocks in the model.

---

[35] In urban areas wind direction may change very frequently.

*Table 4.2: Vegetation scenarios – characteristics of vegetation objects.*

| Name | Type | Vertical density | Crown shape | Height (m) |
|---|---|---|---|---|
| H | Hedge | Densely foliated | - | 1.5 |
| T1 | Row of trees | Sparsely foliated | No distinct | 10 |
| T2 | Row of trees | Densely foliated | Distinct | 10 |

Both trees have a leafless base up to 2 m (Figure 4.5a). While the vertical density of the crown of the sparsely foliated tree increases only slightly between the leaf base and the top, the crown of the densely foliated tree is distinct and reaches its maximum density between 6 and 7 m. All trees have the same height of 10 m. Furthermore, a third vegetation scenario was defined using a hedge of 1.5 m height (H) (Figure 4.5a).

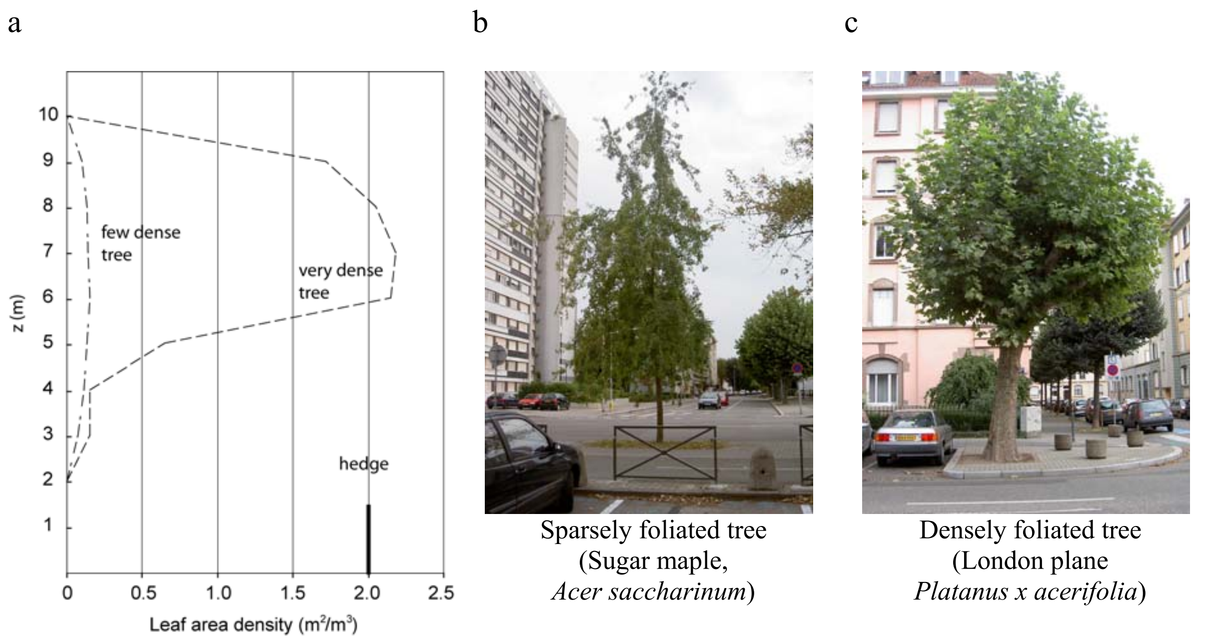


Sparsely foliated tree (Sugar maple, *Acer saccharinum*)

Densely foliated tree (London plane *Platanus x acerifolia*)

*Figure 4.5: Vegetation objects: a) leaf area density profile of the three vegetation objects (source: ENVI-met plant database), b) example of a sparsely foliated tree, and c) example of a densely foliated tree. Note the LAD profiles do not reflect the physical shape of objects.*

Each tree was tested in two different scenarios: 1) continuous row of trees (Figure 4.6b,d) and 2) widely-spaced row of trees (Figure 4.6c,d). For the hedge, only the continuous row applies (Figure 4.6b,d). The distance between buildings and vegetation objects is one grid cell (3 m, Figure 4.6e). The same applies for the spacing between neighboured trees in the situation with the widely-spaced row of trees.

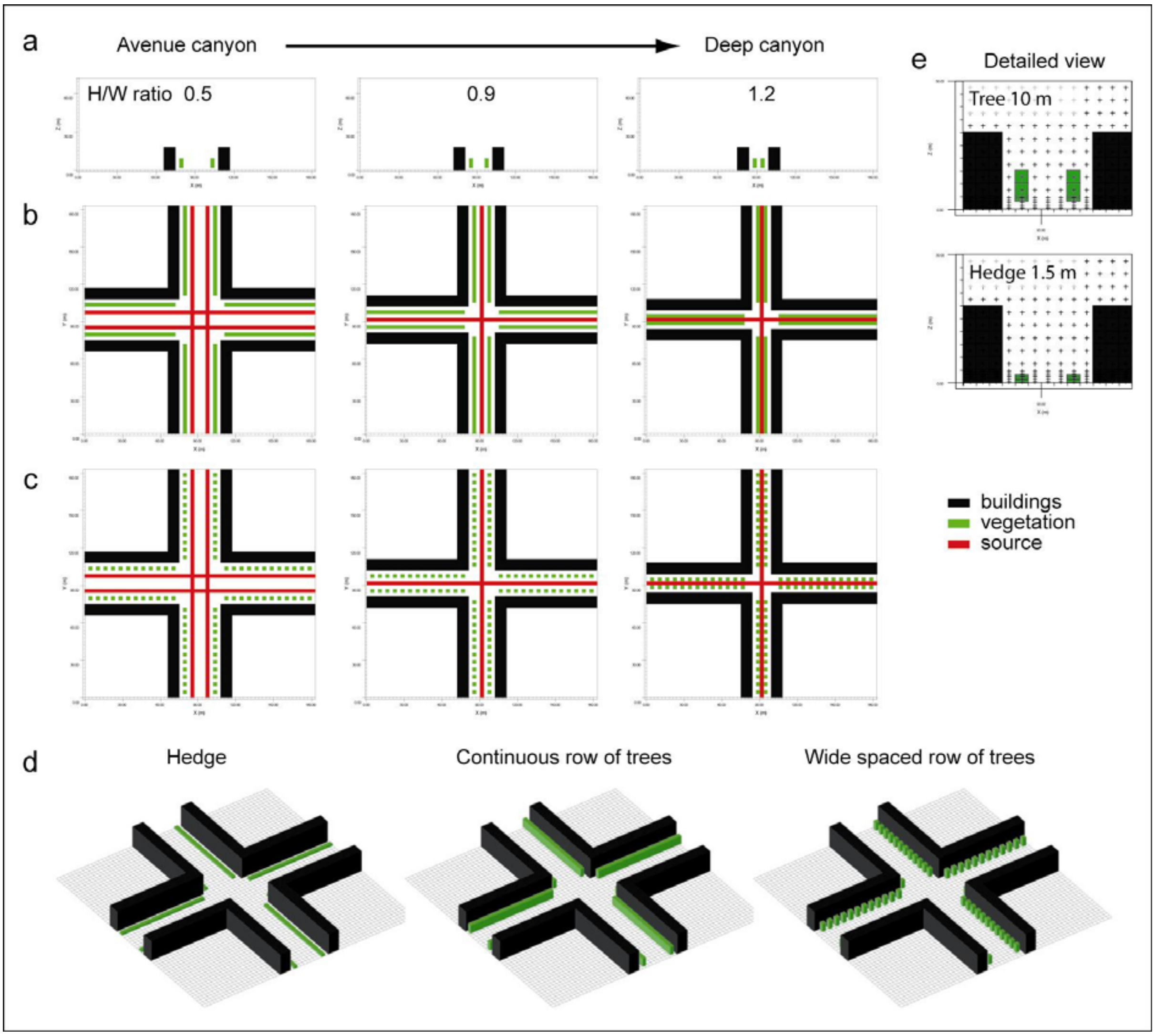


*Figure 4.6: Vegetation scenarios - configuration of model areas: a) vertical cut, b) and c) horizontal cuts of model areas where b) scenario with the continuous row of trees and hedge and c) widely-spaced row of trees. 3D view of model areas (aspect 0.5) with the main vegetation scenarios (d) and detailed views into the canyon (aspect ratio 0.9) (e).*

The simulations that were run are summarized in Figure 4.7. Each aspect ratio was run with all five vegetation scenarios. Each was simulated with the two inflow directions and two wind speeds (four different wind flows per scenario).

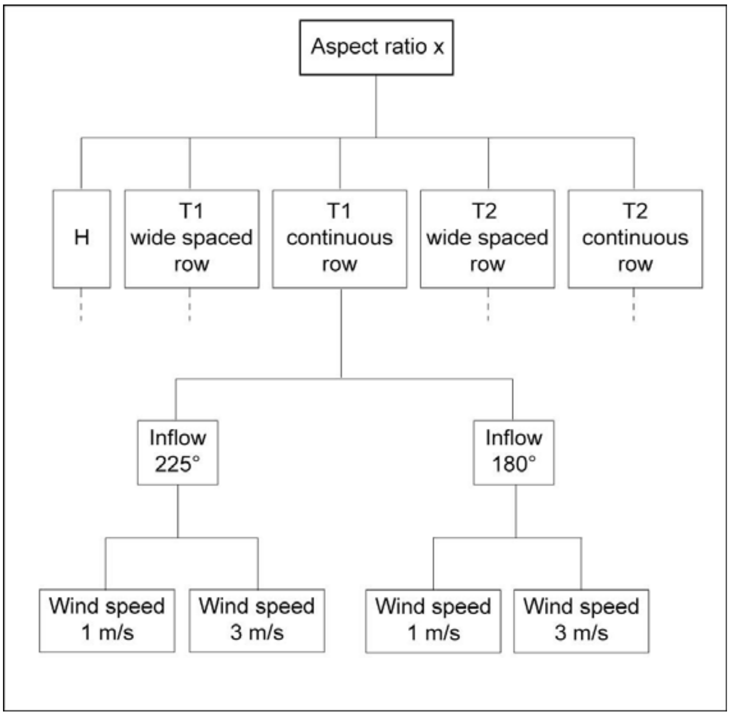


*Figure 4.7: Overview of simulations run for each aspect ratio x. Each aspect ratio was run with five vegetation scenarios and each with two different inflows and wind speeds. H hedge, T1 sparsely foliated tree, T2 densely foliated tree.*

### 4.3.2 Flow and particle dispersion in the situation without vegetation

The influence of vegetation on particle dispersion is directly linked to the modifications of the wind field and retention on the plants surfaces. To analyse the effects of vegetation, it is necessary to understand how particle dispersion is influenced by the general flow field within the canyons. Below, the wind flows are described. Then the resulting particle distribution in the situation without vegetation is described.

#### 4.3.2.1 Wind flow

The climatic conditions within street canyons are primarily controlled by the micrometeorological effects of urban geometry rather than the mesoscale forces controlling the climate of the boundary layer (Hunter *et al.* 1992). Ventilation and consequently particle dispersion depend on the air flows occurring at different levels within the street canyon. They are determined by the local wind field that depends on canyon geometry and the approaching wind flow direction and speed. In the following paragraph, the wind field and resulting particle dispersion are described. Here we show only the results for the canyon with aspect ratio 0.9. The description of the flow field is mainly performed based on the results from the simulations. For the interpretation, the results are compared to other wind tunnel studies, simulations, and measurements.

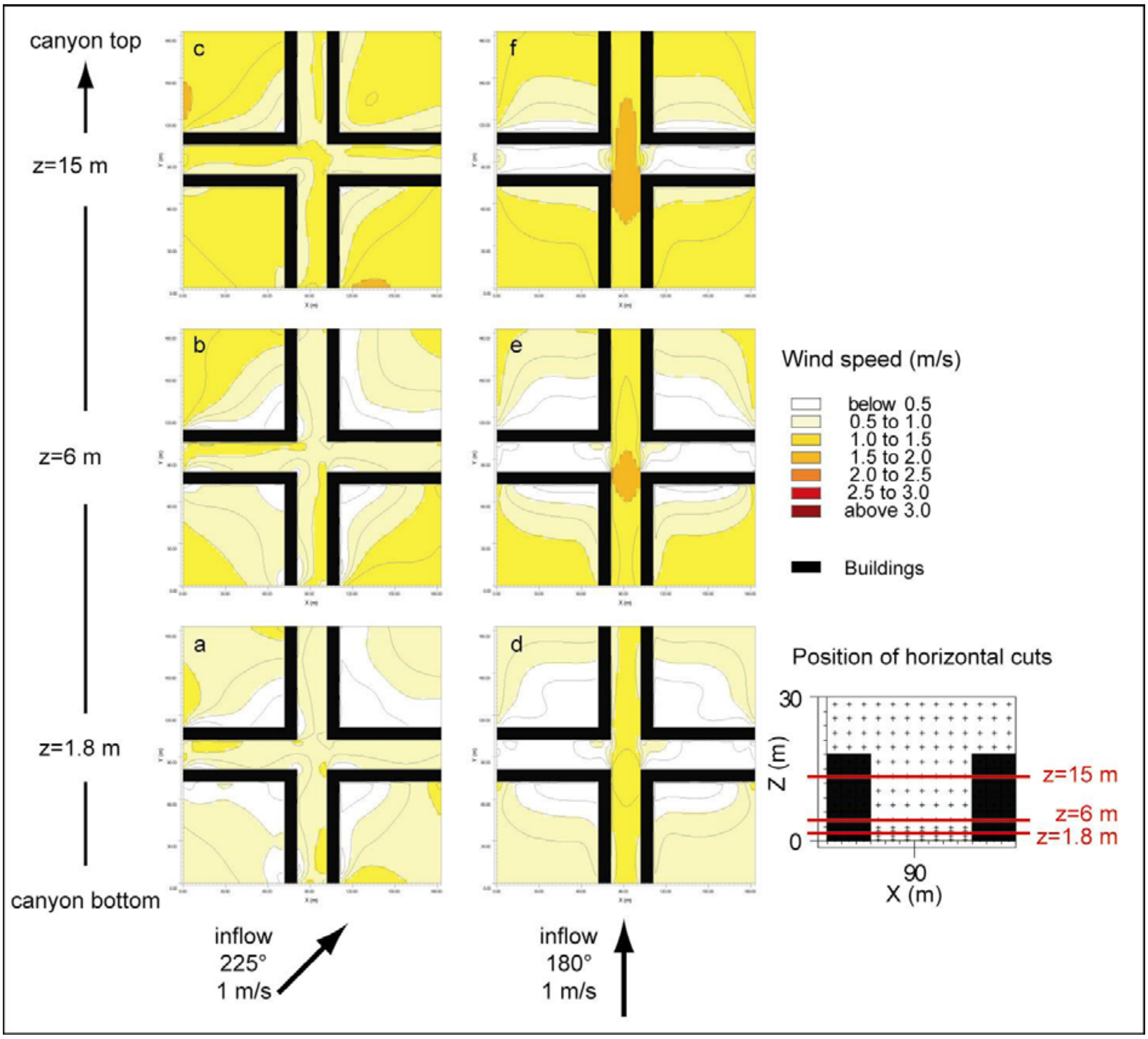


*Figure 4.8: Wind speed in the canyon with aspect ratio 0.9 for the calm wind simulation. Horizontal cuts at heights 1.8 m, 6 m and 15 m, a-c) inflow direction 225°, and d-f) inflow 180°. Distance between isolines is 0.25 m/s. Modification of wind speed by the building structure: wind speed reduction from the top to the bottom of the canyon (c-a and f-d) and formation of lee- and windward zones (a-c). Very low wind speed is observed in sections with perpendicular inflow (d-f). With parallel inflow, longitudinal velocity is proportional to the velocity outside the canyon (d-f). Furthermore, wind speed increases near the intersection towards the canyon top.*

In general, if the spacing between two buildings is large and the height is comparatively low, then their air flow fields do not interact[36]. At closer spacing – this is the case for all three aspect ratios used here – the wakes are disturbed and in fact, the smaller spacing between buildings disrupts the wakes around the buildings. Two main wind flows can be distinguished: the mean wind flow outside the canyon and the secondary wind flow inside the canyon (Figure 4.8). The main flow outside is increasingly modified and experiences deflection and wind speed changes with decreasing distance to the building structure.

[36] The flow field around a building is characterised by three zones of disturbance: 1) a downward flow at the windward face (bolster eddy vortex), 2) a lee eddy behind the building that is drawn into the low pressure zone due to the sharp edges of the building top and sides, and 3) a building wake further downstream characterised by increased turbulence and lower horizontal wind speed (Oke 1988).

Deflection occurs at building walls leading to wind speed reduction, deflection and formation of recirculation regions. In general, increased turbulence and formation of intermittent vortices occur at the corners of buildings (Oke 1988, Ahmad *et al.* 2005). In such short canyons, these vortices induce advection from the building-corners to the mid-block (Hoydysh and Dabberdt 1988).

Wind speed is lower inside the canyon and increases towards the top and at building corners (Figure 4.8a-c,d-f). In case of oblique inflow, lee- and windward regions occur on the respective canyon side (a-c). The size of the region on the windward side increases towards the canyon top. No such zones occur in case of parallel inflow (Figure 4.8 d-f). The longitudinal velocity component is proportional to the velocity above the canopy. Near the intersection a zone with increasing wind speed occurs that increases in size towards the top (Figure 4.8e,f). Canyon sections with perpendicular inflow show a very homogeneous wind field with low velocity (Figure 4.8d-f).

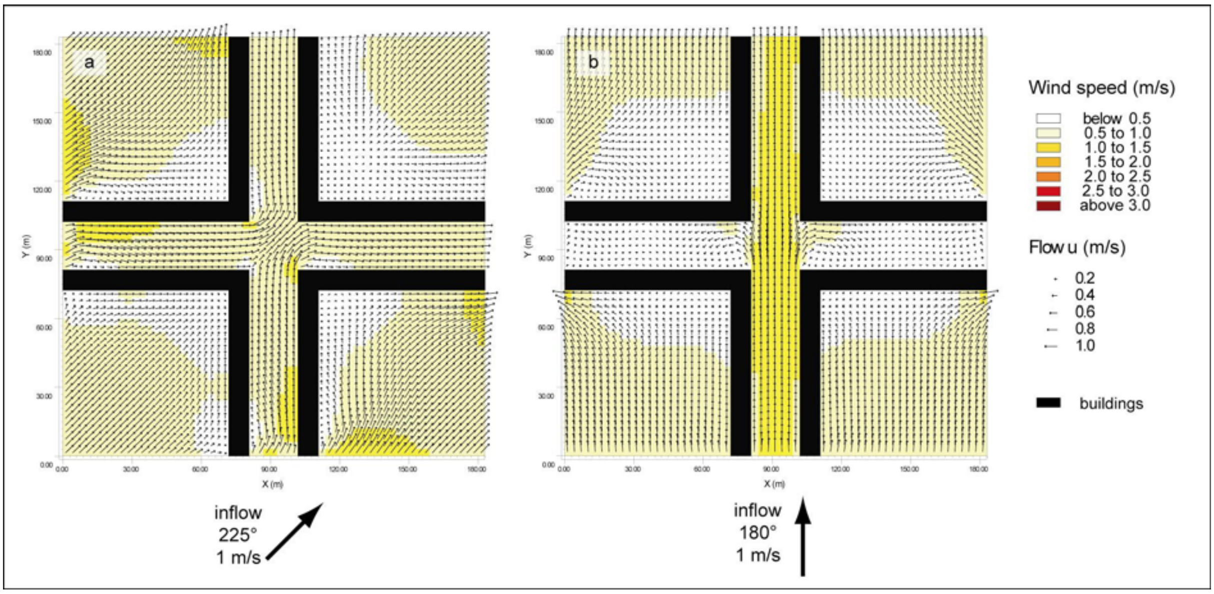


*Figure 4.9: Characteristics of horizontal flow at 1.8 m height in the calm wind simulation for both inflow directions. Example of aspect ratio 0.9. The arrows indicate the flow. Deflection of the flow occurs at building corners and with the convergence of flows at the intersection. Flow is reduced in case of perpendicular inflow (b).*

Deflection occurs where the oblique inflow enters the canyon and decreases the more the flow advances towards the intersection (Figure 4.9a). At the immediate intersection, both flows converge and are consequently separated in two flows continuing towards the upper and right canyon sections where the general slight deflection continues. Perpendicular inflow leads to significantly lower wind speeds inside the canyon and a near absence of flow (very short arrows, Figure 4.9a). In contrast, the sections with along-street wind show a nearly unmodified wind field (Figure 4.9b). Deflections occur at the intersection.

While at higher levels above the canyon, the flow experiences no deflection (straight, horizontal arrows, Figure 4.10), it is deflected up- or downwards near the canyon and modifications of wind speed occur. On the top of the windward building the flow is deflected, resulting in wind speed increase (longer upward arrows). Recirculation zones occur with lower wind speeds on the leeward side of the canyon.

With perpendicular and oblique inflows, the flow inside the canyon is dominated by recirculation, such, that the air at lower levels moves opposite to the direction of the outer flow (see simplified flow with oblique wind in Figure 4.10). Air is blown downwards at the windward canyon wall and, after recirculation at the canyon bottom, it is blown upwards on the leeward canyon wall.

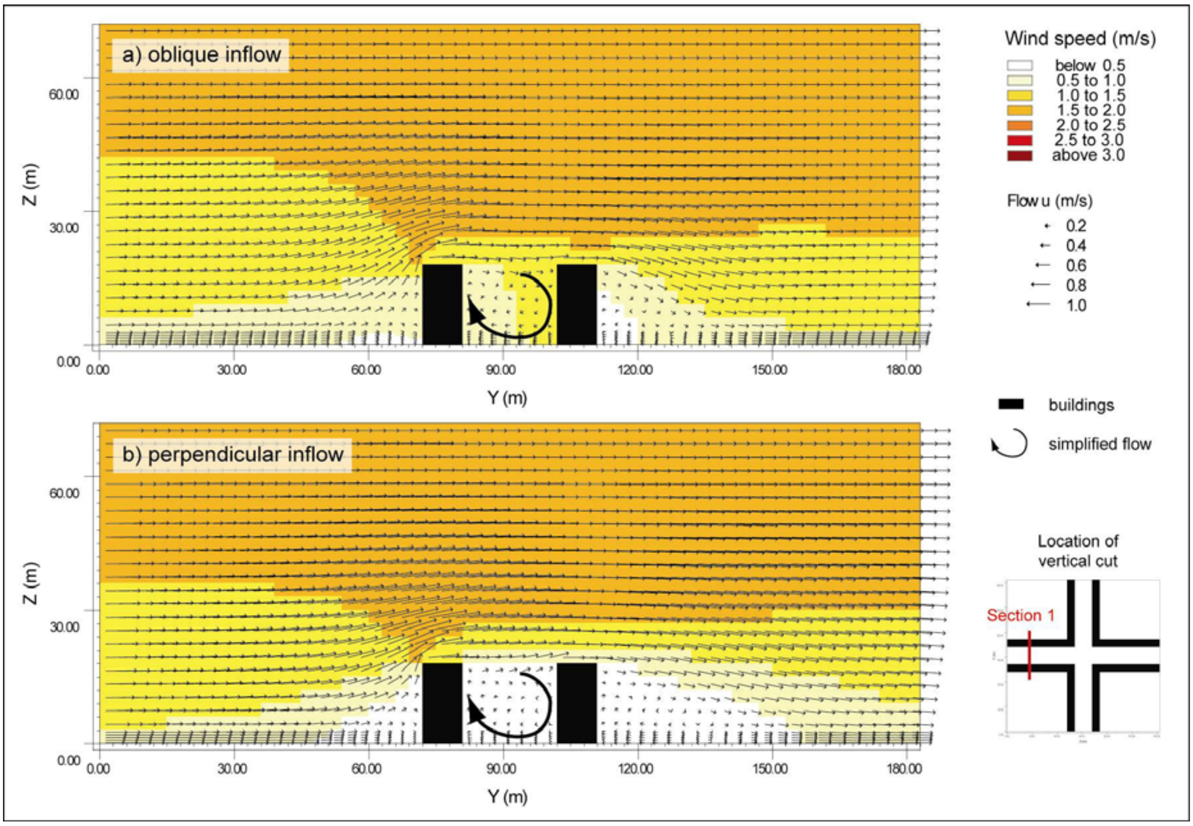


*Figure 4.10: Vertical wind flow ($u_z$) and wind speed for aspect ratio 0.9 at section 1. There is a disturbance of the main flow by the building structure. Deflection at buildings leads to up- and downward flows and lee- and windward canyon sides. Wind speed is reduced inside the canyon. With oblique wind lee- and windward sides occur (a). With perpendicular inflow, the flow inside the canyon is more homogeneous and characterised by very low wind speed (b). Inside the canyon a vortex is induced that rotates along the canyon length with oblique wind; with perpendicular inflow it is a single cross-canyon vortex.*

The smaller the canyon the more the wind field is modified and the more the flow fields of neighboured buildings interfere as the comparison of vertical wind flows in the three canyons in Figure 4.11 shows. The figure shows the vertical air flow in the simulation with high wind speed (the general characteristics can be better observed than with low speed that follows in Figure 4.12).

With oblique inflow, a bulk of downward air flow blows air from above inside the canyon. (Figure 4.11a-c,g-i). Its size decreases with aspect ratio (compare Figure 4.11a with b,c). The flow on the opposite canyon side moves upwards, leading to the conclusion that the air circulates across the canyon. The flow inside deeper canyons with oblique inflow is described as a helical or spiral rotating vortex induced along the length of the canyon. Such a vortex is more stable in urban areas, where it suppresses ventilation (Nakamura and Oke 1988). Before the intersection this vortex is probably less stable due to the influence of the downward bulk that induces better ventilation.

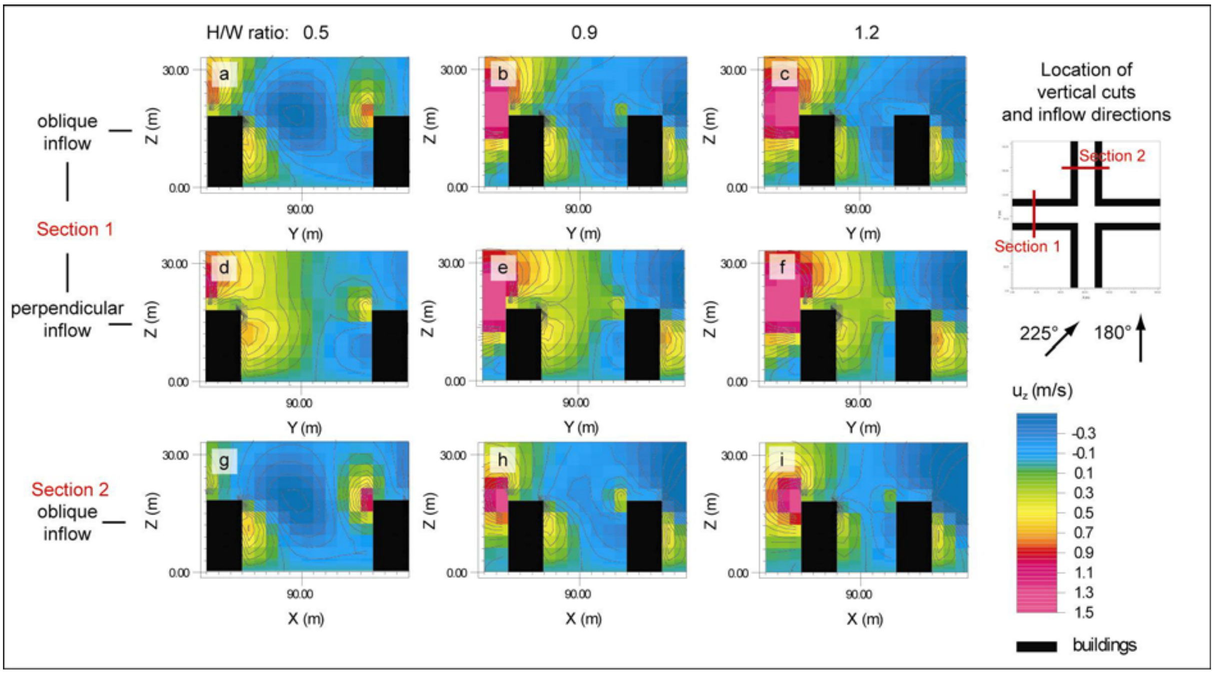


*Figure 4.11: Vertical wind flow ($u_z$) in the three canyons at the higher wind speed (3 m/s for different inflow directions (section 1 and 2). Blue colours indicate downward flow, green to magenta upward flow. The flow inside the canyon is characterised by down-drafts at the windward wall, reverse flow at the bottom and updrafts at the leeward wall. The bulks of downward and upward flows are disturbed with increasing aspect ratio. The distance between isolines is 0.1 m/s.*

The simulation with the perpendicular inflow in the avenue canyon (aspect 0.5) is characterised by secondary flows in the canyon space, where the downward flow is reinforced by deflection down the windward face of the next building downstream (Figure 4.11d). The flow regime is defined as a wake interference flow (Oke 1988). With decreasing distances between the canyon walls, the bulk of the outer flow does not enter the canyon (Figure 4.11e,f). At greater aspect ratios a single cross-canyon vortex is established in the canyon, typical for a skimming flow regime (Oke 1988). It is associated with reduced exchange between the canyon and the flow outside. Nevertheless, at this wind speed, the flow inside the canyon is driven by the flow outside (Nakamura and Oke 1988).

The described relationships also apply to the simulations with a calm wind, but in general, exchange and circulation is reduced. The up- and downward flows are significantly reduced. With oblique wind, a downward bulk from above still enters into the canyon (Figure 4.12a-c,g-i).With perpendicular inflow, it is nearly absent and is cut by an upward flow (Figure 4.12d,e,f). The strength of the up- and downward flows decrease with aspect ratio.

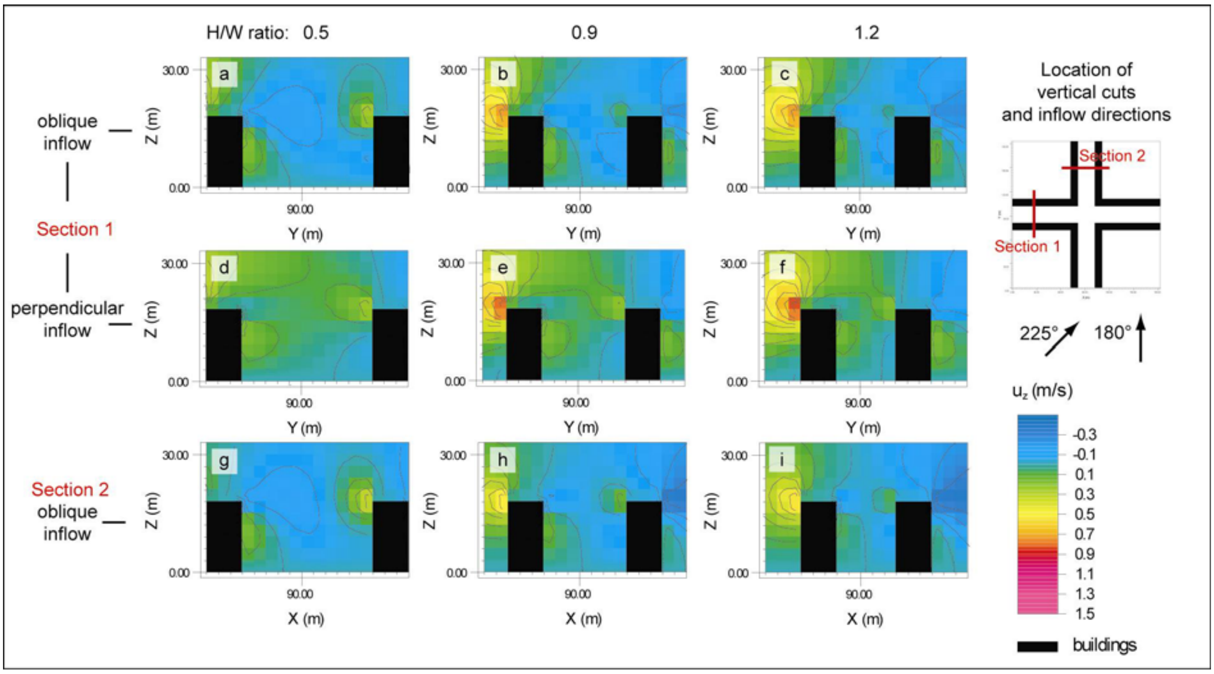


*Figure 4.12: Vertical wind flow ($u_z$) in the three canyons at wind speed 1 m/s for different inflow directions (sections 1 and 2). Blue colours indicate downward flow, green to magenta upward flow. In general, exchange is smaller than at high wind speed (lower velocities). The downward and upward bulks are very low. The distance between isolines is 0.1 m/s.*

### 4.3.2.2 Particle dispersion

The highest particle concentrations occur in close vicinity to the source, and decrease with increasing distance from the source (Figure 4.13). In general, particle concentrations increase with increasing aspect ratio, referring to worsened ventilation (Figure 4.13 a to c and d to f). Besides the volume of the canyon, this is due to the rate at which the canyon can exchange air vertically with the atmosphere above roof-level. As described in 4.3.2, within the avenue canyon, the air flow is mainly influenced by the outer flow thus fresh air penetrates into the canyon, leading to mixing and consequently to dilution of the particle concentration.

The highest values occur at the intersection where the flows and the sources converge (Figure 4.13). Furthermore, concentrations are generally higher after the intersection. This effect is especially visible in the simulation with wind direction 180° (Figure 4.13d-e). In the along-wind street, it leads to significantly higher concentrations after the intersection. At the intersection the flow crosses the left and right streets, resulting in pollutant uptake. With oblique inflow, the increase after the intersection is smaller. In both situations increased deflection and turbulence after the intersection leads to wind speed reduction and fewer particles are blown outside the canyon.

With perpendicular inflow, concentrations tend to increase (Figure 4.13 compare a and d, b and e, c and f). The reason is reduced vertical exchange with the outer flow. Ventilation is reduced in the whole canyon section, while the oblique approaching inflow provides markedly better ventilation.

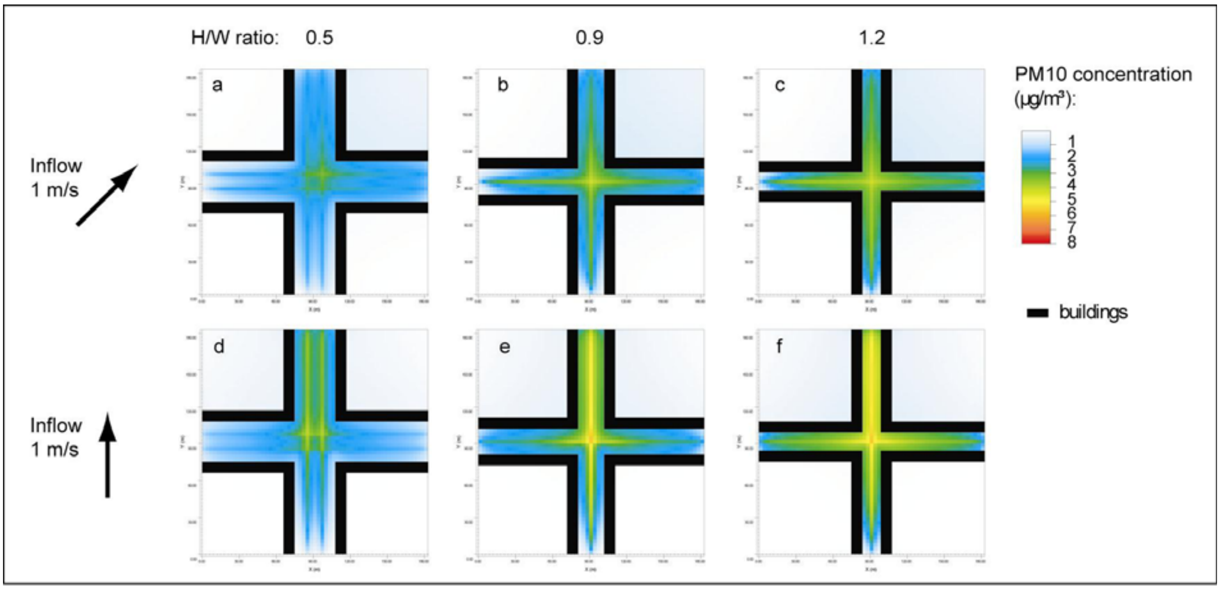


*Figure 4.13: Particle concentration in the simulation with calm wind for inflow 225° (a-c) and 180° (d-f), horizontal cut at 1.8 m. Concentrations increase with aspect ratio. Higher values occur after the intersection. Concentrations are reduced with oblique and increased with perpendicular and parallel inflow.*

Increasing concentrations with aspect ratio for all inflow directions apply also for the vertical dimension. Concentrations are higher after the intersection (Figure 4.14g-l). The canyon with aspect ratio 0.5 is better ventilated, particularly on the walking sides (Figure 4.14a). This effect is mainly induced by the fresh air blowing into the canyon and the helical vortex that is missing in the perpendicular inflow.

The vertical concentration distribution also reveals poorly ventilated regions that are characterised by weak mixing of pollutants, resulting in a long residence time for exhaust emissions and consequently higher concentration rates. The highest particle concentrations, away from the source, are typically found in the wake of the upwind walls (leeward). This effect is stronger in the canyons with ratios 0.9 and 1.2 and visible in the simulation with oblique inflow before the intersection (Figure 4.14b,c). The relationship can be explained by the following process. Fresh air penetrates the street canyon along the downwind walls and leads to lower concentrations at the bottom of the windward buildings. Next, this flow is deflected at the bottom of the canyon towards the leeward buildings and the pollution concentration increases again when the flow crosses the source. Consequently, the air in the leeward side shows higher pollution concentration. Dilution is reduced due to significantly lower wind speeds. Only a few particles are blown up the walls to the top of the canyon. In the deeper canyons only a small amount of the upward air flow leaves the canyon and the recirculation inside leads to a further accumulation of pollutants. After the intersection (oblique wind), differences in concentration between the lee- and windward side of the canyon are smaller and nearly absent in the deeper canyons (Figure 4.14g-i).

Equal concentrations on the lee- and windward side in the simulation with perpendicular inflow again point to a lack of exchange with the main flow outside the canyon (Figure 4.14d-f). In the same section, concentrations are higher with perpendicular inflow (compare Figure 4.14 a-c with d-f).

The highest concentrations even at the top of the canyon occur in the simulation with parallel inflow (Figure 4.14j-l). No fresh air enters into the canyon from outside and consequently no mixing occurs. The upward flow on the building walls transports pollutants towards the canyon top but at low velocity.

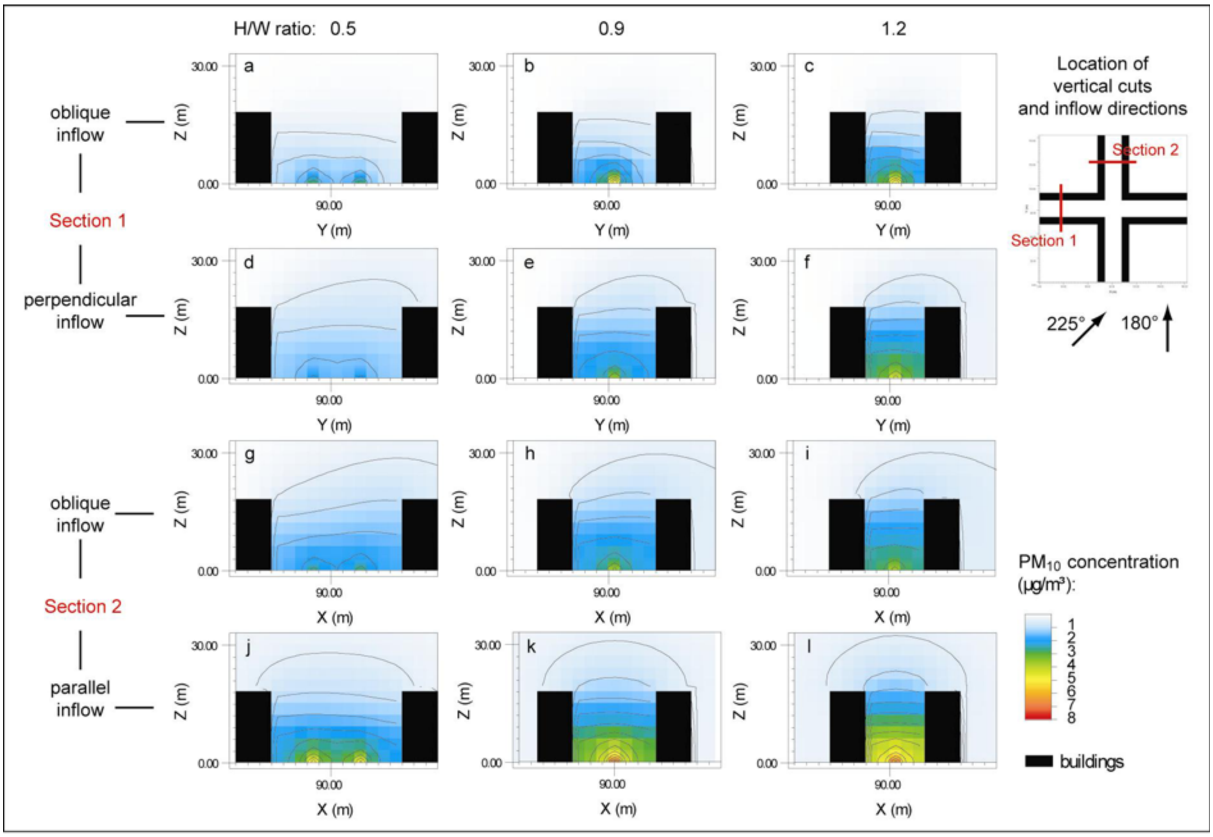


*Figure 4.14: Particle concentration in the calm wind simulation with different inflow directions (section 1 and 2): vertical distribution with oblique inflow (a-c, g-i), perpendicular inflow (d-f), and parallel inflow (j-l). Distance between isolines 0.5 µg/m$^3$. In general, concentrations increase with aspect ratio. With oblique inflow, concentrations are smaller on the windward side (a,b,c). Parallel inflow promotes particle accumulation (j-l).*

The comparison of values on both walking sides for the two sections reveals differences in the pattern of pollutant distribution for different inflow directions. Significant differences between the lee- and windward side occur with oblique inflow before the intersection (Figure 4.15a). Concentrations are higher on the leeward side. These differences decrease when oblique inflow is increasingly modified by building structures and are absent in the two deeper canyons (after the intersection, Figure 4.15b). In the avenue canyon, concentrations are higher on the windward side and in general they are higher than before the intersection. With perpendicular inflow no differences exist between the lee- and windward canyon side (Figure 4.15c). With parallel inflow, differences between both canyons sides[37] decrease with aspect ratio and are absent in the deepest canyon (Figure 4.15d). In this case concentrations reach the highest values for all canyons. The differences in the two wider canyons may refer to the influence of turbulence induced at the intersection that influences the flow pattern inside the canyon and deflects the initial straight flow field.

[37] Even if a distinction between lee- and windward side is not technically correct (as the flow is parallel to both sides), this terminology is used to simplify the discussion.

In general, concentrations are higher after the intersection (compare Figure 4.15 a,c with b,d) and lowest values for all canyons occur with oblique inflow before the intersection when pollution is diluted by the entering fresh air (Figure 4.15a).

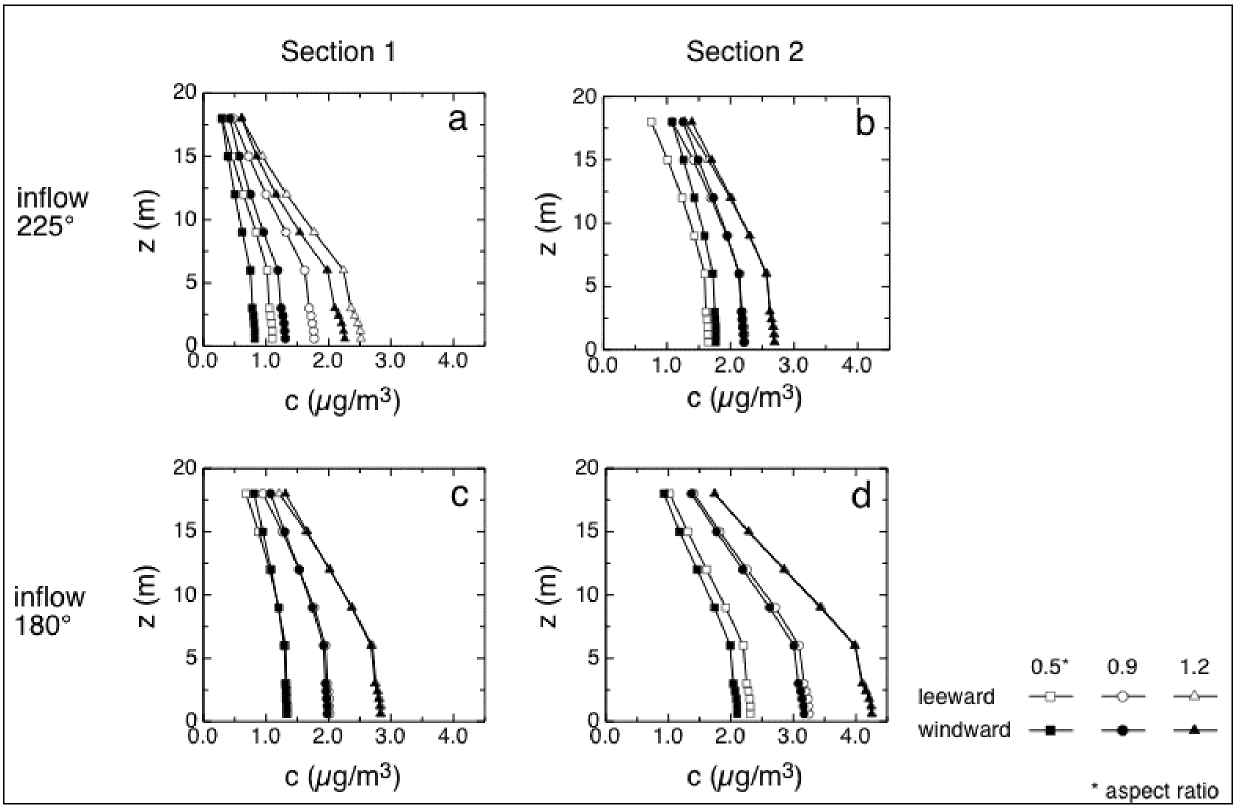


*Figure 4.15: Particle concentration on the lee- and windward side with different inflow directions at section 1 and 2: (a) and (b) oblique inflow, (c) perpendicular, (d) parallel inflow. Shown are the values of the grid cell close to building walls. Mixing with fresh air by oblique inflow leads to concentration differences at the lee- and windward sides in all canyons (a). The spiral vortex inside the canyon is modified after the intersection (b).*

***Influence of wind speed on particle dispersion***

The distribution pattern in the simulation with the higher wind speed is different from that of the calm wind simulation. In general, higher wind speed reduces particle concentration (green colours in Figure 4.16 refer to concentration reduction). With oblique inflow the effect is stronger in the sections before the intersection and on the windward sides (Figure 4.16a-c). The decreasing effect can be explained by the deflection of the flow at the intersection leading generally to more turbulent flows and reduced wind speed after the intersection. Obviously, these changes are in the same dimension as the changes at lower wind speed (relatively). Consequently, more particles are retained inside the canyon.

With parallel inflow the differences are higher in the whole along-wind canyon (reduced concentrations at high wind speed Figure 4.16e-f). In contrast, higher wind speed leads to a concentration increase when the approaching inflow is perpendicular (Figure 4.16e-f). At higher wind speeds the exchange with the main flow outside seems to be inhibited, resulting in higher concentrations. This relationship does not apply for the avenue canyon where faster perpendicular inflow enters the canyon, inducing ventilation (Figure 4.16d).

Again the described effect increases with aspect ratio (i.e. the differences are higher in the canyons with aspect ratio 0.9 and 1.2).

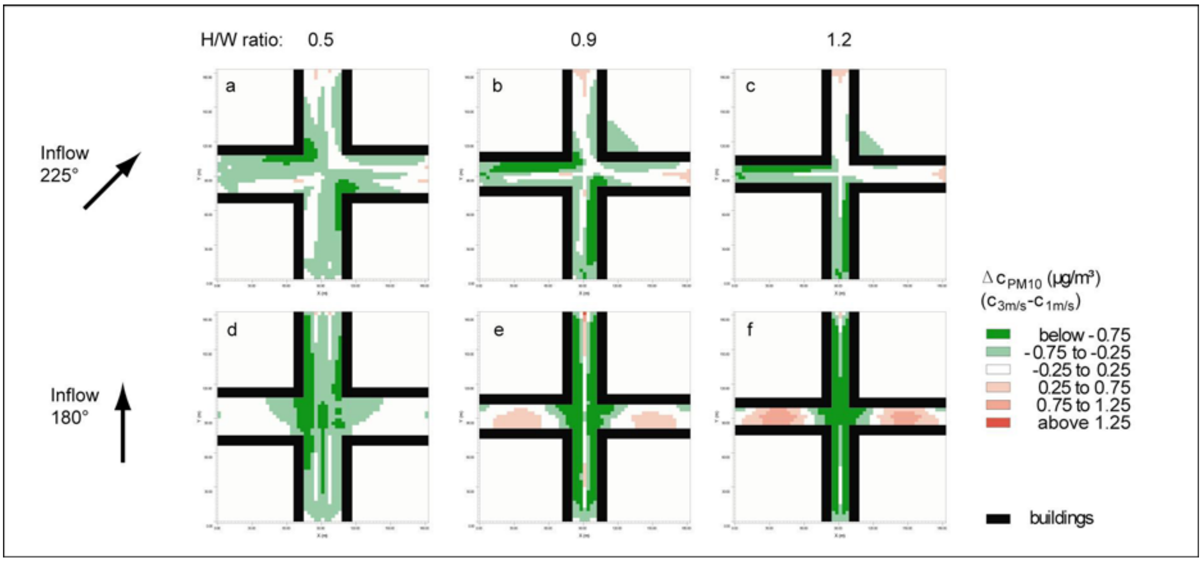


*Figure 4.16: Influence of wind speed on particle concentration. Difference of particle concentrations for inflow 225° (a-c) and 180° (d-f) at 1.8 m height. Green colours indicate higher concentrations in the calm wind simulation. In general, higher wind speed reduces particle concentration except in case of perpendicular inflow, where it leads to concentration increases in the two deeper canyons (e, f).*

The concentration differences induced by higher wind speed are different on the lee- and windward canyon sides. In the simulation with direct oblique inflow, the effect of concentration reduction with higher wind speed is stronger at the bottom of the canyon at the windward side and decreases with height (Figure 4.17a). The differences increase with aspect ratio. Again this refers to better canyon ventilation even with high wind speed and particularly in deep canyons. After the intersection, the differences with oblique inflow are rather low between the bottom and the top, with a slight increase towards the top that might refer to an influence of the flow above the canyon top (Figure 4.17b). In contrast to section 1, the differences decrease with aspect ratio and the highest concentration decrease occurs on the windward side of the canyon with aspect ratio 0.9 followed by the avenue canyon. Even at high wind speed, ventilation is suppressed after the intersection. With perpendicular inflow, concentration changes are low for aspect 0.5 and generally higher on the leeward side (Figure 4.17c). Consequently, ventilation on the leeward side in the deeper canyons is worsened as the faster air transports more particles. Again the differences are higher at the bottom of the canyon. With parallel inflow, concentrations are reduced to the same amount in the two deeper canyons (Figure 4.17d). In the avenue canyon the concentration reduction is different on the lee- and windward side. The reason might be reduced channelling of air and increased turbulence.

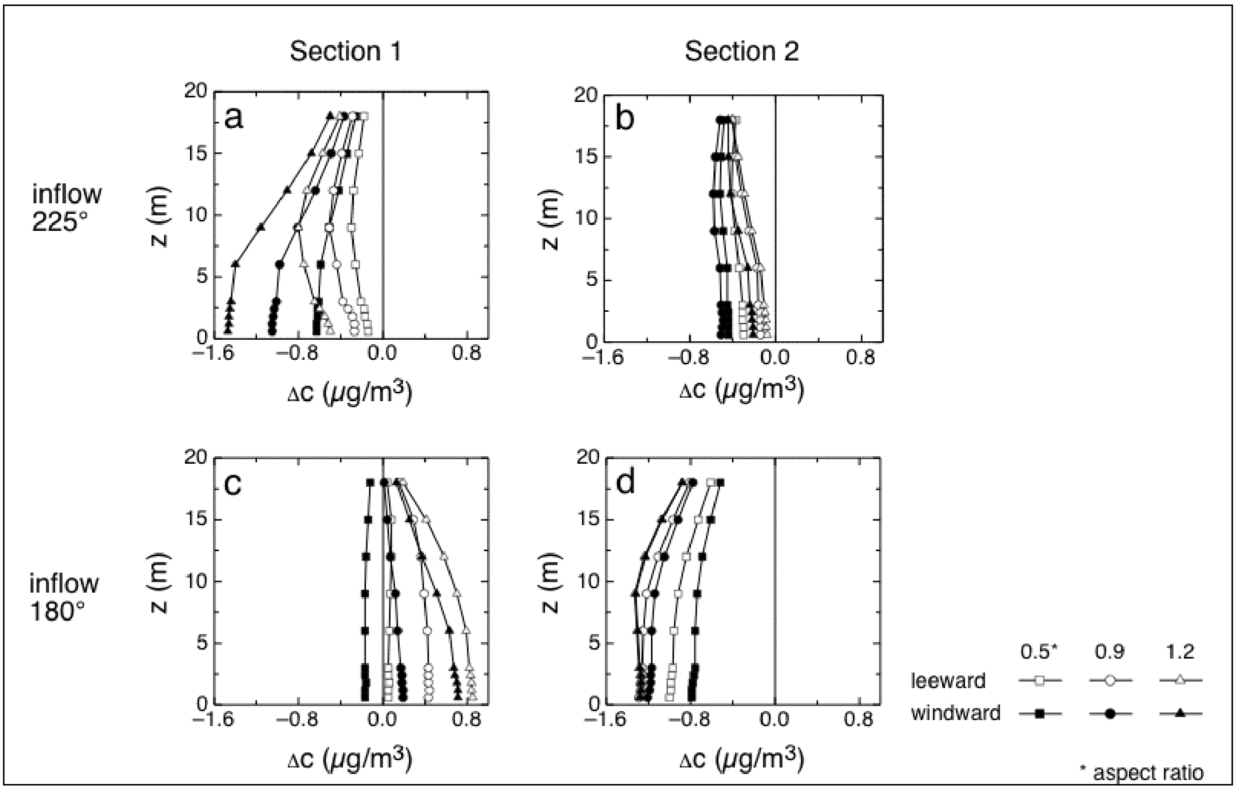


*Figure 4.17: Influence of wind speed on particle concentration inside the canyon (from bottom to building top). Comparison of concentration differences at the lee- and windward side of the canyons with different inflow directions at section 1 and 2 ($\Delta c = c_{3m/s} - c_{1m/s}$) (values of grid cells close to canyon walls). Negative values refer to a concentration decrease induced by high wind speed. Higher wind speed reduces concentrations except with perpendicular inflow direction. It leads to significant concentration reduction with oblique inflow (a,b). The changes are higher at the windward side and before the intersection. With aspect ratio windward differences increase before (a) and decrease after the intersection (b). Higher wind speed with perpendicular direction leads to concentration increase in the deeper canyons (c). The effect is higher on the leeward side and increases with aspect ratio. With parallel inflow concentrations are reduced (d).*

#### 4.3.2.3 Conclusions

These results reveal the influence of dense building structures on particle dispersion and emphasize situations favouring pollutant accumulation. We have shown that particle concentrations in street canyons are closely related to inflow direction, wind speed and aspect ratio. Ventilation is reduced with aspect ratio, leading to an additional accumulation of particles. Oblique inflow generally leads to better ventilation. First, fresh air enters the canyon from the roof level and second, a rotating helical vortex leads to air mixing. Concentrations are higher on the leeward canyon side. The ventilating strength of the vortex is reduced by building structures (after the intersection). In deeper canyons it transforms into a stable vortex, suppressing ventilation. Additionally, particles are accumulated whenever the flow crosses another source. Parallel inflow then leads to accumulation as no exchange with the flow outside the canyon occurs. The single cross-canyon vortex in the case of perpendicular inflow promotes particle accumulation equally on both sides, particularly in deeper canyons.

Concentrations increase with aspect ratio. Besides the canyon volume, decreasing ventilation is an important factor reducing the vertical exchange and particle transport that normally lead to dilution. In general, the vertical exchange is reduced with increasing aspect ratio, and the avenue canyon experiences good ventilation.

High wind speed reduces the concentration level except in the simulation with perpendicular inflow. It leads to better canyon ventilation at oblique inflow, particularly in deeper canyons. Reductions are higher on the windward side and at the canyon bottom. Increased modification of oblique inflow (by building structures) lowers the reducing effect of higher wind speed, particularly at the bottom. Higher wind speed with perpendicular inflow direction leads to increased particle accumulation in deeper canyons and particularly on the leeward side.

### 4.3.3 Influence of vegetation on particle dispersion

To evaluate the influence of vegetation on particle dispersion in the street canyons, the simulation without vegetation (reference) was compared to each of the five vegetation scenarios. The comparison was performed for both wind directions and wind speeds. Accordingly, four comparison results were obtained for each scenario (compare Figure 4.7 in 4.3.1.2).

#### 4.3.3.1 Influence on particle concentration

***Results with low wind speed***

The results for the scenario with hedges on both sides of the canyon reveals slight modifications in the canyons with aspect ratio 0.9 and 1.2 (Figure 4.18b,c). Concentrations are slightly reduced in the streets after the intersection. No changes occur in the avenue canyon (Figure 4.18a). The sparsely foliated tree rows induce no changes (Figure 4.18d-e). The highest changes are induced by the rows of densely foliated trees that lead to a concentration increase in general (Figure 4.18i-o). The increase is higher before the intersection and increases with aspect ratio. The effect is stronger for the continuous row of trees (Figure 4.18l-m).

For an inflow of 180° the same tendencies apply but with a different pattern. Modifications concern above all the along-wind street. The hedge leads to concentration reduction after the intersection in the two deeper canyons and no changes in the avenue canyon (Figure 4.19a-c). The differences are higher than in the simulation with an inflow direction of 225°. The sparsely foliated tree rows induce a slight concentration reduction after the intersection (Figure 4.19d-i). The effect is slightly stronger in the scenario with the widely spaced row of trees (compare Figure 4.19e,f with h,i). Rows of densely foliated trees lead to a concentration increase in the along-wind street before the intersection and in the street with perpendicular inflow (Figure 4.19j-o). The effect is weak in the avenue canyon and increases with aspect ratio. After the intersection the widely spaced row of trees even leads to a slight concentration decrease in the deep canyon (Figure 4.19l).

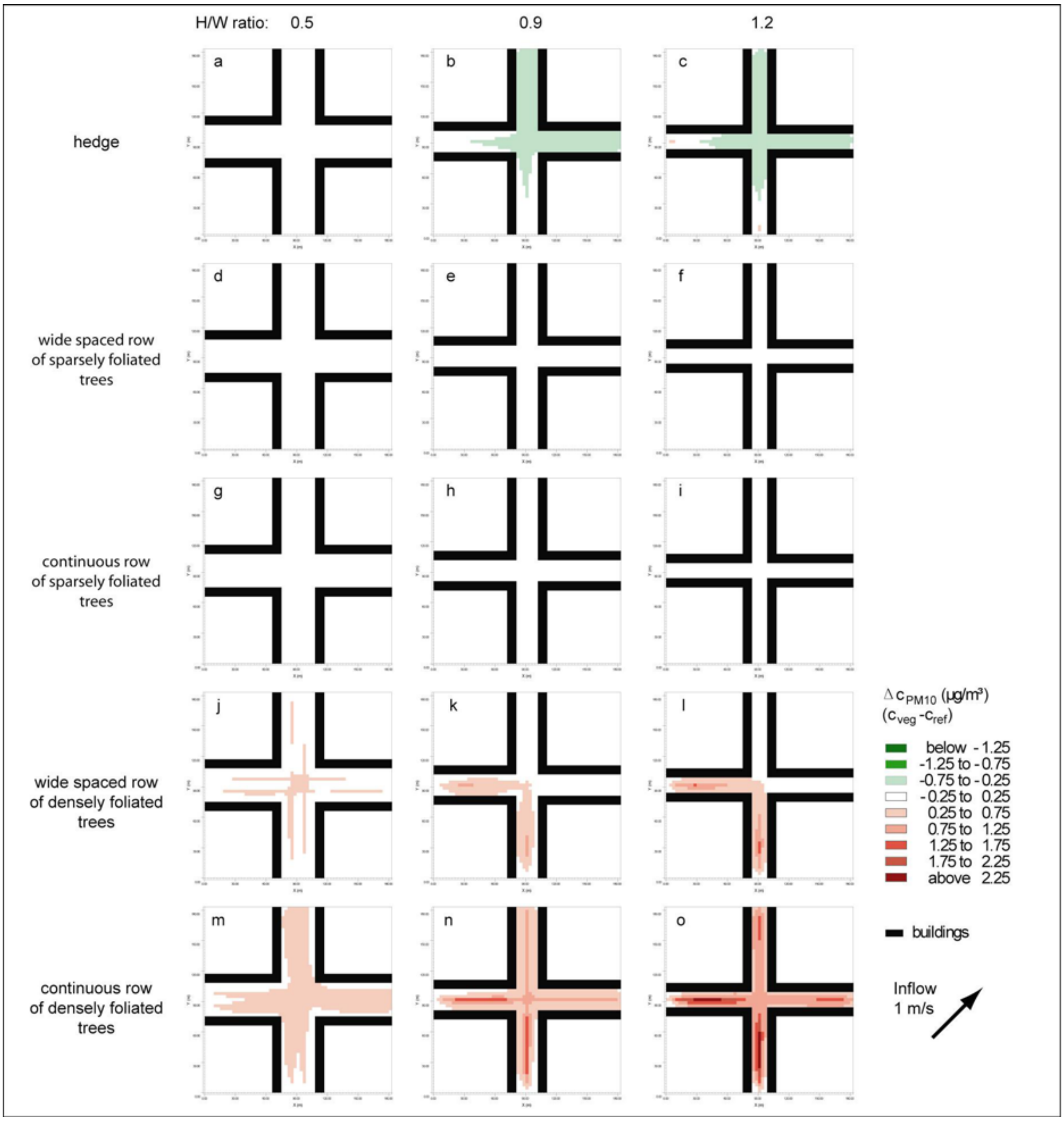


*Figure 4.18: Influence of vegetation on particle concentration for inflow 225° and 1 m/s at 1.8 m height. Comparison of the simulation without vegetation (reference, $c_{ref}$), with the hedge and the four tree scenarios (vegetation scenarios, $c_{veg}$). Red indicates increase and green decrease of concentration induced by vegetation. Hedges slightly reduce particle concentrations after the intersection in the canyons with aspect 0.9 and 1.2 (b,c). Sparsely foliated trees induce no changes (d-i), while densely foliated trees induce higher particle concentrations. The effect increases in each scenario with aspect ratio.*

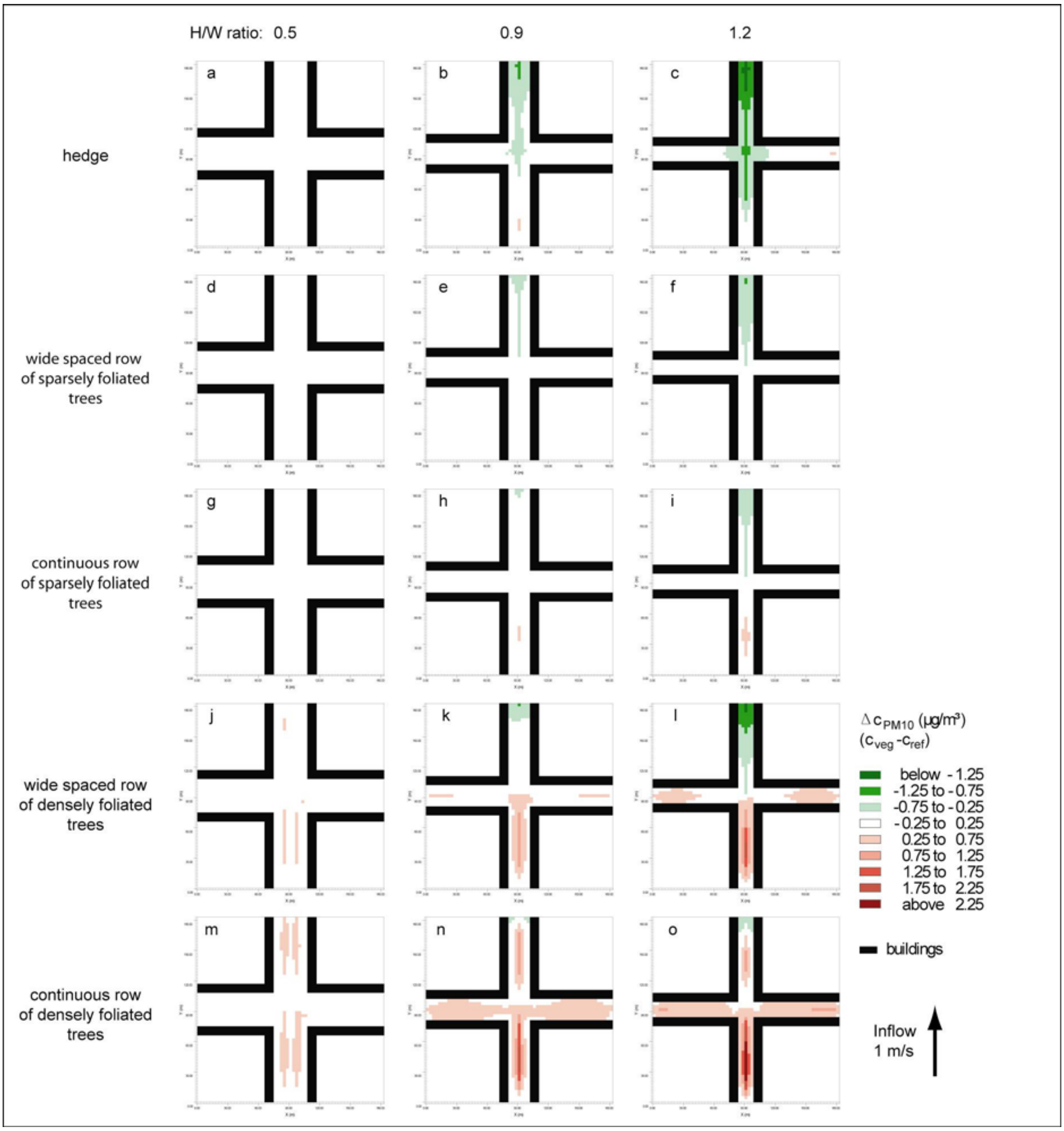


*Figure 4.19: Influence of vegetation on particle concentration for inflow 180° and 1 m/s at 1.8 m height. Comparison of the simulation without vegetation (reference, $c_{ref}$) with the hedge and the two densely foliated tree scenarios (vegetation scenario, $c_{veg}$). Hedges in deeper along-wind street canyons reduce particle concentrations. Densely foliated trees induce an increase in particle concentrations in along-wind streets and streets perpendicular to the inflow. The influence of sparsely foliated trees is very small.*

The analysis of how these effects depend upon height shows similar tendencies to those found at 1.8 m. The modifications induced by the hedge are very small (Figure 4.20). Oblique inflow reduces the concentration near the source at the canyon bottom (Figure 4.20b-c). The reduction after the intersections with oblique and parallel inflow are higher and concern the first 9 m above the bottom (Figure 4.20h-i, k-l). However, the effect is very small. The increasing effect with aspect ratio applies for the canyon height as well, i.e. differences reach higher in the deeper canyon and increase with aspect ratio (compare Figure 4.20h,k with i,l).

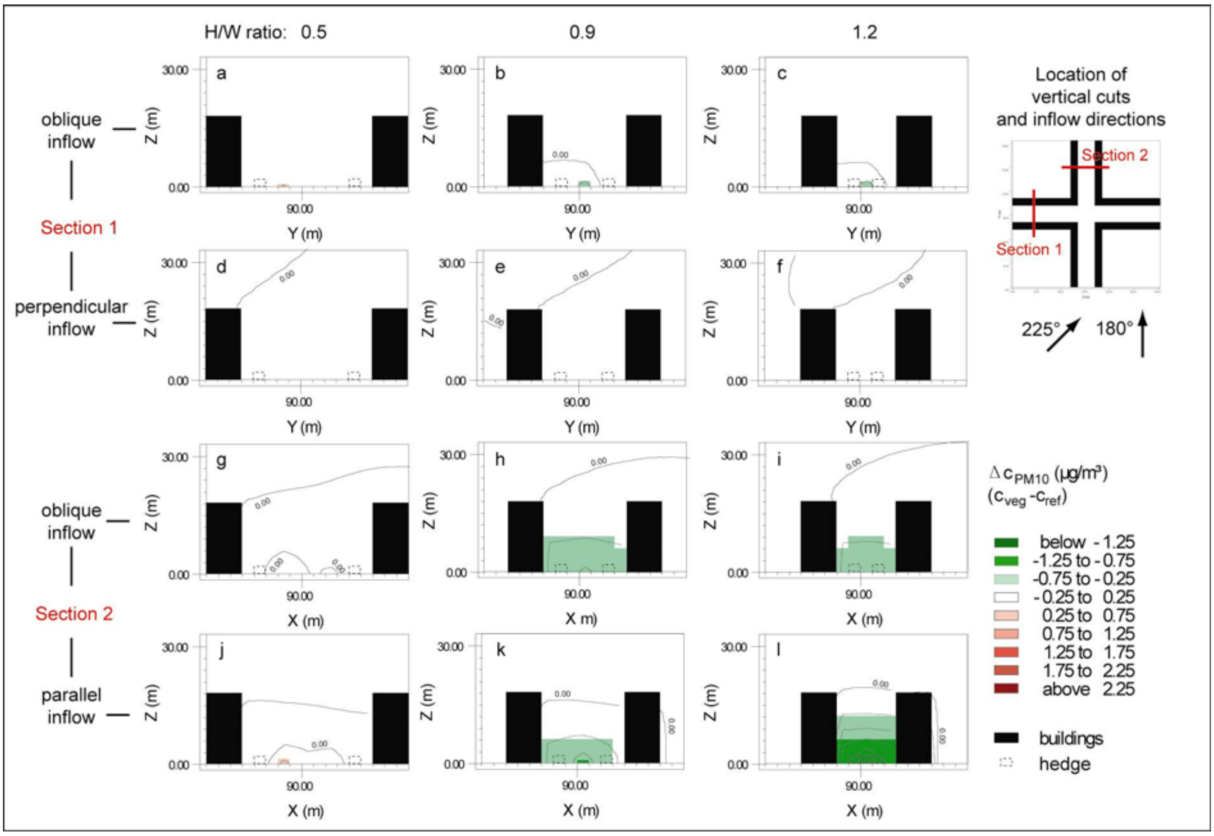


*Figure 4.20: Influence of the hedge rows on particle concentrations at sections 1 and 2. Simulation with wind speed 1 m/s: oblique inflow a-c and g-h, perpendicular inflow d-f, and parallel inflow j-l. In the two deeper canyons differences reach up to 9 m (h-i, k-l). They are small in general. They are higher at the bottom and decrease with height. Distance between isolines is 0.25 µg/m*$^3$.

The effect of the hedge is rather small compared to that of the densely foliated trees. The continuous rows of densely foliated trees induce concentration changes even in the avenue canyon and changes are stronger in the two deeper canyons (e.g. Figure 4.21a-c). The changes are higher in the simulation with oblique wind and in this case, changes are smaller at the windward side (Figure 4.21a-c, g-i). The highest concentration differences occur at the source. Perpendicular inflow induces only slight changes (Figure 4.21d-f). At parallel inflow the increase occurs only in close proximity to the source (Figure 4.21j-l).

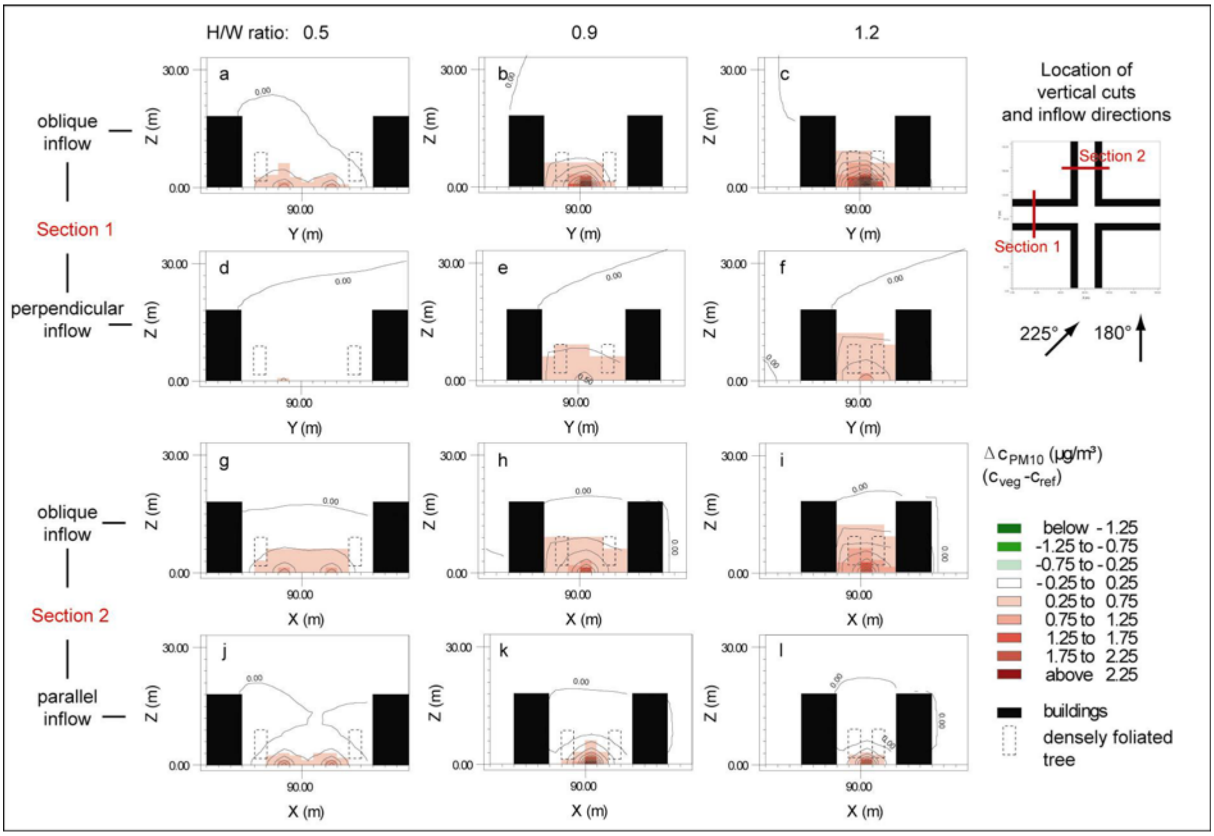


*Figure 4.21: Influence of continuous rows of densely foliated trees on particle concentrations at sections 1 and 2. Simulation with wind speed 1 m/s: oblique inflow a-c and g-h, perpendicular inflow d-f, and parallel inflow j-l. Differences are higher at the bottom near the source and decrease with height. Concentration increase is stronger with oblique inflow. Differences are higher in the two deeper canyons (b-c, h-i). Distance between isolines is 0.25 µg/m³.*

***Summary***

Densely foliated trees flanking both sides of a street induce an increase in particle concentration. The effect is small in avenue canyons and increases with aspect ratio. The higher increase at the source refers to an inhibition of dispersion and consequently dilution inhibition. Furthermore, the increase is higher at the leeward canyon side. Hedges reduce particle concentrations, but the effect is very small.

### 4.3.3.2 Influence on wind speed

It is hypothesised that the concentration changes are related to the modifications of the flow field inside the canyon. The decrease of wind flow within a tree crown depends on the cumulative foliage area and is described in literature by an exponential function (Rauner 1976). Accordingly, the densely foliated tree should reduce wind speed much more than the sparsely foliated tree.

To compare concentration changes and modifications of wind, first, the wind speed close to the bottom is analysed for the calm wind (1 m/s). Remember that in the simulation without vegetation, particle accumulation is higher with perpendicular and parallel inflow (after the intersection), and when the spiral vortex at oblique inflow slows down after the intersection. It is hypothesised that ventilation worsens in these cases when vegetation is present.

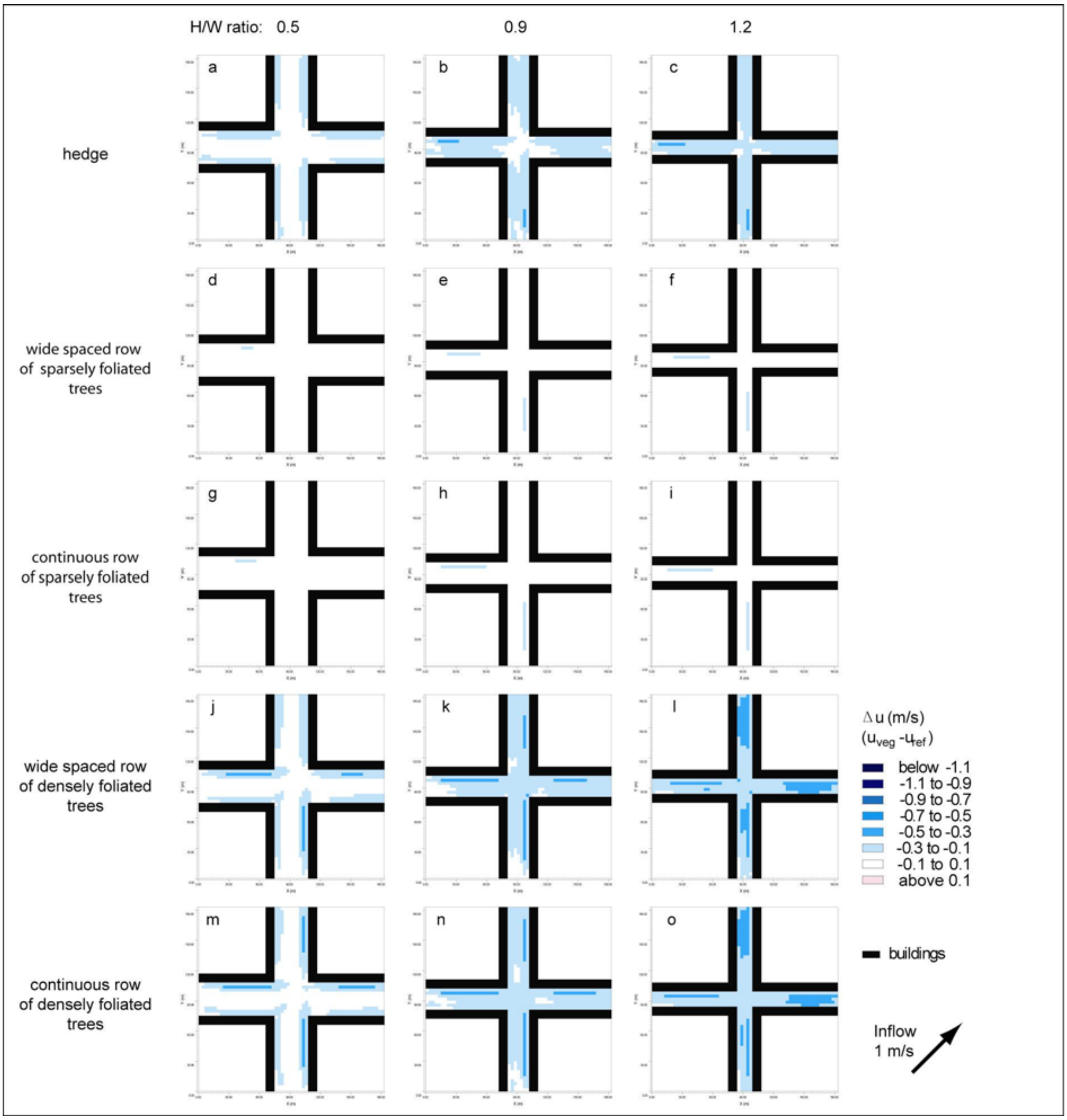


*Figure 4.22: Modification of wind speed by vegetation objects at 1.8 m height. Simulation with inflow of 225° and 1 m/s (wind speed in reference situation $u_{ref}$ and in vegetation scenario $c_{veg}$). Vegetation leads to wind speed reduction. The effect is higher at the windward canyon sides and increases with aspect ratio and vegetation density.*

Wind speed is reduced close to the hedge and tree rows in the simulation with an inflow direction of 225° (Figure 4.22a-c). The highest values occur at the rows on the windward side. With increasing aspect ratio, wind speed reduction affects also the space between vegetation rows (Figure 4.22b,c,k,l,n,o). The highest wind speed reductions are induced by the densely foliated trees after the intersection in the canyon with the highest aspect ratio (Figure 4.22l,o). The sparsely foliated trees induce very few modifications (Figure 4.22d-i).

With inflow at 180°, wind speed is reduced, especially along the walking sides and the hedge and tree rows in the along-wind canyon (Figure 4.23). Again, the highest reductions occur in the deeper canyons, where it affects the whole canyon width (Figure 4.23b-o). The canyon parallel to the inflow shows no modifications at 1.8 m.

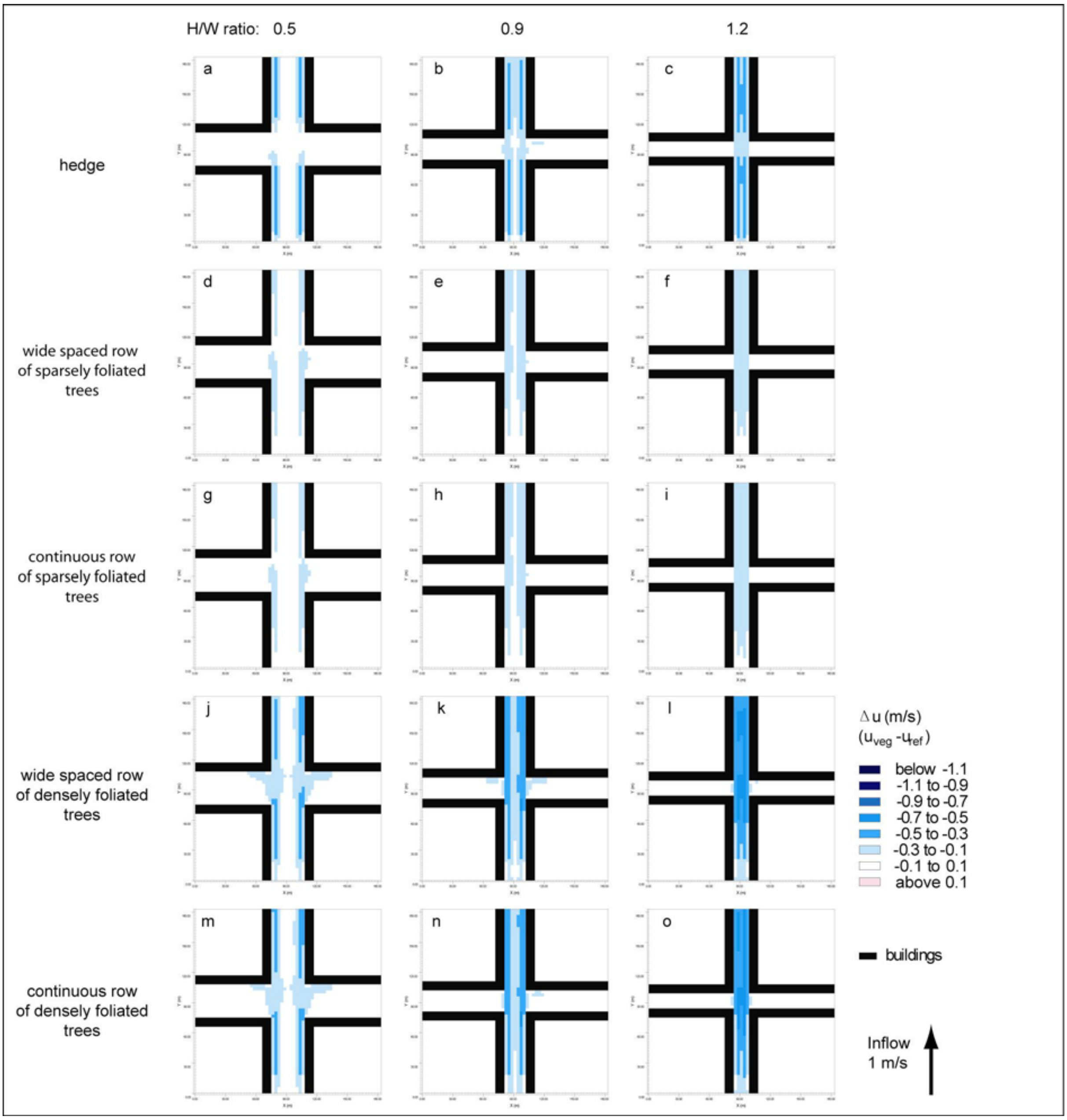


*Figure 4.23: Modification of wind speed by vegetation objects at 1.8 m height. Simulation with inflow of 180° and 1 m/s (wind speed in reference situation $u_{ref}$ and in vegetation scenario $c_{veg}$). Wind speed reduction occurs in close vicinity of hedge and tree rows. The effect is small for the sparsely foliated tree scenarios (d-i). In the deeper canyons higher wind speed reduction occurs also on the walking sides (b-o). The effect increases with aspect ratio and vegetation density.*

Figure 4.24 depicts the vertical modifications of wind speed induced by the hedge and the sparsely and densely foliated trees (continuous row of trees) in the canyon with aspect ratio 0.9. At oblique and parallel inflows, the hedge influences the flow within the first 6 m (remember, the height of the hedge is 1.5 m), leading to wind speed reduction (Figure 4.24a,b,d). As indicated by the results at 1.8 m height, no wind speed changes occur with perpendicular inflow (Figure 4.24b,f,j). Generally, trees lead to a slow down within the crown and a smaller reduction in velocity below the crown. The changes are higher for the densely foliated trees than for the sparsely foliated trees (compare Figure 4.24e,h with i,k,l). As for the hedge, the modifications by the densely foliated trees concern also the first grid cell above the crown. The LAD of both types of vegetation are comparable. With oblique inflow, the modifications are weaker on the leeward side than on the windward side (Figure 4.24a,e,i,c,k). The rows of densely foliated trees induce higher changes with parallel inflow, even between tree rows and buildings.

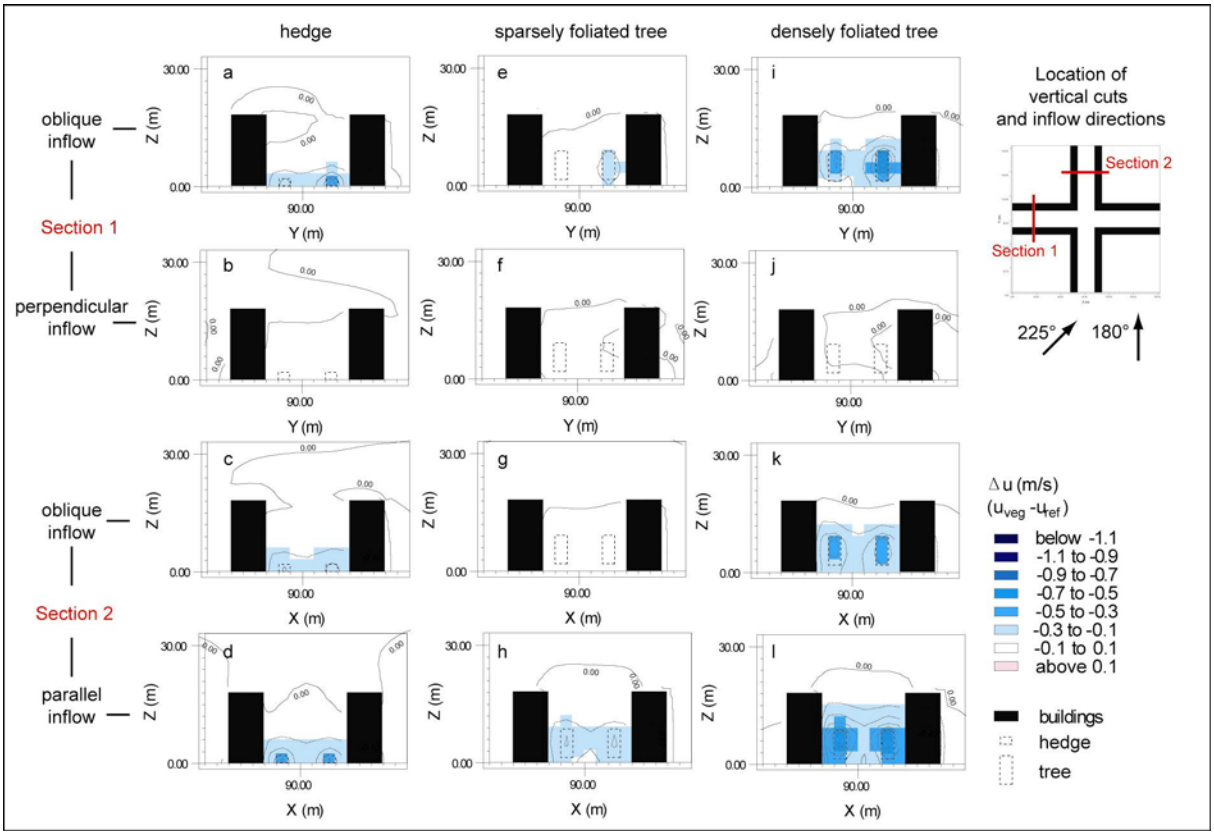


*Figure 4.24: Influence of vegetation on wind speed in the canyon with aspect ratio 0.9 for the simulation with wind speed 1 m/s (wind speed in reference situation $u_{ref}$ and in vegetation scenario $u_{veg}$). Comparison of the scenarios hedge (a-d), sparsely foliated tree (e-h), and densely foliated tree (i-l) (continuous row scenarios) for different approaching inflow directions (section 1 and 2). Distance between isolines 0.1 m/s. In general, vegetation reduces wind speed. The effect is higher on the windward side. The highest reductions are induced by the densely foliated trees with parallel inflow.*

The strength of wind speed reduction by vegetation is different for low and high wind speed. In general, higher speed reduction occurs in the simulation with high wind speed (Figure 4.25a,b,d). No significant changes exist with perpendicular inflow (Figure 4.25c). Significant differences between lee- and windward canyon side can be observed in the simulation with oblique inflow (Figure 4.25a,b). In general, wind speed is reduced more on the leeward side, except for the densely foliated tree scenario with unmodified oblique inflow (Figure 4.25a). At high wind speed a large slow-down effect of the tree can be observed at the bottom on the windward side, inducing a much smaller effect on the leeward side that is even smaller than in the calm wind simulation. For the same high wind speed simulation, the effect of the hedge near the bottom is inverse. A larger slow-down effect can be observed on the leeward side. With calm wind, the differences between hedge and densely foliated trees near the bottom are less significant.

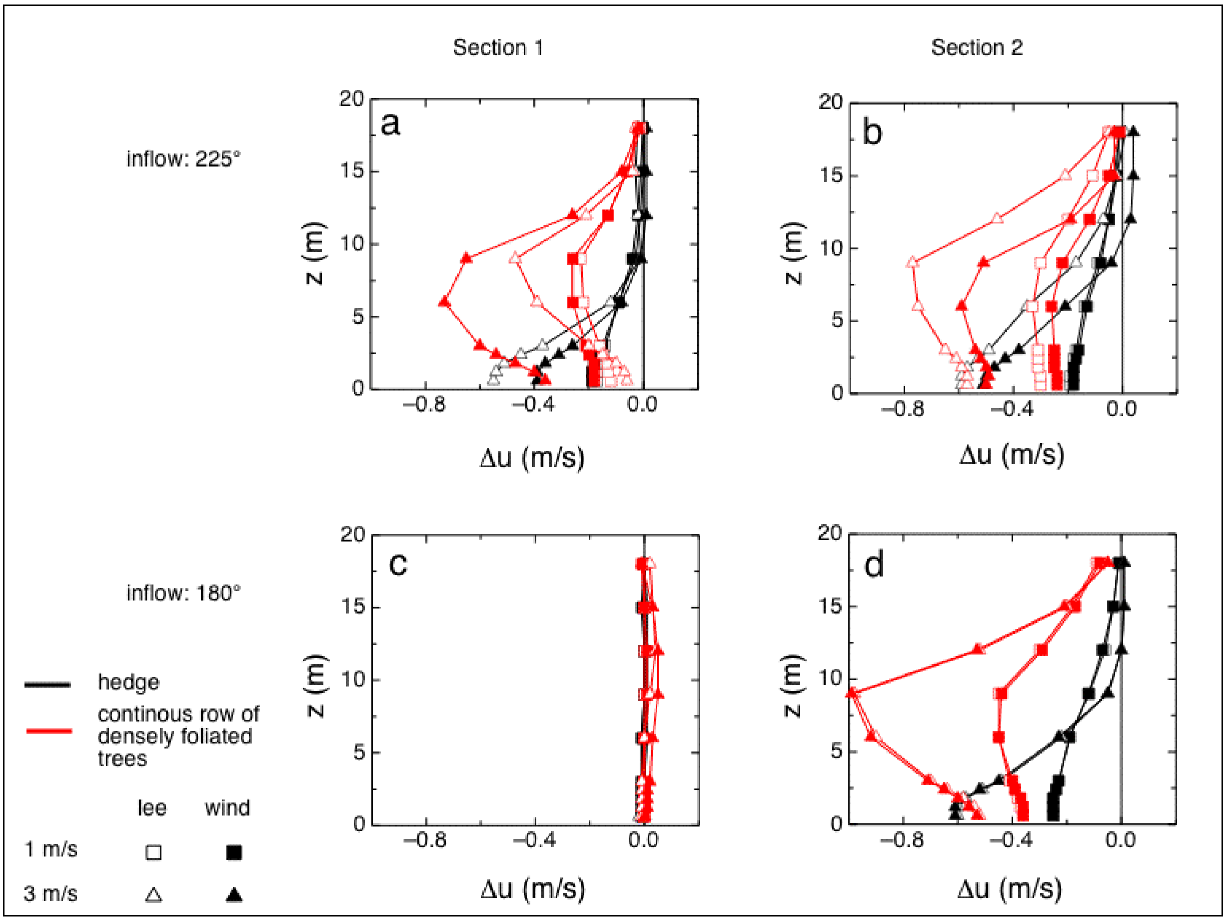


*Figure 4.25: Influence of hedge and densely foliated trees on wind speed in the canyon with aspect ratio 1.2 for different inflow directions. Comparison of vegetation-induced wind speed changes with low and high wind speeds ($\Delta u = \Delta u_{veg} - \Delta u_{ref}$) at sections 1 and 2 (values of grid cells close to canyon walls). Differences between the lee- and windward side occur with oblique inflow (a,b). In general, the hedge reduces wind speed significantly at the bottom while the trees influence the wind flow up to the canyon top. Wind speed reduction by the tree is higher.*

After the intersection, with modified oblique inflow wind speed reductions by vegetation are always higher on the leeward side (Figure 4.25b). The strength of the effect near to the bottom contrasts less with the effect above the hedge or at the height of the tree canopy. In the simulation with high wind speed the effect of the hedge and the tree are very similar near the bottom, but as for all simulations the slowing effect of the tree crown increases with height and decreases again above the canopy. In this section, the effect of the tree at high wind speed reaches even higher and the effect of the hedge is slightly higher than before the intersection. This relationship reveals the inhibiting effect of vegetation, generally worsening the situation in poorly ventilated regions. It is noteworthy that the hedge leads to a wind speed increase near the canyon top. The results for parallel inflow underline the general effect of both vegetation objects (Figure 4.25d). Higher wind speed reduction occurs in the simulation with high wind speed. With low speed the effect of the trees at the bottom is higher than the effect of the hedge. In contrast, at high wind speed the hedge slows down the wind much more near the bottom.

***Summary***

The results of vegetation-induced wind modifications confirm that vegetation leads to wind speed reduction in general. The reductions are higher in the simulation with high wind speed. Velocity differences increase with aspect ratio and vegetation density. While in the wider canyons significant reductions occur close to the hedge and tree rows, they affect the whole canyon bottom in the deep canyon.

Reductions induced on the lee- and windward sides by the hedge are similar. Before the intersection, the trees lead to higher reductions on the windward side and after the intersection reductions are higher on the leeward side. These observations lead to the conclusion that with oblique inflow, the spiral vortex is slowed down, reducing its ventilating effect in the two deeper canyons. In the calm wind simulation, densely foliated tree crowns reduce wind speed more close to the bottom of the canyon than the hedge. With high speed, the reducing effect of the trees near the bottom approaches that of the hedge and is slightly smaller.

With perpendicular inflow modifications of the homogeneous flow field induced by vegetation are not significant. With parallel inflow the trees lead to a larger slow-down of velocities in the simulation with high wind speed. At high wind speed the reducing effect of the hedge is greater within the first two meters.

#### 4.3.3.3 Influence of wind speed on vegetation-induced concentration changes

In the reference situation, it was shown that higher wind speed improves ventilation and reduces particle concentrations, except in case of perpendicular inflow. In the last section it was shown that velocity reduction by vegetation is greater in the simulation with high wind speed, which might reduce the improved ventilation effect. In the following section we analysed how this higher wind speed reduction influences particle concentration values compared to the simulation with calm wind. To analyse the effect, the scenarios with the hedge row and continuous row of densely foliated trees are compared. This is for two reasons. First, the densely foliated trees show the strongest effect and second, we focus on the hedge because of its reducing effect.

Again, differences are smaller in the avenue canyon and increase with aspect ratio. The height of the concentration differences induced by the hedge at both wind speeds differ very little (Figure 4.26a-c). The differences are slightly higher in the simulation with high wind speed (red colours, note that the presented differences do not reflect concentration decreases or increases but only the value). In contrast, the continuous row of densely foliated trees induces much higher concentration differences, with high wind speed after the intersection (Figure 4.26e,f). Before the intersection, concentration differences are higher with low wind speed.

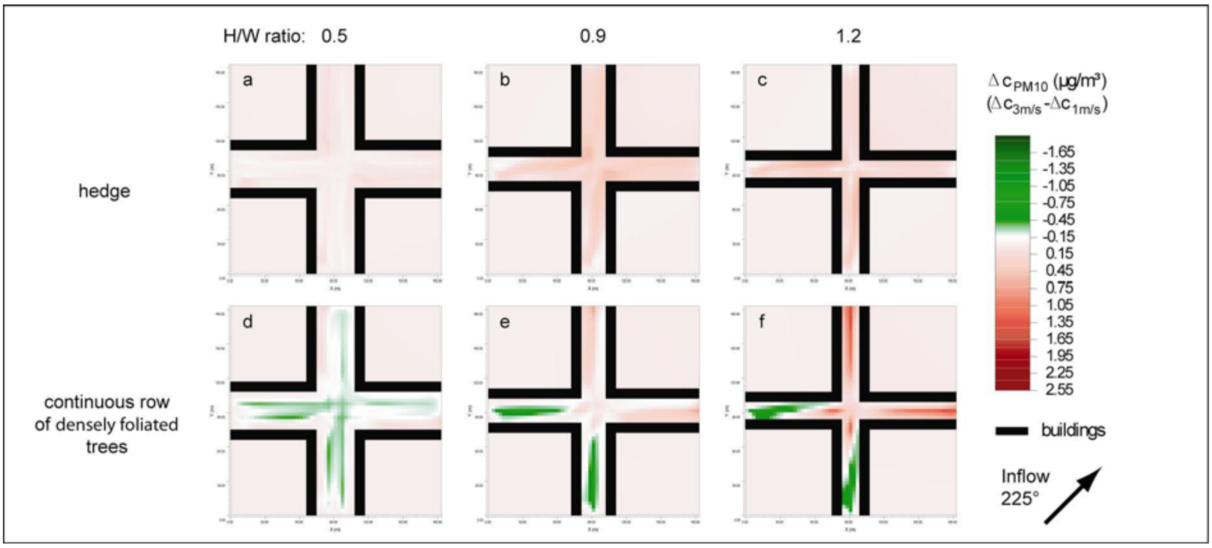


*Figure 4.26: Influence of wind speed on vegetation-induced concentration changes for inflow 225°. Example of scenarios with hedge (a-c) and continuous row of densely foliated trees (d-f). Red colours indicate higher and green colours lower concentration differences at high wind speed. In general, differences induced by the hedge are smaller and slightly higher with high wind speed (note that the presented differences do not reflect concentration decreases or increases but only the value, for values changes see Figure 4.28). Higher wind speed induces higher concentration differences on the windward side before the intersection (b-c). Higher wind speed in the tree scenario leads to higher differences after the intersection (d-f). Before the intersection differences are generally higher with low wind speed (green colours). They are smaller close to building walls.*

High wind speed induces higher concentration changes with perpendicular inflow and on the leeward side (Figure 4.27b-f). For the hedge the differences are even higher than with oblique inflow. For parallel inflow, before the intersection the tree row scenario differences are smaller than in the simulation with calm wind (Figure 4.27d-f). In the deepest canyon, they are even smaller close to the building walls (Figure 4.28f).

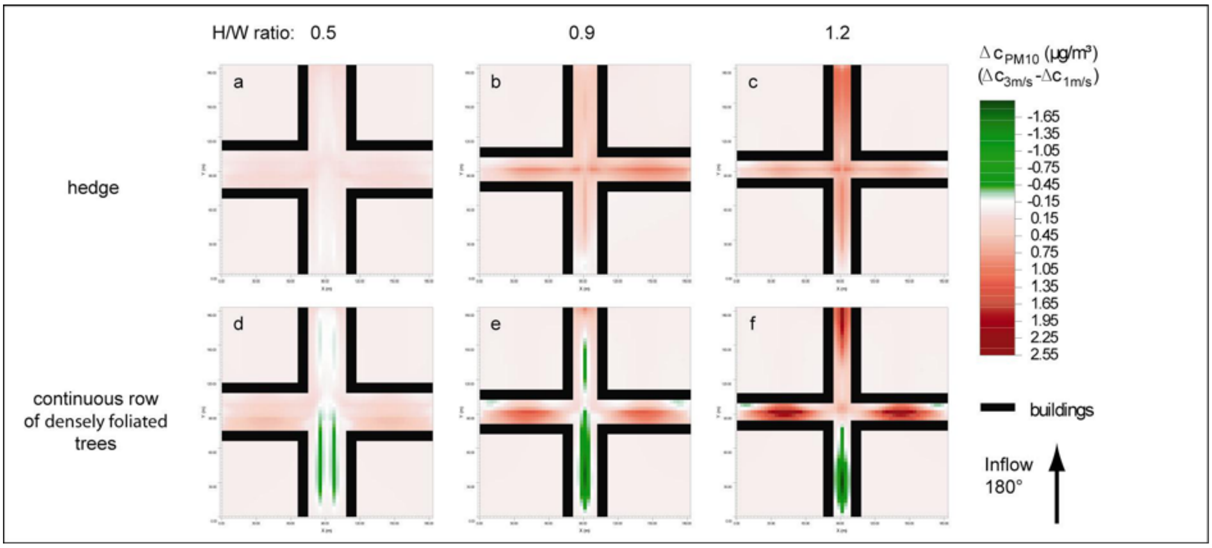


*Figure 4.27: Influence of wind speed on vegetation-induced concentration changes for inflow 180°. Example of scenarios with hedge (a-c) and continuous row of densely foliated trees (d-f). Red colours indicate larger and green colours smaller concentration differences at high wind speed. For the hedge scenario, differences between both wind speeds are higher than with oblique inflow and particularly on the leeward side in the sections with perpendicular inflow (d-f) (note that the presented differences do not reflect concentration decreases or increases but only the value, for values changes see Figure 4.28). High wind speed in the tree scenario leads to higher differences after the intersection (d-f). Before the intersection differences are generally higher with low wind speed (green colours). They are smaller close to building walls.*

Differences induced by different wind speeds are compared at the two sections for the deep canyon (aspect 1.2) in order to show if the changes are negative (reduction) or positive (increase). In this canyon, vegetation-induced modifications show the strongest effect and particularly the hedge and densely foliated tree scenarios.

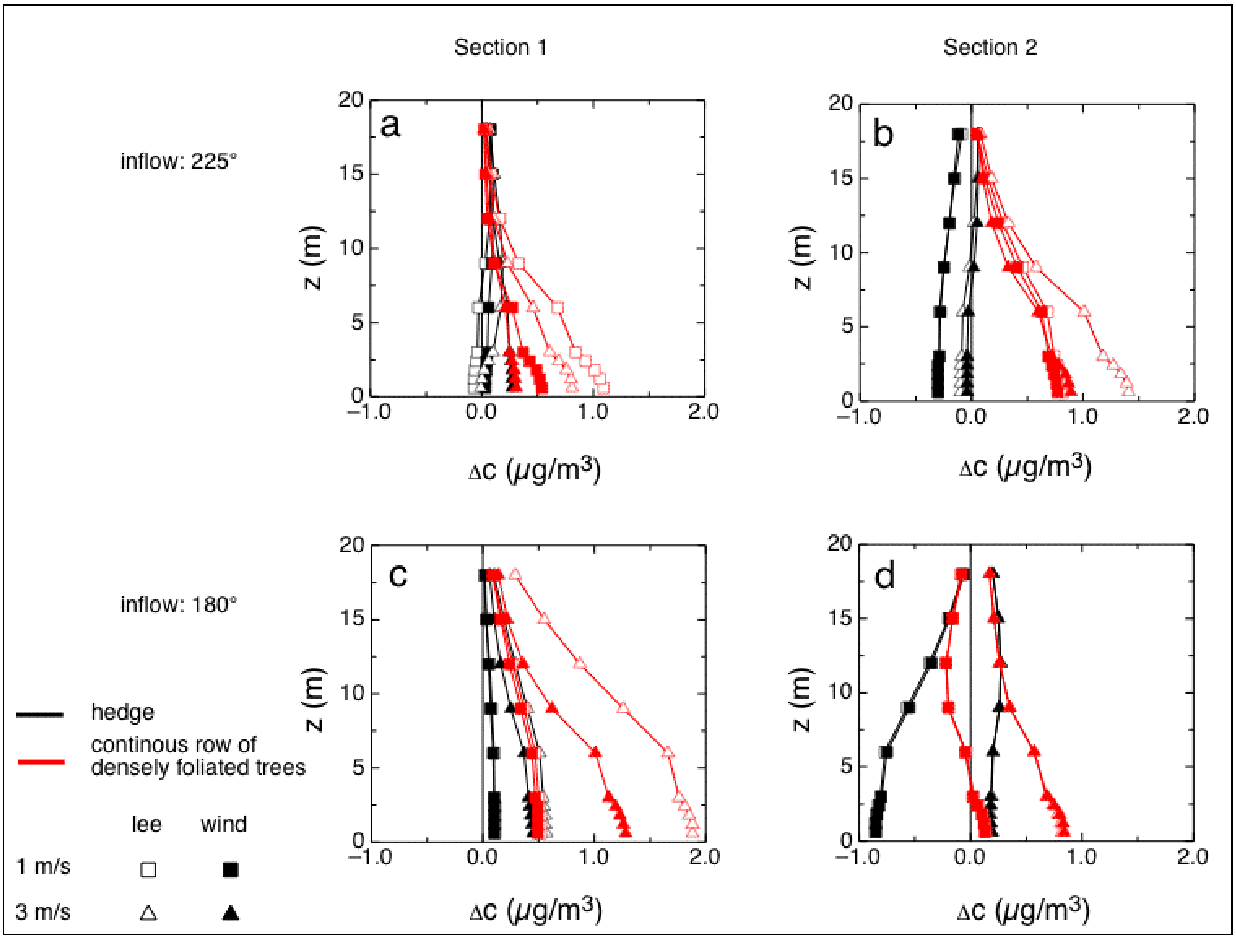


*Figure 4.28: Influence of wind speed on vegetation-induced concentration changes in the canyon with aspect ratio 1.2 ($\Delta c = c_{veg} - c_{ref}$) at sections 1 and 2 (values of grid cells close to canyon walls). Positive values refer to concentration increase induced by vegetation. Comparison of the scenarios with hedge and continuous row of densely foliated trees. Oblique inflow(a) and (b), perpendicular inflow (c), and parallel inflow (d). On the walking sides in the deep canyon, the trees always induce a concentration increase near the bottom. The hedge induces small changes and with calm wind might even reduce concentrations with parallel and oblique inflow (b,d).*

In the densely foliated tree scenario (continuous row), high wind speed generally leads to a concentration increase, especially on the leeward canyon side (Figure 4.28a,b,c). An exception occurs before the intersection where the concentration increase is higher with low wind speed (Figure 4.28a). In general, trees induce higher concentration changes at high wind speed. Even if the effect is small, the hedge shows the tendency to reduce concentrations close to the canyon bottom in the calm wind simulation (Figure 4.28a,b,d).

After the intersection (modified oblique inflow), with higher wind speed the tree row leads to a significant concentration increase at the leeward side (Figure 4.28b). The increase at the windward side equals those of the calm wind simulation (lee- and windward). The hedge reduces concentrations at slow wind speed equally on both canyon sides. This influence disappears with higher velocity.

Highest changes induced by high wind speed occur with perpendicular inflow (Figure 4.28c). They are higher on the leeward side in both the hedge and tree scenarios. In the calm wind simulation, the changes induced by the densely foliated tree scenario are comparable to those of the hedge scenario at high wind speed. While at low wind speed the hedge induces nearly no changes, it increases concentrations slightly at high wind speed.

With parallel inflow, the trees induce significantly higher concentrations in the simulation with high wind speed (Figure 4.28d). Noteworthy is the concentration decrease at the height of the tree canopy and above in the calm wind simulation. The hedge slightly increases concentrations in the simulation with high wind speed but leads to a significant decrease with calm winds.

***Summary***

In the tree scenario, high wind speed leads to higher concentration differences after the intersection and smaller differences than in the calm wind simulation before the intersection. The trees always induce a concentration increase. The only exception occurs with parallel inflow, where the trees reduce concentrations above 5 m in the calm wind simulation.

The hedge always induces higher concentration differences with high wind speed but the effects are small compared to the tree scenario. With calm winds, it leads either to a very small increase or a concentration decrease. The highest increase is induced with high speed perpendicular inflow and the highest decrease with low speed parallel inflow.

With higher wind speed, densely foliated trees worsen the situation in poorly ventilated regions such as the leeward side and with perpendicular inflow. The influence of the hedge is very small and in some cases it might even improve the concentration level.

In general, the concentration increase induced by the trees is much higher at the canyon bottom.

#### 4.3.3.4 Particle removal by plants

The total amount of particles accumulated during the simulation run have been compared (accumulation during one hour). In general, most particles are removed by the hedge followed by the densely foliated trees and the sparsely foliated trees induced the smallest changes (Figure 4.29). More particles are removed in the canyon after the intersection (e.g. Figure 4.29a-c). The amount generally increases with aspect ratio.

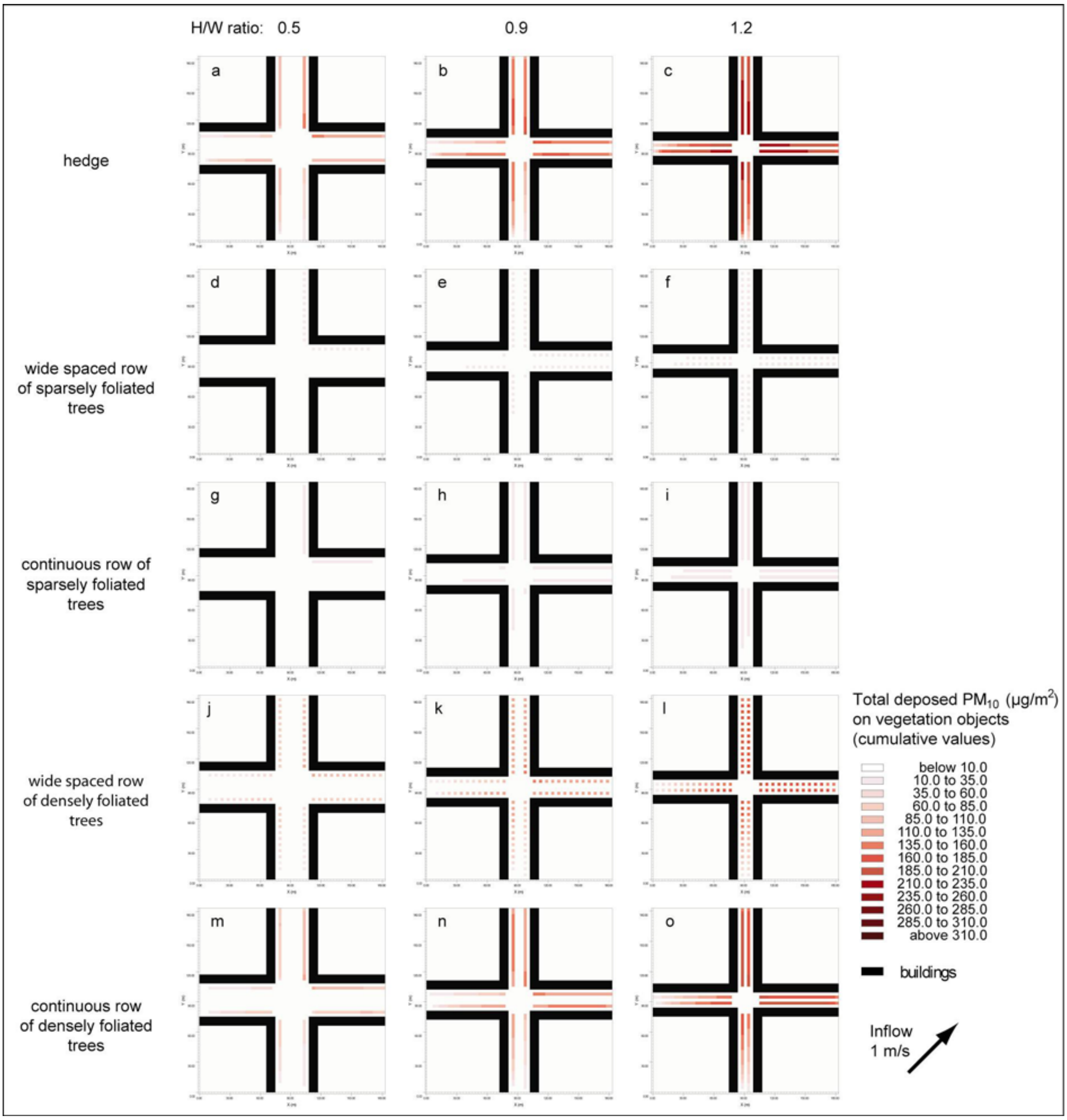


*Figure 4.29: Total deposed particles in the simulation with inflow 225° and 1 m/s (sum of vegetation layers for the simulation time: hedge z1-2, trees z3-6). Dense vegetation objects such as the hedge and densely foliated trees capture more particles than the sparsely foliated trees. The hedge reaches the highest values. A maximum occurs for trees or hedge sections close to the intersection. More particles are deposed after the intersection.*

Perpendicular inflow promotes particle accumulation on plants and leads to the highest removal rates (Figure 4.30a-c, m-o). With parallel inflow removal, rates are higher after the intersections.

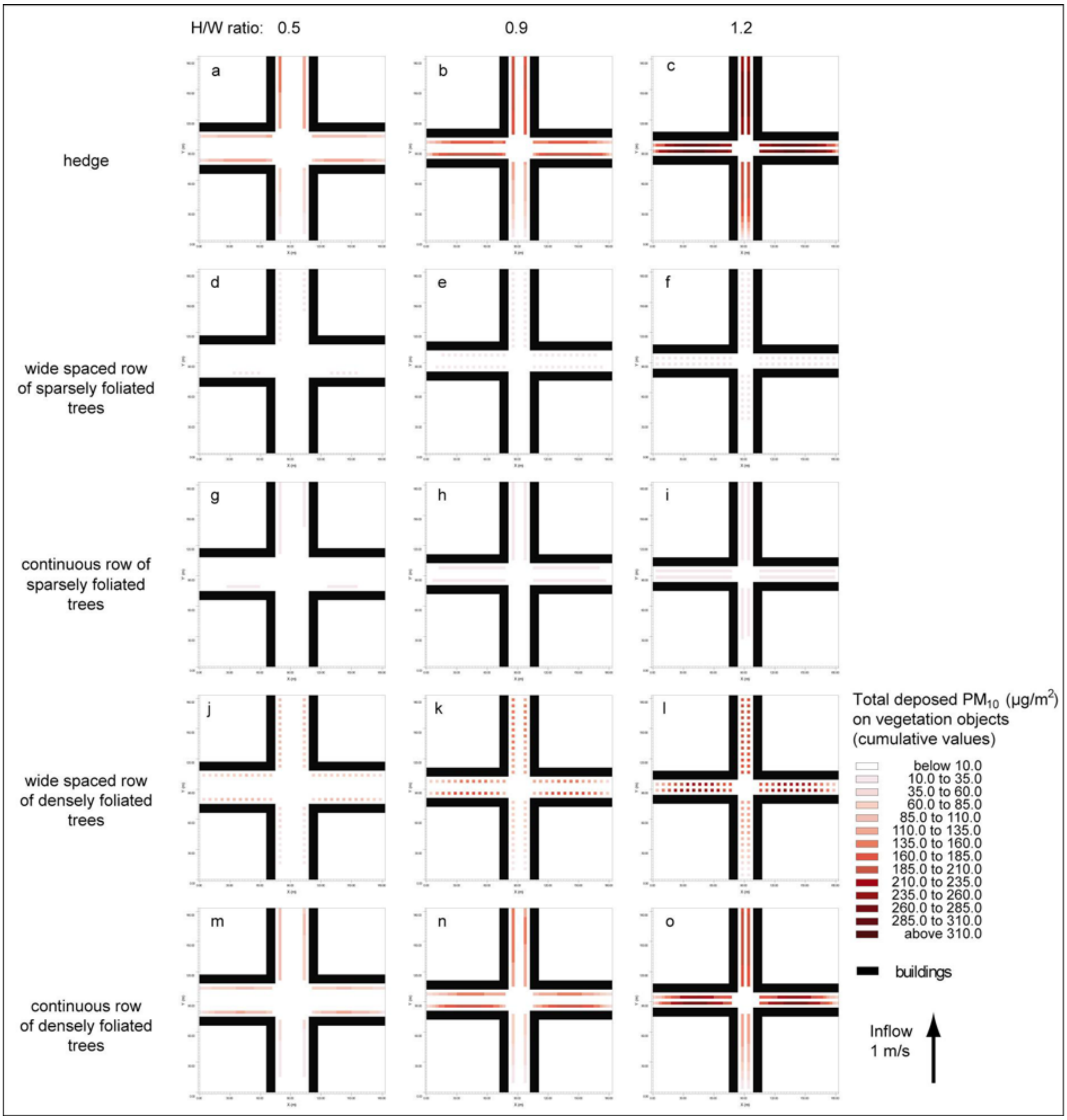


*Figure 4.30: Total deposed particles in the simulation with inflow 180° and 1m/s (sum of vegetation layers: hedge z1-2, trees z3-6). Dense vegetation objects hedge and densely foliated trees capture more particles than the sparsely foliated trees. The hedge reaches the highest values. A maximum occurs for trees or hedge sections close to the intersection. More particles are deposed after the intersection.*

The relations shown for the whole canyon are supported by the example values taken at the two sections. As with the comparison of wind speeds, the results for the hedge and the continuous row of densely foliated trees are compared. As shown by the concentration changes, the hedge leads to concentration reductions at the height of the human respiratory tract, although these changes are small. In contrast, the densely foliated trees almost always induce an increase. It is hypothesized that these decreases and increases are related to the amount of removed particles.

The amount of deposed particles is among others influenced by the wind speed. Wind speed influences the deposition velocity of a particle. At higher wind speed, fewer particles are removed (Figure 4.31a-d). More particles are deposed on vegetation objects at the leeward side of the canyon where generally higher concentrations occur. The differences between the lee- and windward side are higher with unmodified oblique inflow (Figure 4.31a) and in cases of perpendicular inflow (Figure 4.31c). The modified flow after the intersection leads to only slight differences between lee- and windward sides (Figure 4.31b). But the removal rates are higher than with the unmodified oblique inflow. Circulation is reduced in this canyon and additionally slowed down by vegetation, and furthermore, base concentrations are higher in this canyon section. No differences in removal rates on lee- and windward sides occur with parallel inflow (Figure 4.31d).

Another influencing parameter is the LAD, which is high for both the trees and the hedge, but due to the object height, the tree cumulates more leaf area (more LAD layers)[38]. In all analysed cases, the hedge removes more particles than the tree (Figure 4.31a-d). One reason might be the higher concentration of particles near the ground. The leaves of the hedge are closer to the source than those of the tree which start only at 2 m (remember that the hedge reaches up to 1.5 m).

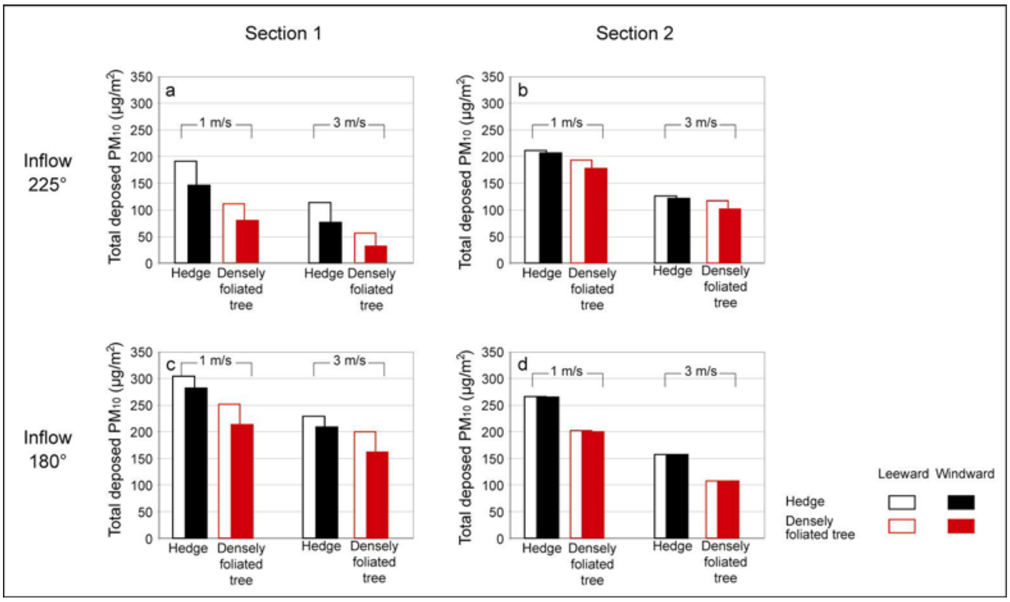


*Figure 4.31: Total deposed particles on a hedge and a densely foliated tree at different wind speeds. Values of hedge/tree in sections 1 and 2 of the canyon with aspect ratio 1.2 (sum of vegetation layers: hedge z1-2, tree z3-6). Simulation with a) and b) oblique inflow, c) perpendicular inflow, and d) parallel inflow. The hedge removes more particles than the densely foliated trees. More particles are deposed on the leeward side and in the simulation with calm wind. Most particles are removed in the canyon with perpendicular inflow (c). Differences between lee- and windward side are higher with oblique inflow before the intersection (a) and with perpendicular inflow (c).*

These observations can be explained as follows. Removal rates are higher after the intersection as concentrations are generally higher too. The same relationship applies for the higher values on the leeward side. Furthermore, increasing removal rates with aspect ratio can be explained by the increasing particle concentrations.

[38] Plant-specific parameters such as leaf diameter are the same for the hedge and the tree (both deciduous).

### 4.3.3.5 Conclusions and planning recommendations

The results reveal the inhibiting effect of vegetation on canyon ventilation and particle dispersion. It was shown that vegetation reduces wind speed at the height of the crown and disturbs the flow field in close vicinity to the plant canopy. With increasing aspect ratio the wind speed reduction increases, and the disturbance of the flow encroaches on the canyon's entire width. The improved ventilation with high wind speeds is suppressed by tree and hedge plantings. In general, vegetation leads to a concentration increase with high wind speeds. The most affected areas are deeper canyons and the leeward canyon sides.

Table 4.3 summarizes the observed effects of the three main vegetation scenarios for all canyon aspect ratios, the three main inflow directions and the two wind speeds. The evaluation was made focusing on the height of the human respiratory tract. In avenue canyons, no significant influence can be observed, with only the densely foliated trees worsening air quality slightly. With increasing aspect ratio, the hedge shows the tendency to improve the situation with oblique and parallel low velocity inflow. The influence tends to be negative with high speed perpendicular inflow. The sparsely foliated trees show a slight positive influence with calm wind and parallel inflow in the deepest canyon. In contrast, the densely foliated trees show a tendency to increase the pollution level. This effect can be already observed in the avenue canyon. It increases with aspect ratio and can be observed in all inflow directions.

*Table 4.3: Summarized overall evaluation of the influence of vegetation on particle concentrations at 1.8 m. Positive +, slight positive (+), slight negative (-), and negative effects. The hedge might reduce concentrations in the two deeper canyons. Rows of sparsely foliated trees induce no concentration changes and a slight positive influence in deeper canyons with parallel inflow. The rows of the densely foliated trees show negative effects, particularly in the deeper canyons. Vegetation has the tendency to reduce the ventilating effect of high wind speed.*

| | | **u = 1 m/s** | | | **u = 3 m/s** | | |
|---|---|---|---|---|---|---|---|
| **Aspect** | | **Oblique inflow** | **Parallel inflow** | **Perpendicular inflow** | **Oblique inflow** | **Parallel inflow** | **Perpendicular inflow** |
| **0.5** | H | **0** | **0** | **0** | **0** | **0** | **0** |
| | T1 | **0** | **0** | **0** | **0** | **0** | **0** |
| | T2 | (-) | (-) | **0** | **0** | **0** | (-) |
| **0.9** | H | **(+)** | **(+)** | **0** | **0** | **0** | (-) |
| | T1 | **0** | **0** | **0** | **0** | **0** | **0** |
| | T2 | - | - | (-) | - | (-) | - |
| **1.2** | H | **(+)** | + | **0** | **0** | **0** | - |
| | T1 | **0** | **(+)** | **0** | **0** | **0** | **0** |
| | T2 | - | - | (-) | - | - | - |

H Hedge, T1 sparsely foliated tree, T2 densely foliated tree

Hedges might partly improve air quality particularly in deep canyons (Table 4.3). A positive influence was observed after the intersection with calm wind. Obviously, concentrations that usually accumulate after the intersection are already reduced by the hedges before the intersection. Remember that the hedge shows higher removal rates than the tree even before the intersection. Accordingly, fewer particles accumulate after the intersection and particles are additionally removed by the hedge rows in this canyon. Removal rates are higher with parallel inflow than with oblique inflow, which might be an explanation for higher concentration reduction rates in this inflow simulation after the intersection. This effect is not observed with higher wind speed (Table 4.3) and it seems that the removal rates do not balance the accumulation of particles in the air. The effect of ventilation inhibition at higher wind speed seems to dominate the influence of particle trapping and suppresses the positive effect of high wind speed observed in the reference case. However, this relationship does not apply for perpendicular inflows (Table 4.3). Here, concentrations and removal rates are both high. The cross-canyon circulation and reduced downward flow in deeper canyons accumulate particles inside the canyon even without vegetation. In the reference case, the accumulation is higher with high wind speed, which partly explains the concentration increase in the vegetation scenarios and the higher increase on the leeward side. The reason for this is the reduced inflow of air from outside the canyon.

Ventilation in the parallel sections worsens when trees are present. Due to wind speed reductions fewer particles are transported, especially in close vicinity to the source. For the sparsely foliated trees and the hedge, no changes occur in the parallel sections. The blocking effect is absent.

The inhibiting effect of vegetation increases with vertical and horizontal leaf area density. Continuous rows of trees worsen ventilation in canyons more than widely-spaced rows. The sparsely foliated trees show no significant increases in pollutant concentrations at the height of the human respiratory tract.

The main outcomes lead to the following recommendations.

- Avoid planting of dense trees in deep canyons.

Dense plantings of densely foliated trees have to be avoided in canyons with ratios higher than 0.5. In such cases, the thermal benefit from street trees can be provided by plantings of very sparsely foliated trees or widely-spaced rows of trees. At the same time, crown closure should be avoided. The inhibition of ventilation should be weighed against the gain in thermal comfort. Such evaluations can be performed using models like ENVI-met.

- Plant trees away from building walls.

Planting of trees close to building walls inhibits the upward flow and mixing of air.

- Avoid tree row plantings close to parks or unpolluted areas.

Tree row or hedge plantings that cut or inhibit penetration of fresh air from unpolluted or less polluted areas should be avoided. It is particularly important to avoid inhibition of the flow close to the bottom.

- Apply pruning methods that favour penetration of air through the canopy.

## 4.4 Simulation of the influence of vegetation on air quality in a real case scenario

Further simulations were run for two reasons. First, we want to show the interest to use models like ENVI-met to evaluate the impact of a planning project on air quality in general. Second, the simulations in the standard scenarios were run for only one hour what does not allow the evaluation of the influence on temperature as thermal effects depend mainly on the temporal changes in radiation during one day and associated heating and cooling of surfaces.

### 4.4.1 Model configuration

The influence of vegetation on traffic-induced $PM_{10}$ concentration and thermal conditions was evaluated based on a planning project that was recently realized in a city district of Strasbourg. In the framework of the construction of a new tram line a street was redesigned. The street is approximately 33 m wide and flanked by buildings of about 20 m height. The facades are discontinuous and smaller streets are crossing the main road. Figure 4.32 shows a view into the street (new design).

*Figure 4.32: View into the street with the new tram line, left and right of the tracks are double traffic lines (view from north-west to south-east, compare Figure 4.33). Before the construction, Horsechestnuts covered the area of the tracks instead of the lawn. Right and left of the tram tracks, sparsely foliated trees have been planted.*

Initially, the double traffic lines were separated by a double row of densely foliated trees with distinct crowns (Figure 4.33a). For the new situation all trees were cut down and replaced by a double tram line. The area between the tracks is covered mostly by lawn (Figure 4.33b). Sparsely foliated trees with no distinct crown were planted widely spaced on both sides of the traffic lines. The main characteristics of the vegetation types before and after the construction of the tram line are listed in Table 4.4.

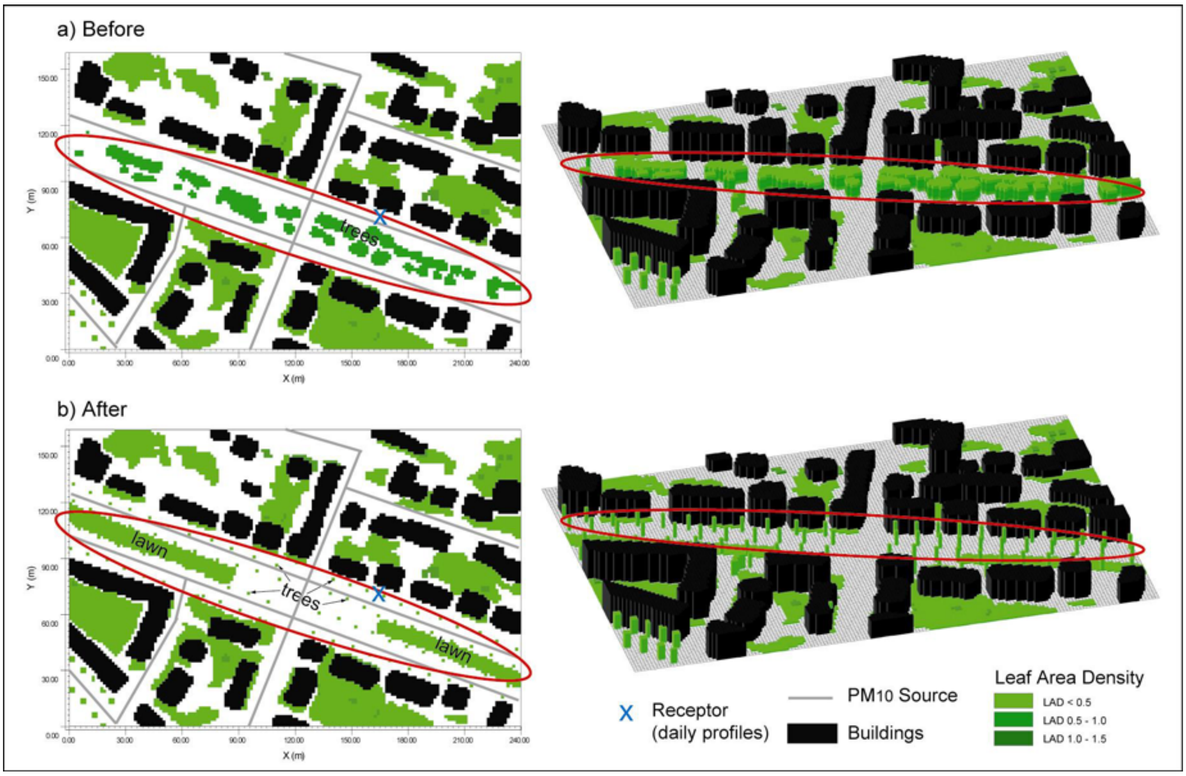


*Figure 4.33: Model area with green design before the construction of the tram line (a) and with the tram line (b). In the situation before the redesign, a double row of trees separated two traffic lines with parking areas under the trees (area inside the red circle). For the construction, all trees were cut down and replaced by a double tram line. The area between the tram tracks is covered by lawn. Sparsely leaved trees were planted on both sides of the traffic lines.*

A simulation was run for a summer day (24 hours, no clouds) with an inflow of 1 m/s and 225° (wind at 10 m, most frequent wind direction in Strasbourg). Furthermore, with the oblique direction a direct inflow in the street should be avoided to simulate rather bad ventilation conditions.

The emission values were taken from the STREET database, i.e. the hourly emission values correspond to the emissions calculated for the respective street in the area.

*Table 4.4: Summary of the vegetation configuration before and after the construction.*

| | **Before** | **After** |
|---|---|---|
| Vegetation type | Trees | Lawn and trees |
| Tree type | Densely foliated trees with distinct crown: 10 m height, LAD 0.75-1.15 $m^2/m^3$ | Small sparsely foliated trees: 3 m height, LAD between 0.07 and 0.15 $m^2/m^3$ |

### 4.4.2 Results

The daily profiles of potential temperature and particle concentration are shown in Figure 4.34 for the receptor indicated in Figure 4.33 (height 1.5 m). The profile of particle concentrations shows two peaks in the morning (8 am) and afternoon (19 pm) that correspond both to the daily rush hours. The impact of the new street design on temperature and particle concentration was compared for 15 pm. Although particle concentrations reach not their maximum, the potential temperature reaches its maximum. For the evaluation of the impact of the redesign project we chose to observe the situation at 15 pm that corresponds to the time of highest thermal discomfort. As in the standard scenarios we focus only on the height of the human respiratory tract (1.5 m).

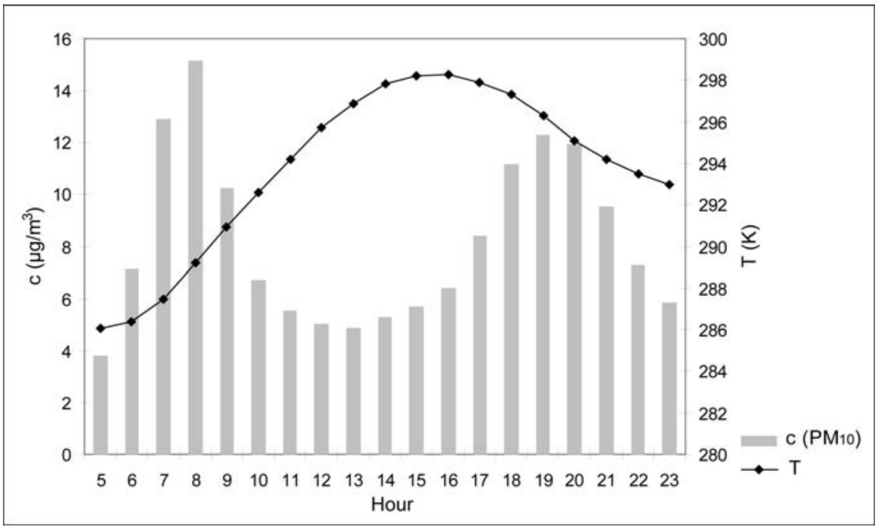


*Figure 4.34: Temperature and particle concentrations throughout the simulation day at the receptor in 1.5 m height (see Figure 4.33, values before 5 am are not presented). The concentration profile shows two peaks at 8 am and 19 pm. The highest temperatures are observed in the early afternoon around 15 pm. Note that concentrations do not include the background concentration.*

Figure 4.35 shows the changes in temperature induced by the new street design. In general, the new design leads to a temperature increase. The highest changes occur in the areas formerly shaded by the trees and the leeward zones of the street. However these changes are very small and reach maximum 1 K. The shade trees induced a temperature decrease but the lawn, replacing the trees in the new street design, obviously has a comparable effect. While the trees induce both shading and humidity increase, increased evapotranspiration in the situation with lawn reduces significantly the amount of sensible heat in general.

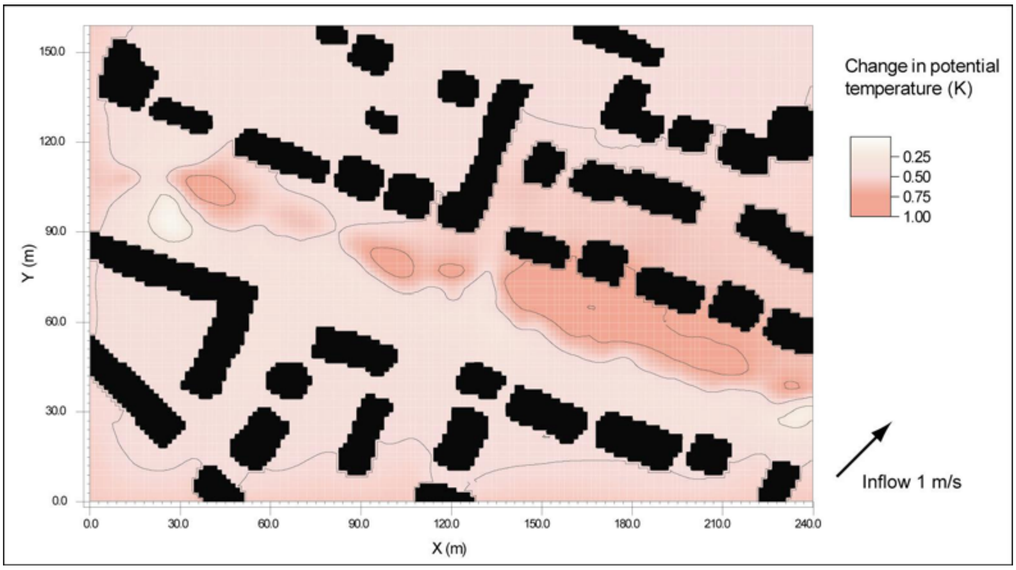


*Figure 4.35: Change in potential temperature induced by the new street design at 15 pm, at 1.5 m height. In general, the potential temperature increases up to 1 K. The highest changes occur in the former location of the tree group and in their downwind. Distance between isolines 0.25 K.*

The change in wind speed is shown in Figure 4.36. The values show a general increase induced by the reduced roughness after the construction. The densely foliated large trees were sheltering the area between the two traffic lines as well as the windward walking side (downwind). After the trees were cut down, the wind speed in these areas increases slightly.

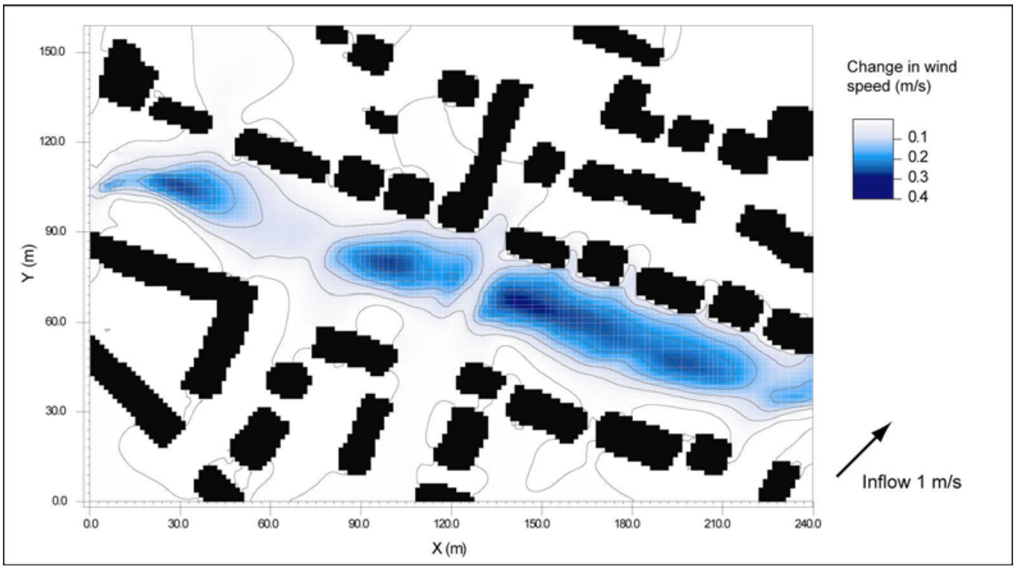


*Figure 4.36: Change in wind speed induced by the new street design at 15 pm, at 1.5 m height. The new street design leads to a slight increase in wind speed in the area initially covered by trees. Distance between isolines 0.05 m/s.*

The increased wind speed generally leads to lower particle concentrations (Figure 4.37). The changes are higher in some locations in the lee of buildings or trees. The highest changes occur at the street intersection. Obviously the large trees in the middle of the street were inhibiting the ventilation even in this wide street canyon.

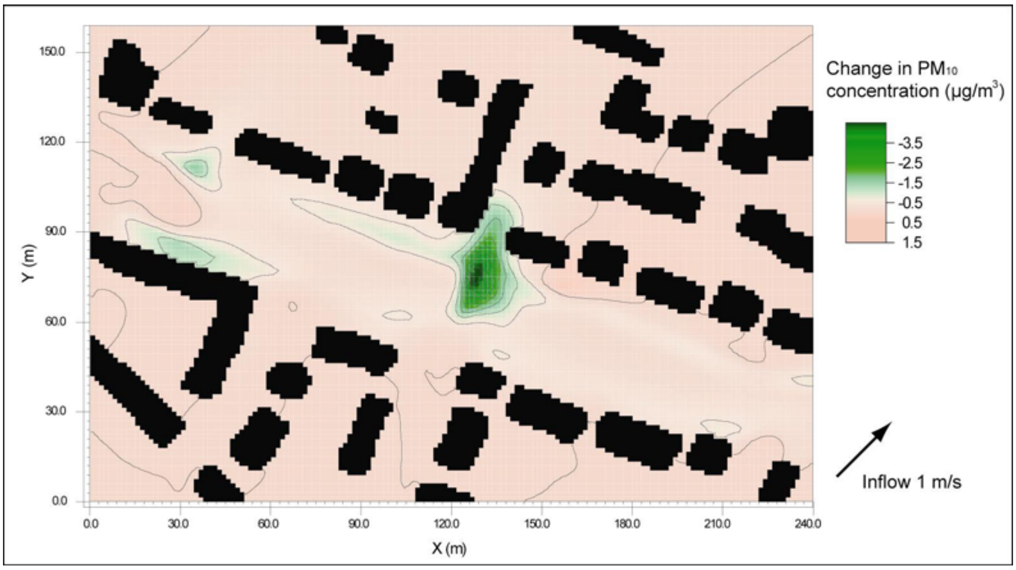


*Figure 4.37: Change in $PM_{10}$ concentration induced by the new street design at 15 pm, at 1.5 m height. The new street design leads locally to reduced concentrations, e.g. in the leeward walking side and downwind of former trees. The highest reduction is observed at the intersection. Distance between isolines 0.5 µg/m³.*

### 4.4.3 Conclusions

The results of the real case scenario confirm the influence of street trees on the thermal conditions and ventilation in the built environment. Trees with large, densely foliated canopies inhibit ventilation and consequently the dispersion of pollutants in streets.

With the new street design pedestrians are exposed to slightly higher temperatures. However, these changes are very small. The changes in particle concentrations are small. Reductions are observed in the lee of buildings and the lee of the former trees. The new street design reduces concentrations at the walking sides near the intersection to up to 2 µg/m³. The new situation especially improves the dispersion of particles at the crossing where base concentrations are generally higher. The new planted sparsely foliated trees show no significant influence but it is estimated that their influence increases in the future (larger crowns inducing ventilation inhibition).

These results indicate that the gain in thermal comfort by shade trees is small compared to the loss of ventilation. During the simulation time and for the chosen receptor the thermal effect of a dense lawn is comparable to that of tree rows.

These results show, that models like ENVI-met help to evaluate the air quality impact of a planning scenario on air quality. For the considered atmospheric conditions (clear summer day) the new street design leads to a rather positive influence on particle dispersion while at the same time the thermal comfort changes only few.

## 4.5 Discussion

The influence of vegetation on the flow field inside canyons was shown using computer modeling. It was possible to describe the general phenomena of dependence on street canyon width. Only the case of continuous facades was evaluated because pollution dispersion is the most critical in such canyons. Simulations were run with the same canyon configuration but with facades interrupted by spacings of 3 m width (from building bottom to top). These results show a slight improvement of ventilation and particularly in the canyons with perpendicular inflow. Fresh air from outside the canyon dilutes the air near the façade openings. However, the inhibiting effect dominates and pollution levels after the canyon (windward side) are slightly increased.

Nevertheless, the changes in pollution concentrations are very small. Although the study was not intended to quantify the effect, it gives some idea of its strength, bearing in mind that we intentionally used an emission value provided by a validated model but that the obtained concentrations are cumulated over one hour. As no chemical reactions occur, concentrations in reality are proportional. Ideally, the described effect has to be verified in field studies, but as it is probably low, it would be difficult to exclude variables that already induce differences between the base simulations in such a study.

The results suggest that the planting of hedges is rather positive. Hedges retain particles and reduce less air ventilation than trees. However, hedges are obstructions to citizens. Roovers *et al*, 2006 reported that a vegetation height of at least 54 cm could be identified as having significant obstructive features. Although their study concentrated on shrubs next to paths in green spaces, hedges in the built environment would probably show a comparable effect. Objects in the built environment are already close to each other and in contrast to trees, hedges may inhibit the field of vision much more.

Our results contradict the general assumptions that are made based on the amount of pollutants removed by urban trees (McPherson *et al.* 1994, Nowak 2006, Escobedo *et al.* in press). Based on the significant cooling effect of trees in streets, Sashua-Bar and Hoffman (2000) even suggest to plant one shade tree per eligible house to offset some of the cars' parking effect in the courtyard. These studies promote generally dense urban tree cover that might lead to precipitate overall conclusions, affecting decisions in planning even of street plantings. We suggest thus to weigh the thermal and air pollution benefit from trees planted in densely built structures against the loss in ventilation. Such evaluations can be done using models like ENVI-met.

If we want to transpose the results to fine and ultra-fine particles, the differences in deposition velocity and aspects of resuspension have to be considered. Ultra-fine particles show higher deposition velocities than fine and coarse particles on both coniferous and broadleaved trees (Freer-Smith *et al.* 2005). We suggest that the removal rates for finer particles would be consequently lower and concentrations higher.

***LAD profiles***

The Leaf Area Density profiles used are standard profiles provided by the model. They are based on profiles described in the literature. Most of the LAD profiles in literature are valuable for forest trees or whole forest parcels. To our knowledge, no LAD profiles have been described for urban trees. In contrast to trees in forests, urban trees are strongly influenced by the urban environment. Urban trees often stand alone and consequently the extension of crowns of urban trees is potentially larger. But most urban trees are regularly pruned, which often leads to densification of leaves within a restrained volume. The vertical and horizontal extension of the crown is accordingly limited, and the tree adapts to the modified conditions by intensified leaf growth near the stem and at the end of the cut branches (Klug *et al.* 2000).

The LAD profiles used in the two tree scenarios represent two extreme cases. A very sparsely foliated and a very densely foliated tree was selected to evaluate each of two real distinct tree types. Sparsely foliated trees usually show no distinct crown. Pruning often results in the formation of an artificial crown or a densified canopy. Furthermore, urban horticulture yields a number of ornamental trees with special growth shapes. It would be interesting to integrate such shapes in simulations. Such aspects can be considered in ENVI-met but with the grid cell size used this would result in enormous trees in form of a staircase. In future versions of ENVI-met object can be simulated by polygons what improves the possibility to simulate different tree shapes.

***Processes induced by plants***

Our results show the role of vegetation in the deposition of particles on plant surfaces. The driving force of deposition is the increased turbulence that is always higher within plant canopies than above or below them (Rauner 1976). The increase within the canopy can be partially explained by leaves and stems fluttering, which converts kinetic energy from the mean flow to turbulent kinetic energy. The role of such turbulence is two-fold. On the one hand, it can facilitate deposition of particles and on the other hand, it can also provide an instantaneous lift force sufficient to detach and re-suspend particles (Ould-Dada and Baghini 2001). Particle deposition and re-suspension may occur simultaneously. The model version we used doesn't take into account re-suspension and normally this would reduce the amount of total deposed particles and consequently increase the overall concentration level. However, plants are effective in trapping particles, and re-suspension rates are estimated to be relatively low compared to the amount deposed (McPherson *et al.* 1994, Ould-Dada and Baghini 2001). Re-suspension depends on the physical characteristics of the particle, the roughness of the surface and the properties of the mean flow. It increases with wind speed, and large particles are re-suspended even at low wind speeds (Ould-Dada and Baghini 2001). Ould-Dada and Baghini (2001) showed that particles with a diameter of 1 μm under constant wind velocities of 5 m/s are likely to pose a relatively small inhalation hazard to humans and a minor source of secondary contamination of adjacent areas (Ould-Dada and Baghini 2001). However, smaller particles like $PM_{10}$ might be more affected by re-suspension due to fewer adhesion force.

In addition to the re-suspension rate, the removal of particles through wash-off by rain or other wet deposition, or trough leaf and twig fall processes that occur under field conditions, were not considered. Thus, tree canopies constitute only a temporary retention site for atmospheric particles. Once trapped on surfaces, particles are temporarily removed from the circulating air, at least for the time of simulation run. In their estimation of $PM_{10}$ removal by the Chicago urban forest, McPherson *et al.* (1994) concluded there was an improvement of air quality by 2.1 % per hour.

In the present study we evaluated the general deposition of particles on plant leaves. The model therefore integrates among others some standard parameters specific to either deciduous or coniferous trees. They concern mainly the aerodynamic behaviour but there are other leaf characteristics such as thickness, stickiness, or slipperiness, which influence the trapping of pollutants as well. It would be interesting to introduce tree-specific deposition velocities and trapping or capture efficiencies in models to better estimate the likely consequences of urban tree planting schemes of planting design and species composition. Freer-Smith et al. (2005) showed that there are a number of species-specific values for particles of different diameters.

***Street canyon configuration***

Dispersion of pollutants in street canyons takes place under the joint influence of natural and vehicle-induced air motions. Turbulence induced by moving vehicles is not considered in the model we used. In calm wind situations, traffic-induced turbulence dominates over the natural winds in the canyon (Kastner-Klein *et al.* 2001). The influence affects the turbulence close to the bottom where highest concentrations occur and affects air flows higher above the road. Kastner-Klein *et al.* (2001) report a pronounced transport of pollutants along the canyon axis for a one-way traffic line. Local concentrations in the street might decrease with vehicle density. Others have shown that traffic motion leads to significant reductions even at the pedestrian level (Pearce and Baker 1997).

As reported in literature the distribution of pollutants within street canyons is also influenced by the roof's shape (Rafailidis 1997, Kastner-Klein and Plate 1999). Accordingly, saddle roofs are more effective for canyon ventilation than flat roofs. Only flat roofs were evaluated as the actual resolution of the model in blocks would create artificial flow obstacles, especially at a resolution of 3 m. It is estimated that the influence of the roof shape on the observed relationship between vegetation and particle dispersion is not significant. Nevertheless, it should be tested, and with the next ENVI-met version (development is ongoing), this should be possible as objects can be defined by polygons. With respect to the roof form, this would facilitate their definition and avoid the staircase form induced by actual block structure.

Another aspect is canyon symmetry. All analysed canyons are symmetric, with equal heights on both canyon sides. In step-down canyons (lower building height of the downwind building) perpendicular inflow induces the same concentrations on the leeward side as the symmetric canyon (Hoydysh and Dabberdt 1988). With high-rise buildings, downwind higher concentrations occur at mid-block due to absence of convergence. It is estimated that this concentration accumulation would be additionally increased by trees. Furthermore, a single high-rise building in the canyon can cause favourable mixing in the windward side but higher concentrations on the leeward side (Ahmad *et al.* 2005).

The role of the L/H ratio, relating the length of the canyon (L, distance between two intersections) to its height, was not addressed in our study. For the avenue canyon L/H reaches 2.3, for the canyon with aspect 0.9 it reaches 3.9 and for the narrowest canyon 5.6 (Ahmad *et al.* 2005). Accordingly, the avenue canyon is considered as a short canyon, the mid-width one as medium canyon and the narrowest one as long canyon. With perpendicular inflow, short canyons provide better ventilation at corners induced by intermittent vortices shed on the building corners (Hoydysh and Dabberdt 1988). A convergence zone in the mid-block is described with maximum concentrations at mid-section. Such a maximum is not observed as no single canyon, but an intersection is analysed. Pollutants are additionally blown inside the canyon from the other canyons, increasing the level near the intersection. However, the described effect may be another reason for the better ventilation of this canyon, and the insignificant influence of vegetation.

Another aspect is the relation between tree and building height. Supposing that higher trees inhibit ventilation more than small trees, it would be interesting to know if the effect is the same for a given tree/building height ratio.

***Model used***

The choice of the model for this study was mainly influenced by its capability to simulate the influence of plants on the atmospheric conditions in a built environment on a microscale. It combines the simulation of processes induced by the plants metabolism with atmospheric processes happening in the upper atmospheric layer of micro environments. The first are commonly modelled by soil-vegetation-atmosphere-transfer models (SVAT) that are often one- or two-dimensional and focus on plant physiological processes (Grünhage and Haenel 1997). These models are not able to simulate processes induced by built objects or sealed surfaces. In contrast, most of the other group of microscale models designed for urban applications do not include processes induced by the plant and plants are considered as porous objects. Models such as MISKAM (Eichhorn 1989) and SCALAR (Johnson and Hunter 1995) are specialised on the simulation of the wind field. The ENVI-met model integrates both aspects.

Another aspect is that the model can be easily accessed and potentially used by planners. City planning has limited financial budgets and tools that are accessible and relatively easy to handle can help to pass the gap between urban climate research outcomes and planning applications as it was shown by Eliasson *et al.* (2000).

# 5 GENERAL CONCLUSIONS

The present work focused on vegetation in urban areas. We have shown that a focus on urban areas is critical to discussions on the future of human life on Earth. Not only do cities house half of the world's population, but they also concentrate most of the world's environmental problems. This relationship implies a particularly high need for a healthy environment that is in turn considered as a main factor for human quality of life. The concept of sustainable development provides a framework for guiding of future development that leads to the emergence of many political actions concerning the urban environment. Urban vegetation is one element identified as a contributor to the sustainable development of a city. Its role in improving the quality of life in cities is widely accepted and indicators of sustainable development commonly include an evaluation of the provision and accessibility to green urban areas.

We adopted an ecosystems approach to present the urban metabolism research and to underline the role of vegetation as an element of the urban ecosystem. The role was presented mainly from a human point of view, which emphasises the benefits to compensate for the detrimental effects of the urban metabolism. All the more, there is a special need to observe vegetation and to analyse its effects in order to optimise its functioning in the urban ecosystem and to benefit as much as possible from its compensating effects. Although there has been substantial research performed on these functions, in our opinion, the functioning of urban vegetation can be better optimised. Actually, political action concerning urban greenspace is among others driven by the general promotion of green. However, we assert that this political aim needs guided planning implementations. Questions of 'how, where, and what should be planted?' have to be addressed in planning projects. Besides aesthetical aspects, these questions should specifically address ecological functions. With the example of air quality, we could show that an increase in vegetation cover, which is generally promoted, is not necessarily linked to an air-quality benefit from the point of view of pollution.

***Microscale air quality simulations to evaluate the influence of vegetation on air quality***

The influence of vegetation on air quality was performed with a microscale air quality model designed for simulations in small-scale urban environments, i.e. at the scale of housing blocks, streets, or a city district. We used ENVI-met because of its ability to simulate processes at the interfaces plant-atmosphere-soil in complex environments such as urban areas. To our knowledge, it is the first model that combines plant-induced exchange processes with the microscale atmospheric processes in built environments that promote generally low air quality.

Based on simulations in standard scenarios, we demonstrated the inhibiting effect on ventilation in deep street canyons. We evaluated the relationship between the height-to-width ratio of streets flanked by buildings and the vertical and horizontal density of vegetation cover. This evaluation of the influence of vegetation on air quality focussed on air quality at the height of the human respiratory tract. The results show that particle concentrations increase with height-to-width ratio and vegetation density. Air quality is additionally worsened in configurations with poor ventilation, such as low wind speed, perpendicular inflow direction, and in deep canyons. Hedges might be an alternative to trees in deep canyons. They retain not only more particles, as they are closer to the source, but may even reduce concentrations at the height of the human respiratory tract. Implementations for planning were formulated from these results: we recommend that planners avoid planting densely foliated trees in canyons with a height-to-width ratio higher than 0.5, plant trees distinctly away from building walls, and apply tree pruning methods that favour penetration of air through the canopy. Furthermore, tree row plantings should be avoided near unpolluted areas to promote the penetration of fresh air into polluted areas.

The impact of the redesigning of a green area within the framework of a planning project was evaluated for a real case scenario. The influence of planted areas on the thermal benefits as well as the influence on pollutant concentrations was confirmed. With the real case scenario we showed that operational air quality models like ENVI-met can be used to evaluate the impact of a planning scenario on the air quality in terms of thermal comfort and exposition to traffic-induced air pollution.

The outcomes of the air quality simulations should encourage planners to consider such aspects much more when defining urban planning projects. One way in which to facilitate their implementation could be through the integration of information about leaf area density for commonly planted urban trees. Although the leaf area density is also a function of pruning, it is possible to differentiate between *a priori* densely and sparsely foliated trees. Planners should also consider the effects of pruning methods on air quality. Such information can be implemented in recommendation lists for urban trees. Although such planning lists are not compulsory, they are a first step towards directed implementation of such information.

***Observation of vegetation with remotely sensed hyperspetral data***

The valuation of vegetation in urban areas and its management requires the observation of urban objects. Remote sensing can provide a valuable source of information. Although it cannot replace precise investigations in the field, it can help monitor tree health and support the updating of databases. We have analysed the potential of hyperspectral data for urban vegetation observation. The performance of different vegetation indices for the detection of vegetated areas was examined. Commonly used vegetation indices like NDVI can not provide correct vegetation estimations in urban areas. We showed that including both the influence of the underlying soil and atmospheric effects in the calculation of a vegetation index significantly improves its performance. For the identification of urban vegetation cover, TSARVI is an index that performs well. Furthermore, the interest to exploit the information at the red-edge was shown. Second order data are simple to derive and useful to exploit data at the red-edge for the detection of senescent vegetation for example.

We examined the possibility of detecting different tree species with hyperspectral data and compared this potential with that of multispectral data. In general, it is possible to detect species, but the success is limited to particular species. This result is above all influenced by the specific effects occurring in all urban remote sensing applications that include mainly the complex illumination conditions and the occurrence of mixed pixels. Additionally, vegetation objects show generally a high inter-object variability that depends mainly on viewing geometry, canopy density and consequently influence of the underlying surface, and different illumination conditions due to the object's 'relief'. Another reason for this limited success is the method we applied. We focussed on supervised classification on a reduced image. Different feature extraction methods were examined in order to evaluate their potential to differentiate spectrally similar classes. We showed that feature extraction based on previously defined classes improves the results of the supervised classification. Decision Boundary Feature Extraction is a useful method for detecting spectrally similar classes. The Maximum Likelihood classifier is commonly applied. Other methods that were especially developed for high dimensional data, performed poorly on the data that we analysed. We believe that this is related to the high inter-object variability in urban vegetation. Detecting the whole object would need the definition of many endmember spectra what would increase the complexity of the analysis. In the future, spectral unmixing should be tested, bearing in mind that the definition of endmembers remains the main problem.

The results of the tree detection were compared with the results obtained on resized multispectral data. The performance of multispectral data is poorer, which underlines our interest in using hyperspectral data for such investigations.

We conclude that very high spatial and spectral resolution data provide precise information on urban vegetation. They can help in detecting tree species, but nevertheless, this potential is limited. The spatial resolution of objects and the complex illumination conditions in urban environments finally are limiting the precision of the obtained information. When considering the pros and cons of the effort required to collect and analyse these data, and the increase in information that they provide, high spatial and spectral resolution data are still too expensive and complex for operational use in planning. However, with the development of technology, this might change in the future.

Finally, we tested the new algorithm for feature selection in hyperspectral images MACLAW. Initially developed for unsupervised classification of large datasets, our interest in testing this algorithm was due to its potential to help to detect possible endmembers and object classes for further analysis. The performance of the algorithm was evaluated on built and non-built objects and compared with a supervised feature selection algorithm. Both band subsets were introduced in a supervised classification. As feature extraction usually yields to better results, the results obtained with both subsets were finally compared to a supervised classification on transformed bands obtained by feature extraction. Although the overall accuracy of the classification on bands selected by MACLAW is smaller, the unsupervised method detects relevant classes that help the user to exploit the data and define classes or endmembers for further analysis.

## 5.1 Perspectives

### Research on urban vegetation and the relevance for planning

The valuation of urban vegetation for the quality of life in urban areas should still be addressed in future research. Despite the large amount of research performed on the subject, some relationships need more confirmation. In this context, it is especially important to make efforts for the implementation of research results in planning. This could be done by means of models but needs close cooperation with a competent person. Planners do not necessarily need to use models that are still rather complex in their application. Furthermore, there is still a gap between planning needs and the demands claimed by researchers concerning data and their interpretability. It seems that a lot has to be done to increase the awareness of the value of the work of each. The most promising solution would be more cooperation between planners and researchers. Unfortunately, this is still very rare and can probably only be managed by political action or legislation.

Much research still needs to be done to evaluate the potential of remote sensing for urban vegetation detection. City planning still uses time consuming methods to build databases and to update them. Although remote sensing cannot entirely replace field observation, it can speed up the process of collecting information. Our own experiences show that planners are not yet convinced of the value of remote sensing for their work. As in the air quality simulations, the methods are too complex and the only way to use these data is in cooperation with researchers. More efforts need to be made to develop well-performing methods that can be applied by planners in their daily work flows. In this context, the application of hyperspectral data can be envisaged only in the distant future.

**Methodologies**

The results obtained with the microscale air quality simulations need further validation, ideally by field validation. However, this poses clear problems in terms of comparability and exclusion of the influence of non-significant parameters. Plants are highly variable objects, and the complex flow patterns in the urban canopy make such experiments rather difficult. A more promising avenue is to improve the reliability of the model. The nesting of microscale models like ENVI-met with models operating on larger scales (e.g. CHIMERE, urban-ADMS) might improve the estimation of some parameters in ENVI-met. However, although effects on the microscale are influenced by processes in the atmosphere above, they depend more on the processes happening in close proximity. Nevertheless, this is still a perspective for the near future.

Another perspective in this context is the validation of the results for smaller particles. The deposition of $PM_{10}$ is generally higher than that of smaller particles, as they remain in suspension longer and are resuspended more quickly from surfaces. In recent years, special attention has been addressed to the latter, as they present a more significant health effect.

It would be interesting to compare our findings with the thermal benefit from shade trees in order to weigh both. Based on this relationship, one could decide if the planting of shade trees provides more benefits than negative effects on pollutant concentrations.

Concerning remote sensing with hyperspectral data, the few examples of research performed on urban vegetation show the need for more studies. In general, hyperspectral data analysis is a research field with a high number of different and often rather complex methods that have proven their performance on built objects, crops or forest canopies, and minerals, with most applications taking place outside urban areas. With their high spectral precision, these data can provide valuable information for object-oriented approaches or can even used to segment objects. Another interesting methodology for the detection of urban trees is the combination with LIDAR data.

# REFERENCES

Adam, K. 1985. Die Stadt als Ökosystem. Geographische Rundschau **37**: 214-225.

Adams, J. B., M. O. Smith, and P. E. Johnston. 1986. Spectral mixture modelling: a new analysis of rock and soil types at the Viking Lander 1 site. Journal of Geophysical Research **91**: 8098-8112.

ADEME. 2002. Classification and criteria for setting up air-quality monitoring stations. Agence de l'Environnement et de la Maîtrise de l'Energie, Paris, France. 63 *pages*.

ADEUS. 1996. Plan vert de la Communauté urbaine de Strasbourg. Analyse de l'état actuel, orientations de programme. Agence de développement et d'urbanisme de l'Agglomération strasbourgeoise, Strasbourg, France. 108 *pages*.

Ahmad, K., M. Khare, and K. K. Chaudhry. 2005. Wind tunnel simulation studies on dispersion at urban street canyons and intersections - a review. Journal of Wind Engineering and Industrial Aerodynamics **93**: 697-717.

Akbari, H. 2002. Shade trees reduce building energy use and $CO_2$ emissions from power plants. Environmental Pollution **116**: S119-S126.

Akbari, H., D. M. Kurn, S. E. Bretz, and J. W. Hanford. 1997. Peak power and cooling energy savings of shade trees. Energy and Buildings **25**: 139-148.

Akbari, H., M. Pomerantz, and H. Taha. 2001. Cool surfaces and shade trees to reduce energy use and improve air quality in urban areas. Solar Energy **70**: 295-310.

Akbari, H., and H. Taha. 1992. The impact of trees and white surfaces on residential heating and cooling energy use in four Canadian cities. Energy **17**: 141-149.

Alberti, M., and J. M. Marzluff. 2004. Ecological resilience in urban ecosystems: Linking urban patterns to human and ecological functions. Urban Ecology **7**: 241-265.

Allemand, S. 2006. Le développement durable. Editions Autrement, Paris, France. 96 *pages*.

Angold, P. G., J. P. Sadler, M. O. Hill, A. Pullin, S. Rushton, K. Austin, E. Small, B. Wood, R. Wadsworth, R. Sanderson, and K. Thompson. 2006. Biodiversity in urban habitat patches. Science of The Total Environment **360**: 196-204.

Arya, S. P. 2001. Introduction to micrometeorology. 2nd edition. Academic Press, San Diego, California. 420 *pages*.

Baize, D., and J. P. Rossignol. 1995. Anthroposols. *In:* D. Baize and M. C. Girard (Eds.). Référentiel pédologique. INRA, Paris, France. pp. 335.

Bannari, A., D. C. He, D. Morin, and H. Anys. 1998. Analyse de l'apport de deux indices de végétation à la classification dans les milieux hétérogènes. Canadian Journal of Remote Sensing **24**: 233-239.

Bannari, A., D. Morin, and F. Bonn. 1995. A review of vegetation indices. Remote Sensing of Environment **13**: 95-120.

Bannari, A., D. Morin, and D. C. He. 1994. High spatial and spectral resolution remote sensing for the management of the urban environment. *In: Proceedings of the* First International Airborne Remote Sensing Conference and Exhibition. Strasbourg, France.

Baret, F., G. Guyot, and D. J. Major. 1989. TSAVI: A vegetation index which minimizes soil brightness effects on LAI and APAR estimation. *In: Proceedings of the* Digest - International Geoscience and Remote Sensing Symposium (IGARSS).

Bariou, R., D. Lecamus, and F. Le Henaff. 1985. Indices de végétation. Université de Rennes, Rennes, France. 150 *pages*.

Barth, H. G., and A. Lang. 2003. Nachhaltige Stadtentwicklung in Deutschland und Frankreich - Instrumente und Umsetzungsmöglichkeiten in ausgewählten Themenbereichen des Umweltschutzes (Luftschadstoff- und Abfallvermeidung). Peter Lang, Frankfurt am Main, Germany. 363 *pages*.

Batzias, F., and C. G. Siontorou. 2007. A novel system for environmental monitoring through a cooperative/synergistic scheme between bioindicators and biosensors. Journal of Environmental Management **82**: 221-239.

Baugh, W. M., F. A. Kruse, and W. W. Atkinson. 1998. Quantitative Geochemical Mapping of Ammonium Minerals in the Southern Cedar Mountains, Nevada, Using the Airborne Visible/Infrared Imaging Spectrometer (AVIRIS). Remote Sensing of Environment **65**: 292-308.

Beckett, K. P., P. H. Freer-Smith, and G. Taylor. 1998. Urban woodlands: their role in reducing the effects of particulate pollution. Environmental Pollution **99**: 347-360.

Beeby, A. 2001. What do sentinels stand for? Environmental Pollution **112**: 285-298.

Ben-Dor, E., N. Levin, and H. Saaroni. 2001. A spectral based recognition of the urban environment using the visible and near-infrared spectral region (0.4-1.1 μm). A case study over Tel-Aviv, Israel. International Journal of Remote Sensing **22**: 2193-2218.

Ben-Dor, E., N. Levin, A. Singer, A. Karnieli, O. Braun, and G. J. Kidron. 2006. Quantitative mapping of the soil rubification process on sand dunes using an airborne hyperspectral sensor. Geoderma **131**: 1-21.

Bennett, J. H., and A. C. Hill. 1973. Absorption of gaseous air pollutants by a standardized plant canopy. Journal of the Air Pollution Control Association **23**: 203-206.

Bergamaschi, L., E. Rizzio, G. Giaveri, S. Loppi, and M. Gallorini. 2007. Comparison between the accumulation capacity of four lichen species transplanted to a urban site. Environmental Pollution **148**: 468-476.

Berkowicz, R., M. Ketzel, S. S. Jensen, M. Hvidberg, and O. Raaschou-Nielsen. 2007. Evaluation and application of OSPM for traffic pollution assessment for a large number of street locations. Environmental Modelling & Software **23**: 296-303.

Berlizov, A. N., O. B. Blum, R. H. Filby, I. A. Malyuk, and V. V. Tryshyn. 2007. Testing applicability of black poplar (Populus nigra L.) bark to heavy metal air pollution monitoring in urban and industrial regions. Science of The Total Environment **372**: 693-706.

Bixler, R. D., and M. F. Floyd. 1997. Nature is scary, disgusting, and uncomfortable. Environment and Behaviour **7**: 443-467.

Bjerke, T., T. Ostdahl, C. Thrane, and E. Strumse. 2006. Vegetation density of urban parks and perceived appropriateness for recreation. Urban Forestry and Urban Greening **5**: 35-44.

Blansché, A., P. Gançarski, and J. J. Korczak. 2006. MACLAW: A modular approach for clustering with local attribute weighting. Pattern Recognition Letters **27**: 1299-1306.

Blume, H.-P. 1998. Böden. *In:* H. Sukopp and R. Wittig (Eds.). Stadtökologie. Gustav Fischer, Stuttgart, Germany. pp. 168-185.

Boardman, J. W. 1989. Inversion of imaging spectrometry data using singular value decomposition. *In: Proceedings of the* IGARSS'89, 12th Canadian Symposium on Remote Sensing. Vancouver, Canada.

Boardman, J. W., F. A. Kruse, and R. O. Green. 1995. Mapping target signatures via partial unmixing of AVIRIS data. Fifth JPL Airborne Earth Science Workshop, JPL Publication 95-1, vol. 1: 23-26.

Bochow, M., K. Segl, and H. Kaufmann. 2007. Automating the build-up process of feature-based fuzzy logic models for the identification of urban biotopes from hyperspectral remote sensing data. *In: Proceedings of the* Urban Remote Sensing Joint Event 2007. Paris, France.

Bolund, P., and S. Hunhammar. 1999. Ecosystem services in urban areas. Ecological Economics **29**: 293-301.

Bonaiuto, M., F. Fornara, and M. Bonnes. 2006a. Perceived residential environment quality in middle- and low-extension italian cities. European Review of Applied Psychology **56**: 23-34.

Bonaiuto, M., F. Fornara, and M. Bonnes. 2006b. Perceived residential environment quality in middle- and low-extension italian cities. European Review of Applied Psychology **56**: 23-34.

Brack, C. L. 2002. Pollution mitigation and carbon sequestration by an urban forest. Environmental Pollution **116**: S195-S200.

Breuste, J. H. 2004. Decision making, planning and design for the conservation of indigenous vegetation within urban development. Landscape and Urban Planning **68**: 439-452.

Bruse, M. 1999. The influences of local environmental design on microclimate (in German). PhD *thesis*. University of Bochum, Bochum, Germany. 196 *pages*.

Bruse, M. 2007. ENVI-met 3. http://www.envi-met.com/. *Accessed* August 2007.

Bruse, M., M. Bürger, A. Ihde, K. Jesionek, and E. Lahme. 2002. Benefits of urban green spaces (BUGS): Measurements and model simulations in WP Micro, Deliverable 18, Part I. Bochum, Germany. 52 *pages*.

Bruse, M., and H. Fleer. 1998. Simulating surface-plant-air interactions inside urban environments with a three dimensional numerical model. Environmental Modelling and Software **13**: 373-384.

Bryant, M. M. 2006. Urban landscape conservation and the role of ecological greenways at local and metropolitan scales. Landscape and Urban Planing **76**: 23-44.

Burgess, E. W. 1925. The growth of the city: an introduction to a research project. *In:* R. E. Park, E. W. Burgess and R. D. McKenzie (Eds.). The city. University of Chicago Press, Chicago. pp. 47-62.

Burgess, J., C. M. Harrison, and M. Limb. 1988. People, Parks and the Urban Green: A Study of Popular Meanings and Values for Open Spaces in the City. Urban Studies **25**: 455-473.

Buyantuyev, A., J. Wu, and C. Gries. 2007. Estimating vegetation cover in an urban environment based on Landsat ETM+ imager: a case study in Phoenix, USA. International Journal of Remote Sensing **28**: 269-271.

Campbell, G. S., and J. M. Normann. 1989. The description and measurement of plant canopy structure. *In:* G. Russell, B. Marshall and P. G. Jarvis (Eds.). Plant canopies: their growth, form and function. Cambridge University Press, Cambridge, UK. pp. 1-19.

Cardelino, C. A., and W. L. Chameides. 1990. Natural hydrocarbons, urbanization and urban ozone. Journal of Geophysical Research **95(D9)**: 13971-13979.

Carter, T., and C. R. Jackson. 2007. Vegetated roofs for stormwater management at multiple spatial scales. Landscape and Urban Planning **80**: 84-94.

CEC. 1990. Greenpaper on the urban environment. COM(90) 218 final, Commission of the European Communities, Brussels, Belgium. 63 *pages*.

CEC. 1991. Council Resolution of 28 January 1991 on the Green Paper on the urban environment. C 33/4, Commission of the European Communities, Brussels, Belgium. 2 *pages*.

CEC. 1996. European Sustainable Cities - report. Commission of the European Communities, Expert Group on the Urban Environment, EC DG XI - Environment, Nuclear Safety and Civil Protection, Brussels, Belgium. 279 *pages*.

CEC. 2001. Environment 2010: Our future, our choice. 6th Environment Action Programme 2001-2010. Commission of the European Communities, Luxembourg. 12 *pages*.

CEC. 2006. Thematic Strategy on the Urban Environment. COM(2005) 718 final, Commission of the European Communities. 12 *pages*.

CEC. 2007. Urban Audit - Assessing the Quality of life of European cities: indicators of urban quality of life. Commission of the European Communities. http://ec.europa.eu/regional_policy/urban2/urban/audit/src/intro.html. *Accessed* September 2007.

Chabrillat, S., G. A.F.H., O. H.W., and K. L. 2002. Use of hyperspectral imagery in identification and mapping of expansive clays in Colorado. Remote Sensing of Environment **82**: 431-445.

Clark, A. N. 1985. Longman dictionary of geography. Longman, Essex, UK. 724 *pages*.

Clark, M. L., D. A. Roberts, and D. B. Clark. 2005. Hyperspectral discrimination of tropical rain forest tree species at leaf to crown scales. Remote Sensing of Environment **96**: 375-398.

Cochrane, M. A. 2000. Using vegetation reflectance variability for species level classification of hyperspectral data. International Journal of Remote Sensing **21**: 2075-2087.

Coles, R. W., and S. C. Bussey. 2000. Urban forest landscapes in the UK -- progressing the social agenda. Landscape and Urban Planning **52**: 181-188.

Coley, R. L., W. C. Sullivan, and F. E. Kuo. 1997. Where does community grow?: the social context created by nature in urban public housing. Environment and Behaviour **7**: 468-494.

Collins, J. P., A. Kinzig, N. B. Grimm, W. F. Fagan, D. Hope, J. Wu, and E. T. Borer. 2000. A new urban ecology. American Scientist **88**: 416-425.

Colvile, R. N., E. J. Hutchinson, J. S. Mindell, and R. F. Warren. 2001. The transport sector as a source of air pollution. Atmospheric Environment **35**: 1537-1565.

Conti, M. E., and G. Cecchetti. 2001. Biological monitoring: lichens as bioindicators of air pollution assessment - a review. Environmental Pollution **114**: 471-492.

Dab, W., C. Ségala, F. Dor, B. Festy, P. Lameloise, Y. Le Moullec, A. Le Tertre, S. Médina, P. Quénel, B. Wallaert, and D. Zmirou. 2001. Pollution atmosphérique et santé: Corrélation ou causalité? Le cas de la relation entre l`exposition aux particules et la mortalité cardio-pulmonaire. Journal of the Air and Waste Management Association **51**: 203-219.

Danson, F. M., M. D. Steven, T. J. Malthus, and J. A. Clark. 1992. High-spectral resolution data for determining leaf water content. International Journal of Remote Sensing **13**: 461-470.

Dare, P. M. 2005. Shadow analysis in high-resolution satellite imagery of Urban Areas. Photogrammetric Engineering and Remote Sensing **171**: 169-177.

De Genst, W., and F. Canters. 2004. Extracting detailed urban land-cover information from hyperspectral imagery. *In: Proceedings of the* UMDS, Application of high resolution remote sensing data.

De Jong, S. M. D., E. J. Pebesma, and B. Lacaze. 2003. Above-ground biomass assessment of Mediterranean forests using airborne imaging spectrometry: the DAIS Peyne experiment. International Journal of Remote Sensing **24**: 1505-1520.

De Lange, R., M. VanTil, and S. Dury. 2004. The use of hyperspectral data in coastal zone vegetation monitoring. EARSeL eProceedings, Vol. 3. www.eproceedings.org/static/vol03_2/03_2_delange1.html.

Demetriades-Shah, T. H., M. D. Steven, and J. A. Clark. 1990. High resolution derivative spectra in remote sensing. Remote Sensing of Environment **33**: 55-64.

Dimoudi, A., and M. Nikolopoulou. 2003. Vegetation in the urban environment: microclimatic analysis and benefits. Energy and Buildings **35**: 69-76.

Douglas, I. (Eds.). 2002. Causes and consequences of global environmental change. Encyclopedia of global environmental change, Vol. 3. John Wiley & Sons, LTD, Chichester, UK. 753 *pages*.

DRIRE. 2000. Plan régional pour la qualité de l`air en Alsace. Direction Régionale de l`Industrie, de la Recherche et de l`Environment, Strasbourg, France. 124 *pages*.

DSD. 2007. http://www.un.org/esa/sustdev. Division for Sustainable Development at the UN Department of Economic and Social Affairs *Accessed* July 2007.

Duhme, F., and S. Pauleit. 1998. Some examples of different landscape systems and their biodiversity potential. Landscape and Urban Planning **41**: 249-261.

Duvigneaud, P. 1980. La synthèse écologique. 2nd edition. Doin éditeurs, Paris, France. 380 *pages*.

Eichhorn, J. 1989. Entwicklung und Anwendung eines dreidimensionalen mikroskaligen Stadtklima-Modells. PhD *thesis*. University of Mainz, Mainz, Germany. 163 *pages*.

Eliasson, I. 2000. The use of climate knowledge in urban planning. Landscape and Urban Planning **48**: 31-44.

Ellenberg, H. 1974. Zeigerwerte der Gefäßpflanzen Mitteleuropas (indicator values of vascular plants in Central Europe). Goltze, Göttingen, Germany. 97 *pages*.

Escobedo, F. J., J. E. Wagner, D. J. Nowak, C. L. De la Maza, M. Rodriguez, and D. E. Crane. in press. Analyzing the cost effectiveness of Santiago, Chile's policy of using urban forests to improve air quality. Journal of Environmental Management **In Press, Corrected Proof**.

Falga, P., and M. Feltin. 2003. Le palmarès des villes vertes. L`Express **16/10/2003**: 94-116.

Fanelli, G., P. Tescarollo, and A. Testi. 2006. Ecological indicators applied to urban and suburban floras. Ecological Indicators **6**: 444-457.

Fenger, J. 1999. Urban air quality. Atmospheric Environment **33**: 4877-4900.

Forrester, J. W. 1961. Industrial dynamics. Pegasus Communications, Walthan, MA. 464 *pages*.

Forrester, J. W. 1969. Urban dynamics. Productivity Press, Wiley, Cambridge, MA. 285 *pages*.

Fowler, D., J. N. Cape, and M. H. Unsworth. 1989. Deposition of atmospheric pollutants on forests. Philosophical Transactions - Royal Society of London **B 324**: 247-265.

Franceschi, E. A. 1996. The ruderal vegetation of Rosario City, Argentina. Landscape and Urban Planning **34**: 11-18.

Freer-Smith, P. H., K. P. Beckett, and G. Taylor. 2005. Deposition velocities to *Sorbus aria, Acer campestre, Populus deltoides x trichocarpa `Beaupre', Pinus nigra* and *x Cupressocyparis leylandii* for coarse, fine and ultra-fine particles in the urban environment. Environmental Pollution **133**: 157-167.

Freer-Smith, P. H., S. Holloway, and A. Goodman. 1997. The uptake of particulates by an urban woodland: Site description and particulate composition. Environmental Pollution **95**: 27-35.

Frischenbruder, M. T. M., and P. Pellegrino. 2006. Using greenways to reclaim nature in Brazilian cities. Landscape and Urban Planning **76**: 67-78.

Fuhrer, J., K. H. Erismann, H. J. Keller, and A. Favre. 1981. A system for quantitative determination of species and vitalities of urban trees on color-infrared photographs. Remote Sensing of Environment **11**: 1-8.

Fukunaga, K. 1990. Introduction to statistical pattern recognition. 2nd edition. Academic Press, Boston, MA. 591 *pages*.

GALK. 2006. Straßenbaumliste. Ständige Konferenz der Gartenamtsleiter beim Deutschen Städtetag. www.galk.de/arbeitskreise/ak_stadtbaeume/akstb_strbaumliste.htm.

Gamon, J. A., and J. S. Surfus. 1999. Assessing leaf pigment content and activity with a reflectometer. New Phytologist **143**: 105-117.

Gançarski, P., A. Blansché, and A. Wania. 2008. Comparison between two coevolutionary feature weighting algorithms in clustering. Pattern Recognition **41**: 983-994.

Gates, D. M., H. J. Keegan, V. R. Schleter, and V. R. Weidner. 1965. Spectral properties of plants. Applied Optics **4**: 11-20.

Gathright, J., Y. Yamada, and M. Morita. 2006. Comparison of the physiological and psychological benefits of tree and tower climbing. Urban Forestry & Urban Greening **5**: 141-149.

Gauthiez, B. 2003. Espace urbain: vocabulaire et morphologie. Monum, éditions du patrimoine, Paris, France. 493 *pages*.

Gayev, Y. A., and E. Savory. 1999. Influence of street obstructions on flow processes within urban canyons. Journal of Wind Engineering and Industrial Aerodynamics **82**: 89-103.

Gerdes, F., and D. Olivari. 1999. Analysis of pollutant dispersion in an urban street canyon. Journal of Wind Engineering and Industrial Aerodynamics **82**: 105-124.

Germann-Chiari, C., and K. Seeland. 2004. Are urban green spaces optimally distributed to act as places for social integration? Results of a geographical information system (GIS) approach for urban forestry research. Forest Policy and Economics **6**: 3-13.

Gilbert, O. L. 1989. The ecology of urban habitats. Chapman & Hall, London, UK. 369 *pages*.

Giordano, S., P. Adamo, S. Sorbo, and S. Vingiani. 2005. Atmospheric trace metal pollution in the Naples urban area based on results from moss and lichen bags. Environmental Pollution **136**: 431-442.

Gitelson, A., and M. N. Merzlyak. 1994. Quantitative estimation of chlorophyll-a using reflectance spectra: Experiments with autumn chestnut and maple leaves. Journal of Photochemistry and Photobiology B: Biology **22**: 247-252.

Gitelson, A. A., and M. N. Merzlyak. 2003. Spectral reflectance changes associated with autumn senescence of *Aesculus hippocastanum* L. and *Acer platanoides* L. leaves. Spectral features and relation to chlorophyll estimation. Journal of Plant Physiology **143**: 286-292.

Givoni, B. 1991. Impact of planted areas on urban environmental quality: A review. Atmospheric Environment **25B**: 289-299.

Godefroid, S. 2001. Temporal analysis of the Brussels flora as indicator for changing environmental quality. Landscape and Urban Planning **52**: 203-224.

Godefroid, S., D. Monbaliu, and N. Koedam. 2007. The role of soil and microclimatic variables in the distribution patterns of urban wasteland flora in Brussels, Belgium. Landscape and Urban Planning **80**: 45-55.

Goheen, P. G. 1970. Victorian Toronto, 1850 to 1900: pattern and process of growth. University of Chicago, Dept. of Geography, Chicago, IL. 478 *pages*.

Gomez, F., L. Gil, and J. Jabaloyes. 2004. Experimental investigation on the thermal comfort in the city: relationship with the green areas, interaction with the urban microclimate. Building and Environment **39**: 1077-1086.

Gonzalez, C. M., L. C. Orellana, S. S. Casanovas, and M. L. Pignata. 1998. Environmental conditions and chemical response of a transplanted lichen to an urban area. Journal of Environmental Management **53**: 73-81.

Grafmeyer, Y., and I. Joseph. 1979. L'école de Chicago - Naissance de l'écologie urbaine. Editions du champ urbain, Paris, France. 335 *pages*.

Grahn, P., and U. A. Stigsdotter. 2003. Landscape planning and stress. Urban Forestry & Urban Greening **2**: 1-18.

Grant, L. 1987. Diffuse and specular characteristics of leaf reflectance. Remote Sensing of Environment **22**: 309-322.

Gratani, L., and L. Varone. 2005. Daily and seasonal variation of $CO_2$ in the city of Rome in relationship with the traffic volume. Atmospheric Environment **39**: 2619-2624.

Gratani, L., and L. Varone. 2006. Carbon sequestration by *Quercus ilex* L. and *Quercus pubescens* Willd. and their contribution to decreasing air temperature in Rome. Urban Ecosystems **9**: 27-37.

Gratani, L., and L. Varone. 2007. Plant crown traits and carbon sequestration capability by *Platanus hybrida* Brot. in Rome. Landscape and Urban Planning **81**: 282-286.

Green, A. A., M. Berman, P. Switzer, and M. D. Craig. 1988. A transformation for ordering multispectral data in terms of image quality with implications for noise removal. IEEE Transactions on Geoscience and Remote Sensing **26**: 65-74.

Grime, J. P. 1979. Plant Strategies and Vegetation Processes. John Wiley & Sons, Chichester, UK. 222 *pages*.

Grime, J. P. 2002. Plant strategies, vegetation processes and ecosystem properties. 2nd edition. Wiley, Chichester, UK. 417 *pages*.

Groves, P., and P. Bajcsy. 2003. Methodology for band and classification model selection. *In: Proceedings of the* IEEE Workshop on Advances in Techniques for Analysis of Remotely Sensed Data, October 27, 2003. Washington DC.

Grünhage, L., and H.-D. Haenel. 1997. PLATIN (PLant-ATmosphere INteraction) I: a model of plant-atmosphere interaction for estimating absorbed doses of gaseous air pollutants. Environmental Pollution **98**: 37-50.

Gulyas, A., J. Unger, and A. Matzarakis. 2006. Assessment of the microclimatic and human comfort conditions in a complex urban environment: Modelling and measurements. Building and Environment **41**: 1713-1722.

Gwinner, K., and M. Schaale. 1997. A case study on the influence of shade and shading on multispectral airborne imaging data. *In: Proceedings of the* Third International Airborne Remote Sensing Conference and Exhibition. Copenhagen, Denmark.

Haala, N., and C. Brenner. 1999. Extraction of buildings and trees in urban environments. ISPRS Journal of Photogrammetry and Remote Sensing **54**: 130-137.

Haeupler, H. 1974. Statistische Auswertung von Punktrasterkarten der Gefäßplanzenflora Süd-Niedersachsens. Scripta Geobotanica **8**: 1-141.

Hannerz, U. 1983. Explorer la ville. Editions de minuit, Paris, France. 419 *pages*.

Hassan, A. A., and J. M. Crowther. 1998. Modelling of fluid flow and pollutant dispersion in a street canyon. Environmental Monitoring and Assessment **52**: 281-297.

Heisler, G. M. 1986. Effects of individual trees on the solar radiation climate of small buildings. Urban Ecology **9**: 337-359.

Hermans, C., M. Smeyers, R. M. Rodriguez, M. Eyletters, R. J. Strasser, and J.-P. Delhaye. 2003. Quality assessment of urban trees: A comparative study of physiological characterisation, airborne imaging and on site fluorescence monitoring by the OJIP-test. Journal of Plant Physiology **160**: 81-90.

Herold, M., M. E. Gardner, and D. A. Roberts. 2003. Spectral resolution requirements for mapping urban areas. IEEE Transactions on Geoscience and Remote Sensing **41**: 1907-1919.

Hill, A. C. 1971. Vegetation: a sink for atmospheric pollutants. Journal of the Air Pollution Control Association **21**: 341-346.

Hinckley, A. D. 1976. Applied ecology: a nontechnical approach. Macmillan, New York, NY. 342 *pages*.

Hoek, G., B. Brunekreef, A. Verhoeff, J. van Wijnen, and P. Fischer. 2000. Daily mortality and air pollution in the Netherlands. Journal of the Air and Waste Management Association **50**: 1380-1389.

Holton, J. R. 1992. An introduction to dynamic meteorology. 3rd edition. Academic Press, Sand Diego, CA. 511 *pages*.

Horler, D. N. H., M. Dockray, J. Barber, and A. R. Barringer. 1983. Red edge measurements for remotely sensing plant chlorophyll content. Advances in Space Research **3**: 273-277.

Hoydysh, W. G., and W. F. Dabberdt. 1988. Kinematics and dispersion characteristics of flows in asymmetric street canyons. Atmospheric Environment (1967) **22**: 2677-2689.

Huang, S.-L., and C.-W. Chen. 2005. Theory of urban energetics and mechanisms of urban development. Ecological Modelling **189**: 49-71.

Huang, S.-L., W.-C. Kao, and C.-L. Lee. 2007. Energetic mechanisms and development of an urban landscape system. Ecological Modelling **201**: 495-506.

Huete, A. R. 1988. A Soil-Adjusted Vegetation Index (SAVI). Remote Sensing of Environment **25**: 295-309.

Hughes, G. F. 1968. On the Mean Accuracy of Statistical Pattern Recognizers. IEEE Transactions on Information Theory **14**: 55-63.

Hunter, L. J., G. T. Johnson, and I. D. Watson. 1992. An investigation of three-dimensional characteristics of flow regimes within the urban canyon. Atmospheric Environment **26B**: 425-432.

ICLEI. 2006. International Council for Local Environmental Initiatives. http://www.iclei.org. *Accessed* August 2006.

Iovan, C., D. Boldo, and M. l. Cord. 2007. Automatic extraction of urban vegetation structures from high resolution imagery and digital elevation model. *In: Proceedings of the* Urban Remote Sensing Joint Event, 2007. Paris, France.

IPCC. 2007. Climate Change 2007 - The IPCC 4th Assessment Report. Intergovernmental Panel on Climate Change. www.ipcc.ch. *Accessed* August 2007.

Jackson, L. E. 2003. The relationship of urban design to human health and condition. Landscape and Urban Planning **64**: 191-200.

Jalas, J. 1955. Hemerobe und hemerochore Pflanzenarten. Ein terminologischer Reformversuch. Acta Societatis pro Fauna et Flora Fennica **72**: 1-15.

Jensen, J. R. 2000. Remote Sensing of the Environment: An earth resource perspective. Prentice Hall, Upper Saddle River, NJ. 544 *pages*.

Jo, H.-K., and G. E. McPherson. 1995. Carbon storage and flux in urban residential greenspace. Journal of Environmental Management **45**: 109-133.

Jo, H. K., and E. G. McPherson. 2001. Indirect carbon reduction by residential vegetation and planting strategies in Chicago, USA. Journal of Environmental Management **61**: 165-177.

Johnson, A. D., and H. D. Gerhold. 2003. Carbon storage by urban tree cultivars, in roots and above-ground. Urban Forestry & Urban Greening **2**: 65-72.

Johnson, G. T., and L. J. Hunter. 1995. A numerical study of dispersion of passive scalars in city canyons. Boundary-Layer Meteorology **75**: 235-262.

Johnson, G. T., and L. J. Hunter. 1999. Some insights into typical urban canyon airflows. Atmospheric Environment **33**: 3991-3999.

Johnston, M. 1997a. The development of urban forestry in the Republic of Ireland. Irish Forestry **54**: 14-32.

Johnston, M. 1997b. The early development of urban forestry in Britain: Part 1. Arboricultural Journal **21**: 107-126.

Jorgensen, E. 1970. Urban forestry in Canada. *In: Proceedings of the* 46$^{th}$ International Shade Tree Conference. University of Toronto, Faculty of Forestry, Shade Tree Research Laboratory, Toronto, Canada.

Kaplan, R., and S. Kaplan. 1989. The experience of nature: A psychological perspective. Cambridge University Press, New York. 339 *pages*.

Kaplan, S. 1995. The restorative benefits of nature: Toward an integrative framework. Journal of Environmental Psychology **15**: 169-182.

Kastner-Klein, P., E. Fedorovich, and M. W. Rotach. 2001. A wind tunnel study of organised and turbulent air motions in urban street canyons. Journal of Wind Engineering and Industrial Aerodynamics **89**: 849-861.

Kastner-Klein, P., and E. J. Plate. 1999. Wind-tunnel study of concentration fields in street canyons. Atmospheric Environment **33**: 3973-3979.

Kaufman, Y. J., and D. Tanre. 1992. Atmospherically resistant vegetation index (ARVI) for EOS-MODIS. IEEE Transactions on Geoscience and Remote Sensing **30**: 261-270.

Keiner, M. 2005. History, definition(s) and models of "sustainable development". ETH E-Collection. http://e-collection.ethbib.ethz.ch/show?type=bericht&nr=416.

Kenneweg, H. 1973. Interpretationen von Luftaufnahmen für die Erforschung und Gestaltung von Vegetationsbeständen in westdeutschen Ballungsräumen. *In: Proceedings of the* Symposium on IUFRO S 6.05 Remote Sensing including Aerial Photography. Freiburg im Breisgau, Germany.

Kent, M., R. A. Stevens, and L. Zhang. 1999. Urban plant ecology patterns and processes: a case study of the flora of the City of Plymouth, Devon, UK. Journal of Biogeography **26**: 1281-1298.

Ketzel, M., and R. Berkowicz. 2004. Modelling the fate of ultrafine particles from exhaust pipe to rural background: an analysis of time scales for dilution, coagulation and deposition. Atmospheric Environment **38**: 2639-2652.

Kieran, J. 1959. A Natural History of New York City. Houghton Mifflin, Boston, MA. 406 *pages*.

Kimes, D. S. 1983. Dynamics of directional reflectance factor distributions for vegetation canopies. Applied Optics **22**: 1364-1372.

Klaffke, K. 1995. Grün- und Freiflächen. *In:* A. f. R. u. Landesplanung (Eds.). Handwörterbuch der Raumplanung. Verlag der ARL, Hannover, Germany. pp. 443-446.

Klotz, S. 1990. Species/area and species/inhabitants relations in european cities. *In:* H. Sukopp, S. Hejný and I. Kowarik (Eds.). Urban ecology–Plants and plant communities in urban environments. SPB Academic Publishing, The Hague, Netherlands. pp. 99–103.

Klug, P., J. Engels, P. Binder, and R. Kastner. 2000. Das Fachwörterbuch für Baumpflege. 1 edition. Arbus, Steinen, Germany. 233 *pages*.

Klumpp, A., W. Ansel, G. Klumpp, P. Vergne, N. Sifakis, M. J. Sanz, S. Rasmussen, H. Ro-Poulsen, A. Ribas, J. Penuelas, H. Kambezidis, S. He, J. P. Garrec, and V. Calatayud. 2006. Ozone pollution and ozone biomonitoring in European cities Part II. Ozone-induced plant injury and its relationship with descriptors of ozone pollution. Atmospheric Environment **40**: 7437-7448.

Konijnendijk, C. C. 2003. A decade of urban forestry in Europe. Forest Policy and Economics **5**: 173-186.

Konijnendijk, C. C., K. Nilsson, T. B. Randrup, and J. Schipperijn (Eds.). 2005. Urban forests and trees, Vol. Springer, Berlin, Germany. 520 *pages*.

Konijnendijk, C. C., S. Sadio, T. B. Randrup, and J. Schipperijn. 2004. Urban and peri-urban forestry in a development context - strategy and implementation. Journal of Arboriculture **30**: 269-276.

Kowarik, I. 1988. Zum menschlichen Einfluss auf Flora und Vegetation. TU Berlin, Berlin, Germany. 280 *pages*.

Kowarik, I. 1990. Some responses of flora and vegetation to urbanization in Central Europe. *In:* H. Sukopp and S. Hejný (Eds.). Urban ecology: plants and plant communities in urban environments. SPB Publishing, The Hague, Netherlands. pp. 45-74.

Kratzer, A. 1956. Das Stadtklima. Vieweg, Braunschweig, Germany. 184 *pages*.

Kruse, F. A. 1988. Use of airborne imaging spectrometer data to map minerals associated with hydrothermally altered rocks in the northern grapevine mountains, Nevada, and California. Remote Sensing of Environment **24**: 31-51.

Kruse, F. A., A. B. Lefkoff, J. W. Boardman, K. B. Heidebrecht, A. T. Shapiro, P. J. Barloon, and A. F. H. Goetz. 1993a. The spectral image processing system (SIPS) - interactive visualization and analysis of imaging spectrometer data. Remote Sensing of Environment **44**: 145-163.

Kruse, F. A., A. B. Lefkoff, and J. B. Dietz. 1993b. Expert system-based mineral mapping in northern death valley, California/Nevada, using the Airborne Visible/Infrared Imaging Spectrometer (AVIRIS). Remote Sensing of Environment **44**: 309-336.

Kühn, I., R. Brandl, and S. Klotz. 2004. The flora of German cities is naturally species rich. Evolutionary Ecology Research **6**: 749–764.

Kühn, I., and S. Klotz. 2006. Urbanization and homogenization - Comparing the floras of urban and rural areas in Germany. Biological Conservation **127**: 292-300.

Kumar, L., K. Schmidt, S. Dury, and A. Skidmore. 2001. Imaging spectrometry and vegetation science. *In:* F. D. van der Meer and S. M. de Jong (Eds.). Imaging spectrometry: basic principles and prospective applications. Kluwer Academic Publishers, Dordrecht, Netherlands. pp. 111-156.

Künzli, N., R. Kaiser, S. Medina, M. Studnicka, O. Chanel, P. Filliger, M. Herry, J. F. Horak, V. Puybonnieux-Texier, P. Quenel, J. Schneider, R. Seethaler, J. C. Vergnaud, and H. Sommer. 2000. Public-health impact of outdoor and traffic-related air pollution: a European assessment. The Lancet **356**: 795-801.

Kuo, F. E., and W. C. Sullivan. 2001. Environment and crime in the inner city: does vegetation reduce crime? Environment and Behaviour **5**: 343-367.

Kuttler, W. 1998. Stadtklima. *In:* H. Sukopp and R. Wittig (Eds.). Stadtökologie. Fischer, Stuttgart, Germany. pp. 125-167.

Kweon, B. S., W. C. Sullivan, and A. R. Wiley. 1998. Green common spaces and the social integration of inner-city older adults. Environment and Behaviour **11**: 832-858.

Landgrebe, D. A. 1999. Information extraction principles and methods for multispectral and hyperspectral image data. *In:* C. H. Chen (Eds.). Information Processing for Remote Sensing. World Scientific, Singapore. pp. 3-38.

Landsberg, H. E. 1970. Men-made climatic changes. Science **170**: 1265-1274.

Lavorel, S., and E. Garnier. 2002. Predicting changes in community composition and ecosystem functioning from plant traits: revisiting the Holy Grail. Functional Ecology **16**: 545-556.

Le Coeur, C., J. P. Amat, L. Dorize, and E. Gautier. 2002. Elément de géographie physique. Bréal, Rosny-sous-Bois, France. 447 *pages*.

Le Gallou, F., and B. Bouchon-Meunier (Eds.). 1992. Systémique - théorie et applications, Vol. Technique et Documentation Lavoisier, Paris, France. 341 *pages*.

Lee, C. L., and D. A. Landgrebe. 1993. Feature extraction based on decision boundaries. IEEE Transactions on Pattern Analysis and Machine Intelligence **15**: 388-400.

Lennon, M., G. Mercier, and L. Hubert-Moy. 2002. Classification of hyperspectral images with nonlinear filtering and support vector machines. *In: Proceedings of the* Geoscience and Remote Sensing Symposium, IGARSS '02. Toronto, Canada.

Leopold, A. C., and P. E. Kriedemann. 1975. Plant growth and development. 2nd edition. McGraw-Hill, New York. 545 *pages*.

Leser, H. 1994. Westermann-Lexikon Ökologie und Umwelt. Westermann, Braunschweig, Germany. 667 *pages*.

Lhomme, S. 2005. Identification du bâtiment à partir d`images satellitaires à très hautes résolutions spatiales. PhD *thesis*. Université de Sherbrooke/ Université Louis-Pasteur, Sherbrooke/ Strasbourg. 258 *pages*.

Lichtenberger, E. 1998. Stadtökologie und Sozialgeographie. *In:* H. Sukopp and R. Wittig (Eds.). Stadtökologie. Fischer, Stuttgart, Germany. pp. 13-48.

Lillesand, T. M., R. W. Kiefer, and J. W. Chipman. 2004. Remote sensing and image interpretation. 5th edition. J. Wiley & Sons, New York. 763 *pages*.

Lohmeyer, A., W. Baechlin, and M. Ketzel. 2000. The Draft of the New German Guideline VDI 3782/8 to Model Automobile Exhaust Dispersion. Environmental Monitoring and Assessment **65**: 381-387.

Lombardo, M., R. M. Melati, and S. Orecchio. 2001. Assessment of the quality of the air in the city of Palermo through chemical and cell analyses on Pinus needles. Atmospheric Environment **35**: 6435-6445.

MA. 2005. Millenium Ecosystem Assessment. www.millenniumassessment.org. *Accessed* August 2007.

Maillet, L., and C. Bourgery. 1993. L'arboriculture urbaine. Institut pour le Développement Forestier, Paris, France. 318 *pages*.

Maurer, U., T. Peschel, and S. Schmitz. 2000. The flora of selected urban land-use types in Berlin and Potsdam with regard to nature conservation in cities. Landscape and Urban Planning **46**: 209-215.

McHale, M. R., E. Gregory McPherson, and I. C. Burke. 2007. The potential of urban tree plantings to be cost effective in carbon credit markets. Urban Forestry & Urban Greening **6**: 49-60.

McPherson, E. G. 2001. Sacramento's parking lot shading ordinance: environmental and economic costs of compliance. Landscape and Urban Planning **57**: 105-123.

McPherson, E. G., L. P. Herrington, and G. M. Heisler. 1988. Impacts of vegetation on residential heating and cooling. Energy and Buildings **12**: 41-51.

McPherson, E. G., D. J. Nowak, and R. A. Rowntree. 1994. Chicago's Urban Forest Ecosystem: Results of the Chicago Urban forest Climate Project. GTR-NE-186, USDA, Syracuse, NY. 201 *pages*.

McPherson, E. G., K. I. Scott, and J. R. Simpson. 1998. Estimating cost effectiveness of residential yard trees for improving air quality in Sacramento, California, using existing models. Atmospheric Environment **32**: 75-84.

McPherson, E. G., and J. R. Simpson. 2002. A comparison of municipal forest benefits and costs in Modesto and Santa Monica, California, USA. Urban Forestry & Urban Greening **1**: 61-74.

McPherson, E. G., and J. R. Simpson. 2003. Potential energy savings in buildings by an urban tree planting programme in California. Urban Forestry & Urban Greening **2**: 73-86.

Meadows, D. H., D. I. Meadows, J. Randers, and W. W. Behrens III. 1972. The limits to growth. Universe Books, New York, NY. 207 *pages*.

Meeus, J. 2000. How the Dutch city of Tilburg gets to the roots of the agricultural `kampen' landscape. Landscape and Urban Planning **48**: 177-189.

Mensink, C., F. Lefebre, L. Janssen, and J. Cornelis. 2006. A comparison of three street canyon models with measurements at an urban station in Antwerp, Belgium. Environmental Modelling & Software **21**: 514-519.

Millard, A. 2004. Indigenous and spontaneous vegetation: Their relationship to urban development in the city of Leeds, UK. Urban Forestry and Urban Greening **3**: 39-47.

Moeller, M. S., and T. Blaschke. 2006. A new index for the differentiation of vegetation fractions in urban neighborhoods based on satellite imagery. *In: Proceedings of the* ASPRS 2006 Annual Conference. Reno, Nevada.

Munzi, S., S. Ravera, and G. Caneva. 2007. Epiphytic lichens as indicators of environmental quality in Rome. Environmental Pollution **146**: 350-358.

Myeong, S., D. J. Nowak, and M. J. Duggin. 2006. A temporal analysis of urban forest carbon storage using remote sensing. Remote Sensing of Environment **101**: 277-282.

Nakamura, Y., and T. R. Oke. 1988. Wind, temperature and stability conditions in an E-W oriented urban canyon. Atmospheric Environment **22**: 2691-2700.

Newman, P. W. G. 1999. Sustainability and cities: extending the metabolism model. Landscape and Urban Planning **44**: 219-226.

Nichol, J., and M. S. Wong. 2007. Remote sensing of urban vegetation life form by spectral mixture analysis of high-resolution IKONOS satellite images. International Journal of Remote Sensing **28**: 985-1000.

Nowak, D. J. 2006. Institutionalizing urban forestry as a "biotechnology" to improve environmental quality. Urban Forestry & Urban Greening **5**: 93-100.

Nowak, D. J., K. L. Civerolo, S. Trivikrama Rao, S. Gopal, C. J. Luley, and D. E. Crane. 2000. A modeling study of the impact of urban trees on ozone. Atmospheric Environment **34**: 1601-1613.

Nowak, D. J., and D. E. Crane. 2002. Carbon storage and sequestration by urban trees in the USA. Environmental Pollution **116**: 381-389.

Nowak, D. J., D. E. Crane, and J. C. Stevens. 2006. Air pollution removal by urban trees and shrubs in the United States. Urban Forestry & Urban Greening **4**: 115-123.

Odum, E. P. 1959. Fundamentals of ecology. Press of W.B. Saunders Company, Philadelphia, PA. 546 *pages*.

Odum, H. T. 1983. Systems ecology. Wiley, New York. 644 *pages*.

OFD. 2002. Mesurer le développement durable. Un aperçu de MONET - le système suisse de monitoring. Office Fédéral de la Statistique, Neuchâtel, Switzerland. 26 *pages*.

Oguz, D. 2000. User surveys of Ankara's urban parks. Landscape and Urban Planning **52**: 165-171.

Oke, T. R. 1980. Climate Impact of Urbanization. *In: Proceedings of the* Interactions of Energy and Climate. Münster, Germany.

Oke, T. R. 1987. Boundary layer climates. Methuen, London, UK. 435 *pages*.

Oke, T. R. 1988. Street design and urban canopy layer climate. Energy and Buildings **11**: 103-113.

Oke, T. R. 1989. The micrometeorology of the urban forest. Philosophical Transactions of the Royal Society of London **B324**: 335-351.

Ould-Dada, Z., and N. M. Baghini. 2001. Resuspension of small particles from tree surfaces. Atmospheric Environment **35**: 3799-3809.

Ouma, Y. O., T. G. Ngigi, and R. Tateishi. 2006. On the optimization and selection of wavelet texture for feature extraction from high-resolution satellite imagery with application towards urban-tree delineation. International Journal of Remote Sensing **27**: 73-104.

Park, C. 2001. The Environment - principles and applications. 2nd edition. Routledge, New York. 660 *pages*.

Pauleit, S., and F. Duhme. 2000. Assessing the environmental performance of land cover types for urban planning. Landscape and Urban Planning **52**: 1-20.

Pearce, W., and C. J. Baker. 1997. Wind-tunnel investigation of the effect of vehicle motion on dispersion in urban canyons. Journal of Wind Engineering and Industrial Aerodynamics **69-71**: 915-926.

Pfeifer, T., W. Frank, W. J. Kost, and F. Droescher. 1996. Das Screening-Modell STREET. TUEV Energie und Umwelt GmbH, Filderstadt, Germany. *pages*.

Phillips, P. 2000. Real estate impacts of urban parks. Issue paper. Washington, DC. 8 *pages*.

Pickett, S. T. A., W. R. Burch, S. Dalton, T. W. Foresman, J. M. Grove, and R. A. Rowntree. 1997. A conceptual framework for the study of human ecosystems in urban areas. Urban Ecosystems **1**: 185-199.

Pickett, S. T. A., M. L. Cadenasso, J. M. Grove, C. H. Nilon, R. V. Pouyat, W. C. Zipperer, and R. Costanza. 2001. Urban ecological systems: linking terrestrial ecological, physical, and socioeconomic components of metropolitan areas. Annual review of ecology and systematics **32**: 127-157.

Portigal, F., R. Holasek, G. Mooradian, P. Owensby, M. Dickison, M. Fene, M. Elliot, E. Hall, and D. Driggett. 1997. Vegetation classification using red-edge first derivative and green peak statistical moment indices with the Advanced Airborne Hyperspectral Imaging System (AAHIS). *In: Proceedings of the* Third International Airborne Remote Sensing Conference and Exhibition. Copenhagen, Denmark.

Price, C. 2003. Quantifying the aesthetic benefits of urban forestry. Urban Forestry & Urban Greening **1**: 123-133.

Price, J. C. 1992. Variability of high resolution crop reflectance spectra. International Journal of Remote Sensing **14**: 2593-2610.

Price, J. C. 1994. How unique are spectral signatures? Remote Sensing of Environment **49**: 181-186.

Puissant, A., J. Hirsch, and C. Weber. 2003. The utility of texture analysis to improve per-pixel classification for high to very high spatial resolution imagery. International Journal of Remote Sensing **26**: 733-745.

Pyšek, P., and A. Pyšek. 1990. Comparison of vegetation and flora of West Bohemian towns. *In:* H. Sukopp and S. Hejný (Eds.). Urban ecology: plants and plant communities in urban environments. SPB Publishing, The Hague, Netherlands. pp. 105-112.

Rafailidis, S. 1997. Influence of Building Areal Density and Roof Shape on the Wind Characteristics Above a Town. Boundary-Layer Meteorology **85**: 255-271.

Randrup, T. B., C. C. Konijnendijk, M. K. Dobbertin, and R. Prüller. 2005. The concept of urban forestry in Europe. *In:* C. C. Konijnendijk, K. Nilsson, T. B. Randrup and J. Schipperijn (Eds.). Urban forests and trees. Springer, Berlin, Germany. pp. 9-21.

Rauner, J. U. L. 1976. Deciduous Forests. *In:* J. L. Monteith (Eds.). Vegetation and the atmosphere. Academic Press, London, UK. pp. 241-264.

Raunkiaer, C. 1934. The Life Forms of Plants and Statistical Plant Geography. Oxford University Press, Oxford, UK. 632 *pages*.

Rees, W. E. 1997. Urban ecosystems: the human dimension. Urban Ecosystems **1**: 63-75.

Riain, C. M. N., B. Fisher, C. J. Martin, and J. Littler. 1998. Flow Field and Pollution Dispersion in a Central London Street. Environmental Monitoring and Assessment **52**: 299-314.

Richards, J. A., and X. Jia. 1999. Remote sensing digital image analysis: An introduction. 3rd edition. Springer Verlag, Berlin, Germany. 363 *pages*.

Richardson, A. J., and C. L. Wiegand. 1977. Distinguishing vegetation from soil background information. Photogrammetric Engineering and Remote Sensing **43**: 1541-1552.

Richter, G. 1981. Handbuch Stadtgrün. BLV Verlagsgesellschaft, München, Germany. 319 *pages*.

Ricotta, C., L. Celesti Grapow, G. Avena, and C. Blasi. 2001. Topological analysis of the spatial distribution of plant species richness across the city of Rome (Italy) with the echelon approach. Landscape and Urban Planning **57**: 69-76.

Ries, K., and J. Eichhorn. 2001. Simulation of effects of vegetation on the dispersion of pollutants in street canyons. Meteorologische Zeitschrift **10**: 229-233.

Roessner, S., K. Segl, U. Heiden, and H. Kaufmann. 2001. Automated differentiation of urban surfaces based on airborne hyperspectral imagery. IEEE Transactions on Geoscience and Remote Sensing **39**: 1525-1532.

Roovers, P., B. Dumont, H. Gulinck, and M. Hermy. 2006. Recreationists' perceived obstruction of field and shrub layer vegetation. Urban Forestry & Urban Greening **4**: 47-53.

Roovers, P., M. Hermy, and H. Gulinck. 2002. Visitor profile, perceptions and expectations in forests from a gradient of increasing urbanisation in central Belgium. Landscape and Urban Planning **59**: 129-145.

Rouse, J. W., R. W. Haas, J. A. Schell, D. W. Deering, and J. C. Harlan. 1974. Monitoring the vernal advancement and retrogradation (Greenwave effect) of natural vegetation. NASA/GSFCT Type III Final Report, Greenbelt, MD. 93 *pages*.

RSI. 2004. Spectral analysis with ENVI. Research Systems Inc., Boulder, CO. 92 *pages*.

Saaroni, H., E. Ben-Dor, A. Bitan, and O. Potchter. 2000. Spatial distribution and microscale characteristics of the urban heat island in Tel-Aviv, Israel. Landscape and Urban Planning **48**: 1-18.

Sagrado, A. P. G., J. van Beeck, P. Rambaud, and D. Olivari. 2002. Numerical and experimental modelling of pollutant dispersion in a street canyon. Journal of Wind Engineering and Industrial Aerodynamics **90**: 321-339.

Samaali, M., D. Courault, M. Bruse, A. Olioso, and R. Occelli. 2007. Analysis of a 3D boundary layer model at local scale: Validation on soybean surface radiative measurements. Atmospheric Research **85**: 183-198.

Samadzadegan, F., A. Azizi, M. Hahn, and C. Lucas. 2005. Automatic 3D object recognition and reconstruction based on neuro-fuzzy modelling. ISPRS Journal of Photogrammetry and Remote Sensing **59**: 255-277.

Sampson, R. J., S. W. Raudenbush, and F. Earls. 1997. Neighbourhoods and violent crime. Science **277**: 918-924.

Sanders, R. A. 1986. Urban vegetation impacts on the hydrology of Dayton, Ohio. Urban Ecology **9**: 361-376.

Sandström, U. G. 2002. Green infrastructure planning in urban Sweden. Planning Practice and Research **17**: 373-385.

Sandström, U. G., P. Angelstam, and A. Khakee. 2006a. Urban comprehensive planning - identifying barriers for the maintenance of functional habitat networks. Landscape and Urban Planning **75**: 43-57.

Sandström, U. G., P. Angelstam, and G. Mikusinski. 2006b. Ecological diversity of birds in relation to the structure of urban green space. Landscape and Urban Planning **77**: 39-53.

Sanesi, G., and F. Chiarello. 2006. Residents and urban green spaces: The case of Bari. Urban Forestry and Urban Greening **4**: 125-134.

Sanger, J. E. 1971. Quantitative investigation of leaf pigments from their interception in buds through autumn coloration to decomposition in falling leaves. Ecology **52**: 1075-1089.

Savard, J.-P. L., P. Clergeau, and G. Mennechez. 2000. Biodiversity concepts and urban ecosystems. Landscape and Urban Planning **48**: 131-142.

Schmidt, K. S., and A. K. Skidmore. 2003. Spectral discrimination of vegetation types in a coastal wetland. Remote Sensing of Environment **85**: 92-108.

Schulte, G. 1995. Der naturwissenschaftliche Zugang zur Stadtökologie. *In:* E.-H. Ritter (Eds.). Zeitschrift für Angewandte Umweltforschung, Sonderheft 6. Analytica, Berlin. pp. 25-31.

Schwartz, M. W., J. H. Thorne, and J. H. Viers. 2006. Biotic homogenization of the California flora in urban and urbanizing regions. Biological Conservation **127**: 282-291.

SDUD. 2007. Berlin Digital Environmental Atlas, Senate Department for Urban Development, Berlin, Germany. www.stadtentwicklung.berlin.de/umwelt/umweltatlas. *Accessed* August 2007.

Segl, K., S. Roessner, U. Heiden, and H. Kaufmann. 2003. Fusion of spectral and shape features for identification of urban surface cover types using reflective and thermal hyperspectral data. ISPRS Journal of Photogrammetry and Remote Sensing **58**: 99-112.

Seinfeld, J. H., and S. N. Pandis. 2006. Atmospheric chemistry and physics: From air pollution to climate change. 2nd edition. Wiley, Hoboken, NJ. 1203 *pages*.

Serpico, S. B., and L. Bruzzone. 2001. A new search algorithm for feature selection in hyperspectral remote sensing images. IEEE Transactions on Geoscience and Remote Sensing **39**: 1360-1367.

Shafer, C. S., B. K. Lee, and S. Turner. 2000. A tale of three greenway trails: user perceptions related to quality of life. Landscape and Urban Planning **49**: 163-178.

Shashua-Bar, L., and M. E. Hoffman. 2000. Vegetation as a climatic component in the design of an urban street: An empirical model for predicting the cooling effect of urban green areas with trees. Energy and Buildings **31**: 221-235.

Shashua-Bar, L., and M. E. Hoffman. 2003. Geometry and orientation aspects in passive cooling of canyon streets with trees. Energy and Buildings **35**: 61-68.

Shippert, P. 2003. Introduction to hyperspectral image analysis. Online Journal of Space Communication, Vol. 3. http://satjournal.tcom.ohiou.edu/pdf/shippert.pdf.

Sieghardt, M., E. Mursch-Radlgruber, E. Paoletti, E. Couenberg, A. Dimitrakopoulus, F. Rego, A. Hatzistathis, and T. B. Randrup. 2005. The abiotic environment: impact of urban growing conditions on urban vegetation. *In:* C. C. Konijnendijk, K. Nilsson, T. B. Randrup and J. Schipperijn (Eds.). Urban forests and trees. Springer, Berlin, Germany. pp. 281-323.

Simpson, J. R., and E. G. McPherson. 1998. Simulation of tree shade impacts on residential energy use for space conditioning in Sacramento. Atmospheric Environment **32**: 69-74.

Sims, D. A., and J. A. Gamon. 2002. Relationships between leaf pigment content and spectral reflectance across a wide range of species, leaf structures and developmental stages. Remote Sensing of Environment **81**: 337-354.

Sitte, P., E. W. Weiler, J. W. Kadereit, A. Bresinsky, and C. Körner. 2002. Strasburger - Lehrbuch der Botanik. 35 edition. Spektrum Akademischer Verlag, Heidelberg, Berlin, Germany. 1123 *pages*.

Small, C. 2001. Estimation of urban vegetation abundance by spectral mixture analysis. International Journal of Remote Sensing **22**: 1305-1334.

Small, C. 2003. High spatial resolution spectral mixture analysis of urban reflectance. Remote Sensing of Environment **88**: 170-186.

Smardon, R. C. 1988. Perception and aesthetics of the urban environment: Review of the role of vegetation. Landscape and Urban Planning **15**: 85-106.

Snep, R. P. H., P. F. M. Opdam, J. M. Baveco, M. F. WallisDeVries, W. Timmermans, R. G. M. Kwak, and V. Kuypers. 2006. How peri-urban areas can strengthen animal populations within cities: A modeling approach Biological Conservation **127**: 345-355.

Song, C. 2005. Spectral mixture analysis for subpixel vegetation fractions in the urban environment: How to incorporate endmember variability? Remote Sensing of Environment **95**: 248-263.

Söyrinki, N. 1991. On the alien flora of the province of Buenos Aires, Argentina. Annales botanici Fennici **28**: 59-79.

Stabler, L. B., C. A. Martin, and A. J. Brazel. 2005. Microclimates in a desert city were related to land use and vegetation index. Urban Forestry and Urban Greening **3**: 137-147.

Stanners, D., and P. Bourdeau. 1995. Europe's Environment: The Dobris assessment. European Environmental Agency, Copenhagen, Denmark. 676 *pages*.

Straub, B. M., and C. Heipke. 2001. Automatic extraction of trees for 3D city models from images and height data. *In: Proceedings of the* Automatic extraction of man-made objects from aerial and space images, third workshop. Ascona, Switzerland.

Strauss, B., and R. Biedermann. 2005. The use of habitat models in conservation of rare and endangered leafhopper species (Hemiptera, Auchenorrhyncha). Journal of Insect Conservation **9**: 245-259.

Stülpnagel, A., M. Horbert, and H. Sukopp. 1990. The importance of vegetation for the urban climate *In:* H. Sukopp and S. Hejný (Eds.). Urban ecology - Plants and plant communities in urban environments. SPB Publishing, The Hague, Netherlands. pp. 175-193.

Sugumaran, R., M. K. Pavuluri, and D. Zerr. 2003. The use of high-resolution imagery for identification of urban climax forest species using traditional and rule-based classification approach. IEEE Transactions on Geoscience and Remote Sensing **41**: 1933-1939.

Sukopp, H. 1976. Dynamik und Konstanz in der Flora der Bundesrepublik Deutschland. Schriftenreihe für Vegetationskunde **10**: 9-27.

Sukopp, H. 1990. Urban ecology and its application in Europe. *In:* H. Sukopp and S. Hejný (Eds.). Urban ecology - Plants and plant communities in urban environments. SPB Publishing, The Hague, Netherlands. pp. 1-22.

Sukopp, H. 1998. Urban Ecology - Scientific and Pratical Aspects. *In:* J. Breuste, H. Feldmann and O. Uhlmann (Eds.). Urban Ecology. Springer, Berlin, Germany. pp. 3-17.

Sukopp, H. 2004. Human-caused impact on preserved vegetation. Landscape and Urban Planning **68**: 347-355.

Sukopp, H., and P. Werner. 1983. Urban environments and vegetation. *In:* W. Holzner, M. J. A. Werger and I. Ikusima (Eds.). Man's impact on vegetation. Junk, The Hague, Netherlands. pp. 13.

Sukopp, H., and R. Wittig. 1998. Stadtökologie. 2nd edition. Fischer, Stuttgart, Germany. 474 *pages*.

Swain, P. H., and S. M. Davis. 1978. Remote sensing: the quantitative approach. McGraw-Hill, New York, NY. 396 *pages*.

Taha, H. 1996. Modeling impacts of increased urban vegetation on ozone air quality in the South Coast Air Basin. Atmospheric Environment **30**: 3423-3430.

Taha, H., S. Douglas, and J. Haney. 1997. Mesoscale meteorological and air quality impacts of increased urban albedo and vegetation. Energy and Buildings **25**: 169-177.

Takashi, N., T. Guo, and Y. Yoshifumi. 2002. Simulated recovery of information in shadow areas on IKONOS image by combining ALS data. *In: Proceedings of the* GIS development.

Tapia Silva, F. O., A. Wehrmann, H.-J. Henze, and N. Model. 2006. Ability of plant-based surface technology to improve urban water cycle and mesoclimate. Urban Forestry & Urban Greening **4**: 145-158.

Tarvainen, O., A. M. Markkola, and R. Strommer. 2003. Diversity of macrofungi and plants in Scots pine forests along an urban pollution gradient. Basic and Applied Ecology **4**: 547-556.

Taylor, G. R., A. H. Mah, F. A. Kruse, K. S. Kierein-Young, R. D. Hewson, and B. A. Bennett. 1996. Characterization of saline soils using airborne radar imagery. Remote Sensing of Environment **57**: 127-142.

Tello, M. L., M. Tomalak, R. Siwecki, J. Gáper, E. Motta, and E. Mateo-Sagasta. 2005. Biotic urban growing conditions - threats, pests and diseases. *In:* C. C. Konijnendijk, K. Nilsson, T. B. Randrup and J. Schipperijn (Eds.). Urban forests and trees. Springer, Berlin, Germany. pp. 325-365.

Thomas, N., and M. Lennon. 2005. Mission de télédétection hyperspectrale aéroportée CASI sur la ville de Strasbourg, Final Report. Actimar, Brest, France. 46 *pages*.

Thönnessen, M. 2002. Elementdynamik in Fassadenbegrünendem Wein (Parthenocissus tricuspidata) – Nährelemente, anorganische Schadstoffe, Platin-Gruppen-Elemente, Filterleistung, immissionshistorische Aspekte, Methodische Neu- & Weiterentwicklungen. Kölner Geographische Arbeiten **78**, 136 *pages*.

Timms, D. W. G. 1971. The urban mosaic - towards a theory of residential differentiation. Cambridge University Press, Cambridge, UK. 277 *pages*.

Tjallingii, S. 2002. Green and red: enemies or allies? The Utrecht experience with green structure planning. Built Environment **29**: 107-116.

Todorova, A., S. Asakawa, and T. Aikoh. 2004. Preferences for and attitudes towards street flowers and trees in Sapporo, Japan. Landscape and Urban Planning **69**: 403-416.

Tomášek, W. 1979. Die Stadt als Ökosystem - Überlegungen zum Vorentwurf Landschaftsplan Köln (The town as ecological system - thoughts to the concept of the landscape plan Cologne). Landschaft und Stadt **11**: 51-60.

Trepl, L. 1990. Research on the anthropogenic migration of plants and naturalisation. *In:* H. Sukopp and S. Hejný (Eds.). Urban ecology: plants and plant communities in urban environments. SPB Publishing, The Hague, Netherlands. pp. 75-99.

Tyrväinen, L. 1997. The amenity value of the urban forest: an application of the hedonic pricing method. Landscape and Urban Planning **37**: 211-222.

Tyrväinen, L. 2001. Economic valuation of urban forest benefits in Finland. Journal of Environmental Management **62**: 75-92.

Tyrväinen, L., and A. Miettinen. 2000. Property Prices and Urban Forest Amenities. Journal of Environmental Economics and Management **39**: 205-223.

Tyrväinen, L., S. Pauleit, K. Seeland, and S. de Vries. 2005. Benefits and uses of urban forests and trees. *In:* C. C. Konijnendijk, K. Nilsson, T. B. Randrup and J. Schipperijn (Eds.). Urban forests and trees. Springer, Berlin, Germany. pp. 81-114.

Tzilkowski, W. M., J. S. Wakeley, and L. J. Morris. 1986. Relative use of municipal street trees by birds during summer in state college, Pennsylvania. Urban Ecology **9**: 387-398.

Tzoulas, K., K. Korpela, S. Venn, V. Yli-Pelkonen, A. Kazmierczak, J. Niemela, and P. James. 2007. Promoting ecosystem and human health in urban areas using Green Infrastructure: A literature review. Landscape and Urban Planning **81**: 167-178.

Ulrich, R. S. 1984. View through a window may influence recovery from surgery. Science **224**: 420-421.

Ulrich, R. S., R. F. Simons, B. D. Losito, E. Fiorito, M. A. Miles, and M. Zelson. 1991. Stress recovery during exposure to natural and urban environments. Journal of Environmental Psychology **11**: 201-230.

UN. 1992. Agenda 21. United Nations Department of Economic and Social Affairs, Division for Sustainable Development. www.un.org/esa/sustdev/documents/agenda21/english/agenda21toc.htm. *Accessed* August 2007.

UN. 2006. World Population Prospects: The 2006 Revision Population Database. United Nations Population Division. http://esa.un.org/unpp/. *Accessed* July 2007.

UN. 2007a. Human Settlements Programme UN-Habitat. United Nations. www.unhabitat.org. *Accessed* July 2007.

UN. 2007b. The millenium development goals report. United Nations. www.un.org/millenniumgoals/. *Accessed* August 2007.

Underwood, E., S. Ustin, and D. Dipietro. 2003. Mapping nonnative plants using hyperspectral imagery. Remote Sensing of Environment **86**: 150-161.

UNEP. 2007. http://www.unep.org. United Nations Environment Programme. *Accessed* July 2007.

UNFPA. 2007. State of world population 2007 - Unleashing the potential of urban growth. United Nations Population Fund. http://www.unfpa.org/upload/lib_pub_file/695_filename_sowp2007_eng.pdf. *Accessed* August 2007.

Van de Garde, H. J. J. 1976. Present application of false colour photography in Holland. *In: Proceedings of the* Practical Application of Remote sensing, summer school. Alpbach/ Tyrol, Austria.

Van der Meer, F. 1996. Metamorphic facies zonation in the Ronda peridotites mapped from GER imaging spectrometer data. International Journal of Remote Sensing **17**: 1633-1657.

Van der Meer, F. D., S. De Jong, and S. M. Bakker. 2001. Imaging spectrometry: Basic analytical techniques. *In:* F. D. Van der Meer and S. De Jong (Eds.). Imaging spectrometry: Basic principles and prospective applications. Kluwer Academic Publishers, Dordrecht. pp. 17-61.

Van Herzele, A., and T. Wiedemann. 2003. A monitoring tool for the provision of accessible and attractive urban green spaces. Landscape and Urban Planning **63**: 109-126.

Vardoulakis, S., B. E. A. Fisher, K. Pericleous, and N. Gonzalez-Flesca. 2003. Modelling air quality in street canyons: A review. Atmospheric Environment **37**: 155-182.

Vicari, J. 1981. Agir sur la ville. Editions du Moniteur, Paris, France. 279 *pages*.

Villarreal, E. L., A. Semadeni-Davies, and L. Bengtsson. 2004. Inner city stormwater control using a combination of best management practices. Ecological Engineering **22**: 279-298.

Von Haaren, C., and M. Reich. 2006. The german way to greenways and habitat networks. Landscape and Urban Planning **76**: 7-22.

Walker, C. 2004. Beyond recreation: A broader view of urban parks. The Urban Institute, Washington, DC. 7 *pages*.

Walmsley, A. 1995. Greenways and the making of urban form. Landscape and Urban Planning **33**: 81-127.

Wania, A., I. Kühn, and S. Klotz. 2006a. Plant richness patterns in agricultural and urban landscapes in Central Germany - spatial gradients of species richness. Landscape and Urban Planning **75**: 97-110.

Wania, A., D. Nafaa, J. Hirsch, and C. Weber. 2006b. Analysing spectral characteristics of urban objects. *In: Proceedings of the* International Conference on Spatial Analysis and GEOmatics SAGEO, 11-13 September 2006, Strasbourg, France.

Wania, A., and C. Weber. 2007. Hyperspectral imagery and urban green observation. *In: Proceedings of the* Urban Remote Sensing Joint Event, 11-13 April 2007, Paris, France.

Warner, T. A., and M. C. Shank. 1997. Spatial autocorrelation analysis of hyperspectral imagery for feature selection. Remote Sensing of Environment **60**: 58-70.

WCED. 1987. Our common future. World Commission on Environment and Development. 374 *pages*.

Weber, C. 1997. Système urbain et informations multisources. State doctorate *thesis*. Université Louis Pasteur, Strasbourg, France. 147 *pages*.

Werquin, A. C., B. Duhem, G. Lindholm, B. Oppermann, S. Pauleit, and S. Tjallingii. 2005. Green structure and urban planning, final report COST Action C11. European Commission, Brussels, Belgium. 440 *pages*.

Whitney, G. G. 1985. A quantitative analysis of the flora and plant communities of a representative midwestern U.S. town. Urban Ecology **9**: 143-160.

WHO. 2007. The urban environment. World Health Organisation. www.who.int/heli/risks/urban/urbanenv. *Accessed* September 2007.

Wittig, R. 1996. Die mitteleuropäische Großstadtflora. Geographische Rundschau **48**: 640-646.

Wittig, R. 1998. Flora und Vegetation. *In:* H. Sukopp and R. Wittig (Eds.). Stadtökologie. Fischer, Stuttgart, Germany. pp. 219-265.

Wittig, R., and H. Sukopp. 1998. Was ist Stadtökologie? *In:* H. Sukopp and R. Wittig (Eds.). Stadtökologie. Fischer, Stuttgart, Germany. pp. 1-12.

Wolman, A. 1965. The metabolism of cities. Scientific American **213**: 179-190.

Wolterbeek, B. 2002. Biomonitoring of trace element air pollution: principles, possibilities and perspectives. Environmental Pollution **120**: 11-21.

Xiao, Q., and E. G. McPherson. 2002. Rainfall interception by Santa Monica's municipal urban forest. Urban ecosystems **6**: 291-302.

Xiao, Q., S. L. Ustin, and E. G. McPherson. 2004. Using AVIRIS data and multiple-masking techniques to map urban forest tree species. International Journal of Remote Sensing **25**: 5637-5654.

Yang, J., J. McBride, J. Zhou, and Z. Sun. 2005. The urban forest in Beijing and its role in air pollution reduction. Urban Forestry & Urban Greening **3**: 65-78.

Zhang, Y., Z. Yang, and W. Li. 2006a. Analyses of urban ecosystem based on information entropy. Ecological Modelling **197**: 1-12.

Zhang, Y., Z. Yang, and X. Yu. 2006b. Measurement and evaluation of interactions in complex urban ecosystem. Ecological Modelling **196**: 77-89.

# GLOSSARY OF TERMS

**Archaeophytes:** Archaeophytes (plants) are ancient immigrants that reached central Europe before 1500 usually due to agriculture.

**Azimut:** Solar azimuth is the horizontal direction of the Sun above the horizon (usually true north) expressed in degrees.

**Biotope**: The living space of plants and animals with uniform living conditions determining the function of the biosystem. It is considered as the spatial unit of the biosystem.

**Biocoenosis:** describes all the interacting organisms living together in a specific habitat (or biotope).

**Boundary layer:** A boundary layer is defined as the layer of fluid (liquid or gas) in the immediate vicinity of a material surface in which significant exchange of momentum, heat, or mass takes place between the surface and the fluid. Sharp variations in the properties of the flow, such as velocity, temperature, and mass concentration, also occur in the boundary layer. The atmospheric or **planetary boundary layer** (PBL) is formed as a consequence of the interactions between the atmosphere and the underlying surface (land or water). The height of the PBL depends on the rate of surface cooling and heating. With continuous heating of the surface during the day the depth of the PBL increases resulting in thermal mixing. Cooling of surfaces during the night suppresses mixing and the PBL is consequently shrinking.

**Cavity:** The cavity is a zone of recirculating flow occuring in the case of flow separation induced when a viscous flow meets a bluff body. The primary cause of flow separation is a loss of mean kinetic energy in the boundary layer of any surface. It is characterised by low speeds but large wind shears and high-turbulence intensities. Buildings are 'surrounded' by a three-dimensional cavity (flow separation from the roof and building sides). Dimensions of a cavity envelope of a building depend on the width-to-height and length-to-height ratios of the buildings and the characteristics of the approach flow.

**Canopy:** In this study, the term is used either to describe the urban canopy or the vegetation canopy. In both cases it describes the whole of objects (e.g. a forest canopy is the whole of a forest).

**Classification accuracy:** It is the averaged percentage of correct classifications used to asses the accuracy of a classification. It is determined empirically, by selecting a sample of pixels from the thematic map (or classified image) and checking their labels against classes determined from reference or ground truth data (training samples). **User accuracy** is the probability that a ground truth class is B given that the pixel has been labelled B (on the thematic image) by the classifier. In contrast, the **Producer's accuracy** is the probability that the classifier has labelled the image pixel as B given that the ground truth class is B.

**Confusion matrix:** Also called error or contingency matrix. Is the most common means of expressing classification accuracy comparing, on a category-by-category basis, the relationship between known reference data (ground truth) and the corresponding results of an automated classification (square matrix).

**Diffusion:** The exchange of fluid parcels between regions in space by apparently random motions on a very small (usually molecular) scale.

**Ecosystem services:** Benefits from a multitude of resources and processes that are supplied by natural ecosystems are considered as ecosystem services. They include products like clean drinking water and processes like the decomposition if waste. Services can be subdivided into five categories: **provisioning** such as the production of food and water; **regulating**, such as the control of climate and disease; **supporting**, such as nutrient cycles and crop pollination; **cultural**, such as spiritual and recreational benefits; and **preserving**, which includes guarding against uncertainty through the maintenance of diversity.

**Eddies** are parcels of air that transport energy and mass from one location to another.

**Endmember:** They are defined as spectrally "pure" features (e.g. vegetation, soil, etc.). Pure spectral endmembers are usually defined under idealized in situ or laboratory conditions where reflectance spectra are acquired using a portable spectroradiometer focussed only on a single surface (e.g. a single leaf from a maple tree). When in situ measurements are not possible, spectral endmembers can also be derived from "pure" features in the imagery

**Energy balance:** The energy balance at an ideal surface assuming to have no mass and heat capacity, is described as $R_N=H+H_L+H_G$ where $R_N$ is the net radiation, H and $H_L$ the sensible and latent heat fluxes to or from the air, and $H_G$ the ground heat flux to or from the submedium (e.g. the soil). During the day, the surface receives radiative energy ($R_N >0$), which is partitioned into sensible and latent heat fluxes to the atmosphere and the heat flux to the submedium (H, $H_L$, $H_G$ are positive). At night, the surface losses energy by outgoing radiation that is compensated by gains of heat from the air and the soil, and from the latent heat of condensation released during dew formation.

**Evaporation:** The process by which a liquid is transformed into a gas, in the atmosphere usually water changing to water vapour.

**Evapotranspiration**: The combined loss of water to the atmosphere by evaporation and transpiration.

**Flux:** rate of flow of some quantity.

**Inversion:** A departure from the usual decrease of increase with height of an atmospheric property. Most commonly refers to a temperature inversion when temperatures increase. Inversions represent important layers in the atmosphere suppressing the mixing of air in the layer below. Inversions might be due to warming (induced by sinking air masses) or cooling (induced by surface cooling).

**Irradiation:** Total radiant flux received by unit area of a given surface.

**Kappa:** An indicator used to assess the accuracy of a classification. Used to asses the extent to which the percentage correct values of a confusion matrix are due to true agreements (approaching 1) or ‘chance’ agreements (approaching 0).

**Latent heat:** Latent heat is the heat which is not sensed as a temperature heat. It is the heat required to enable a substance to change from liquid at a given temperature to vapour at the same temperature.

**Leaf area density:** The area of leaves per volume unit ($m^2/m^3$).

**Long-wave radiation:** Radiation observed in the range 3.0-100 µm (radiant wavelengths of the Earth-Atmosphere system).

**Momentum:** That property of a particle which is given by the product of its mass with its velocity.

**Multispectral images:** Remotely sensed images characterised by several spectral bands, e.g. Landsat TM, Quickbird, Ikonos. In contrast to hyperspectral images that have many narrow bands, these images are defined by few and broad bands (large bands, low spectral resolution).

**Nature:** The word is derived from the latin word ‘nasci’ that means to be born, emerge from itself without foreign action. Accordingly, as nature are considered all phenomena and processes emerging without the influence of humans.

**Neophytes:** Neophytes are plants that arrived after 1500 with the discovery of the Americas and the expansion of trade.

**Potential temperature:** The temperature a parcel of dry air would have if brought adiabatically from its present position to standard pressure of 100 kPa.

**Radiation:** The process by which electromagnetic radiation is propagated through free space by virtue of joint undulatory variations in the electric and magnetic fields in space.

**Reflection:** Reflection is the physical process where an incident ray of light or wave is reflected back into the medium due to interaction on an interface. The reflected energy is equal to the incident energy reduced by the energy that is either absorbed or transmitted.

**Ruderal:** A ruderal species is a plant species that is first to colonise disturbed lands. The disturbance may be natural (e.g. wildfires or avalanches), or man-made - constructional (e.g. road construction, building construction or mining), or agricultural (e.g. abandoned farming fields or abandoned irrigation ditches).

**Run-off:** The water, derived from precipitation, that ultimately reaches stream channels.

**Scattering:** The process by which small particles suspended in a medium of a different index of refraction diffuse a portion of the incident radiation in all directions.

**Scavenging:** The sweeping out of airborne particles by rain or snow.

**Sensible heat:** Sensible heat is when the addition or subtraction of energy to a body is sensed as a rise or fall in its temperature. Used in contrast to latent heat.

**Short-wave radiation:** Radiation in the range 0.15-3.0 µm, also termed solar radiation.

**Test samples:** A sample of pixels additionally defined to assess classification accuracy and evaluate the performance of a classifier. In contrast to training samples it serves not for the classification.

**Therophytes:** A plant which survives unfavourable seasons in the form of seeds, and completes its life-cycle during favourable seasons. Annual species are therophytes.

**Total suspended particles** (TSP) is the term generally used for describing suspended particles that range in size from a few nanometers (nm) to tens of micrometers (μm) in diameter.

**Training set:** A sample of pixels used to train a supervised classifier and to test classification accuracy.

**Transpiration:** The process by which water in plants is transferred as water vapour to the atmosphere.

**Troposphere:** The lowest 10-20 km of the atmosphere, characterised by decreasing temperature with height, appreciable water vapour and vertical motion, and weather.

**Turbulence:** A turbulence is a characteristic of flows in general. Turbulent flows are irregular and random. The velocity components vary at any location randomly with time.

**Wake:** The wake of a building is the region of flow immediately surrounding and following the main recirculation cavity (or recirculating zone). All bluff and streamline bodies have wakes. Some may have recirculating cavity in their lee (lee-side cavity region or wake cavity).

**Zenith:** That point in the sphere surrounding an observer that lies directly above him.

# ABBREVIATIONS

| | |
|---|---|
| ARVI | Atmospherically Resistant Vegetation Index |
| ASPA | Association pour la Surveillance et l'Etude de la Pollution Atmosphérique en Alsace |
| AVIRIS | Airborne Visible Infrared Imaging Spectrometer |
| BRDF | bidirectional reflectance distribution function |
| CASI | Compact Airborne Spectrographic Imager |
| CFD | Computational Fluid Dynamics |
| CIR | colour infrared |
| DAFE | Discriminant Analysis Feature Extraction |
| DBFE | Decision Boundary Feature Extraction |
| FWHM | full width half mean |
| GIS | Geographic Information System |
| IGN | Institut Géographique National |
| LAD | leaf area density |
| LAI | leaf area index |
| MACLAW | Modular Approach for Clustering with Local Attribute Weighting |
| mNDVI | Modified Red Edge Normalized Difference Vegetation Index |
| ML | Maximum Likelihood |
| MNF | Minimum Noise Fraction |
| MS | multispectral |
| NDVI | Normalized Difference Vegetation Index |
| NIR | near infrared |
| PAN | peroxyacetyl nitrate |
| PBL | Planetary Boundary Layer |
| PC | principal component |
| $PM_{10}$ | particulate matter with a diameter < 10µm |
| RAD | root area density |
| SAM | Spectral Angle Mapper |
| SAVI | Soil Adjusted Vegetation Index |
| SLRA | Soil Line Resistant to Atmospheric |
| SVAT | soil-vegetation-atmosphere-transfer |
| TSAVI | Transformed Soil Adjusted Vegetation Index |
| TSARVI | Transformed Soil Atmospherically Resistant Vegetation Index |
| UBL | Urban Boundary Layer |
| UFP | ultra-fine particles |
| VOC | volatile organic compounds |

# EXTENDED SUMMARY IN FRENCH / RÉSUMÉ EN FRANÇAIS

**Titre de la thèse** : Urban vegetation – detection and function evaluation for air quality assessment

**Nom du candidat** : Annett Wania

Le contexte général de la thèse est la végétation en ville et son rôle pour la qualité de vie. La végétation est considérée comme un élément de l'écosystème urbain ayant des fonctions sociales, psychologiques et écologiques. Elle est ainsi reconnue comme un élément capable de compenser en partie les effets de l'urbanisation et en conséquence reconnue dans les politiques d'aménagement des villes. Cette reconnaissance se conjugue plus au moins aisément à travers les contraintes du développement des systèmes urbains. De plus, l'analyse des pratiques de planification montre que les choix sur les caractéristiques et la localisation de la végétation sont avant tout influencés par des critères esthétiques et le simple argument de la présence de végétation dans l'espace public. Ainsi, on remarque une quasi absence d'un questionnement permettant d'évaluer la fonctionnalité de la végétation à un lieu donné. Idéalement, cette fonctionnalité devrait tenir compte des différentes fonctions, non seulement la fonction psychologique ou sociale mais aussi des fonctions écologiques. Or il semble d'autant plus nécessaire d'optimiser l'intégration de cet élément urbain dans l'aménagement de l'espace urbain. Les fonctions écologiques sont complexes mais importantes pour la compréhension des interactions entre les éléments du système. Elles sont difficiles à étudier dans l'ensemble. C'est pourquoi dans la thèse on s'est appliqué à étudier l'influence de la végétation sur la qualité de l'air et plus particulièrement sur la rétention des particules émises par le trafic. Pour réaliser ces travaux deux étapes ont été identifiées : (1) la caractérisation de la végétation et (2) la modélisation de l'impact de la rétention dans différentes configurations de bâti.

La thèse s'organise en trois parties. La première présente le cadre général du travail exposé c'est-à-dire la qualité de vie en milieu urbain dans une logique de développement durable. Elle positionne l'intérêt de la végétation urbaine dans ce contexte. La seconde partie se focalise sur les moyens disponibles de localiser et d'identifier la végétation urbaine en s'appuyant sur des images satellites peu utilisées jusqu'à présent dans ce contexte. Enfin, la dernière partie développe une modélisation micro-climatique permettant de réfléchir sur le lien existant entre végétation et polluants atmosphériques dans une optique d'aménagement urbain.

# PARTIE I : CADRE THEORIQUE

## Chapitre 1 : Développement durable et villes

La population dans les villes du monde augmente de manière continue et, en 2008, plus de la moitié de la population mondiale vivra en milieu urbain (UNFPA 2007). Parallèlement, les villes concentrent la plupart des problèmes environnementaux : forte pollution de l'air, des eaux, des sols, disparition de la biodiversité, etc. Paradoxalement, les villes présentent en même temps la meilleure chance d'assurer un futur durable, car elles concentrent plus de la moitié de la population sur une surface terrestre très réduite. La question de la qualité de vie se pose particulièrement en ville et le concept de développement durable propose un cadre d’action politique qui réfère directement aux questions de la qualité de vie. Le concept réclame une action sociétale et politique couvrant la satisfaction des besoins de chacun sans compromettre ceux des générations futures (WCED 1987). Dans ce contexte, l’environnement urbain fait sens pour de nombreuses actions politiques et la réflexion sur la forme urbaine (compacte ou éclatée) et les éléments urbains cohérents continue.

Dans ce contexte, la végétation en ville est reconnue comme un élément urbain capable de compenser en partie les effets négatifs d’une urbanisation dynamique. Elle est d’ailleurs considérée comme étant un élément clé de la qualité de vie en milieu urbain. Sa valeur dans les approches et développements scientifiques et opérationnels est visible par sa prise en compte dans les systèmes d’indicateurs de développement durable urbain et les nombreux projets de recherches à l’échelle européenne. Cette thèse contribue à la réflexion en se focalisant plus particulièrement sur l’évaluation des fonctions de la végétation en milieu urbain.

## Chapitre 2 : La végétation – un élément de l’écosystème urbain

### L’écosystème urbain

Pour pouvoir évaluer les différentes fonctions de la végétation, nous nous sommes appuyé sur le concept d’écosystème. Ce concept considère une unité comme étant l’ensemble des organismes vivants, leurs relations entre eux ainsi qu’avec leur environnement inorganique. Nous avons défini l’écosystème urbain comme étant l’ensemble des éléments biotiques, abiotiques et des éléments crées par l’homme que nous avons appelés techniques. La figure 1 montre les trois groupes d’éléments liés par des interactions.

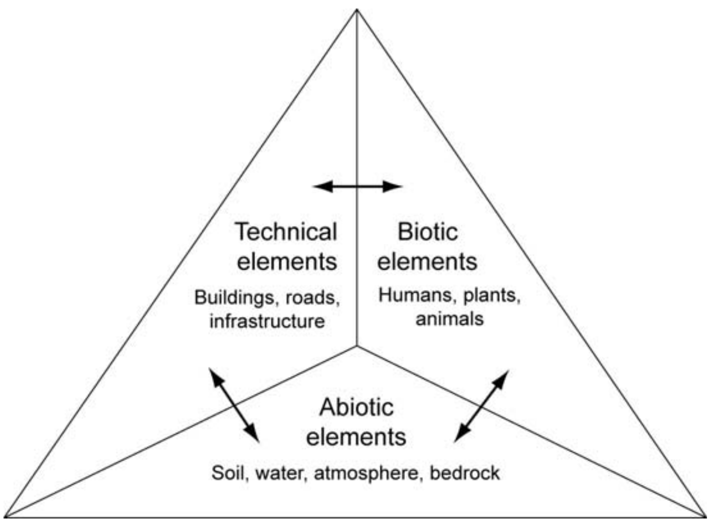


*Figure 1 : L’écosystème urbain d’après Tomášek (1979). L’écosystème urbain est composé d’éléments biotiques et abiotiques ainsi que des éléments techniques qui sont créés par l’homme. Les éléments sont liés par des interactions (flèches).*

Pour une compréhension écologique (dans le sens des sciences dures), il est impossible de délimiter le système urbain basé uniquement sur des chiffres de population (Pickett *et al.* 2001). De manière générale, on considère la ville-même, ses banlieues ou quartiers moins densément peuplés, les corridors les reliant mais aussi l’ensemble des espaces associés à la ville par des fonctions diverses (approvisionnement, aménités, interdépendance, etc.), les 'hinterland'. L'écosystème urbain est donc un système complexe qui ne peut pas être décrit de la même manière que les écosystèmes 'naturels'[39] mais dont il est possible de s'inspirer (Douglas 2002). Le métabolisme urbain, comme pour tout organisme, défini par la consommation d'énergie et de substances, est principalement induit par l'être humain. C'est l'acteur principal de ce système. S'ajoutent au métabolisme des éléments abiotiques et biotiques qui sont intégrés dans le système où l'homme a une prépondérance en tant que 'consommateur'. Contrairement aux écosystèmes naturels, l'équilibre dynamique dans ce cas ne peut être maintenu que par un supplément d'énergie, ce qui le met en déséquilibre par rapport à d'autres écosystèmes (Collins *et al.* 2000). Le soleil, comme source d'énergie principale des écosystèmes naturels, n'est pas une ressource énergétique suffisante pour maintenir le fonctionnement du système urbain. L'empreinte de l'écosystème urbain va donc loin au delà des frontières physiques du système et induit une forte pression sur les ressources naturelles comme par exemple le sol ou l'eau (Pickett *et al.* 2001). Les villes dépendent de leur 'hinterland' et la probabilité d'endommager les régions environnantes augmente avec la taille de la ville et l'intensité de l'influence humaine (Douglas 2002). Le métabolisme des écosystèmes urbains est l'objet d'étude de différentes recherches, les travaux pionniers sont ceux d'Odum H.T. (1983), dont le principal objectif est l'évaluation des effets du processus d'urbanisation. Ces approches quantitatives permettent de quantifier le métabolisme urbain, même si la description de l'ensemble du système est quasiment impossible.

Après avoir défini la ville comme un écosystème, nous avons décrit plus particulièrement les caractéristiques environnementales de cet écosystème. Nous avons notamment précisé les principales modifications des sols et des eaux en détaillant plus particulièrement celles de l'atmosphère. Les sols en milieu urbain sont caractérisés par des processus divers : pollution, compaction, imperméabilisation et une forte altération des conditions hydriques. Ainsi, les fonctions environnementales initiales sont fortement réduites et modifiées (ex. la croissance végétale, la fonction de filtre, le stockage, l'interception). Concernant l'atmosphère, nous avons présenté les phénomènes les plus marquants pour le climat urbain tel que l'îlot de chaleur, la modification des flux à l'intérieur de la couche limite urbaine et ceux proches de la surface, ainsi que les phénomènes de pollution atmosphérique. Les principales raisons de ces situations sont la rugosité élevée, la modification du budget énergétique, ainsi que l'émissions des polluants mobiles et fixes.

### La végétation comme un élément de l'écosystème

Dans une deuxième partie de ce chapitre, nous avons considéré la végétation comme étant un élément de l'écosystème urbain. Tout d'abord, nous avons montré les différentes définitions qui dépendent principalement de l'observateur et qui vont de la plante, l'association de plantes, de catégories d'occupation du sol jusqu'au réseau composé de différentes catégories d'occupation du sol. La figure 2 montre les différentes échelles d'observation.

[39] Nous comprenons ici comme étant naturel tout ce qui émerge de soi-même sans influence d'autrui. Par conséquence, le mot 'nature' est utilisé pour tout processus ou phénomène dont l'origine n'est pas humaine.

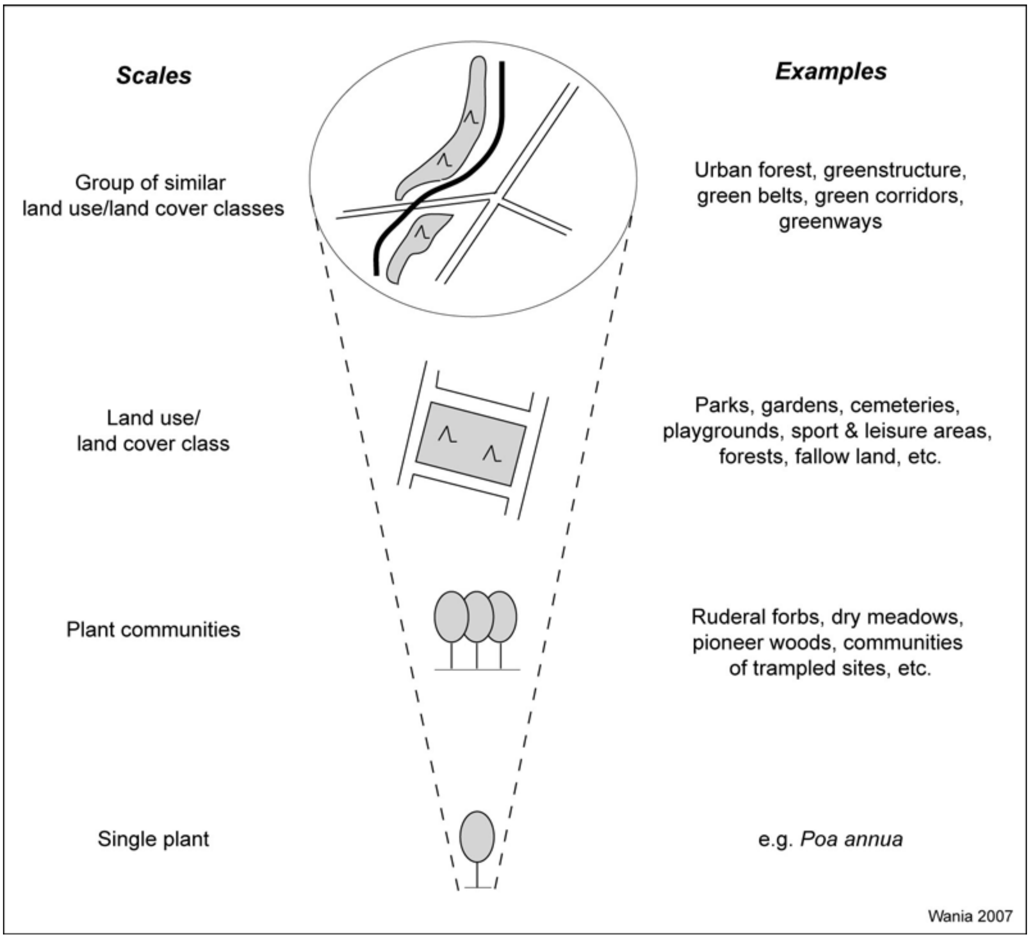


*Figure 2 : Les échelles de la végétation en milieu urbain. A gauche, les termes utilisés par les deux observateurs principaux, le botaniste et l'agent de l'aménagement, et à droite, des exemples pour chaque échelle.*

Nous avons distingué deux observateurs principaux qui sont le botaniste et un agent d'aménagement. Le premier observe la végétation dans le sens stricte du terme ou alors la flore urbaine, considérée comme étant spécifique à une ville dans une région particulière (Wittig 1996). Nous pouvons différenciér la flore urbaine en flore spontanée et flore plantée. Alors que la dernière est limitée aux plantes ornementales ou plantées principalement dans des lieux publics, le groupe spontané comprend l'ensemble des plantes qui existent de manière 'naturelle', donc sans influence humaine. Dans l'écosystème urbain, 60 à 70 % sont plantées (Gilbert 1989). Quant à l'agent de l'aménagement qui n'utilise pas les termes du botaniste, au lieu d'observer une seule plante ou une communauté de plantes, il observe un paysage urbain en termes de catégories d'occupation du sol. Contrairement au botaniste, celui-ci inclut souvent des surfaces non végétales. Souvent, on s'appuie sur la fonction de la surface considérée, sa propriété ou encore la valeur écologique. Ainsi plusieurs termes sont utilisés. En plus des différentes catégories d'occupation du sol, il existe une variété de termes qui désignent l'ensemble ou une grande partie des surfaces végétales. La plupart ont en commun l'objectif de la conservation d'un environnement écologique sain, c'est-à-dire d'espaces jugés importants pour assurer les fonctions écologiques de la végétation, sur lesquelles nous allons revenir plus tard.

### L'élément et ses interactions

En s'appuyant sur le concept d'écosystème, nous avons ensuite défini les différentes fonctions de la végétation dans l'écosystème urbain. La figure 3 montre les différentes interactions dégagées. Les interactions avec le sol, l'eau, et l'atmosphère sont directement induites par le métabolisme de la plante qui en tant que telle représente également un système. De plus, les plantes font partie de la chaîne d'alimentation des animaux, certaines plantes profitent également des animaux. Les interactions avec l'être humain se définissent d'une part par les éléments techniques que l'homme installe et qui induisent soit la disparition de la plante, soit la perturbation de son fonctionnement. D'autre part, la plante a des influences sur l'être humain qui sont principalement psychologiques ou sociales.

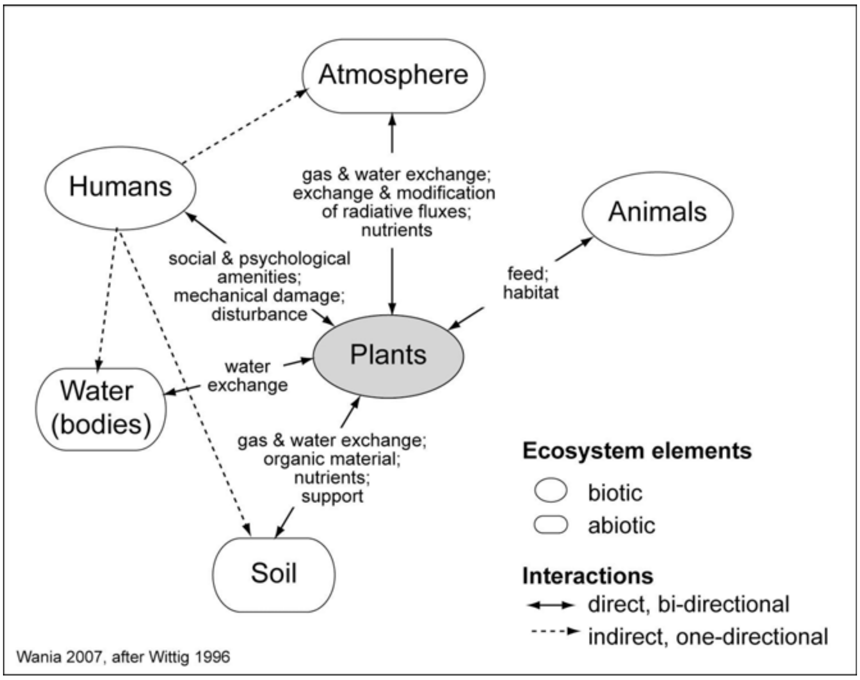


*Figure 3 : La plante dans l'écosystème urbain : interactions directes avec les autres éléments abiotiques et biotiques. Les interactions présentées focalisent sur la végétation, ainsi les interactions entre les autres éléments ne sont pas représentées. Les éléments techniques sont représentés par les être humains. Les influences indirectes concernent la modification des conditions environnementales qui induit soit la disparition des plantes, soit la modification des échanges avec les éléments sol, eau et atmosphère. L'influence directe de l'être humain se définit par la destruction ou la perturbation par l'influence mécanique*

### Qualité environnementale et végétation

Les interactions entre la végétation et les éléments atmosphère, sol, eau et animaux, identifiées auparavant définissent le cadre du rôle de la plante pour la qualité de l'environnement en milieu urbain. Dans cette partie, nous avons fait un état de l'art des différentes interactions. Cet état de l'art est basé sur les résultats de recherches publiés dans la littérature scientifiques.

Tout d'abord, la végétation peut servir d'indicateur environnemental par ces réactions sur les changements de conditions de vie. Le domaine de l'écologie des plantes a identifié certains indicateurs qui servent à la gestion des conditions environnementales telles que la sécheresse, la pollution de l'air, des sols et des eaux. D'autres indicateurs permettent d'évaluer l'intensité de l'influence humaine. Les autres fonctions sont écologiques, sociales, psychologiques, esthétiques et économiques. Parmi les fonctions écologiques, nous avons identifié les fonctions pour le climat telles que le rafraîchissement de l'air et la rétention et la filtration des polluants. L'influence sur l'eau se définit principalement par la rétention et l'interception des eaux de pluies. La végétation urbaine joue donc un rôle particulier en termes de biodiversité suite à son originalité écologique et sa fonction d'habitat en ville qui fait le lien avec les écosystèmes à l'extérieur de la ville.

Finalement, son rôle pour la qualité de vie en ville se définit aussi par son effet psychologique, social et esthétique. La végétation contribue à la diminution de l'impact du stress lié à la vie urbaine et les citoyens perçoivent l'effet positif sur la qualité de vie. Les espaces verts, les forêts urbaines, les coulées vertes sont des lieux de récréation, de détente et d'activité physique. En plus des espaces verts de taille importante, les squares ou les petits parcs sont des lieux de rencontre sociale. La végétation est aussi un élément d'architecture et d'urbanisme. Elle sert de coupure, de discontinuités et de liaison ; elle permet de cacher aussi ou d'agrémenter des paysages inesthétiques.

La végétation connaît aussi une fonction économique qui se définit d'une part par sa valeur de consommation telle que l'exploitation du bois, la récolte des fruits et légumes. Une attention spéciale est portée à sa valeur en tant que bien fonctionnel.

Par ses fonctions écologiques, la végétation peut aussi indirectement aider à réduire la consommation d'énergie, notamment par l'ombrage en été et la protection des vents forts en hiver.

# PARTIE II : DETECTION DE LA VEGETATION URBAINE

## Chapitre 3 : Détection de la végétation en milieu urbain à l'aide des images hyperspectrales

Le deuxième objectif principal de cette thèse a été l'évaluation du potentiel des données hyperspectrales pour la localisation et la caractérisation du couvert végétal en ville. Cette nouvelle génération de données de télédétection est caractérisée par une haute résolution spectrale (plusieurs bandes spectrales étroites et continues) et spatiale (quelques mètres) et semble être ainsi plus particulièrement adaptée pour les études en milieu urbain, connu pour son hétérogénéité que ce soit au niveau spatial ou spectral. Ces données pourraient compléter les méthodes de suivi actuellement appliquées à des bases de données de végétation urbaine. Dans le cadre de cette étude, nous avons exploité une image CASI à 32 bandes acquise en septembre 2005 sur la ville de Strasbourg. Elle couvre les longueurs d'ondes entre 430-950 nm et sa résolution spatiale au sol est de 2 m.

Dans un premier temps, nous avons testé différents indices de végétation pour créer un masque de végétation utilisé dans les analyses suivantes. Nous avons notamment comparé l'indice NDVI (Rouse *et al.* 1974), qui reste l'indice le plus souvent utilisé, et deux indices hybrides dont TSAVI (Baret *et al.* 1989), un indice qui tient compte de l'influence du signal du sol sous-jacent, et TSARVI (Bannari *et al.* 1994), qui lui tient compte non seulement de l'influence du sol mais aussi des effets atmosphériques. Ce dernier a prouvé sa performance en milieu urbain et en milieu à couverture végétale éparse sur des données multispectrales (Bannari *et al.* 1994, 1998). Les résultats de cette analyse confirment ce qui a été observé dans ces applications. Contrairement au TSARVI, les résultats du NDVI et TSAVI montrent des fausses estimations de couvert, plus particulièrement dans les zones ombragées (voir Figure 4).

De plus nous avons exploité la partie étroite du passage des longueurs d'onde du rouge au proche infrarouge, appelé « red-edge », pour montrer l'intérêt d'utiliser la méthode de la première dérivée pour caractériser l'état sanitaire de la couverture végétale.

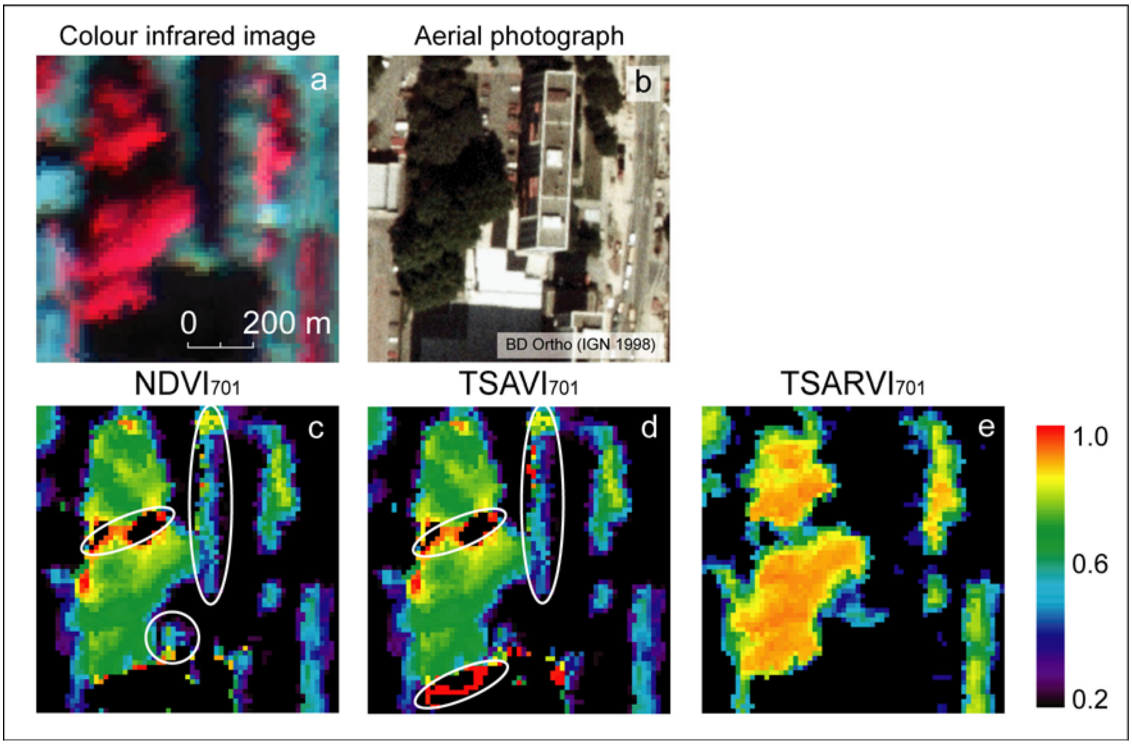


*Figure 4 : Comparaison de la performance de différents indices de végétation pour extraire la végétation. Exemple de comparaison entre NDVI (c), TSAVI (d) et TSARVI (e). Les cercles indiquent des erreurs dans la détection du couvert végétal.*

Dans une deuxième partie, nous avons procédé à l'extraction de l'information sur le couvert végétal en passant par la méthode de classification supervisée. L'application des méthodes telles que le Maximum de Vraisemblance nécessite une réduction des dimensions initiales de l'image. Pour cela, nous avons testé l'influence de différentes méthodes d'extraction dont un groupe de méthodes effectuant une transformation sur la globalité des données ('non-supervisée') et un autre groupe effectuant une extraction basée sur les statistiques de classes préalablement définies. Dans le premier cas, la méthode globale a été la Minimum Noise Fraction Transformation (MNF), dans le deuxième cas, les deux méthodes basées sur les classes ont été la Discriminant Feature Extraction Analysis (DAFE) et la Decision Feature Boundary Extraction (DBFE). La motivation de tester chacune résidait dans le fait que les classes à extraire, nous nous sommes concentrés sur les arbres, sont des classes qui se ressemblent fortement au niveau spectral. Les résultats montrent une meilleure performance des deux méthodes basées sur la statistique des classes. La figure 5 (image de gauche) montre le meilleur résultat obtenu sur des bandes extraites avec la méthode DBFE. Malgré le bon taux de classification, beaucoup de classes définies ne semblent pas uniques et seules quelques classes ont pu être extraites finalement. Ces résultats sont certainement liés aux conditions particulières en milieu urbain telles que les effets liés à l'illumination (effets environnementaux, de radiation diffuse, d'ombre) et à l'hétérogénéité du milieu ainsi qu'au problème des mixels. De plus, des effets liés au couvert végétal comme la forte variation de la canopée (végétale) de manière générale, les effets d'ombre à l'intérieur d'une canopée, l'influence des surfaces sous-jacentes rendent la définition de classes difficile.

Afin de pouvoir évaluer la performance des images hyperspectrales, nous avons comparé le meilleur résultat de classification obtenu avec une image multispectrale (Figure 5).

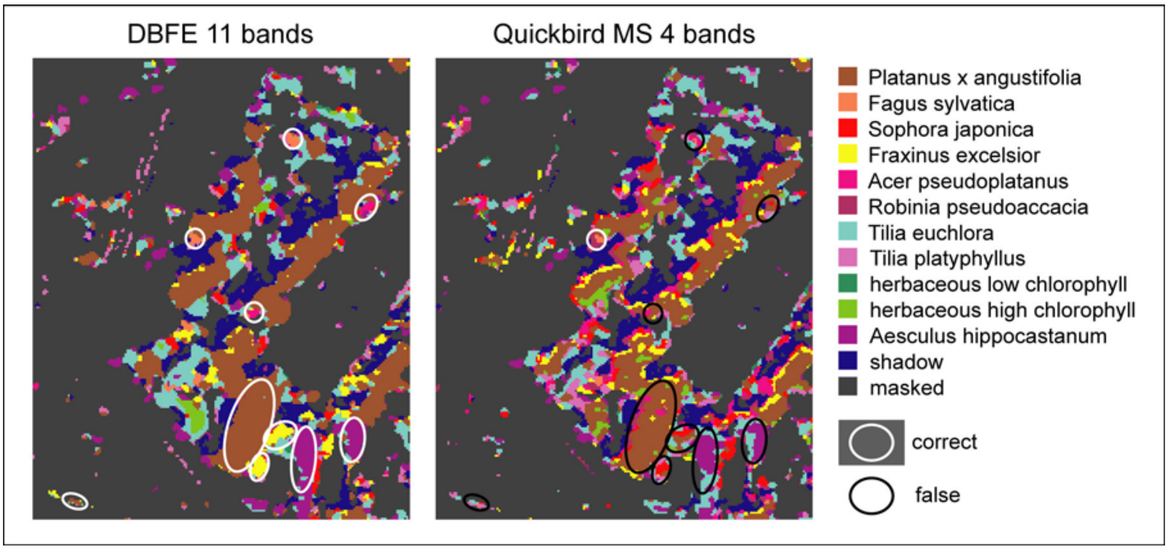


*Figure 5 : A gauche, les meilleurs résultats obtenus avec la méthode de classification du Maximum de Vraisemblance sur des bandes extraites avec la Decision Boundary Feature Extraction. A droite, les résultats du Maximum de Vraisemblance sur les bandes multispectrales.*

Finalement, un nouvel algorithme de classification non-supervisée a été testé. Il s'agit du Modular Approach for Clustering with Local Attribute Weighting (MACLAW) (Blansché *et al.* 2006), qui utilise les approches génétiques et de pondération de bandes. Ce dernier est particulièrement intéressant pour la sélection de bandes dans les images hyperspectrales. L'intérêt de cet algorithme a été son potentiel pour l'exploitation des données hyperspectrales et notamment pour la définition de classes spectrales, ce qui correspond à la phase la plus critique dans le traitement de ces images avec les méthodes de classification supervisées.

# PARTIE III APPLICATION ET MODELISATION

## Chapitre 4 : Evaluation de l'effet sur la qualité de l'air à l'aide des simulations microclimatiques

Le quatrième chapitre a été destiné à évaluer une fonction écologique de la végétation en ville. Il s'agit de l'effet sur la qualité de l'air et plus précisément sur la qualité de l'air en termes de pollution atmosphérique. La végétation est reconnue pour pouvoir filtrer et retenir certains polluants. A l'aide du modèle micro-climatique ENVI-met (Bruse and Fleer 1998), la qualité de l'air et plus précisément la répartition des polluants atmosphériques a été simulée d'une part dans des scénarii standardisés et d'autre part dans un cas réel d'un tissu urbain dans la ville de Strasbourg.

Les simulations dans des scénarii standardisés ont permis d'évaluer l'influence des arbres d'alignement dans des rues-canyons de différentes tailles sur la répartition des particules

$PM_{10}$. Nous avons notamment analysé l'influence du rapport hauteur-largeur (H/W) et de la direction du vent sur les concentrations à hauteur de l'appareil respiratoire humain. L'influence principale peut être décrite par une inhibition de la ventilation à l'intérieur de la rue qui se présente par une modification des flux circulants. Les résultats montrent que l'effet a tendance à être négatif pour les arbres à feuillage dense et augmente avec le rapport H/W (Figure 6). La présence d'arbres dans les rues étroites bloque la ventilation et aggrave les conditions dans des situations de faible ventilation par exemple avec un vent perpendiculaire et de vitesse faible. Au contraire, les haies peuvent aider à réduire le niveau de concentrations à hauteur de l'appareil respiratoire humain et pourraient être une alternative à la plantation d'arbres.

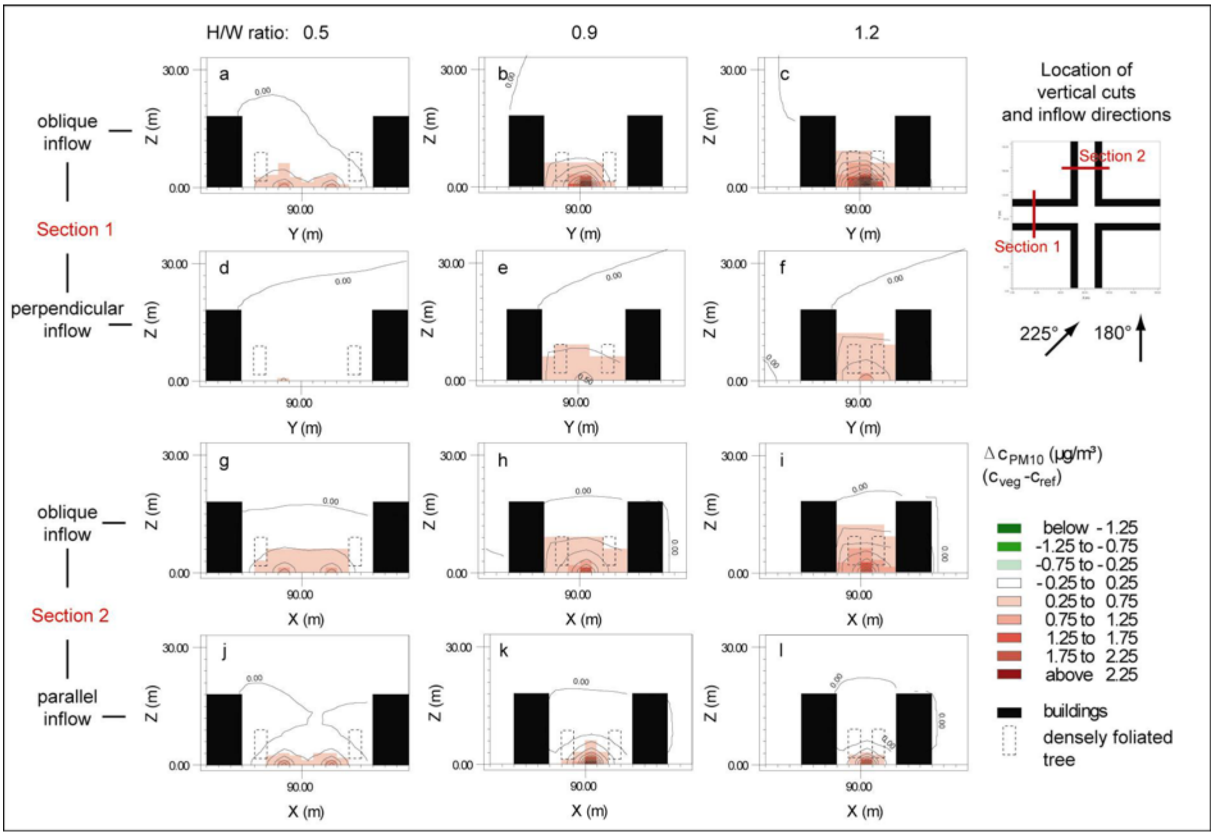


*Figure 6 : Influence d'un alignement d'arbres à feuillage dense sur la concentration de particules. Coupe verticale de trois rues à différents ratios hauteur-largeur (H/W). L'inhibition de la ventilation augmente avec le ratio H/W. Les arbres à feuillage dense coupent la circulation à l'intérieur de la rue qui induit initialement une dilution de polluants.*

A partir de ces résultats, nous avons formulé des recommandations pour l'aménagement urbain à l'échelle de la rue :

1. De manière générale, la plantation des arbres dans des rues étroites flanquées de bâtiments des deux côtés doit être évitée (H/W supérieur à 0.5).

2. Planter des arbres d'alignement à distance des bâtiments avoisinants.

3. Eviter de planter des alignements d'arbres proches des parcs ou des aires peu polluées.

4. Appliquer des méthodes d'élagage qui favorisent la pénétration d'air à l'intérieur de la canopée.

La simulation d’un cas réel de tissu urbain a servi à l’évaluation de l’impact d’un projet de construction d’une nouvelle ligne de tram dans un quartier de Strasbourg dans le cadre duquel la couverture végétale a été modifiée (Figure 7a et b). Les arbres de taille importante ont notamment été remplacés par une surface herbeuse. La comparaison des résultats à 15 heures et pour la hauteur de l’appareil respiratoire humain (1.5 m) montre que les températures varient de 1 K, ce qui indique que l’influence de la surface herbeuse en termes de confort thermique se rapproche de celles des arbres (Figure 7d). En termes de pollution, le fait d’avoir enlevé les arbres améliore la ventilation dans cette rue large surtout au niveau du carrefour (Figure 7e).

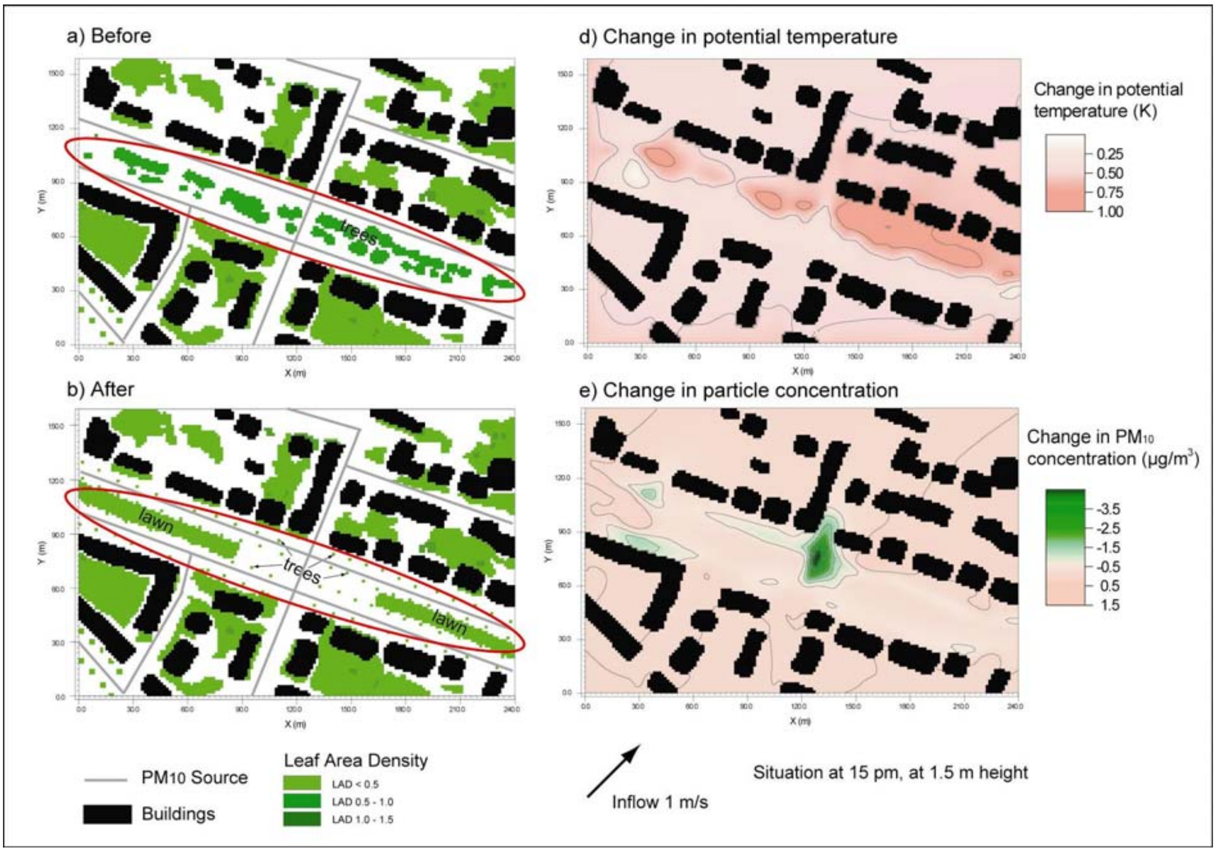


*Figure 7 : Evaluation des modifications de la qualité de l’air induites par une modification de la couverture végétale dans le cadre d’un projet d’aménagement à l’échelle de la rue. Le remplacement des arbres par une surface herbeuse (a et b) induit une légère augmentation des températures (d) et réduit localement la concentration des particules (e).*

## CONCLUSIONS

Les résultats de cette thèse contribuent à la mise en valeur de la végétation urbaine. Ils démontrent l’intérêt d’étudier cet élément urbain qui permet d’assurer une certaine qualité de vie en ville. Ils montrent aussi que des actions plus ciblées sont nécessaire pour valoriser ces fonctions, par exemple sa fonction vis-à-vis de la qualité de l’air. Nous avons pu montrer l’intérêt de mettre en place des recommandations concrètes pour l’aménagement qui vont au-delà des aspects actuellement considérés dans un projet de planification.

L’observation de la végétation urbaine à partir d’images satellitaires reste une piste à suivre dans le futur. Avec les nouvelles générations de capteurs qui offrent non seulement une résolution spatiale plus adaptée au milieu urbain mais aussi une résolution spectrale plus fine, l'hétérogénéité du milieu urbain peut être étudié de manière plus détaillée. Jusqu'à l'heure actuelle, les images hyperspectrales ont été peu exploitées pour l'étude du couvert végétal et nous avons montré que, malgré la complexité des données et du milieu-même, elles présentent une source d'information prometteuse.

# ANNEX

## CHAPTER 2

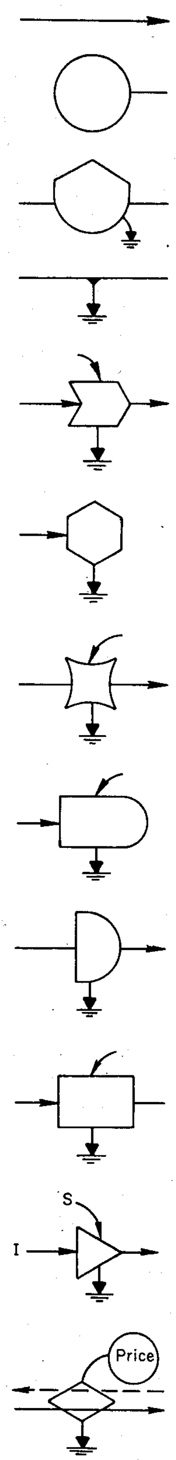


*Energy circuit* (Chapters 1–3). A pathway whose flow is proportional to the quantity in the storage or source upstream.

*Source* (Chapter 7). Outside source of energy delivering forces according to a program controlled from outside; a forcing function.

*Tank* (Chapter 3). A compartment of energy storage within the system storing a quantity as the balance of inflows and outflows; a state variable.

*Heat sink* (Chapter 7). Dispersion of potential energy into heat that accompanies all real transformation processes and storages; loss of potential energy from further use by the system.

*Interaction* (Chapter 8). Interactive intersection of two pathways coupled to produce an outflow in proportion to a function of both; control action of one flow on another; limiting factor action; work gate.

*Consumer* (Chapters 9 and 20). Unit that transforms energy quality, stores it, and feeds it back autocatalytically to improve inflow.

*Switching action* (Chapter 6). A symbol that indicates one or more switching actions.

*Producer* (Chapters 8 and 19). Unit that collects and transforms low-quality energy under control interactions of high-quality flows.

*Self-limiting energy receiver* (Chapter 10). A unit that has a self-limiting output when input drives are high because there is a limiting constant quantity of material reacting on a circular pathway within.

*Box* (Chapter 6). Miscellaneous symbol to use for whatever unit or function is labeled.

*Constant-gain amplifier* (Chapters 8 and 9). A unit that delivers an output in proportion to the input *I* but changed by a constant factor as long as the energy source *S* is sufficient.

*Transaction* (Chapter 23). A unit that indicates a sale of goods or services (solid line) in exchange for payment of money (dashed). Price is shown as an external source.

*Figure AC2-1: Symbols of the energy circuit language (Odum 1983).*

# ANNEX CHAPTER 3

*Table AC3-1 : Detection of vegetation. Confusion matrix for the ML classification on 9 MNF bands (training samples) (for classes see Table 3.6).*

| | Ground Truth (%) | | | | | | | | | | | | |
|---|---|---|---|---|---|---|---|---|---|---|---|---|---|
| Class | PA | FS | SJ | FE | AP | RP | TE | TP | HerbL | HerbH | AH | shadow | Total |
| PA | 93.17 | 0.87 | 5.56 | 7.69 | 0.89 | 0.00 | 0.73 | 0.00 | 0.00 | 0.00 | 0.00 | 0.33 | 13.66 |
| FS | 0.80 | 96.52 | 0.00 | 0.00 | 1.79 | 0.00 | 0.00 | 0.00 | 0.00 | 0.00 | 0.00 | 0.00 | 3.33 |
| SJ | 1.00 | 0.00 | 81.48 | 19.23 | 2.68 | 0.81 | 0.73 | 2.34 | 0.00 | 0.00 | 0.00 | 0.00 | 3.30 |
| FE | 1.00 | 0.00 | 3.70 | 70.51 | 0.89 | 0.00 | 1.46 | 0.78 | 0.00 | 1.35 | 0.00 | 0.00 | 2.28 |
| AP | 1.20 | 2.61 | 2.78 | 1.28 | 89.29 | 0.00 | 0.00 | 0.00 | 0.00 | 0.00 | 0.00 | 0.00 | 3.22 |
| RP | 0.00 | 0.00 | 5.56 | 0.00 | 0.00 | 91.06 | 0.00 | 6.25 | 0.00 | 0.00 | 0.00 | 0.98 | 3.67 |
| TE | 2.41 | 0.00 | 0.00 | 0.00 | 0.89 | 0.00 | 94.89 | 0.00 | 0.26 | 0.00 | 6.11 | 0.00 | 4.58 |
| TP | 0.20 | 0.00 | 0.93 | 1.28 | 3.57 | 8.13 | 0.00 | 90.63 | 0.00 | 0.00 | 0.00 | 0.33 | 3.81 |
| HerbL | 0.00 | 0.00 | 0.00 | 0.00 | 0.00 | 0.00 | 0.00 | 0.00 | 99.21 | 0.00 | 0.00 | 0.00 | 21.37 |
| HerbH | 0.00 | 0.00 | 0.00 | 0.00 | 0.00 | 0.00 | 0.00 | 0.00 | 0.13 | 98.65 | 0.00 | 0.00 | 25.04 |
| AH | 0.20 | 0.00 | 0.00 | 0.00 | 0.00 | 0.00 | 2.19 | 0.00 | 0.40 | 0.00 | 93.89 | 0.98 | 7.29 |
| shadow | 0.00 | 0.00 | 0.00 | 0.00 | 0.00 | 0.00 | 0.00 | 0.00 | 0.00 | 0.00 | 0.00 | 97.38 | 8.45 |
| Total | 100.00 | 100.00 | 100.00 | 100.00 | 100.00 | 100.00 | 100.00 | 100.00 | 100.00 | 100.00 | 100.00 | 100.00 | 100.00 |

*Table AC3-2: Detection of vegetation. Confusion matrix for the ML classification on 9 MNF bands + homogeneity 7x7 (training samples) (for classes see Table 3.6).*

| | Ground truth (%) | | | | | | | | | | | | |
|---|---|---|---|---|---|---|---|---|---|---|---|---|---|
| Class | PA | FS | SJ | FE | AP | RP | TE | TP | HerbL | HerbH | AH | shadow | Total |
| PA | 94.38 | 0.87 | 5.56 | 6.41 | 0.89 | 0.00 | 0.73 | 0.00 | 0.00 | 0.00 | 0.00 | 0.33 | 13.80 |
| FS | 0.80 | 97.39 | 0.00 | 0.00 | 1.79 | 0.00 | 0.00 | 0.00 | 0.00 | 0.00 | 0.00 | 0.00 | 3.36 |
| SJ | 1.61 | 0.00 | 83.33 | 15.38 | 4.46 | 0.00 | 0.73 | 2.34 | 0.00 | 0.00 | 0.00 | 0.00 | 3.39 |
| FE | 1.00 | 0.00 | 2.78 | 73.08 | 0.89 | 0.81 | 0.00 | 0.78 | 0.00 | 1.35 | 0.00 | 0.00 | 2.28 |
| AP | 0.80 | 1.74 | 1.85 | 0.00 | 90.18 | 0.00 | 0.00 | 0.00 | 0.00 | 0.00 | 0.00 | 0.33 | 3.13 |
| RP | 0.00 | 0.00 | 5.56 | 0.00 | 0.00 | 95.93 | 0.00 | 7.81 | 0.00 | 0.00 | 0.00 | 0.98 | 3.90 |
| TE | 1.00 | 0.00 | 0.00 | 3.85 | 0.00 | 0.00 | 97.81 | 0.00 | 0.13 | 0.00 | 4.96 | 0.00 | 4.44 |
| TP | 0.20 | 0.00 | 0.93 | 1.28 | 1.79 | 3.25 | 0.00 | 89.06 | 0.00 | 0.00 | 0.00 | 0.00 | 3.50 |
| HerbL | 0.00 | 0.00 | 0.00 | 0.00 | 0.00 | 0.00 | 0.00 | 0.00 | 99.34 | 0.00 | 0.00 | 0.00 | 21.40 |
| HerbH | 0.00 | 0.00 | 0.00 | 0.00 | 0.00 | 0.00 | 0.00 | 0.00 | 0.26 | 98.65 | 0.00 | 0.00 | 25.07 |
| AH | 0.20 | 0.00 | 0.00 | 0.00 | 0.00 | 0.00 | 0.73 | 0.00 | 0.26 | 0.00 | 95.04 | 0.33 | 7.23 |
| shadow | 0.00 | 0.00 | 0.00 | 0.00 | 0.00 | 0.00 | 0.00 | 0.00 | 0.00 | 0.00 | 0.00 | 98.03 | 8.51 |
| Total | 100.00 | 100.00 | 100.00 | 100.00 | 100.00 | 100.00 | 100.00 | 100.00 | 100.00 | 100.00 | 100.00 | 100.00 | 100.00 |

*Table AC3-3: Detection of vegetation. Confusion matrix for the ML classification on 6 DAFE bands (training samples) (for classes see Table 3.6).*

| | Ground Truth (%) | | | | | | | | | | | | |
|---|---|---|---|---|---|---|---|---|---|---|---|---|---|
| Class | PA | FS | SJ | FE | AP | RP | TE | TP | HerbL | HerbH | AH | shadow | Total |
| PA | 93.78 | 0.87 | 2.78 | 0.00 | 0.00 | 0.00 | 2.19 | 0.00 | 0.00 | 0.00 | 0.00 | 0.00 | 13.49 |
| FS | 0.00 | 92.17 | 0.00 | 2.56 | 7.14 | 0.00 | 0.00 | 0.00 | 0.00 | 0.00 | 0.00 | 0.00 | 3.30 |
| SJ | 0.40 | 0.00 | 91.67 | 0.00 | 0.00 | 0.00 | 0.73 | 1.56 | 0.00 | 0.00 | 0.00 | 0.00 | 2.96 |
| FE | 1.41 | 0.00 | 0.00 | 88.46 | 0.89 | 0.00 | 3.65 | 4.69 | 0.00 | 0.11 | 0.00 | 0.00 | 2.53 |
| AP | 0.00 | 6.09 | 0.00 | 2.56 | 87.50 | 0.00 | 0.73 | 2.34 | 0.00 | 0.00 | 0.00 | 0.00 | 3.16 |
| RP | 0.00 | 0.00 | 1.85 | 0.00 | 0.00 | 92.68 | 0.00 | 8.59 | 0.00 | 0.00 | 0.00 | 1.64 | 3.76 |
| TE | 4.02 | 0.00 | 0.00 | 1.28 | 0.00 | 0.00 | 90.51 | 0.00 | 0.00 | 0.22 | 7.25 | 0.00 | 4.72 |
| TP | 0.00 | 0.87 | 3.70 | 5.13 | 4.46 | 5.69 | 0.00 | 82.81 | 0.00 | 0.45 | 0.00 | 0.00 | 3.73 |
| HerbL | 0.20 | 0.00 | 0.00 | 0.00 | 0.00 | 0.00 | 0.00 | 0.00 | 99.74 | 0.00 | 0.00 | 0.00 | 21.51 |
| HerbH | 0.00 | 0.00 | 0.00 | 0.00 | 0.00 | 0.00 | 0.00 | 0.00 | 0.13 | 99.21 | 0.00 | 0.00 | 25.18 |
| AH | 0.20 | 0.00 | 0.00 | 0.00 | 0.00 | 0.00 | 2.19 | 0.00 | 0.13 | 0.00 | 92.75 | 0.66 | 7.11 |
| shadow | 0.00 | 0.00 | 0.00 | 0.00 | 0.00 | 1.63 | 0.00 | 0.00 | 0.00 | 0.00 | 0.00 | 97.70 | 8.54 |
| Total | 100.00 | 100.00 | 100.00 | 100.00 | 100.00 | 100.00 | 100.00 | 100.00 | 100.00 | 100.00 | 100.00 | 100.00 | 100.00 |

*Table AC3-4: Detection of vegetation. Confusion matrix for the ML classification on 11 DBFE bands (training samples) (for classes see Table 3.6).*

| | Ground Truth (%) | | | | | | | | | | | | |
|---|---|---|---|---|---|---|---|---|---|---|---|---|---|
| Class | PA | FS | SJ | FE | AP | RP | TE | TP | HerbL | HerbH | AH | shadow | Total |
| PA | 96.39 | 0.00 | 1.85 | 2.56 | 0.00 | 0.00 | 0.73 | 0.00 | 0.00 | 0.00 | 0.00 | 0.33 | 13.83 |
| FS | 0.00 | 100.00 | 0.00 | 0.00 | 0.89 | 0.00 | 0.00 | 0.00 | 0.00 | 0.00 | 0.00 | 0.00 | 3.30 |
| SJ | 0.20 | 0.00 | 96.30 | 0.00 | 0.00 | 0.00 | 0.00 | 0.78 | 0.00 | 0.00 | 0.00 | 0.00 | 3.02 |
| FE | 0.40 | 0.00 | 0.00 | 94.87 | 0.00 | 0.00 | 0.00 | 1.56 | 0.00 | 0.00 | 0.00 | 0.00 | 2.22 |
| AP | 0.20 | 0.00 | 1.85 | 0.00 | 99.11 | 0.00 | 0.00 | 0.00 | 0.00 | 0.00 | 0.00 | 0.00 | 3.24 |
| RP | 0.00 | 0.00 | 0.00 | 0.00 | 0.00 | 96.75 | 0.00 | 0.78 | 0.00 | 0.00 | 0.00 | 1.64 | 3.56 |
| TE | 2.41 | 0.00 | 0.00 | 1.28 | 0.00 | 0.00 | 94.89 | 0.00 | 0.13 | 0.90 | 5.34 | 0.00 | 4.72 |
| TP | 0.20 | 0.00 | 0.00 | 1.28 | 0.00 | 3.25 | 0.73 | 96.88 | 0.00 | 0.00 | 0.00 | 0.00 | 3.73 |
| HerbL | 0.00 | 0.00 | 0.00 | 0.00 | 0.00 | 0.00 | 0.00 | 0.00 | 99.87 | 0.00 | 0.00 | 0.00 | 21.51 |
| HerbH | 0.00 | 0.00 | 0.00 | 0.00 | 0.00 | 0.00 | 0.00 | 0.00 | 0.00 | 99.10 | 0.00 | 0.00 | 25.13 |
| AH | 0.20 | 0.00 | 0.00 | 0.00 | 0.00 | 0.00 | 3.65 | 0.00 | 0.00 | 0.00 | 94.66 | 0.66 | 7.29 |
| shadow | 0.00 | 0.00 | 0.00 | 0.00 | 0.00 | 0.00 | 0.00 | 0.00 | 0.00 | 0.00 | 0.00 | 97.38 | 8.45 |
| Total | 100.00 | 100.00 | 100.00 | 100.00 | 100.00 | 100.00 | 100.00 | 100.00 | 100.00 | 100.00 | 100.00 | 100.00 | 100.00 |

*Table AC3-5: Detection of vegetation. Confusion matrix for the ML classification on Quickbird data (4 bands, multispectral) (for classes see Table 3.6).*

| | Ground Truth (%) | | | | | | | | | | | | |
|---|---|---|---|---|---|---|---|---|---|---|---|---|---|
| Class | PA | FS | SJ | FE | AP | RP | TE | TP | HerbL | HerbH | AH | shadow | Total |
| PA | 75.70 | 0.00 | 5.56 | 5.13 | 0.00 | 0.00 | 2.19 | 2.34 | 0.00 | 9.09 | 0.00 | 0.00 | 13.49 |
| FS | 0.00 | 69.57 | 0.00 | 2.56 | 14.29 | 8.13 | 0.00 | 12.50 | 0.00 | 0.00 | 0.00 | 0.00 | 3.53 |
| SJ | 6.43 | 0.87 | 81.48 | 38.46 | 18.75 | 0.00 | 0.73 | 7.81 | 0.00 | 0.00 | 0.00 | 0.00 | 5.21 |
| FE | 1.41 | 4.35 | 3.70 | 43.59 | 2.68 | 0.00 | 3.65 | 7.81 | 0.00 | 0.00 | 0.00 | 0.00 | 1.94 |
| AP | 1.41 | 11.30 | 2.78 | 6.41 | 43.75 | 4.88 | 5.11 | 20.31 | 0.00 | 0.00 | 0.00 | 0.00 | 3.30 |
| RP | 0.80 | 11.30 | 0.00 | 0.00 | 12.50 | 85.37 | 0.00 | 7.03 | 0.00 | 0.00 | 0.00 | 1.64 | 4.27 |
| TE | 1.00 | 0.00 | 0.00 | 0.00 | 0.89 | 0.00 | 71.53 | 10.94 | 0.26 | 0.00 | 14.50 | 0.66 | 4.55 |
| TP | 4.82 | 2.61 | 6.48 | 3.85 | 7.14 | 0.81 | 9.49 | 31.25 | 0.13 | 0.79 | 0.00 | 0.66 | 3.10 |
| HerbL | 0.00 | 0.00 | 0.00 | 0.00 | 0.00 | 0.00 | 0.00 | 0.00 | 98.02 | 0.00 | 0.00 | 0.00 | 21.12 |
| HerbH | 8.43 | 0.00 | 0.00 | 0.00 | 0.00 | 0.00 | 0.00 | 0.00 | 0.79 | 90.12 | 0.00 | 0.00 | 24.22 |
| AH | 0.00 | 0.00 | 0.00 | 0.00 | 0.00 | 0.00 | 7.30 | 0.00 | 0.79 | 0.00 | 85.50 | 0.33 | 6.86 |
| shadow | 0.00 | 0.00 | 0.00 | 0.00 | 0.00 | 0.81 | 0.00 | 0.00 | 0.00 | 0.00 | 0.00 | 96.72 | 8.42 |
| Total | 100.00 | 100.00 | 100.00 | 100.00 | 100.00 | 100.00 | 100.00 | 100.00 | 100.00 | 100.00 | 100.00 | 100.00 | 100.00 |

*Table AC3-6: Validation of the MACLAW algorithm. Confusion matrix for the ML classification on 8 MNF bands.*

| | Ground truth (%) | | | | | | | |
|---|---|---|---|---|---|---|---|---|
| Class | Asphalt & flat roof 2 | Vegetation | Painted asphalt | Red tile roof… | bitumen roof | Shadow | Water | Total |
| Asphalt&flat roof 2 | 97.32 | 0.00 | 0.00 | 0.00 | 3.06 | 1.13 | 0.00 | 20.23 |
| Vegetation | 0.00 | 98.58 | 1.67 | 0.00 | 0.00 | 0.00 | 0.00 | 21.46 |
| Painted asphalt | 0.00 | 1.26 | 98.33 | 0.00 | 0.00 | 0.00 | 0.00 | 8.28 |
| Red tile roof… | 0.17 | 0.16 | 0.00 | 100.00 | 0.00 | 0.85 | 0.00 | 14.00 |
| Flat bitumen roof | 2.51 | 0.00 | 0.00 | 0.00 | 96.94 | 1.69 | 0.00 | 10.42 |
| Shadow | 0.00 | 0.00 | 0.00 | 0.00 | 0.00 | 96.05 | 1.70 | 11.82 |
| Water | 0.00 | 0.00 | 0.00 | 0.00 | 0.00 | 0.28 | 98.30 | 13.79 |
| Total | 100.00 | 100.00 | 100.00 | 100.00 | 100.00 | 100.00 | 100.00 | 100.00 |

*Table AC3-7: Validation of the MACLAW algorithm. Confusion matrix for the ML classification on 4 DAFE bands.*

| | Ground truth (%) | | | | | | | |
|---|---|---|---|---|---|---|---|---|
| Class | Asphalt & flat roof 2 | Vegetation | Painted asphalt | Red tile roof… | bitumen roof | Shadow | Water | Total |
| Asphalt&flat roof 2 | 96.82 | 0.16 | 0.00 | 0.00 | 7.48 | 2.82 | 0.00 | 20.81 |
| Vegetation | 0.00 | 99.84 | 0.84 | 0.00 | 0.00 | 0.00 | 0.00 | 21.66 |
| Painted asphalt | 0.00 | 0.00 | 99.16 | 0.00 | 0.00 | 0.00 | 0.00 | 8.07 |
| Red tile roof… | 0.34 | 0.00 | 0.00 | 100.00 | 0.00 | 0.00 | 0.00 | 13.90 |
| Flat bitumen roof | 2.85 | 0.00 | 0.00 | 0.00 | 92.52 | 1.41 | 0.00 | 10.01 |
| Shadow | 0.00 | 0.00 | 0.00 | 0.00 | 0.00 | 95.76 | 0.00 | 11.55 |
| Water | 0.00 | 0.00 | 0.00 | 0.00 | 0.00 | 0.00 | 100.00 | 14.00 |
| Total | 100.00 | 100.00 | 100.00 | 100.00 | 100.00 | 100.00 | 100.00 | 100.00 |

*Table AC3-8: Validation of the MACLAW algorithm. Confusion matrix for the ML classification on 6 DBFE bands.*

| | Ground truth (%) | | | | | | | |
|---|---|---|---|---|---|---|---|---|
| Class | Asphalt & flat roof 2 | Vegetation | Painted asphalt | Red tile roof… | bitumen roof | Shadow | Water | Total |
| Asphalt&flat roof 2 | 96.82 | 0.16 | 0.00 | 0.00 | 6.46 | 0.28 | 0.00 | 20.40 |
| Vegetation | 0.00 | 99.84 | 0.84 | 0.00 | 0.00 | 0.00 | 0.00 | 21.66 |
| Painted asphalt | 0.00 | 0.00 | 99.16 | 0.00 | 0.00 | 0.00 | 0.00 | 8.07 |
| Red tile roof… | 0.17 | 0.00 | 0.00 | 100.00 | 0.00 | 1.41 | 0.00 | 14.03 |
| Flat bitumen roof | 3.02 | 0.00 | 0.00 | 0.00 | 93.54 | 1.98 | 0.24 | 10.25 |
| Shadow | 0.00 | 0.00 | 0.00 | 0.00 | 0.00 | 96.33 | 0.00 | 11.61 |
| Water | 0.00 | 0.00 | 0.00 | 0.00 | 0.00 | 0.00 | 99.76 | 13.96 |
| Total | 100.00 | 100.00 | 100.00 | 100.00 | 100.00 | 100.00 | 100.00 | 100.00 |

*Table AC3-9: Validation of the MACLAW algorithm. Confusion matrix for the ML classification on 8 bands selected by MACLAW.*

| | Ground truth (%) | | | | | | | |
|---|---|---|---|---|---|---|---|---|
| Class | Asphalt & flat roof 2 | Vegetation | Painted asphalt | Red tile roof… | bitumen roof | Shadow | Water | Total |
| Asphalt&flat roof 2 | 95.81 | 0.16 | 0.00 | 0.00 | 5.78 | 0.56 | 0.00 | 20.16 |
| Vegetation | 0.00 | 96.54 | 0.00 | 1.48 | 0.00 | 0.00 | 0.00 | 21.08 |
| Painted asphalt | 0.00 | 0.00 | 97.49 | 0.00 | 0.00 | 0.00 | 0.00 | 7.94 |
| Red tile roof… | 1.17 | 3.31 | 2.51 | 98.52 | 0.00 | 1.13 | 0.00 | 14.92 |
| Flat bitumen roof | 3.02 | 0.00 | 0.00 | 0.00 | 94.22 | 4.80 | 0.00 | 10.63 |
| Shadow | 0.00 | 0.00 | 0.00 | 0.00 | 0.00 | 89.27 | 2.68 | 11.14 |
| Water | 0.00 | 0.00 | 0.00 | 0.00 | 0.00 | 4.24 | 97.32 | 14.13 |
| Total | 100.00 | 100.00 | 100.00 | 100.00 | 100.00 | 100.00 | 100.00 | 100.00 |

*Table AC3-10: Validation of the MACLAW algorithm. Confusion matrix for the ML classification on 8 bands selected with Bhattacharyya distance.*

| | Ground truth (%) | | | | | | | |
|---|---|---|---|---|---|---|---|---|
| Class | Asphalt & flat roof 2 | Vegetation | Painted asphalt | Red tile roof… | Flat bitumen roof | Shadow | Water | Total |
| Asphalt&flat roof 2 | 97.49 | 0.16 | 0.00 | 0.00 | 0.68 | 1.13 | 0.00 | 20.06 |
| Vegetation | 0.00 | 99.53 | 2.09 | 0.00 | 0.00 | 0.00 | 0.00 | 21.70 |
| Painted asphalt | 0.00 | 0.31 | 97.91 | 0.00 | 0.00 | 0.00 | 0.00 | 8.04 |
| Red tile roof… | 0.34 | 0.00 | 0.00 | 100.00 | 0.00 | 0.28 | 0.00 | 13.93 |
| Flat bitumen roof | 2.18 | 0.00 | 0.00 | 0.00 | 99.32 | 3.67 | 0.00 | 10.83 |
| Shadow | 0.00 | 0.00 | 0.00 | 0.00 | 0.00 | 94.35 | 2.43 | 11.72 |
| Water | 0.00 | 0.00 | 0.00 | 0.00 | 0.00 | 0.56 | 97.57 | 13.73 |
| Total | 100.00 | 100.00 | 100.00 | 100.00 | 100.00 | 100.00 | 100.00 | 100.00 |

# ANNEX CHAPTER 4

## Analysis of Street configurations in the city of Strasbourg

### Street configurations referenced in STREET

The street configurations used to simulate the influence of vegetation on particle dispersion were compared to those referenced in the model STREET[40] for the city of Strasbourg. STREET is a screening model for mesoscale air quality simulations used above all for the evaluation of the achievement of limit values and localisation of high pollution concentrations in urban areas (Lohmeyer *et al.* 2000). Annual average pollution and 98-percentiles can be calculated for each street section based on traffic volume and pattern, background concentration, the meteorological parameters wind direction and mean wind speed and finally the street configuration. The model uses dimensionless results of dispersion and flow for different building configurations precalculated by the microscale model MISKAM[41] (Eichhorn 1989). They are stored in a database and used to calculate emissions with STREET.

For the city of Strasbourg[42] each street section is characterized among others by a configuration type and concentration and emission values for benzene, CO, COV, $NO_X$, $PM_{10}$ and $SO_2$. Focus for the analysis was on the street configuration types, all in all 98 street and intersection types are identified in the database. Each is defined either by three, four, or five of the following characteristics:

- Road type (straight line, intersection in X or T form[43]),
- Disposition of flanking buildings (e.g. without, on one side, on both sides),
- Number of traffic lines (two, four or more),
- Continuity of building façade (five types),
- Aspect ratio (ratio height/width) or in case of buildings flanking only one side the distance from the centre of the road to the building façade.

---

[40] STREET is used to calculate automobile exhaust dispersion in built-up areas. It was developed by order of the ministry of the environment of the Land Baden-Württemberg (Pfeifer *et al.* 1996) and recommended in the draft of the guideline of the German Society of Engineers (VDI) (Ausbreitungsrechnung fuer KFZ-Emissionen, VDI 3782, Blatt 8, 1998).

[41] Like ENVI-met MISKAM is a microscale, non hydrostatic, three-dimensional flow model with an Eulerian dispersion model. Like in ENVI-met the calculation of the flow and dispersion regime accounts for the influence of building structures but contrarily to ENVI-met MISKAM does not include a vegetation model.

[42] The used data mainly consist in emission and concentration data (STREET model, version 3.1) calculated based on traffic data for 2000. Streets and intersections are those referenced in the BD Topo of IGN® (1989). Information source ASPA 05052302-ID.

[43] According to their traffic load intersections are characterised either by a ratio of 50/50 (same traffic load on both streets) or 80/20 (80 % traffic on one and 20 % on the other street). As we consider only equal traffic load this difference is not considered any further here.

## Analysis of street configuration types

Among these characteristics aspect ratio and building façade were further investigated. The analysed data cover the municipality of Strasbourg ("Commune de Strasbourg"). Considered are only streets between buildings which line up continuously along both sides.

Four aspect ratios occur within the limits of the municipality of Strasbourg: 0.33, 0.5, 0.66, and 1.0 (Table AC4-1). The relative occurrence of each was analysed focussing on the relation to city districts and their building pattern. Concerning the aspect ratio, most streets are classified as avenue canyons. 80 % if the streets are classified as wide or avenue canyons with about 37 % aspect ratio 0.33 and 43 % ratio 0.5. Nevertheless, about 12 % of the streets and intersections are deeper canyons with ratio 0.66 and 1.0.

Concerning the building façade flanking the streets with the respective aspect ratio, it is noteworthy that streets with ratio 0.33 are entirely characterised by an interrupted façade with dominating non-built spaces (interrupted front > building front) (Table AC4-1). With increasing ratio façades tend to be more closed. Canyons with aspect ratio 1.0 (regular canyons) are flanked by dense and nearly continuous building façades.

*Table AC4-1: Aspect ratio and building façades within Strasbourg municipality as referenced in the STREET database (total number of street sections 4468). Streets with buildings flanking only one side are not listed (7.4 %). '% total' indicates the percentage of each aspect ratio on the total number of street sections. The four columns on the right indicate the percentage of building façade types for each aspect ratio. Building density increases from left to right. A fifth façade type (not mentioned here) is the transition from a continuous to a discontinuous façade and occurs only for aspect ratio 1.0 (0.8 %).*

| | | Building density → | | | |
|---|---|---|---|---|---|
| **H/W ratio** | **% of total** | **% façade non - built > built** | **% façade non - built < built (%)** | **% façade interrupted by small accesses*** | **Length of continuously built façade up to 60 m (%)** |
| 0.33 | 36.8 | 100 | 0 | 0 | 0 |
| 0.5 | 42.9 | 4.4 | 71.5 | 13.4 | 10.7 |
| 0.66 | 0.9 | 0 | 100 | 0 | 0 |
| 1.0 | 12.0 | 0 | 0 | 51.4 | 47.8 |

* Small spacings between buildings that are not considered as roads; access to backyards or parking places.

The analysis of the spatial occurrence of ratios and façade types in Figure AC4-1 reveals a link to the dominating building structure of city districts. Deeper canyons with aspect ratio 1.0 occur predominantly in the old city districts mainly built in the 18$^{th}$ and 19$^{th}$ century such as the city centre and the surrounding older districts (south and northeast) as well as the district of Neudorf (Figure AC4-1b). Both are densely built-up. Here, either high rise buildings with up to eight floors or smaller buildings (five/six floors) flanking smaller roads dominate. Configurations where the building height is half the street width (aspect 0.5) occur also in the mentioned city districts but mainly dominate in the older suburbs (e.g. Robertsau, Cronenbourg, Meinau) characterised by single family houses or houses with four or five floors. Streets with such an aspect ratio occur in industrial areas as well (e.g. Plaine des Bouchers, harbour districts).

Concerning the characteristics of the façade, older residential densely built-up districts close to the city centre show the tendency of more closed façades than residential districts in the outer suburbs (Figure AC4-1a). Again, these are the centre, Neudorf and the districts south and north-east to the centre. Nevertheless, these façade types also occur in the old industrial area of Plaine des Bouchers. Façades in the suburbs are less continuous but nevertheless the built-up part dominates.

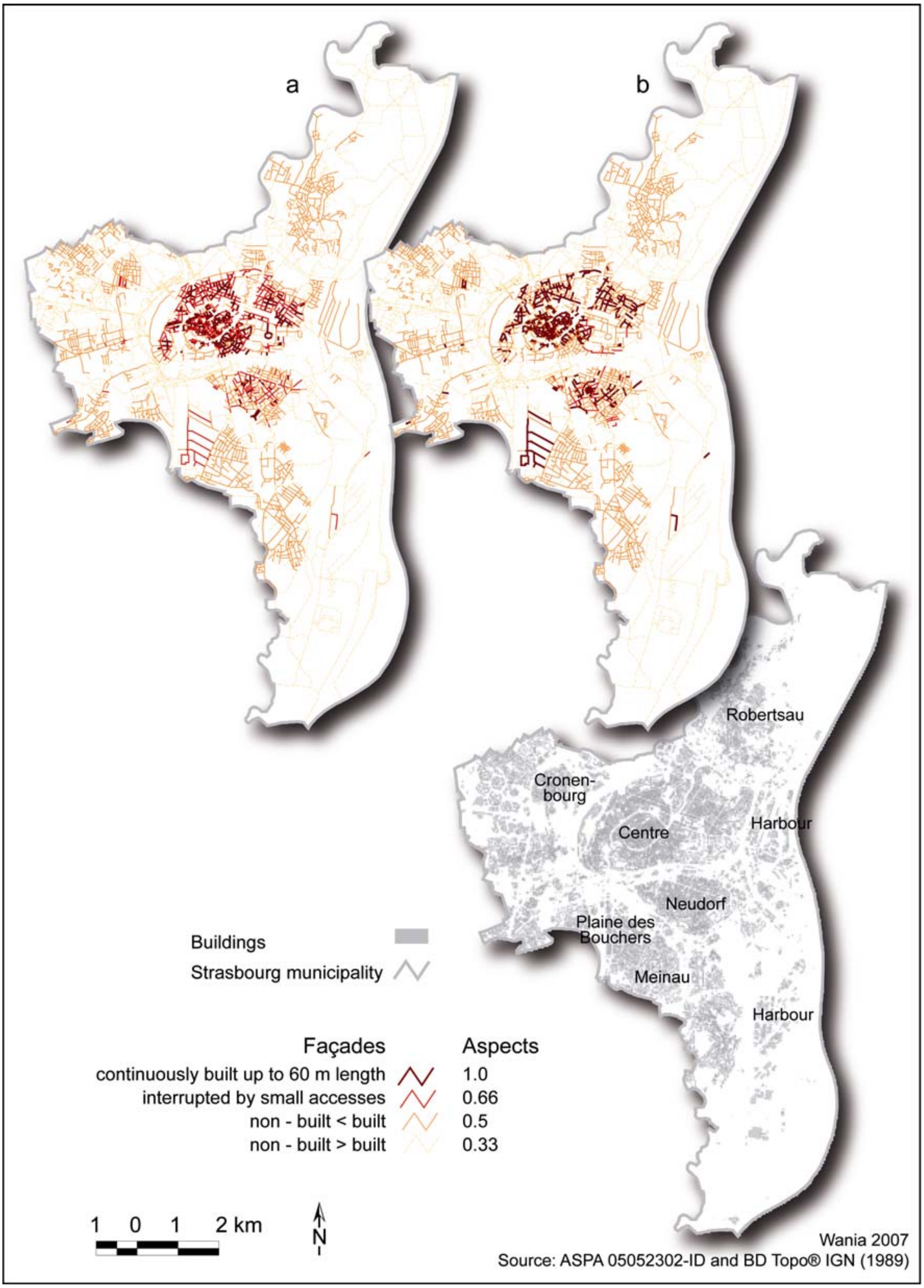


*Figure AC4-1: Spatial occurrence of different aspect ratios and facades within the limit of Strasbourg municipality: a) continuity of façades and b) aspect ratio.*

## Occurrence of vegetation

The occurrence of vegetation in streets was analyzed regarding the configuration types referenced in the database. Information about vegetation cover was extracted from image data (see Part II) using a vegetation index. As this index does not provide information about the vegetation type (trees, bushes or herbaceous plants), the information was completed in the field (random tests).

In general, vegetation occurs in every configuration type. Typical for the city of Strasbourg are large avenues flanked by tree lines on both sides (Figure AC4-2a). Often the tree lines tend to be continuous as tree crowns touch each other, particularly in case of old trees. These avenues are frequent in the city centre and usually flanked by continuous façades (e.g. Figure AC4-2a,b). Double tree lines also occur in deeper canyons with aspect ratios about 1.0 (Figure AC4-2b). Other frequently occurring vegetation configurations are one single row of trees or rows of trees on both sides of the traffic lane (four tree rows). Hedges are rarely flanking streets.


*Figure AC4-2: Two examples for streets with continuous rows of trees on both sides: a) avenue canyon (aspect 0.66) and b) canyon with aspect ratio 1.0.*

## Conclusions

The street configurations used for the microscale air quality simulations cover the range of canyon types referenced in the model STREET for the city of Strasbourg. Although the used configurations are mainly intersections, they are also representative for street sections. Generally, streets in densely built-up city districts show the tendency of higher aspect ratios and closed façades. Wide streets with aspect ratio 0.33 are flanked by only few buildings. Contrarily, streets with higher aspect ratios tend to have continuously built façades. Regarding general results obtained in air quality assessment studies it can be supposed that the risk of pollution accumulation increases with the aspect ratio (ADEME 2002). The highest aspect ratio referenced in Strasbourg is 1.0 and covers ten percent of all referenced streets. Such streets occur mainly in areas where most of the population concentrates like city centres and the residential districts close to the centre.

The analysis of street configurations in Strasbourg municipality shows the relevance of those defined to study the influence of vegetation on the dispersion of traffic induced particles. Wide canyons with dense buildings flanking both sides are represented by the model canyon with aspect ratio 0.5. According to ADEME (2002) canyons with smaller ratios present no risk of pollution accumulation what is supported by the finding that wider canyons are rarely flanked by a continuous building façade. Deeper canyons that tend to be more densely built are represented by aspect ratios 0.9 and 1.2.

Vegetation occurs in all canyon types. Tree lines are common to the street design in Strasbourg and most of the cities in the mid latitudes. They occur in wide and deep canyons, densely built or not.

**Comparison between two coevolutionary feature weighting algorithms in clustering**

P. Gançarski, A. Blansché and A. Wania

**Pattern recognition, 2008, Vol. 41, Issue 3, Pages 983-994**
**Part Special issue: Feature Generation and Machine Learning for Robust Multimodal Biometrics**

**2007 Urban Remote Sensing Joint Event**

# Hyperspectral imagery and urban green observation

Annett Wania and Christiane Weber
Image et Ville UMR 7011 CNRS/ULP
Louis Pasteur University
Strasbourg, France
{wania, weber}@lorraine.u-strasbg.fr

***Abstract*— Urban vegetation is known to play a major role in improving urban environmental conditions and to contribute to urban life quality. Consequently, nowadays most central European cities take special care on green spaces management and research on the effects is performed in different disciplines. Both need precise and up-to-date information, also beyond public areas. Using remote sensing is therefore valuable and especially since high resolution data are available for urban studies. Hyperspectral data are potentially interesting for such highly heterogeneous areas. However, there has been limited evaluation of the use of hyperspectral images and processing techniques for mapping urban vegetation. Here, we discuss the potential to use hyperspectral data for vegetation detection in urban areas. For our study we analyze field spectra and an image acquired by the Compact Airborne Spectral Imager (CASI) in September 2005 over Strasbourg city area (France). We present the first results on evaluation of coherence between field and image data. For image processing, a vegetation mask and minimum noise fraction transformation (MNF) is applied to reduce and compress the data. The following Spectral Angle Mapper (SAM) classification aims at vegetation identification at species level. We finally discuss our experiences and illustrate the difficulties encountered with urban vegetation detection.**

## I. INTRODUCTION

Today, more than 50 % of the world's population live in urban areas and by 2030 this percentage will presumably increase to 60 % (United Nations world population prospects 2004). At the same, cities concentrate most of the environmental problems. Air, water and soil pollution are on the daily agenda and the urban heat island influences local climate conditions. Urban ecosystems are no self regulating systems with high energy and material input and excessive output (waste, heat, pollutants). These ecosystems are a high load for the hinterland receiving these outputs. Nevertheless, cities remain the living place for a considerable number of humans. Discussions about life quality are ongoing and much research is performed to understand system processes and to possibly intervene in or interrupt cycles that menace our living environment, the fundament of life on Earth.

Nowadays, most of European city municipalities take care about quality of life, environmental preservation or biodiversity assessment. In such context green space development and maintenance constitute a complex issue related to aesthetic, social, ecological factors. On the one hand vegetation is part of the urban environment and contributes to life. On the other hand, urban vegetation is exposed to extreme living conditions (dryness, missing nutrient supply, light, oxygen, space etc.) affecting tree health and shortening life duration. Consequently, regular observation of trees in cities is important to avoid accidental events, diseases and to maintain habitats for plants and trees. Therefore information about vegetation (species, vegetation type, health conditions) is necessary and has to be up-dated regularly. But it is still very time consuming and expensive to assure the updating of such databases.

The automatic object detection with remote sensing offers a valuable alternative and it is worth to precise that individual vegetation object detection in urban areas was nearly impossible until the availability of high-resolution data. Since high spatial and spectral resolution sensors are available there is an increasing interest in urban remote sensing applications as these sensors are probably more powerful for the analysis of the particular heterogeneous environment ([1], [2], [3]). An adequate alternative to aerial photographic products usually used for planning purposes or decision support activities are Ikonos or Quickbird images. These data already provide relevant spatial resolution for object detection and characterization (automatic or not) and numerical capacities enabling data collection and structuring. However these multispectral data are somehow limited in spectral resolution constraining the detection and identification of urban reality objects in a short range of wavelength (visible and near infrared light) and with coarse spectral resolution (three or four channels). Comparatively, hyperspectral data offer both high spatial and spectral resolution capacities potentially interesting for highly heterogeneous areas such as urban areas.

Nevertheless, among urban application studies there are few about vegetation analysis in urban areas ([4], [5], [6]) and even less studies use hyperspectral data ([7]). As for multispectral data hyperspectral data are mostly used for agricultural, forest applications or biodiversity studies ([8], ([9], [10]). Some of these studies encourage the usage of these data for vegetation analysis. In [8] a promising study on discrimination of vegetation types based on field spectra analysis was performed.

It is especially difficult to identify urban vegetation elements, even using geometrical characteristics like forms because these elements are often in small groups or in line rather sparsely located; restrained patches or small areas (excluding urban forest of course). The focus of this article is to discuss possibilities to use hyperspectral data for urban

1-4244-0712-5/07/$20.00 ©2007 IEEE.

vegetation analyses in a perspective of vegetation monitoring or updating official databases. Regarding possible image processing approaches (per pixel or object oriented), we decide to promote the first option to extract vegetation information from hyperspectral images

## II. DATA

We analyze reflectance data of a CASI image acquired in mid September 2005 on Strasbourg city area, France. Flight campaign was initially started in May but due to a technical failure of the sensor, the campaign was interrupted. The 32 bands of the CASI image cover a spectral range between 429 and 954 nm with bandwidths between 11.4 and 11.8 nm. The spatial resolution is 2 m. Initial size of the image is about 143 km² covering mainly the city of Strasbourg with its outskirts and partly the rural landscape outside the city. For our analysis the image was subset to an area of 1254 x 908 pixels covering half of the densely built city center and two city quarters. Fig. 1 shows the image subset.


Figure 1. CASI image subset of Strasbourg 2.5 x 1.8 km.

The center of Strasbourg (lower left part Fig. 1) is entirely surrounded by the river Ill crossing the city from southwest to north. It is densely built with few vegetation cover. Dominating vegetation objects are trees on squares, backyards and vegetation along the riverside. Outside the Ill-island vegetation is much more present. The old German quarter in the north and east of the center is less densely built and dominated by relatively large building blocs surrounding larger backyards with vegetation. Several main avenues cross this part of the city, most of them with tree lines on both roadsides. Furthermore, there are three large parks and a smaller park near the center. All parks show an important amount of big, old trees (50-100 years). In the lower right part of the image high and elongated buildings refer to city planning during the seventies. The university campus is situated here. This younger part of the town is less densely built and besides the buildings often much younger and smaller trees as well as larger herbaceous surfaces (lawn, flower beds) are more present.

The dominating tree species in Strasbourg are chestnut, plane, lime and maple. They are the dominating tree species in the big avenues. Furthermore, trees like acacia, birch, poplar and ornamental trees are interspersed in the urban pattern.

In our study we analyze also field spectra registered during the mentioned flight campaign. These data were acquired with a handheld radiometer type TriOS RAMSES-ARC (TriOS GmbH, Oldenburg, Germany). The instrument has a spectral sampling interval of approximately 3 nm and a field view of 7°. Field spectra were acquired in 229 bands of 3 nm spectral band range. The initial field spectra covering 229 bands from 309 – 1050 nm were transformed to the 32 bands of the CASI image. During the flight campaign as well as the week before a total of 93 field spectra were acquired. For this study we analyzed only vegetation spectra, all in all 51.

### *A. Experiences with urban vegetation observation in CASI image*

As for every object in urban areas main problems for vegetation detection originate from object size and shadow. Generally, the spatial resolution of an image determines the minimum size of objects possible to detect. Theoretically, in the CASI image we use, only objects covering more than 4 m² are detectable. Smaller objects are mixed with neighboring objects (built or non-built) leading to a mixed pixel. The probability to detect a pure pixel increases with the objects size. Vegetation shows highly varying object sizes. In case of trees for example, size is strongly linked to the species, different species showing different growing shapes and sizes. In general, object size naturally increases with trees age but urban trees rarely reach sizes comparable to trees grown under natural conditions. Either they die before or they are limited in spatial extension by pruning, stress or due to near obstacles (buildings).

Tab. I shows urban vegetation objects in two groups separated by the CASI image pixel size.

TABLE I. SPATIAL RESOLUTION OF URBAN VEGETATION OBJECTS AND THEORETICAL OBJECT DETECTION LIMIT IN CASI IMAGE

Increasing object size

| Covered area | Vegetation object | Object composition |
|---|---|---|
| < 4 m² | balconies | C |
| | facades | S |
| | flower beds | C |
| | front gardens | C |
| | small shrubs | S, C |
| | small single trees | S |
| > 4 m² | big single trees | S |
| | dense tree lines & groups | S, C |
| | backyard gardens | S, C |
| | herbaceous areas | S, C |
| | parks and allotment gardens | C |

S single species, C composition of several species

On one hand, this table shows the limit for complete urban vegetation cover detection. On the other hand, it shows that even single objects are mixed in their composition, an important aspect for spectral signal interpretation. The object list is of course not exhaustive and exceptions occur usually.

Our aim was to test CASI data for species discrimination based on spectral characteristics. Consequently, detectable target objects are above all trees covering an important area like big single trees or dense tree lines and tree groups. Furthermore homogeneous herbaceous areas (lawn) were identified as a target group. Highly mixed vegetation objects like shrub groups, parks and gardens where not considered supposing that they are composed of single objects. Anyhow, the latter two are composed of smaller objects like trees, shrubs and herbaceous areas and are better identified in an object-oriented approach.

One of the main difficulties encountered in species detection is the determination of the tree crown for identification of relevant training sets. This is complicated additionally by the need to identify a relevant number of canopies for one species. Canopy reflectance is highly varying between species or even within one single tree ([11]). The canopy spectral reflectance is influenced by 1) architecture and composition of the canopy, 2) background spectral reflectance and 3) atmospheric composition ([12]). Even if we suppose the latter is the same for one image, canopy effects and the background signal highly vary within one tree (Fig. 2a) and between canopies of the same species (Fig. 2b). Fig. 2a shows varying reflectance of a big single plane tree canopy with differences up to 30 %. Content of chlorophyll, water, the plants age and health are biological (physiological) factors, leaf geometry, orientation and distribution are physical factors influencing reflectance properties of the canopy ([13], [11]). Variability is a natural factor in vegetation reflectance. The difference in canopy reflectance characteristics between a pruned plane (extremely limited tree extension) and a single big plane for example (Fig. 2b) might be due to highly different physical tree properties.

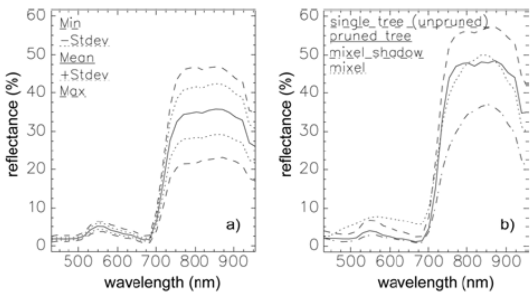


Figure 2. Spectral characteristics of plane trees: a) variations in the canopy of one single tree and b) between species in different environments and of different growth shapes.

Another main influence in urban areas stems from the underlying soil varying from bare nature like soil to artificial materials like concrete, asphalt or differently colored pavement stones. Again, depending on canopy density the underlying background signal influence may highly modify the captured signal of the same species. It is especially difficult to evaluate if the difference between two trees of the same species is due to health conditions, tree's growth shape or to the underlying soil. Foliage is defined by a spectral shape and the same a spectral shape should define the other factors. Fig. 2b shows the reflectance curve of a small tree under normal illumination (mixel) and an equivalent one covered by shadow (mixel shadow). On one hand, the spectral profiles show that both canopies are mixed with surrounding objects (no plateau in the NIR). On the other hand, reflectance intensity is reduced by shadow. The latter is a general observation made and it seems that possible differences between species are reduced by this signal attenuation.

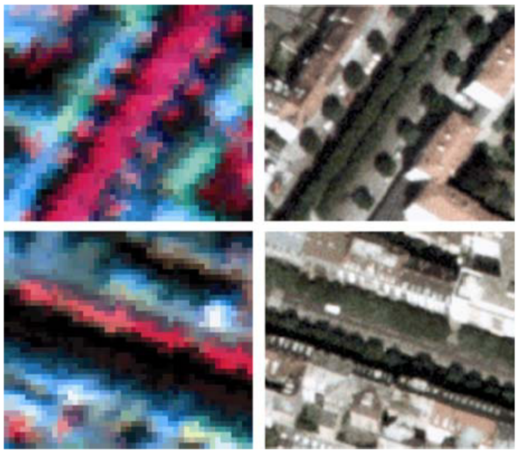

Figure 3. Example subsets of typical vegetation formations in Strasbourg, left CASI image, right aerial photograph BD Ortho. Upper line: a central double dense line of pruned planes separates car lines, the outer tree lines along the walking sides are less dense, with smaller single trees. Below: Tree lines along both roadsides in an avenue, the lower line is hidden by shadow.

Fig. 3 shows three CASI image subsets and the corresponding subsets of the aerial photographs of BD Ortho (© Institut Géographique National, from Mai 1998). Spatial resolution of the Orthophoto is 0.5 m. The comparison of both images clearly shows the difficulty to identify relevant training sets for small sized vegetation objects and tree crown detection. Furthermore, the image shows the influence of shadow from surrounding buildings.

## III. METHODS

### *A. Comparison field spectra and image spectra*

To evaluate relevance between the measured vegetation field spectra and the CASI image we compared field spectra with the spectral profile of the corresponding image pixel. On the one hand we compared them visually. On the other hand we used the Spectral Analyst in ENVI software 4.3 for quantitative evaluation of spectra similarity. Initially this tool is made for labeling endmembers (pure pixels) but we used it to evaluate how field spectra fit to image spectra by quantifying the similarity between two spectra. The idea is above all to evaluate relevance of field spectra for object detection in the

**2007 Urban Remote Sensing Joint Event**

image. Additionally, these results give a first insight of spectral characteristics of vegetation objects and class definition.

In a first step valuable spectra pairs were determined by identification of the representative image pixel for each field measurement. Even if the spatial resolution of the image is rather high, it was impossible to identify all measured vegetation objects in the image. Concerned are above all small trees or hedges covering less than the surface of the pixel or that are situated at the edge of a pixel and thus mixed with surrounding objects. Finally, image and field spectra of 27 vegetation objects were evaluated. We used the Spectral Angle Mapper (SAM) and the Spectral Feature Fitting (SFF) method in the Spectral Analyst to evaluate similarity between the field and the image spectra. For the evaluation both scores and the visual comparison of both spectra were taken into account. The SAM algorithm determines spectral similarity between two spectra by calculating an angle between the spectra in n-Dimensional space. Accordingly smaller angles represent closer matches ([14]). The SFF uses a least-squares technique to compare two spectra. It is an absorption-feature-based methodology where reference spectra (in our case the field spectra) are scaled to match the image spectra after the continuum is removed from both data sets (for more information see ([15]). Result of both methods is a score between 0 and 1. Higher scores indicate closer match and ideally approach 1.

*B. Vegetation mask*

To concentrate further analysis on urban vegetation, we decided in a first step to built a vegetation mask. An approved method to differentiate between built areas and vegetated areas is the calculation of a vegetation index (VI). Nowadays, there exists a variety of VI and generally they are divided into ratio, orthogonal and hybrid indices. Some of them have been already used with hyperspectral data ([12], [16]). We tested the performance of some of these indices to finally chose a VI that provides the best information for our data and the aim of the study. Besides the most often used ratio index Normalized Difference Vegetation Index (NDVI, see (1), [17]), we tested above all hybrid indices that account for the influence of soil background. In urban areas the influence of the soil background is especially important and surfaces are highly varying. Most surfaces in urban areas are artificial. Besides the more nature like soils in gardens, backyards or parks, most of the soils are sealed with asphalt, concrete or other stones. Even if these soils are different from soils in the open landscape, they behave - compared to vegetation - very similar in terms of reflectance, i.e. they are part of the soil line. Vegetation indices based on the concept of the soil line are largely accepted in remote sensing analysis. Among the variety of soil adjusted indices we chose to test three: Modified Soil Adjusted Vegetation Index (MSAVI, see (2), [18]), Transformed Soil Adjusted Vegetation Index (TSAVI, see (3), [19]) and Transformed Soil Atmospherically Resistant Vegetation Index (TSARVI, see (4), [20]). MSAVI and TSAVI are modifications of the first Soil Adjusted Vegetation Index (SAVI) developed by [21] and are less sensitive to the influence of bare soil to better estimate low vegetation cover. Generally vegetation indices are developed for agriculture or forest science applications. The first index developed in an urban context is the TSARVI and in [22] it was shown that this index provides better vegetation estimates than the NDVI. TSARVI is the only index that uses a hybrid channel (RB) calculated from a red (R) and blue (B) channel instead of the red channel (see (5)).

$$NDVI = \frac{NIR - R}{NIR + R} \tag{1}$$

$$MSAVI = \frac{2NIR + 1 - \sqrt{(2NIR+1)^2 - 8(NIR - R)}}{2} \tag{2}$$

$$TSAVI = \frac{[a(NIR - aR - b)]}{[(R + aNIR - ab + X(1 + a^2))]} \tag{3}$$

$$TSARVI = \frac{[a_{rb}(NIR - a_{rb}RB - b_{rb})]}{[(RB + a_{rb}NIR - a_{rb}b_{rb} + X(1 + a_{rb}^2))]} \tag{4}$$

$$RB = R - \gamma(R - B) \tag{5}$$

Bare soil pixels for the calculation of slope $a$ and ordinate $b$ of the soil line used in TSAVI and TSARVI were detected within the 2D-Scatterplot of the red and near infrared band (NIR). $\gamma$ is an atmospheric self-correcting factor, which depends on aerosol types ([20]). According to [20] $\gamma$ was set to 1. Consequently, the hybrid channel equals the blue band.

The blue, red and NIR bands used to calculate the VI were obtained in a former study where field spectra were analyzed to obtain object groups (see [23]). Among the 229 bands an optimal band subset was identified for object group discrimination. Selection of equivalent CASI bands for vegetation index calculations was done based on this subset. We used the most relevant bands: B = 429 nm, R = 667 nm and NIR = 904 nm. The resulting image was used to define a mask enabling to avoid indeterminate zones characterized by border values.

*C. Training set definition*

As already mentioned, the selection of training sets for hyperspectral image analysis in urban areas is difficult especially in case of vegetation. First, the spatial variation of urban vegetation complicates the detection of representative training sets. Second, even if hyperspectral data are reduced in dimensionality before classification, the number of bands finally used remains still higher than in usual multispectral data analysis. Training set size definition has to account for this increased dimensionality. For an image with n bands the training set should at least include 10 x n pixels ([24]). Furthermore, it is important to have additionally test sites to assure quality evaluation of the results. We defined training sets on vegetation objects in groups covering at least 10 x n pixels and appearing in several locations in the analyzed image extract. Class separability was evaluated for the transformed image (see next paragraph) with the Jeffrey-Matusita distance ([24]).

1-4244-0712-5/07/$20.00 ©2007 IEEE.

**2007 Urban Remote Sensing Joint Event**

*D. Feature reduction*

We used the Minimum Noise Fraction (MNF) Transformation for feature extraction in software ENVI 4.3. MNF aims at data decorrelation, noise-signal separation and inherent dimensionality determination. The transformation consists of two cascaded Principal Components (PC) transformations ([25]). The first PC transformation decorrelates and rescales noise in the data. The second is a standard PC transformation of the noise-whitened data. Initial dimension is reduced to only a few bands with high eigenvalues and coherent spatial information. For detailed information see [26] and [27].

*E. Classification method*

Image classification was performed with the Spectral Angle Mapper (SAM) algorithm in ENVI 4.3. The SAM classifier compares two reflectance spectra, the image pixel spectrum and a reference spectrum ([14]). Both spectra are defined by multispectral vectors and the angle between both spectra is calculated. The range of angles is between 0 and 1. Smaller angles indicate closer match to the reference spectra. In our case reference spectra were derived from the image and more precisely the mean of the training set classes. For each class a spectral angle image is calculated (abundance image). A derivative product of these images is a classified map based on small angles to each class.

## IV. Results

*A. Field spectra evaluation*

The results of the similarity analysis clearly show the difficulties encountered when comparing field and image spectra. In some cases the SAM score reaches satisfying values while the SFF score is rather unsatisfying, or while a high score in SAM induced similarity the visual comparison was unsatisfying. More herbaceous vegetation objects than trees show good similarities between measured and image spectra. This might be due to the problem of mixed pixels in images. Fig. 4 shows two examples for a good fit (high SAM and SFF scores).

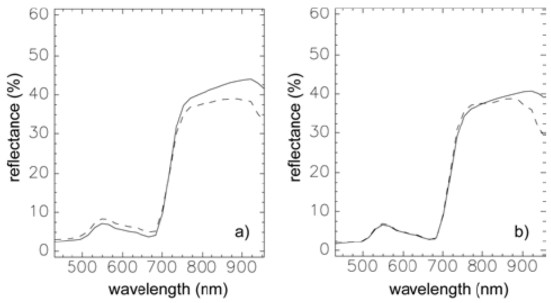


Figure 4. Comparison of spectral signatures obtained from field measurements (solid) and the corresponding image pixel (dashed) for two vegetation objects: a) fallow land with Chenopodium album and b) dense lawn.

However, in general the scores are rather high between vegetation objects as they show the same absorption features and peaks. Real differences exist between photosynthetic and non-photosynthetic vegetation or dense and low vegetation cover.

*B. Vegetation mask*

Relevance of the calculated vegetation indices was evaluated by comparing pixel values with the equivalent spectral profiles in the CASI image. One of the problems with index calculation stems from shadow. In the CASI image subset two kinds of shadow were detected: shadow on built surfaces and on vegetated surfaces. Fig. 5 shows a selection of typical shadow signatures found in the image subset. Typical for both are very low reflectance values in the whole spectral range (see reflectance scale). But shadow on vegetation nevertheless is different from shadow on built areas. While on the latter reflectance values generally decrease with increasing wavelength, shadow on vegetation shows the typical peaks and absorption features of vegetation (green peak, chlorophyll absorption of red light and the red-NIR shift). Consequently, it should be possible to detect vegetation hidden by shadow. We decided to include shadow in our vegetation mask.

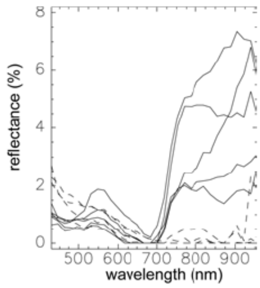


Figure 5. Spectral profiles of shadow pixels: solid lines vegetation and dashed lines built areas covered by shadow.

In general, TSAVI and TSARVI provide better vegetation cover estimations than NDVI and MSAVI. Fig. 6 shows a small subset of the image with the corresponding VI results (light grey/white = high VI value). Values between 0.6 and 1 are displayed. MSAVI shows higher values than NDVI unless its correction for the soil signal. Furthermore, both indices identify shadow on built areas as vegetation cover with highest values (see red circles in the NDVI image). TSAVI and TSARVI give better estimates concerning shadow and it seems that TSARVI identifies the best vegetation cover. The two visible tree groups are of different height, the group below being higher than the smaller group above. Due to these overlapping canopies a shadow zone separates both groups. While the TSAVI shows very high values for this shadow, the TSARVI shows quite low values and seems to better estimate tree canopy limits. It seems that the use of the hybrid channel improves vegetation cover estimates in shadowed areas. Nevertheless, TSARVI gives false estimates for red tile roofs what affects negatively the overall result. We finally decided to use the TSAVI for the mask even if vegetation areas are slightly overestimated. It was built on the value range 0.6 – 1.

1-4244-0712-5/07/$20.00 ©2007 IEEE.

**2007 Urban Remote Sensing Joint Event**

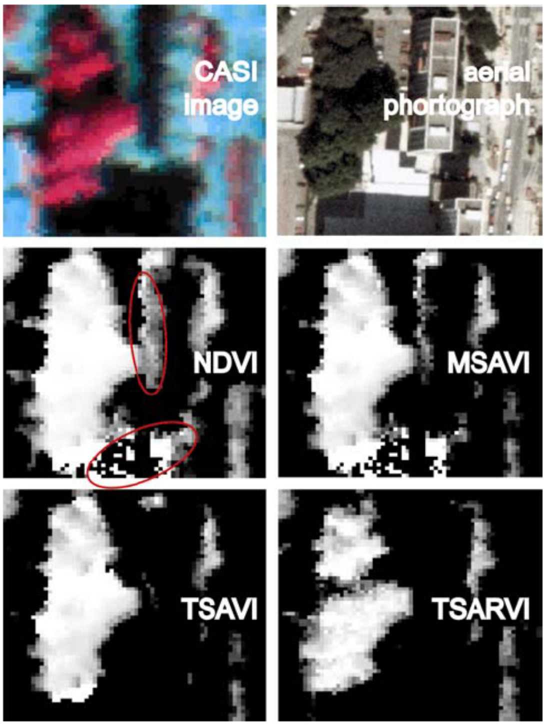


Figure 6. Comparison of NDVI, MSAVI, TSAVI and TSARVI calculated for the CASI image. Range for each VI 0.6-1. Red circles in the NDVI image refer to incorrect vegetation detection.

## C. *Vegetation classification*

Seven thematic classes were retained for classification, namely four different tree groups, two herbaceous classes and a shadow class (spectral profiles of training sets see Fig. 7a). SAM classification was performed on five MNF bands with no angle set. One band with a high percentage of explained variance (12.2%) had to be excluded as it showed clearly noise due to the movement of the airplane (flight lines). The five retained bands explain 64.6 % of total variance. Overall classification accuracy is 97.9 % with a Kappa 0.97.

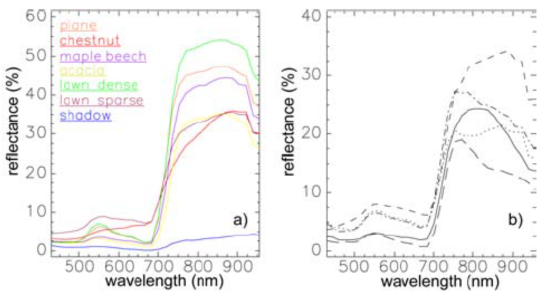


Figure 7. a) Spectral profiles of training sets and b) Spectral profiles of typical unclassified pixels.

TABLE II. CONFUSION MATRIX OF SAM CLASSIFICATION ON FIVE MNF BANDS

| | Ground Truth (pixels) | | | | | | | |
|---|---|---|---|---|---|---|---|---|
| **Class** | *plane* | *chest-nut* | *lawn dense* | *shadow* | *lawn sparse* | *acacia* | *maple, beech* | *total* |
| unclassified | 0 | 0 | 0 | 0 | 1 | 0 | 0 | 1 |
| plane | 108 | 0 | 0 | 0 | 4 | 0 | 0 | 112 |
| chestnut | 0 | 71 | 0 | 1 | 2 | 0 | 0 | 74 |
| lawn dense | 0 | 0 | 105 | 0 | 1 | 0 | 0 | 106 |
| shadow | 0 | 0 | 0 | 135 | 0 | 0 | 0 | 135 |
| lawn sparse | 0 | 0 | 0 | 0 | 67 | 0 | 0 | 67 |
| acacia | 0 | 0 | 0 | 0 | 0 | 56 | 4 | 60 |
| maple, beech | 0 | 0 | 0 | 0 | 0 | 0 | 75 | 75 |
| total | 108 | 71 | 105 | 136 | 75 | 56 | 79 | 630 |

Tab. II shows the confusion matrix and Fig. 8 shows a subset of the classified image. In general, the defined classes are correctly classified. Shadow is the dominating class in the analyzed image. In the German quarter this shadow includes a high amount of street trees hidden by the shadow of buildings with a mean height of 25 m. After classification, the defined four tree classes include pixels with nearly spectral response. The chestnut class for example includes generally damaged trees (senescence) as well as small trees in avenues showing especially low reflectance values. The plane class is rather unique in the image, i.e. only plane trees are classified. On the other hand, planes are sometimes classified in the acacia class. This is especially the case for pruned planes. Obviously, differences exist between reflectance characteristics of regularly pruned and natural grown trees (see Fig. 2b). Most of the street trees in big avenues are regularly pruned avoiding extension of branches over streets. Consequently, the canopy of pruned plane trees is less complex and dense, leafs often concentrate at only one height. Contrarily, naturally grown trees span a wide crown over a much larger area and leafs are overlapping at different heights. However, in other locations pruned trees are classed in the plane class, obviously not only the shape modifies the signal. The acacia and maple, beech (more precisely copper beech) class were defined only on these species but gather after classification most of the pixels on shrub groups or the mixed tree-shrub areas along the riverside or even small trees on lawn areas. It seems that the maple, beech class gathers pixels with higher reflectance values. This class was merged due to high spectral similarity of both species. Both span wide canopies and show higher reflectance values than the acacia class with its rather sparse crown and the probably higher influence of the underlying soil.

Chestnuts are easily detectable due to their typical spectral signature of non-photosynthetic vegetation (see Fig. 7a). Since a while these trees are affected every year by the horse chestnut leaf-miner and during image acquisition leafs were already damaged with visible pigment changes and leaf senescence. The two lawn classes are correctly classified in most cases. Dense lawn is sometimes confounded with plane and the sparse lawn class often appears at the margins of objects.

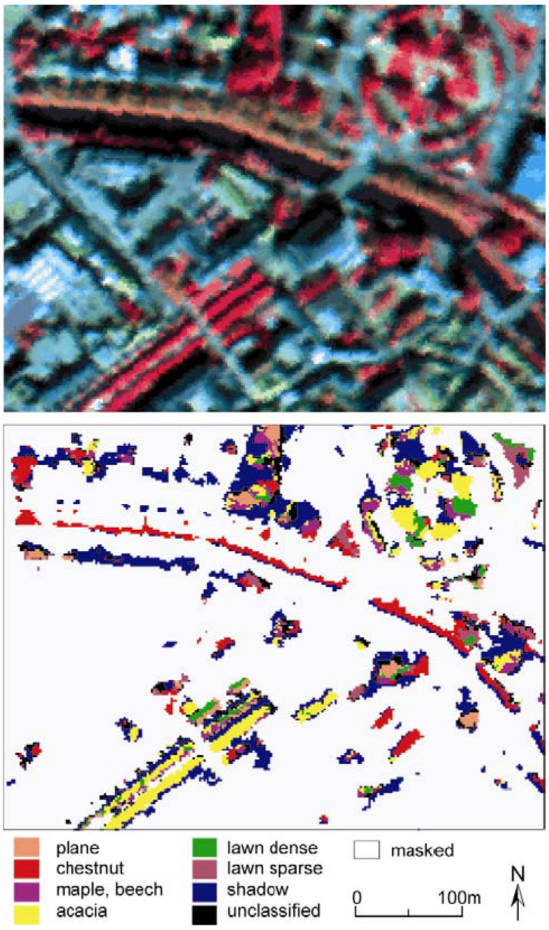


Figure 8. Result of SAM classification with corresponding image subset.

Nevertheless there are high numbers of unclassified pixels. In most cases these are highly mixed pixels either on the limit of a vegetation object or mixed due to the object's spatial resolution (small street trees). Fig. 7b shows the spectral characteristics of some of these unclassified pixels. In any case these pixels have low reflectance values in common and a spectral profile close to vegetation. The abrupt decrease in NIR reflectance of some pixels refers again to mixed objects.

## V. Discussion

The results of our study clearly show the problems encountered with vegetation detection in urban areas. Main problem originates from spatial resolution and mixed pixels. Even if the CASI image has a rather high spatial resolution, small objects like bushes, young trees or trees with a small crown perimeter are mixed with neighboring or even surrounding objects and can not be properly detected. Considered trees are birch, poplar, lime, willow and almost all ornamental trees. The latter are more often intentionally small growing cultivars. The definition of relevant training sets is strongly influenced by the spatial resolution problem. First, we had to limit our classes on large sized vegetation objects occurring several times in the image subset. But the frequency of vegetation objects in an urban area is rather limited compared to built objects. Second, the definition of the tree crown perimeter is a special challenge. And consequently, the question raises to which extent the variance within a canopy is representative for a class? Trees are three-dimensional objects with varying illumination conditions contrarily to buildings or most of the built surfaces. One can say that even every tree crown is unique in different locations in the image probably depending on the growth conditions and the underlying soil. However, these objects can be classified according to their growth shape, health, underlying soil and possible shadow effects. A study on standardized tree foliage examples could show that spectra discrimination between different tree species already poses problems [11]. Like [8] [11] suggests to focus on spectral regions for species discrimination. However, these authors analyzed field spectra or spectra obtained under controlled laboratory conditions.

Shadow is another problem encountered in this study. We do not investigate it further but the classification shows to what large extent shadow hides vegetation objects in the CASI image. Shadow is widely present and covers a high amount of vegetation in avenues, backyards, besides high or very high buildings. Shadow casts from buildings or even vegetation itself. It is not sure if shadow completely hides spectral differences between species. Probably an object-oriented classification approach might help to overcome this problem if proximity rules are used, for example in the case of tree alignments where one tree line is hidden by shadow but the parallel line is visible. Classification of urban objects with a per pixel approach shows concrete limits due to the heterogeneity of the urban pattern. In another study an object-oriented approach should be tested. Several authors already showed promising results on multispectral data but not on a species level ([5], [6]).

Results of the classification are not very satisfying but give a first insight into the complex problems with urban vegetation detection. The high amount of unclassified pixels is probably due to class definition and the classifier chosen. The SAM classifier compares two spectra and if the angle is higher than the maximum angle 1 the pixel is not classified in the concerned class. SAM uses endmembers to class pixels ideally pure pixels derived from field spectra. In our analysis they were derived from the training sets initially covering a certain spectral range in each band. This range is not considered in the SAM classifier what might be the main reason for the high amount of unclassified pixels. Nevertheless, this classifier is better adapted to hyperspectral data whereas the Maximum likelihood classifier leads to unacceptable results.

Another reason for the high amount of unclassified pixels might also be the result of data decompression. Even if it is applied on potential vegetation pixels determined with the TSAVI the mask covers a huge amount of mixed pixels and the dominance of shadow might disadvantageously influence the overall result for the vegetation pixels. But even if this problem

1-4244-0712-5/07/$20.00 ©2007 IEEE.

## 2007 Urban Remote Sensing Joint Event

can be solved the problem with relevant class definition remains.

Nevertheless, in general it is possible to detect vegetation in urban areas using vegetation indices like TSAVI or TSARVI. TSARVI seems to perform even better as this index does not saturate in shadow regions. But the use of a hybrid channel leads to some erroneous detection of built areas. First tests were performed to optimize TSARVI on only vegetation objects using TSARVI calculations in different NIR bands. Probably it is better to calculate vegetation indices on more than one band combination and to profit from the spectral resolution of these data.

### REFERENCES


[1] S. Barr and M. Barnsley, "Reducing structural clutter in land cover classifications of high spatial resolution remotely sensed images for urban land use mapping," *Computers and Geosciences*, vol. 26, pp. 433-449, 2000.

[2] P.M. Dare, "Shadow analysis in high resolution satellite imagery of urban areas," *Photogrammetric Engineering and Remote Sensing*, vol. 71, pp. 169-177, 2005.

[3] X.Y. HU, C.V. Tao and B. Prenzel, "Automatic segmentation of high resolution satellite imagery by integrating texture, intensity, and color features," *Photogrammetric Engineering and Remote Sensing*, vol. 71, pp. 1399-1406, 2005.

[4] G. Zhu, F. Bian and M. Zhang, "A flexible method for urban vegetation cover measurement based on remote sensing images," ISPRS Joint Workshop High Resolution Mapping from Space, Hannover, Germany, Definiens, 2003.

[5] X. Zhang, and X. Feng, "Detecting urban vegetation from IKONOS data using an object-oriented approach," IGARSS 2005 Symposium, Seoul, Korea, 2005.

[6] M. S. Moeller, and T. Blaschke, "A new index for the differentiation of vegetation fractions in urban neighborhoods based on satellite imagery," ASPRS 2006 Annual Conference, Reno, Nevada, 2006.

[7] A. Jung, P. Kardevan and L. Tőkei, "Detection of urban effect on vegetation in a less built-up Hungarian city by hyperspectral remote sensing," *Physics and Chemistry of the Earth*, vol. 30, pp. 255-259, 2005.

[8] K. S. Schmidt and A. K. Skidmore, "Spectral discrimination of vegetation types in a coastal wetland," *Remote Sensing of Environment*, vol. 85, pp. 92-108, 2003.

[9] E. Underwood, S. Ustin and D. Dipietro, "Mapping nonnative plants using hyperspectral imagery," *Remote Sensing of Environment*, vol. 86, pp. 150-161, 2003.

[10] F. Tsai, E.-K. Lin and H.-H. Wang, "Detecting invasive plant species using hyperspectral satellite imagery," International Geoscience and Remote Sensing Symposium IGARSS '05. Seoul, Korea, 2005.

[11] M. A. Cochrane, "Using vegetation reflectance variability for species level classification of hyperspectral data," *International Journal of Remote Sensing*, vol. 21, pp. 2075-2087, 2000.

[12] N. H. Broge, and E. Leblanc, "Comparing prediction power and stability of broadband and hyperspectral vegetation indices for estimation of green leaf area index and canopy chlorophyll density," *Remote Sensing of Environment*, vol. 76, pp. 156-172, 2000.

[13] A. Bannari, D. Morin and F. Bonn, "A review of vegetation indices," *Remote Sensing of Environment*, vol. 13, pp. 95-120, 1995.

[14] F. A. Kruse, A. B. Lefkoff, J. B. Boardman, K. B. Heidebrecht, A. T. Shapiro, P. J. Barloon and A. F. H. Goetz, "The Spectral Image Processing System (SIPS) - Interactive Visualization and Analysis of Imaging spectrometer Data," *Remote Sensing of Environment*, vol. 44, pp. 145 – 163, 1993.

[15] R. N. Clark, A. J. Gallagher and G. A. Swayze, "Material absorption band depth mapping of imaging spectrometer data using the complete band shape least-squares algorithm simultaneously fit to multiple spectral features from multiple materials," Third Airborne Visible/Infrared Imaging Spectrometer (AVIRIS) Workshop, JPL, 1990.

[16] O. Mutanga and A. K. Skidmore, "Hyperspectral band depth analysis for better estimation of grass biomass (Cenchrus ciliaris) measured under controlled laboratory conditions," *International Journal of Applied Earth Observation*, vol. 5, pp. 87-96, 2004.

[17] J. W. Rouse, R. W. Haas, J. A. Schell, D. W. Deering and J. C. Harlan, "Monitoring the vernal advancement and retrogradation (Greenwave effect) of natural vegetation," Greenbelt, MD, USA, NASA/GSFCT Type III Final Report, 1974.

[18] J. Qi, A. Chehbouni, A. R. Huete, Y. H. Kerr and S. Sorooshian, "A modified soil adjusted vegetation index," *Remote Sensing of Environment*, vol. 47, pp. 1-25, 1994.

[19] F. Baret and G. Guyot, "Potentials and limits of vegetation indices for LAI and APAR assessment," *Remote Sensing of Environment*, vol. 35, pp. 161-173, 1991.

[20] A. Bannari, D. Morin and F. Bonn, "A review of vegetation indices," *Remote Sensing of Environment*, vol. 13, pp. 95-120, 1995.

[21] A. R. Huete, "A Soil-Adjusted Vegetation Index (SAVI)," *Remote Sensing of Environment*, vol. 25, pp. 295-309, 1988.

[22] A. Bannari, D. C. He, D. Morin and H. Anys, "Analyse de l'apport de deux indices de végétation à la classification dans les milieux hétérogènes," *Canadian Journal of Remote Sensing*, vol. 24, pp. 233-239, 1998.

[23] A. Wania, D. Nafaa, J. Hirsch and C. Weber, "Analysing spectral characteristics of urban objects," International Conference on Spatial Analysis and GEOmatics SAGEO, 2006.

[24] J.A. Richards and X. Jia, *Remote sensing digital image analysis: an introduction*. Springer, Berlin, 1999.

[25] RSI Research Systems Inc., *Spectral analysis with ENVI*. Boulder, 2004.

[26] A. A. Green, M. Berman, P. Switzer and M. D. Craig, "A transformation for ordering multispectral data in terms of image quality with implications for noise removal," *IEEE Transactions on Geoscience and Remote Sensing*, vol. 26, pp. 65-74, 1988.

[27] J. B. Boardman and F. A. Kruse, "Automated spectral analysis: a geological example using AVIRIS data, north Grapevine Mountains, Nevada," *Proceedings, ERIM Tenth Thematic Conference on Geologic Remote Sensing*, Environmental Research Institute of Michigan, Ann Arbor, MI: I-407 - I-418, 1994.

# Analysing spectral characteristics of urban objects

**Annett Wania, Dhikrane Nafaa, Jacky Hirsch and Christiane Weber**

*Laboratoire Image et Ville, UMR 7011 CNRS/ULP*
*3,rue de l'Argonne*
*67000 Strasbourg*
*annett.wania@lorraine.u-strasbg.fr*

*ABSTRACT. The analysis of narrowband reflectance spectra for different objects is of particular interest since hyperspectral images are used for the analysis of the earth's surface. Acquired in very narrow and continuous bands these data can be used for labelling object groups identified in knowledge extraction (data mining processes) and unsupervised classification (image multi-strategy classification approach, research project ACI FoDoMust). In this paper the results of data analysis performed on narrowband reflectance spectra acquired with a field spectroradiometer during a hyperspectral image acquisition campaign in September 2005, are presented, aiming to identify object group characteristics. Results will be introduced into a dictionary of urban objects compiled for multiscale image classification and data mining. Identified objects gather non-vegetated surfaces and different vegetation types and species. Firstly, groups are identified through spectra recognition and multivariate analysis. Additionally, discriminant bands are identified and consequently used for a first criterion for object group characterisation.*

*RÉSUMÉ. L'arrivée des images hyperspectrales avec des bandes étroites et continues est particulièrement intéressante pour l'analyse des spectres de réflectance en milieu urbain. Ces données servent à l'identification de groupes d'objets particuliers en fournissant une information spectrale plus riche. De telles données sont utiles pour accompagner une démarche d'extraction de connaissances et de classification multistratégie développée dans le cadre de l'ACI FoDoMust. Le présent article présente les résultats d'une analyse effectuée sur des spectres de réflectance acquis par spectroradiomètre de terrain dans le cadre d'une campagne couplée à un survol hyperspectral de Strasbourg en Septembre 2005. Le but est l'identification des caractéristiques de groupes d'objets pouvant être introduites dans un « dictionnaire d'objets urbains » utilisé ensuite par les algorithmes de fouilles et d'extraction de connaissances. La gamme des objets identifiés s'étend des surfaces non-végétales jusqu'aux différents types de végétation voire d'espèces. Dans un premier temps des méthodes de statistique multivariée sont appliquées pour générer des groupes d'objets. La méthode appliquée permet en plus d'identifier les bandes les plus discriminantes qui seront utilisées ensuite pour la définition d'un premier critère de caractérisation de ces groupes d'objets.*

*KEYWORDS: reflectance spectroscopy, vegetation, urban objects, multivariate analysis.*

*MOTS-CLÉS : spectroscopie, réflectance, végétation, objets urbains, analyse multivariée.*

SAGEO'2006, pages 1 à 12

**1. Introduction**

Hyperspectral data offer new opportunities for the analysis of the earth's surface and differentiation of objects based on spectral characteristics. Acquired in very narrow and continuous bands, these reflectance spectra propose very precise spectral information. Hyperspectral image classification uses reference spectra provided in spectral libraries for object identification and to study spectral fingerprints of terrestrial targets. Actually a variety of spectral libraries is available (e.g. ASTER spectral library 1998, USGS 2003). Ground reflectance spectra for spectral libraries are either measured during an image acquisition along the covered area (e.g. Ben-Dor *et al.* 2001) or collected especially to built a general reference spectral library (e.g. Herold *et al.* 2004).

To date there are few spectral libraries that can be used for urban remote sensing applications even though several studies showed the particular interest of hyperspectral data for urban studies (Liu *et al.* 1999, Ben-Dor *et al.* 2001, Roessner *et al.* 2001, Herold *et al.* 2004, Kruse & Boardman 2004). The complex characteristics of urban objects and their heterogeneity pose a particular challenge and usual multispectral sensors show limitations for the mapping of such complex environments. In their study Herold *et al.* (2004) showed that bands of multispectral sensors often lie outside or near the boundaries of spectral narrow band ranges identified as optimal bands for object discrimination. Furthermore small spectral variations are not considered in multispectral images.

In September 2005 the Laboratory "Image et Ville" performed a hyperspectral image acquisition campaign over the Strasbourg city area (France) with the airborne sensor CASI-2. At the same time, field measurements were performed with a handheld spectrometer acquiring spectra in the 300 and 1050 nm region with 3 nm band width. The objective of the field campaign was to get spectra for the maximum of objects present in the urban area of Strasbourg. The targets measured reached from non-vegetated surfaces such as roofs, impervious, permeable surfaces to different vegetation types (different species as well as vegetation types). Altogether, 200 data sets were acquired.

In this paper we present the methodology applied for the exploration of these data aiming at data structuring and especially object group determination. To identify object groups and bands suitable for object group's discrimination, we use multivariate classification procedures. Group definition should aim at object group characteristics identification that might be introduced into a dictionary of urban objects. This dictionary was compiled for multiscale and multi-strategy image classification and data mining in the research project FoDoMust. This project focuses on the development of methods and tools that allow to use multiple knowledge sources and images to identify and locate elements of the urban pattern. The dictionary is a tool developed within this multi-strategy approach to describe spatial and spectral characteristics of singular and composed objects in reality and in the image.

After data presentation, the results of the classification methodology – object groups – and a first criterion for object group discrimination are presented.

## 2. Data and methods

During the field campaign 200 spectra were collected, 122 vegetation and 78 mineral/built surfaces spectra. The field campaign took place at the end of May and in mid September 2005 (flight campaign in May was interrupted because technical failure of the sensor, the image was acquired in September). Collection of vegetation targets included different lawns (e.g. park lawn, football areas, playgrounds), different trees typically present in central European urban areas (e.g. plane, maple, chestnut, poplar, willows as broadleaved-trees; pine, thuja, cedar, fir as coniferous trees and several shrubs). Furthermore measurements on vegetated fallow land, flowerbeds and agricultural areas were performed. The group of mineral/built surfaces cover targets like different roof materials (metal, tiles, gravel), asphalt (different ages), sand, gravel, different paving stones and plates (sandstone, concrete). Data were acquired with a handheld radiometer type TriOS RAMSES-ARC (TriOS GmbH, Oldenburg, Germany). The instrument is a stand-alone highly integrated hyperspectral radiometer for the UV and/or VIS spectral range sampling a spectral range of 300 – 1050 nm (Actimar 2005). The instrument has a spectral sampling interval of approximately 3 nm and a field view of 7°. For our study data were acquired in 229 bands of 3 nm spectral band range.

For further analysis initial spectral range was reduced to the spectral range of the CASI-2 image (429 to 954 nm) as the main objective of our study is the identification of relevant bands for urban objects discrimination. Thus only 165 out of 229 bands were used for statistical analysis. The initial band resolution of the ground measurements was remained.

Data were compiled in a spectral library using ENVI 4.2 software (Research Systems Inc.) assigning a code to each spectra. Regarding object types each spectra was assigned to one of the main categories vegetated, mineral, built, water surfaces as well as sub-categories (e.g. vegetated surfaces: herbaceous plants, coniferous trees and shrubs, broadleaved trees and shrubs).

We applied multivariate statistical analysis firstly to generate target groups and secondly to identify the most relevant bands for targets discrimination (target groups). Thus we combine cluster analysis (statistical software SPSS version 12.0) and discriminant analysis (BMDP 7.0), respectively to generate spectra groups and to assess the results. *Cluster analysis* identifies homogeneous groups within a heterogeneous data population. Although reflectance spectra are highly correlated, we privileged the fact that generation of groups is performed only on statistical measures and is not only based on subjective visual object group interpretation. As measure for the aggregation of groups mean distance between classes was used with the Euclidean distance interval. Special interest was given to the homogeneity of each group. Clusters are generated according to the users choice on the maximum number of clusters. With regard to the total number of objects a high maximum number was chosen for main groups generation. In the following step groups generated by cluster analysis are assessed and improved by stepwise *discriminant analysis*. Discriminant analysis is a method designed to optimise variance between groups and to identify the combination of variables (in our case the spectral bands) that best predicts the group to which a case (object signature) belongs. Cases are classified according to their distances from the centres of groups. Classification matrix shows stability of groups and eventual gains or losses.

## 3. Results

### *3.1 Generating groups*

*Cluster analysis*

Cluster analysis initially generated maximum 25 groups with different numbers of objects. Some of the groups consisted even only of one spectra. Discriminant analysis can be performed only on groups with at least two objects and consequently the initial 25 groups were studied with regard to their content (shape of spectra). We decided to exclude rare spectra from further analysis (groups consisting only in one object) and to divide some of the groups. Finally, 150 spectra remained.

At the end 25 groups were retained for further discriminant analysis (Table 1). Cluster analysis combined vegetation spectra in nine groups mainly based on different reflectance levels in the near infrared (NIR) (see Table 1 reflectance levels in percent). Three mineral surface groups were identified including one gravel group and two groups of sand, sand 1 showing lower reflectance values through the whole spectrum than sand 2. Built surfaces are pooled in 12 groups. The three asphalt groups seem to refer to the material's age: asphalt 1 including exclusively asphalt that is obviously fresher while asphalt 2 and 3 are brighter and include also paving stones. The five paving stones groups differ particularly among each other as they include different materials. Roof materials are combined in four groups with one metal roof (zinc), two different coloured gravel roof groups and one red tile roof group.

| N° | Group | Description (objects) |
|---|---|---|
| 1 | Vegetation 1 | coniferous and broadleaved trees, low NIR reflectance (20-25%) |
| 2 | Vegetation 2 | fallow and agricultural land, high green and red and low NIR reflectance (30-35%) |
| 3 | Asphalt 1 | dark-grey |
| 4 | Gravel roof 1 | gravel roofs (gravel compacted with asphalt) and one brown tile roof, homogeneous colour |
| 5 | Zinc roofs | metal |
| 6 | Gravel | parking places and river bank, bright-grey |
| 7 | Asphalt 2 | bright-grey, asphalt and gravel |
| 8 | Sand 1 | lower reflectance values |
| 9 | Gravel roof 2 | gravel roof and bright-grey gravel paving stone, heterogeneous colour |
| 10 | Asphalt 3 | mean bright-grey, asphalt and paving stone |
| 11 | Pavement 1 | very bright-grey, paving stone and gravel |
| 12 | Red tile roofs | red tiles (clay) |
| 13 | Water | water of lakes and rivers |
| 14 | Sand 2 | higher reflectance values |
| 15 | Pavement 2 | bright concrete, swirl surface, parking place |
| 16 | Pavement 3 | bright-grey paving stones, concrete like, rough surface |
| 17 | Pavement 4 | grey paving stones with regularly interspersed plants |
| 18 | Pavement 5 | bright coloured (grey and very bright rose) |
| 19 | Vegetation 3 | coniferous and broadleaved trees, low NIR reflectance (35-40%) |
| 20 | Vegetation 4 | broadleaved trees and herbaceous plants, mean NIR reflectance (45-55%) |
| 21 | Vegetation 5 | broadleaved trees, high green and red, mean NIR (45-55%) reflectance |
| 22 | Vegetation 6 | broadleaved trees, high NIR reflectance (50-70%) |
| 23 | Vegetation 7 | broadleaved trees, highest NIR reflectance values (75-90%) |
| 24 | Vegetation 8 | broadleaved trees, high NIR reflectance (65-80%) |
| 25 | Vegetation 9 | broadleaved trees, highest NIR reflectance values (90-100%) |

**Table 1.** *Final groups generated by cluster analysis and spectra evaluation. Group definition and description (in percent reflectance values for vegetation groups).*

*Discriminant analysis*

Groups generated by cluster analysis where evaluated by stepwise discriminant analysis. 95,3 % of objects are correctly classified. Table 2 shows the classification matrix with few possible changes between classes (see numbers in bold). Considered classes represent exclusively vegetation.

| | | Number of cases identified into group | | | | | | | | | | | | | | | | | | | | | | | | |
|---|---|---|---|---|---|---|---|---|---|---|---|---|---|---|---|---|---|---|---|---|---|---|---|---|---|---|
| | **% correct** | **1** | **2** | **3** | **4** | **5** | **6** | **7** | **8** | **9** | **10** | **11** | **12** | **13** | **14** | **15** | **16** | **17** | **18** | **19** | **20** | **21** | **22** | **23** | **24** | **25** |
| **1** | 90,0 | 18 | **1** | 0 | 0 | 0 | 0 | 0 | 0 | 0 | 0 | 0 | 0 | 0 | 0 | 0 | 0 | 0 | 0 | **1** | 0 | 0 | 0 | 0 | 0 | 0 |
| **2** | 100,0 | 0 | 3 | 0 | 0 | 0 | 0 | 0 | 0 | 0 | 0 | 0 | 0 | 0 | 0 | 0 | 0 | 0 | 0 | 0 | 0 | 0 | 0 | 0 | 0 | 0 |
| **3** | 100,0 | 0 | 0 | 4 | 0 | 0 | 0 | 0 | 0 | 0 | 0 | 0 | 0 | 0 | 0 | 0 | 0 | 0 | 0 | 0 | 0 | 0 | 0 | 0 | 0 | 0 |
| **4** | 100,0 | 0 | 0 | 0 | 3 | 0 | 0 | 0 | 0 | 0 | 0 | 0 | 0 | 0 | 0 | 0 | 0 | 0 | 0 | 0 | 0 | 0 | 0 | 0 | 0 | 0 |
| **5** | 100,0 | 0 | 0 | 0 | 0 | 2 | 0 | 0 | 0 | 0 | 0 | 0 | 0 | 0 | 0 | 0 | 0 | 0 | 0 | 0 | 0 | 0 | 0 | 0 | 0 | 0 |
| **6** | 100,0 | 0 | 0 | 0 | 0 | 0 | 3 | 0 | 0 | 0 | 0 | 0 | 0 | 0 | 0 | 0 | 0 | 0 | 0 | 0 | 0 | 0 | 0 | 0 | 0 | 0 |
| **7** | 100,0 | 0 | 0 | 0 | 0 | 0 | 0 | 3 | 0 | 0 | 0 | 0 | 0 | 0 | 0 | 0 | 0 | 0 | 0 | 0 | 0 | 0 | 0 | 0 | 0 | 0 |
| **8** | 100,0 | 0 | 0 | 0 | 0 | 0 | 0 | 0 | 7 | 0 | 0 | 0 | 0 | 0 | 0 | 0 | 0 | 0 | 0 | 0 | 0 | 0 | 0 | 0 | 0 | 0 |
| **9** | 100,0 | 0 | 0 | 0 | 0 | 0 | 0 | 0 | 0 | 2 | 0 | 0 | 0 | 0 | 0 | 0 | 0 | 0 | 0 | 0 | 0 | 0 | 0 | 0 | 0 | 0 |
| **10** | 100,0 | 0 | 0 | 0 | 0 | 0 | 0 | 0 | 0 | 0 | 4 | 0 | 0 | 0 | 0 | 0 | 0 | 0 | 0 | 0 | 0 | 0 | 0 | 0 | 0 | 0 |
| **11** | 100,0 | 0 | 0 | 0 | 0 | 0 | 0 | 0 | 0 | 0 | 0 | 2 | 0 | 0 | 0 | 0 | 0 | 0 | 0 | 0 | 0 | 0 | 0 | 0 | 0 | 0 |
| **12** | 100,0 | 0 | 0 | 0 | 0 | 0 | 0 | 0 | 0 | 0 | 0 | 0 | 2 | 0 | 0 | 0 | 0 | 0 | 0 | 0 | 0 | 0 | 0 | 0 | 0 | 0 |
| **13** | 100,0 | 0 | 0 | 0 | 0 | 0 | 0 | 0 | 0 | 0 | 0 | 0 | 0 | 3 | 0 | 0 | 0 | 0 | 0 | 0 | 0 | 0 | 0 | 0 | 0 | 0 |
| **14** | 100,0 | 0 | 0 | 0 | 0 | 0 | 0 | 0 | 0 | 0 | 0 | 0 | 0 | 0 | 3 | 0 | 0 | 0 | 0 | 0 | 0 | 0 | 0 | 0 | 0 | 0 |
| **15** | 100,0 | 0 | 0 | 0 | 0 | 0 | 0 | 0 | 0 | 0 | 0 | 0 | 0 | 0 | 0 | 3 | 0 | 0 | 0 | 0 | 0 | 0 | 0 | 0 | 0 | 0 |
| **16** | 100,0 | 0 | 0 | 0 | 0 | 0 | 0 | 0 | 0 | 0 | 0 | 0 | 0 | 0 | 0 | 0 | 2 | 0 | 0 | 0 | 0 | 0 | 0 | 0 | 0 | 0 |
| **17** | 100,0 | 0 | 0 | 0 | 0 | 0 | 0 | 0 | 0 | 0 | 0 | 0 | 0 | 0 | 0 | 0 | 0 | 2 | 0 | 0 | 0 | 0 | 0 | 0 | 0 | 0 |
| **18** | 100,0 | 0 | 0 | 0 | 0 | 0 | 0 | 0 | 0 | 0 | 0 | 0 | 0 | 0 | 0 | 0 | 0 | 0 | 2 | 0 | 0 | 0 | 0 | 0 | 0 | 0 |
| **19** | 91,3 | 0 | **1** | 0 | 0 | 0 | 0 | 0 | 0 | 0 | 0 | 0 | 0 | 0 | 0 | 0 | 0 | 0 | 0 | 21 | **1** | 0 | 0 | 0 | 0 | 0 |
| **20** | 100,0 | 0 | 0 | 0 | 0 | 0 | 0 | 0 | 0 | 0 | 0 | 0 | 0 | 0 | 0 | 0 | 0 | 0 | 0 | 0 | 13 | 0 | 0 | 0 | 0 | 0 |
| **21** | 100,0 | 0 | 0 | 0 | 0 | 0 | 0 | 0 | 0 | 0 | 0 | 0 | 0 | 0 | 0 | 0 | 0 | 0 | 0 | 0 | 0 | 5 | 0 | 0 | 0 | 0 |
| **22** | 81,2 | 0 | 0 | 0 | 0 | 0 | 0 | 0 | 0 | 0 | 0 | 0 | 0 | 0 | 0 | 0 | 0 | 0 | 0 | 0 | **1** | 0 | 13 | 0 | **2** | 0 |
| **23** | 100,0 | 0 | 0 | 0 | 0 | 0 | 0 | 0 | 0 | 0 | 0 | 0 | 0 | 0 | 0 | 0 | 0 | 0 | 0 | 0 | 0 | 0 | 0 | 13 | 0 | 0 |
| **24** | 100,0 | 0 | 0 | 0 | 0 | 0 | 0 | 0 | 0 | 0 | 0 | 0 | 0 | 0 | 0 | 0 | 0 | 0 | 0 | 0 | 0 | 0 | 0 | 0 | 7 | 0 |
| **25** | 100,0 | 0 | 0 | 0 | 0 | 0 | 0 | 0 | 0 | 0 | 0 | 0 | 0 | 0 | 0 | 0 | 0 | 0 | 0 | 0 | 0 | 0 | 0 | 0 | 0 | 3 |

**Table 2.** *Classification matrix: percent of correct classification for each group, number of cases (grey) and identified changes (bold).*

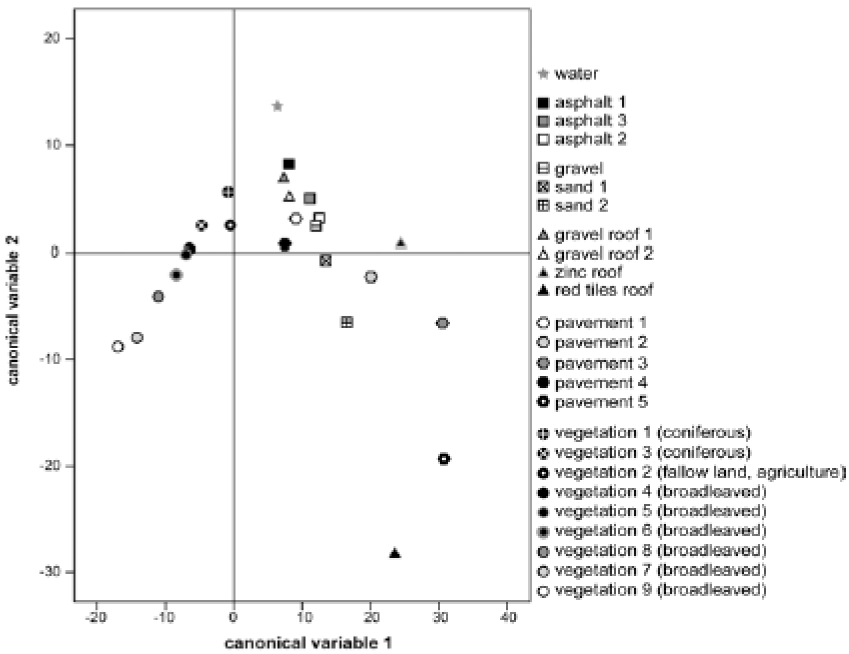


**Figure 1.** *Group means projected on the first and second canonical variables (asphalt and vegetation: grey scale gradation corresponds to reflectance levels, i.e. increasing overall reflectance values from black to white).*

Figure 1 shows the distances between groups for the most discriminating two canonical variables. Most of the discrimination is provided by the first two canonical variables with 63 and 20 % proportion of total dispersion explained (third and forth variable: 12 and 4 % respectively).

Distinct distances exist between the two main object groups vegetation and mineral/built surfaces. Vegetation group means show negative values on the first canonical variable. In the opposite, mineral/built and the water surface group show positive values on this variable. As already mentioned different vegetation groups are mainly based on different reflectance intensities in the NIR region (see Table 1). Highest NIR reflectance of broadleaved trees group vegetation 9 are in distinct opposition to the low reflecting coniferous dominated groups vegetation 1 and 3. The distance between vegetation group 4 and 5 is very small, both groups seem to be quite similar. Originally, both groups belong to one cluster but it was decided to separate them due to much higher reflectance values in the green and red region for vegetation 5. The suggested difference was not confirmed by discriminant analysis.

The mineral/built surfaces groups seem to be quite distinct except groups asphalt 2 and gravel. This might be due to similar colours, both are light-grey. Compared to the other asphalt groups (asphalt 1 and 3) asphalt 2 has higher reflectance values and seems to be brighter. Concerning roofs, there are three distinct groups: red tile roofs and zinc roofs show high distances to all groups and to both gravel roof groups (gravel roof 1 and 2). Again, the darker gravel roof group 1 approaches the darker asphalt group 1, the same applies for the brighter gravel roof group 2 approaching the mean bright asphalt group 3.

*Discriminant spectral regions*

Discriminant analysis indicates 11 most significant bands for object group discrimination. Table 3 shows the list of discriminating bands and the order of inclusion in the discriminant function (step number, spectral definition of bands, total number of bands included at each step and F-value of the entered band). The most important bands are a NIR and a red band. Both are potentially useful for calculating a vegetation index (see below). Consequently, the most important characteristic for group discrimination lies thus in the red - NIR shift and probably discriminates in a first step vegetation from non-vegetated surfaces. The following bands lie in the visible region (VIS) what might indicate the influence of object colour. Altogether, seven out of eleven bands lie in the VIS region.

| Step No. | Wavelength (nm) | Spectral region | No. of bands included | F-value to enter |
|---|---|---|---|---|
| 1 | 907,69 | NIR | 1 | 262,66 |
| 2 | 674,69 | Red | 2 | 266,79 |
| 3 | 504,01 | Green | 3 | 112,80 |
| 4 | 428,23 | Blue | 4 | 25,62 |
| 5 | 625,59 | Red | 5 | 11,39 |
| 6 | 694,28 | Red | 6 | 6,45 |
| 7 | 454,59 | Blue | 7 | 4,04 |
| 8 | 687,75 | Red | 8 | 2,59 |
| 9 | 817,70 | NIR | 9 | 2,40 |
| 10 | 910,89 | NIR | 10 | 1,35 |
| 11 | 775,62 | NIR | 11 | 1,23 |

**Table 3.** *Most discriminant bands and their spectral definition.*

Figure 2 shows mean spectra of six distinct groups (high distances) and the position of the mentioned eleven discriminant bands. These are examples of identified object groups and the figure reveals the importance of the first two most discriminating bands for the differentiation between the two vegetation groups and the four mineral and built surfaces groups. While the first have high reflectance values in the NIR and lower in the red band, the differences of reflectance values of both bands is clearly smaller for the mineral and built surfaces. Furthermore, one can see the aspect of the spectra for the red tile roofs group reflecting the

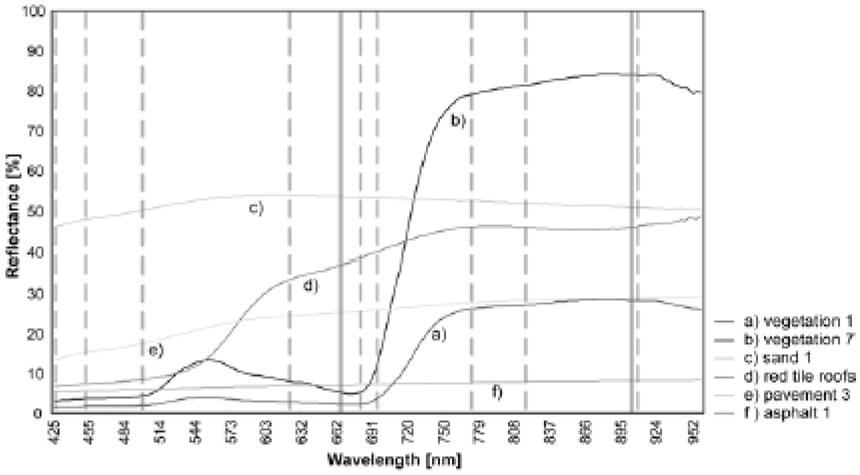


particularity of this group (see figure 1).

**Figure 2.** *Mean spectra of six distinct groups and position of the eleven discriminant bands (vertical grey lines, most discriminating two bands continuous lines: λ = 674,69nm and 907,69nm), other bands dashed lines.*

### *3.2 Object discrimination criteria extraction*

Based on the results and especially the relevant bands, a first criterion can be retained for the discrimination of the two main object groups vegetation and mineral/built surfaces. The criterion refers to the concept of vegetation index consisting in the steep slope between the red and NIR, a unique feature of green vegetation (Horler *et al.* 1983). Vegetation indices are based on the sharp reflectance changes in the red - NIR region. Green vegetation shows low red reflectance due to chlorophyll absorption and in the opposite especially high reflectance values in the NIR due to high internal leaf scattering (Horler *et al.* 1983). Both values vary with the chlorophyll content in opposite direction.

Normalised difference vegetation index NDVI was calculated using the two most discriminant bands (λ = 907,69 nm and 674,69 nm). The nine vegetation groups have high NDVI values (0,67-0,92) (see Table 4) whereas mineral/built surfaces show significantly lower values. Furthermore it seems that the simple reflectance difference between both bands is sufficient for the discrimination of both groups. Vegetation groups show higher differences than non-vegetated surfaces.

| Group N° | Group name | $R_{908}$-$R_{675}$ | NDVI ($R_{908}$-$R_{675}$/ $R_{908}$+$R_{675}$) |
|---|---|---|---|
| 1 | Vegetation 1 | 2595,31 | **0,85** |
| 2 | Vegetation 2 | 2757,52 | **0,67** |
| 3 | Asphalt 1 | 104,99 | 0,07 |
| 4 | Gravel roof 1 | 524,65 | 0,24 |
| 5 | Zinc roofs | -794,63 | -0,13 |
| 6 | Gravel | 263,90 | 0,06 |
| 7 | Asphalt 2 | 120,38 | 0,03 |
| 8 | Sand 1 | 338,73 | 0,06 |
| 9 | Gravel roof 2 | 546,61 | 0,19 |
| 10 | Asphalt 3 | 79,59 | 0,03 |
| 11 | Pavement 1 | 682,26 | 0,18 |
| 12 | Red tile roofs | 810,85 | 0,10 |
| 13 | Water | -213,05 | -0,77 |
| 14 | Sand 2 | 721,15 | 0,09 |
| 15 | Pavement 2 | 58,38 | 0,01 |
| 16 | Pavement 3 | -262,14 | -0,03 |
| 17 | Pavement 4 | 1616,11 | 0,32 |
| 18 | Pavement 5 | -37,56 | 0,00 |
| 19 | Vegetation 3 | 3847,34 | **0,86** |
| 20 | Vegetation 4 | 4832,43 | **0,92** |
| 21 | Vegetation 5 | 4480,67 | **0,84** |
| 22 | Vegetation 6 | 5747,13 | **0,91** |
| 23 | Vegetation 7 | 7899,42 | **0,89** |
| 24 | Vegetation 8 | 6728,75 | **0,87** |
| 25 | Vegetation 9 | 9293,86 | **0,90** |

**Table 4.** *Difference in reflectance values in the two most discriminant bands and NDVI for each group (R reflectance with rounded band mean).*

**4. Discussion and Conclusions**

These results represent the first step of information extraction for urban object recognition. The results will be introduced in a dictionary compiled for multiscale image analysis and data mining (FoDoMust project). The dictionary will be used to complete an ontology designated to provide knowledge for unsupervised image classification. The idea of this multi-strategy approach is to combine different unsupervised classifiers to optimise classification results. According to spatial resolution of the analysed images, the dictionary differentiates between single objects (e.g. single tree) and composite objects (e.g. park where the tree is located) and each is characterised by its (1) 'reality' and (2) image characteristics. Ground measurements analysed in this study are considered as reality and consequently are analysed for object 'reality' characteristics extraction. In the present study potential object groups were identified and a first criterion was retained to differentiate between vegetation and mineral/built surfaces. Further analysis will focus on extraction of object group characteristics that allow differentiating between different mineral/built surfaces or different vegetation types.

The identified object groups based on these ground measurements present only some pixels in the image while the same object group in the image is defined by a much higher number of 'objects' (pixels). Consequently, object groups and differences retained for object discrimination in the dictionary have to be validated by image analysis. Coherency between 'reality' and 'image' characteristics is fundamental. Furthermore, in future analysis spectral discrimination of identified groups should be evaluated using spectral distance measures such as the Jeffries-Matusita distance (Schmidt & Skidmore 2003, Herold *et al.* 2004). This distance measure is commonly used for analysis of narrowband reflectance spectra acquired in the VIS-SWIR region.

With regard to significant bands for group discrimination our results are coherent with those of Herold *et al.* (2004) in their study on spectra in the VIS-SWIR region. They found that most of the optimal bands for object discrimination lie in the VIS region. Fewer bands were identified in the NIR and short wave infrared region. The high number of discriminant bands in the VIS region and their ranking in our study indicate that VIS wavelengths are important for object differentiation. Nevertheless our study concerns only the VIS and NIR region and one band in the NIR region is identified as the most relevant band. Together with the second most relevant red band, vegetation and mineral/built surfaces are obviously discriminated. The influence of the last three NIR bands might be important to distinguish between the different vegetation groups but should be tested on their discriminating force for mineral/built surfaces. The importance of the VIS bands for mineral/built surface distinction has to be analysed.

**Acknowledgements**

This research is supported by the research project FoDoMust (ACI Action Concertée Incitative Fouille de Données Multi-stratégie, responsible P. Gançarski), Pôle Image Strasbourg and the network of alsacian environmental research laboratories REALISE (Réseau Alsace de Laboratoires en Ingénieries et Sciences pour l'Environnement).

**References**

*Actimar, Mission de télédétection hyperspectrale aéroportée CASI sur la ville de Strasbourg, Rapport final, Brest 2006, 46 pages.*

ASTER spectral library, http://speclib.jpl.nasa.gov/, 1998 (accessed: May 2006).

Ben-Dor E., Levin N. & Saaroni H., A spectral based recognition of the urban environment using the visible and near infra-red spectral region (0,4-1,1 µm). A case study over Tel-Aviv, Israel. *International Journal of Remote Sensing*, vol. 22, n°11, 2001, p. 2193-2218.

Herold M., Roberts A. D., Gardner M. E. & Dennison P. E., Spectrometry for urban area remote sensing – Development and analysis of a spectral library from 350 – 2400 nm, *Remote Sensing of Environment*, vol. 91, n° 3-4, 2004, p. 304-319.

Horler D.N., Dockray M. & Barber J., The red edge of plant leaf reflectance, *International Journal of Remote Sensing*, vol. 4, n° 2, 1983, p. 273-288.

Kruse F.A. & Boardman J.W., Using hyperspectral data for urban baseline studies, Boulder, Colorado, *Proceedings of the 13th JPL Airborne Geoscience Workshop, Jet Propulsion Laboratory*, 31 March – 21 April 2004, Pasadena, Canada.

Liu J., Zhang L. & Tong Q., Extraction and Recognition of urban objects by hyperspectral remote sensing, *Proceedings of the 20th Asian Conference on Remote Sensing*, 22-25 November 1999, Hong Kong, China.

Roessner S., Segl K., Heiden U. & Kaufmann H., Automated differentiation of urban surfaces based on airborne hyperspectral imagery, *IEEE Transactions on Geoscience and Remote Sensing*, vol. 39, n° 7, 2001, p. 1525-1532.

Schmidt K.S. & Skidmore A.K., Spectral discrimination of vegetation types in a coastal wetland, *Remote Sensing of Environment*, vol. 85, n° 1, 2003, p. 92-108.

USGS spectral library splib05a, http://speclab.cr.usgs.gov/spectral-lib.html, 2003 (accessed: May 2006).